SAFETY OF RAILROAD PASSENGER VEHICLE DYNAMICS

OMNISIM Simulation and Test Correlations for Passenger Rail Cars

U.S. Department
of Transportation

**Federal Railroad
Administration**

Office of Research
and Development
Washington, DC 20590

DOT/FRA/ORD-01/07

Final Report
July 2002

REPORT DOCUMENTATION PAGE

Form Approved
OMB No. 0704-0188

1. AGENCY USE ONLY *(Leave blank)*	2. REPORT DATE	3. REPORT TYPE AND DATES COVERED
	July 2002	Final Report January 1997 – March 2000

4. TITLE AND SUBTITLE
Safety of Railroad Passenger Vehicle Dynamics: OMNISIM Simulation and Test Correlations for Passenger Rail Cars

5. FUNDING NUMBERS
DTFR53-95-C-00049

6. AUTHOR(S)
Gopal Samavedam, John Gomes

7. PERFORMING ORGANIZATION NAME(S) AND ADDRESS(ES)
Foster-Miller, Inc.
350 Second Avenue
Waltham, MA 02451-1196

8. PERFORMING ORGANIZATION REPORT NUMBER

9. SPONSORING/MONITORING AGENCY NAME(S) AND ADDRESS(ES)
U.S. Department of Transportation
Federal Railroad Administration
1120 Vermont Avenue NW
MS20
Office of Research and Development
Washington, D.C. 20592

10. SPONSORING/MONITORING AGENCY REPORT NUMBER
DOT/FRA/ORD-01/07

11. SUPPLEMENTARY NOTES

12a. DISTRIBUTION/AVAILABILITY STATEMENT
This document is available to the publish through the National Technical Information Service, Springfield, VA 22161

12b. DISTRIBUTION CODE
N/A

13. ABSTRACT *(Maximum 200 words)*

The purpose of the work is to validate the safety assessment methodology previously developed for passenger rail vehicle dynamics, which requires the application of simulation tools as well as testing of vehicles under different track scenarios. This report specifically addresses the evaluation of the tasks in the methodology related to measurement of vehicle and track parameters, test conduct, and correlation of the test results with computer simulation results.

This report presents a summary of the testing and correlation with OMNISIM computer simulation results for two different rail passenger rail car designs. The first design had non-equalized trucks and the second had equalized trucks. The tests and OMNISIM simulation correlations included vehicle response to variations in vertical alignment, steady curving, dynamic curving, yaw and sway, twist and roll, pitch and bounce, and hunting with initial alignment defects. For each dynamic test, a description and correlation are provided. Summary tables are provided for the measured and simulated maximum and RMS force levels of each test.

It is concluded that the methodology can be used to adequately evaluate the safety issues involved in the dynamic behavior of the passenger rail vehicles as they negotiate a variety of track conditions.

14. SUBJECT TERMS	15. NUMBER OF PAGES
passenger rail vehicles, non-equalized trucks, equalized trucks, OMNISIM, rail vehicle dynamics	48
	16. PRICE CODE: N/A

17. SECURITY CLASSIFICATION OF REPORT	18. SECURITY CLASSIFICATION OF THIS PAGE	19. SECURITY CLASSIFICATION OF ABSTRACT	20. LIMITATION OF ABSTRACT
Unclassified	Unclassified	Unclassified	Unlimited

NSN 7540-01-280-5500

Standard Form 298 (Rev. 2-89)
Prescribed by ANSI Std. 239-18

SI* (MODERN METRIC) CONVERSION FACTORS

APPROXIMATE CONVERSIONS TO SI UNITS

Symbol	When You Know	Multiply By	To Find	Symbol
	LENGTH			
in	inches	25.4	millimeters	mm
ft	feet	0.305	meters	m
yd	yards	0.914	meters	m
mi	miles	1.61	kilometers	km
	AREA			
in^2	square inches	645.2	millimeters squared	mm^2
ft^2	square feet	0.093	meters squared	m^2
yd^2	square yards	0.836	meters squared	m^2
ac	acres	0.405	hectares	ha
mi^2	square miles	2.59	kilometers squared	km^2
	VOLUME			
fl oz	fluid ounces	29.57	milliliters	ml
gal	gallons	3.785	liters	l
ft^3	cubic feet	0.028	meters cubed	m^3
yd^3	cubic yards	0.765	meters cubed	m^3

NOTE: Volumes greater than 1000 l shall be shown in m^3.

	MASS			
oz	ounces	28.35	grams	g
lb	pounds	0.454	kilograms	kg
T	short tons (2000 lb)	0.907	megagrams	Mg
	TEMPERATURE (exact)			
°F	Fahrenheit temperature	5(F-32)/9 or (F-32)/1.8	Celcius temperature	°C
	ILLUMINATION			
fc	foot-candles	10.76	lux	l
fl	foot-Lamberts	3.426	candela/m^2	cd/m^2
	FORCE and PRESSURE or STRESS			
lbf	poundforce	4.45	newtons	N
psi	poundforce per square inch	6.89	kilopascals	kPa

APPROXIMATE CONVERSIONS FROM SI UNITS

Symbol	When You Know	Multiply By	To Find	Symbol
	LENGTH			
mm	millimeters	0.039	inches	in
m	meters	3.28	feet	ft
m	meters	1.09	yards	yd
km	kilometers	0.621	miles	mi
	AREA			
mm^2	millimeters squared	0.0016	square inches	in^2
m^2	meters squared	10.764	square feet	ft^2
m^2	meters squared	1.195	square yards	ac
ha	hectares	2.47	acres	mi^2
km^2	kilometers squared	0.386	square miles	
	VOLUME			
ml	milliliters	0.034	fluid ounces	fl oz
l	liters	0.264	gallons	gal
m^3	meters cubed	35.71	cubic feet	ft^3
m^3	meters cubed	1.307	cubic yards	yd^3
	MASS			
g	grams	0.035	ounces	oz
kg	kilograms	2.202	pounds	lb
Mg	megagrams	1.103	short tons (2000 lb)	T
	TEMPERATURE (exact)			
°C	Celcius temperature	1.8C + 32	Fahrenheit temperature	°F
	ILLUMINATION			
lx	lux	0.0929	foot-candles	fc
cd/m^2	candela/m^2	0.2919	foot-Lamberts	fl
	FORCE and PRESSURE or STRESS			
N	newtons	0.225	poundforce	lbf
kPa	kilopascals	0.145	poundforce per square inch	psi

* SI is the symbol for the International System of Units

CONTENTS

Section Page

ILLUSTRATIONS

Figure **Page**

TABLES

PREFACE

This report presents results of testing and correlation with the OMNISIM computer simulation for two passenger rail cars. The first car had non-equalized trucks and the second had equalized trucks. The testing for both cars was performed at the Transportation Technology Center (TTC), Pueblo, CO.

For the first car, all testing was done from June to August 1997. The vehicle response to variations in vertical alignment tests and the dynamic curving tests were conducted from July 28-29 on the Wheel Rail Mechanisms (WRM) loop. The hunting test with initial alignment defects was conducted on July 24 on the Railroad Test Track (RTT). The steady curving with spirals tests were conducted in the months of June and July on the RTT. Testing on the Precision Test Track (PTT) was done on August 1. The PTT is used for the yaw and sway, twist and roll, and pitch and bounce tests.

For the second car, the testing was done from February to March 1999. The constant curving tests on spirals and the dynamic curving tests were conducted on March 4 on the WRM loop. Testing on the PTT was done on March 5. The vehicle response to variations in vertical alignment tests were conducted from March 9-11 on the WRM.

The work reported here has been performed under the contract DTFR53-95-C-00049 from the FRA. Dr. Thomas Tsai of the FRA is the Technical Monitor. The authors wish to thank Dr. David Wormley, Dr. Fred Blader, and Mr. John Elkins for their valuable technical inputs throughout the program. The technical input from Dr. Herbert Weinstock of the Volpe Center is gratefully acknowledged.

The support of Dr. Andrew Kish of the Volpe Center in the initial development of the OMNISIM code is also acknowledged.

The authors wish to thank Mr. Steve Belport, Mr. Scott Cummings, and Ms. Huimin Wu of Transportation Technology Center, Inc. (TTCI) for the conduct of the tests. Thanks are also due to Messrs. Ken Laine and David Cackovic of TTCI for their test support.

1. INTRODUCTION

The Federal Railroad Safety Authorization Act of 1994 requires that the FRA establish regulations for minimum safety standards of conventional railroad passenger vehicles. As a part of this mission, FRA initiated the development of a methodology for vehicle dynamic safety evaluations. The methodology is described in Refs. (1,2), and requires the application of simulation tools as well as testing of vehicles under different track scenarios. Passenger rail vehicles have to operate on a variety of track geometries: tangent, curved and spirals connecting tangents to constant radius curves. The maximum levels of vertical and lateral misalignment and the maximum amount of crosslevel variation that can be safely negotiated are important in safety evaluations. Derailments occur for a variety of reasons, including track failures, equipment failures, and improper train operation. The scenarios need to be identified for investigation including vehicle transient response to vertical and lateral perturbations in the track alignment, steady-state curving, dynamic curving, and truck hunting.

The report is organized as follows. Section 2 presents the safety methodology and a brief description of the simulation program, OMNISIM. Section 3 gives a description of the rail cars and vehicle/track models used in all the tests. Section 4 provides a summary of the instrumentation. Section 5 presents the stationary testing which includes track stiffness, static suspension system characterization, rigid body modal characterization, and track and wheel profile measurements. Section 6 provides test scenarios and procedures. The summary of the results and overall conclusions of practical interest derived from the study are presented in Section 7.

The dynamic test results and correlations with simulation results are presented in the Appendices.

1.1 Objectives

The overall objective of the full-scale testing is to validate the proposed rail vehicle safety evaluation methodology through testing two different types of passenger rail vehicles under several track scenarios. The specific objectives followed in this work are:

1. Evaluate the dynamic performance of a bi-level vehicle with non-equalized trucks and a bi-level vehicle with equalized trucks under conditions of vertical track perturbations, steady curving, dynamic curving, yaw and sway, twist and roll, pitch and bounce, and hunting. Identify unsafe behavior of the car, such as wheel climb and wheel lift.

2. Characterize the parameters of vehicles and the track segments required for the OMNISIM simulation code to predict the observed response.

3. Compare the OMNISIM simulation results with the test data on lateral and vertical loads and accelerations. Evaluate the OMNISIM code capability to predict the unsafe vehicle behavior observed in the tests.

4. Identify the inadequacies, if any, in the overall safety methodology and the limitations of the code and test techniques.

2. SAFETY METHODOLOGY AND SIMULATION TOOL

2.1 Safety Methodology

Figure 1 indicates the overall methodology being pursued for vehicle safety evaluation. Tasks 1 to 4 in this figure represent determination of car and track parameters, which are inputs to the analysis. Task 5 focuses on wheel climb/wheel lift failure modes for application in the methodology. In Task 6, OMNISIM has been chosen as a candidate tool for safety evaluations. Using this tool, vehicle dynamic response and safety have been studied for several scenarios such as:

- Hunting.
- Steady curving.
- Dynamic curving.
- Gage narrowing.
- Response to individual and combined lateral and vertical track perturbations.

This report specifically addresses the evaluation of the tasks in the methodology related to measurement of vehicle and track parameters, test conduct, and correlation of the test results with computer simulation results. These are critical tasks in the overall safety methodology and require direct evaluation. In this evaluation a rail car with non-equalized trucks and a rail car with equalized trucks are considered.

2.2 Simulation Tool - OMNISIM

OMNISIM (3) has been used for the evaluation of the dynamic performance of commuter passenger rail vehicles. OMNISIM is a multi-body system simulation program, modeling both vehicle and supporting structures in a generalized manner. Each system modeled is represented as a group of bodies, each having its own inertial properties and position in space. These bodies are connected by appropriate interconnections, which may be defined as having special properties, such as suspensions or the rolling connection between the wheel and rail, or being very stiff such as metal-to-metal contact. The program can predict the behavior of the bodies in transient and steady-state response in the time domain. OMNISIM also permits the bodies to be represented as having simple flexible properties. This is useful, for example, to simplify the representation of the torsional rigidity of a vehicle body when negotiating track crosslevel variations.

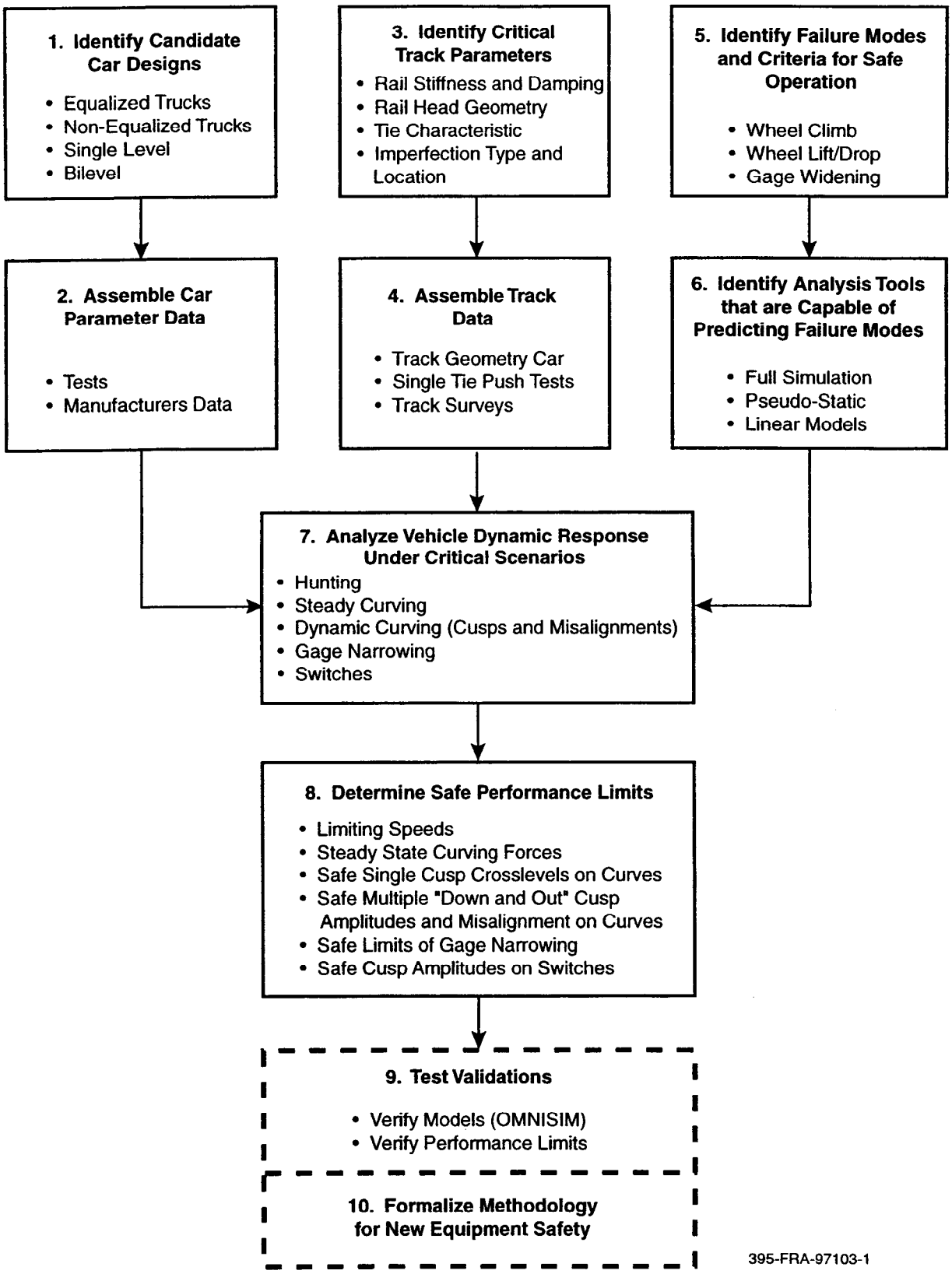

Figure 1. Overall methodology

OMNISIM can work with English or metric units and with measured or analytically constructed inputs or a combination of both. It presents a unified approach to predicting rail vehicle response to a variety of inputs, such as those from the track, actuator or wind forces. Vehicle ride quality may also be assessed. The flexible structure of the input allows the user to model any new or existing vehicle design. In addition to the main run processor, pre- and post-processing programs have also been created. Each system is defined in a text file called the definition file, using an appropriate word processor. This file is then preprocessed to the required format and units by the preprocessing program DEFINE. This program rearranges the data and the system units and permits the user to see the system in diagrammatic form, displaying its geometry and characteristics. DEFINE will also display previously pre-processed files.

Means are provided in the definition file to identify the degrees of freedom for each body required in the model. The potential choices include all translational and rotational rigid body motions and the first beamlike free-free flexible modes in twist and in vertical and lateral bending. The interaction of rigid or flexible bodies is defined through hard or soft connections (e.g., metal to metal or suspension elements). The program requires the user to define a vehicle and track system model with inertial and geometric properties, connection characteristics, wheel/rail geometry data, and displacement or force inputs.

There are a number of different types of track and vehicle interbody connections available. Their characteristics range from simple spring and damper pairs in parallel or in series to more complex friction elements. The characteristic of each spring and damper is defined using piecewise linear functions of displacement and velocity, respectively. Hysteresis requires two piecewise linear functions that represent the asymptotic loading and unloading curves. Additional information, such as that which controls the speed of closure to the asymptote in hysteresis, may also be specified.

The present wheel/rail connection assumes no roll rotation of the rail, with the vehicle and track system in the same moving coordinates. This is equivalent to a track model that generates the same behavior at the wheel as the vehicle moves down the track. Although useful in identifying rail motions, further improvements are contemplated. These will allow the rails to be modeled as a stationary continuum with a potential reduction in the number of degrees of freedom, and will release the rail support model from moving with the vehicle.

Each individual wheel/rail connection uses a look-up table representing the required variables at the point of contact between the wheel and rail so that the rolling contact forces may be calculated for the steel wheels on steel rails. The profile data tables are precomputed using a more flexible version of Law and Cooperrider's program WHRAILA (4), named PROFIT, for PROfile FIT. A four-dimensional look-up table of creep force coefficients, according to Kalker (5) and as adapted by British Rail, is used in determining the forces and moments on each wheel. The rotational speed of the wheel or axle, which may be a solid or have independently rotating wheels, is regarded as a special variable and is required to obtain the wheel/rail forces. The method assumes that the dominant changes in the wheel/rail contact geometry are those due to local relative displacement between each wheel and the rail to which it is connected.

The inputs to the system under study may be measured or analytically constructed in segments using several optional functions. Those representative of laboratory simulation, generally as a function of time, can be formed in the input text file that is read directly by the stepping processor at commencement. A swept frequency sine wave allows vibration testing of a stationary vehicle. However, at the option of the user, the input file may request some or all of the data from a file of either measured or analytically defined histories, formed using the preprocessor called INFORM. This may be filtered and is formatted as digital information in steps along a chosen path or track. If measured data is to be used, it is called into INFORM, from a measured track geometry file. INFORM uses a text setup file to identify the source and preprocess the path and input data that may be of mixed measured and analytic origins.

The short wavelength inputs are regarded as local perturbations, and are introduced as variations in lateral or vertical position of the rails or guideway. For the analytically defined inputs, a repeated shape and amplitude for a segment of the rail may be chosen from a combination of cusps, bends, or sine waves. The long wavelength variations define the overall path and are linearly interpolated from positions along the track at which curvature and superelevation are either chosen analytically or taken from the measured data set. These are transformed into components of the connection strokes, so that the degrees of freedom for each body remain those relative to its local inertial coordinate system. Provision is made to allow both external displacement and forcing inputs to the model. Rail perturbations are an example of displacement inputs; whereas coupler loads due to train action is an example of a forcing input.

For post-processing, PLOTS produces graphs of the output for monitor display or for hardcopy output. TEXTS produces numerical information for viewing or passing to other post-processors, such as a spreadsheet, for further manipulation. Much of the work in this report was postprocessed using a spreadsheet program.

3. DESCRIPTION OF VEHICLES AND MODELS

3.1 The Test Vehicles

The vehicles used for testing are modern bi-level passenger cars. The first has non-equalized trucks while the second has equalized trucks.

3.1.1 Vehicle with Non-Equalized Trucks

The vehicle with non-equalized trucks has an axle load of 34 kips. It uses an H truck frame and bolster with outside journal bearings. A schematic of a generic non-equalized truck is shown in Figure 2. The frame is welded steel and consists of two box sections for the side beams and two circular sections for the lateral beams. The truck bolster is a welded box structure that is

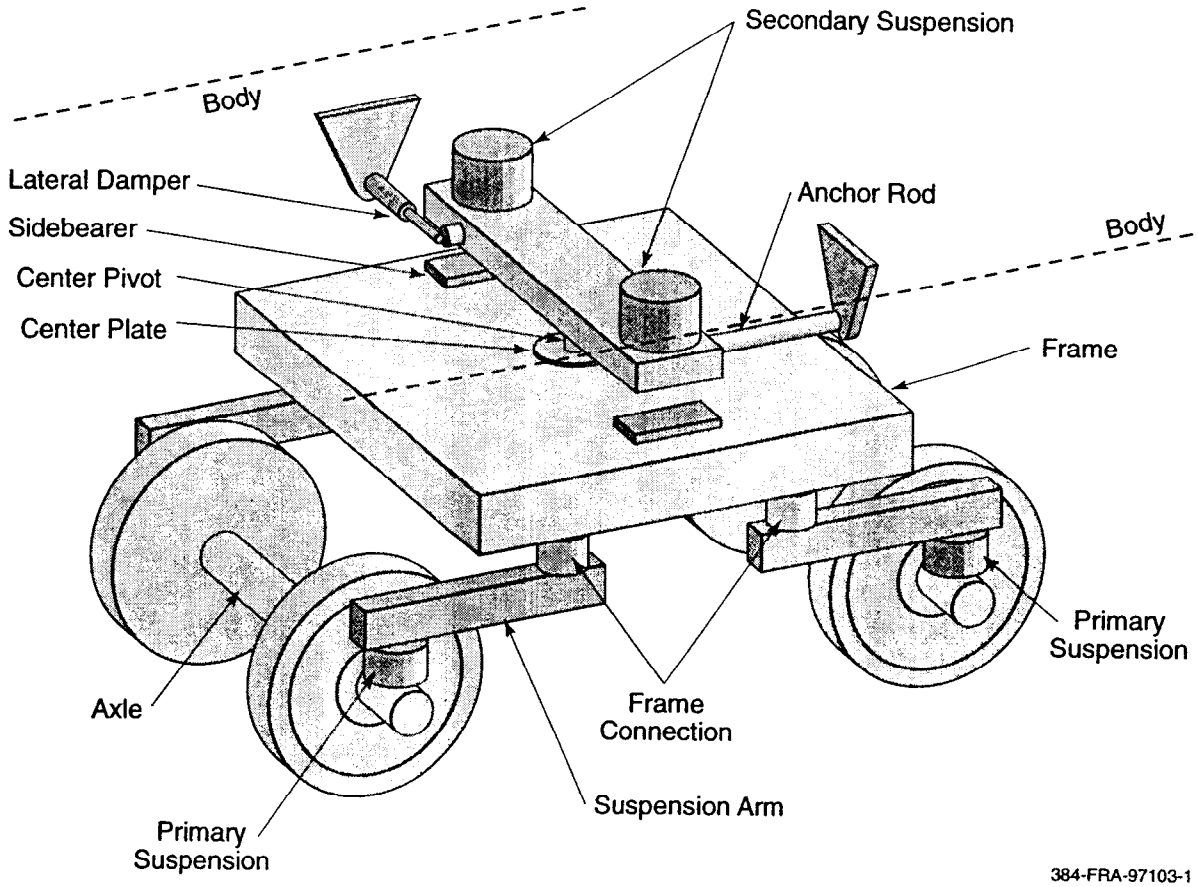

Figure 2. Schematic of non-equalized truck

also used as an auxiliary air supply for the air springs. A center pivot provides the interface between the frame and truck bolster with a nylon bushing.

A radius arm between the truck frame and the journal bearing provides wheelset guidance. The primary suspension is a set of steel coil springs supported on the journal bearing through a rubber pad.

The vehicle uses an air bag secondary suspension. An air spring with a back-up rubber spring is used as an emergency if air is lost. There are stops to limit both vertical and lateral movement. The lateral stops are on the truck bolster and the vertical stops are between the carbody and truck bolsters. Rotary dampers provide damping in the lateral and vertical directions and are connected between the truck bolster and carbody.

3.1.2 Vehicle with Equalized Trucks

The vehicle with equalized trucks has an axle load of 39.7 kips. It uses a rigid H truck frame and bolster with outside journal bearings. A schematic of a generic equalized truck is shown in Figure 3. The frame is cast steel with a center hole and side bearing to accommodate the truck bolster. The truck bolster is a welded structure with a center pin arrangement.

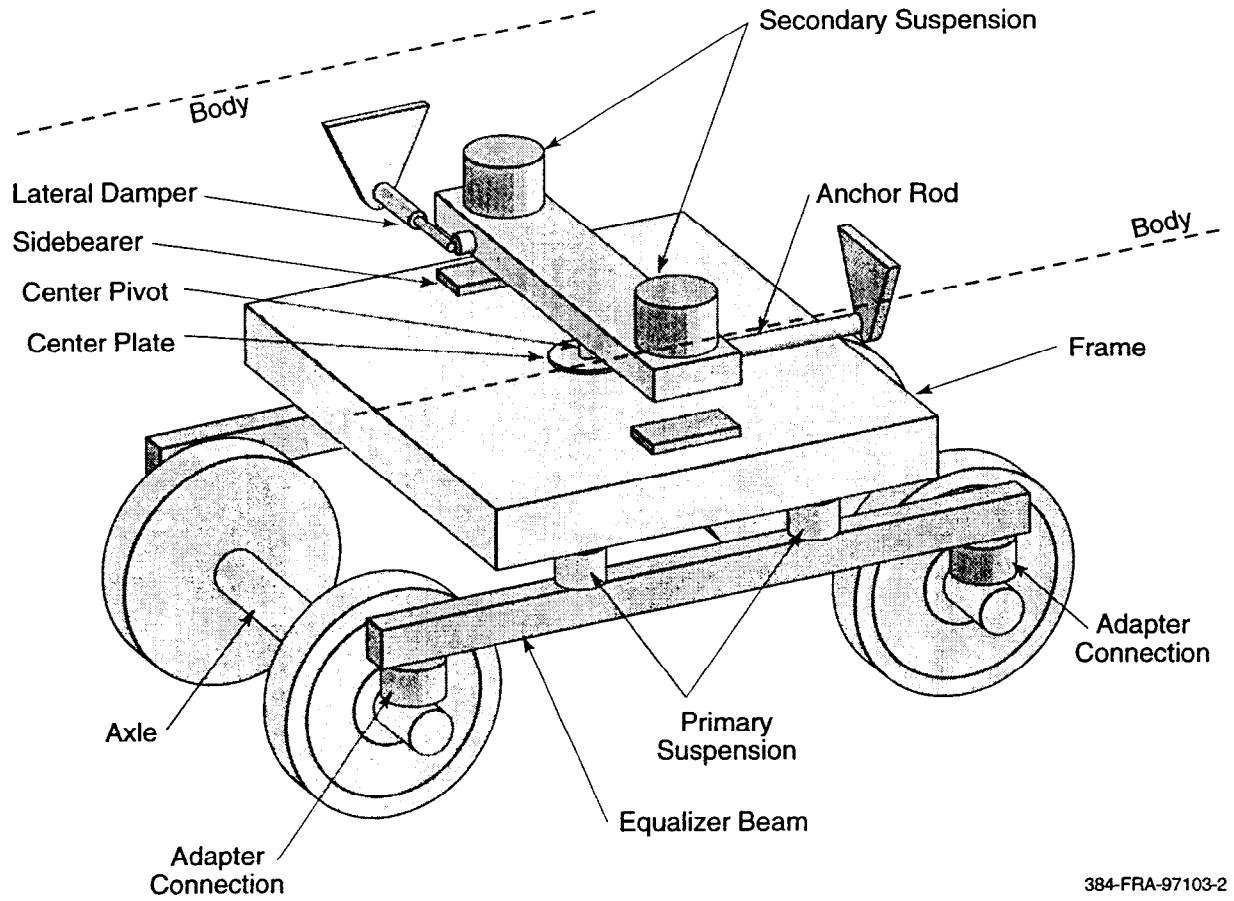

Figure 3. Schematic of equalized truck

The pedestal guides provide wheelset guidance for the journal bearing housings. The primary suspension is a pair of steel coil springs supported between each equalizer beam and side of the truck frame. The pedestal guides provide lateral and longitudinal wheelset restraint.

The vehicle uses two coil spring packs for the secondary suspension. The coil springs are between the truck bolster and the underframe of the car. There is a lateral damper and a vertical damper connected between the end of the truck bolster and the carbody for a total of four per truck.

3.2 The Vehicle Models

Each vehicle is represented by a multi-body model consisting of springs, dampers and masses that represent the carbody, primary and secondary suspensions, trucks, axles, and wheels. The track structure is also represented with springs, dampers and masses. These parameters are identified on the basis of manufacturer's data or measured by testing as explained in Section 4.

Each carbody is represented with lateral, vertical, pitch, yaw, roll, torsional and bending degrees of freedom (DOF). The suspension between the carbody is represented with longitudinal, lateral, and vertical DOF. The truck is represented with longitudinal, lateral, vertical, pitch, yaw and roll DOF. The primary suspension between the truck and axle is represented with longitudinal, lateral, and vertical DOF. Each wheelset has longitudinal, vertical, lateral, pitch and roll DOF. The wheel-rail contact model uses the Kalker formulation. The model parameters are summarized in Tables 1 and 2 for the vehicle with non-equalized trucks and the vehicle with equalized trucks, respectively. These parameters are assembled from the manufacturer's data and from car characterization tests as discussed in Section 5.

Table 1. Car physical characteristics (non-equalized trucks)

Unit	Parameter Description	Value
lb-s^2/in.	Carbody mass	257.91
lb-s^2/in.	Truck bolster mass	5.24
lb-s^2/in.	Truck frame mass	15.86
lb-s^2/in.	Wheelset mass	11.33
in.	Truck wheelbase	102
in.	Truck center spacing	714
in.	Wheel radius	18
in.	Carbody center of gravity from top of rail	84.80
in.	Bolster center of gravity from top of rail	30.21
in.	Truck frame center of gravity from top of rail	23.40
in.	Wheelset center of gravity from top of rail	18.00
in.	Transverse secondary spring spacing	79.02
in.	Transverse secondary damper spacing	107.01
in.	Transverse bolster anchor rod spacing	107.01
in.	Transverse wear plate spacing	45.67
in.	Transverse primary spring spacing	79.02
in.	Center of air spring height from top of rail	40.04
in.	Center of lateral damper height from top of rail	33.10
in.	Center of bolster anchor rod height from top of rail	20.95
lb-s^2-in.	Carbody roll moment of inertia	9.89E+05
lb-s^2-in.	Carbody pitch moment of inertia	2.70E+07
lb-s^2-in.	Carbody yaw moment of inertia	2.70E+07
lb-s^2-in.	Truck bolster roll moment of inertia	5.98E+03
lb-s^2-in.	Truck bolster pitch moment of inertia	2.21E+02
lb-s^2-in.	Truck bolster yaw moment of inertia	5.78E+03
lb-s^2-in.	Truck frame roll moment of inertia	1.31E+04
lb-s^2-in.	Truck frame pitch moment of inertia	1.56E+04
lb-s^2-in.	Truck frame yaw moment of inertia	2.83E+04
lb-s^2-in.	Wheelset roll moment of inertia	8.03E+03
lb-s^2-in.	Wheelset pitch moment of inertia	1.49E+03
lb-s^2-in.	Wheelset yaw moment of inertia	8.03E+03
lb/in.	Primary longitudinal stiffness (per wheel)	5.60E+04
lb/in.	Primary lateral stiffness (per wheel)	4.20E+04
lb/in.	Primary vertical stiffness (per wheel)	4.49E+03
lb/in.	Secondary suspension lateral stiffness (per spingset)	1.29E+03
lb/in.	Secondary suspension vertical stiffness (per spingset)	3.82E+03
lb-s/in.	Secondary lateral damping (per truck)	5.60E+02
lb-s/in.	Secondary vertical damping (per truck)	2.80E+02

Table 2. Car physical characteristics (equalized trucks)

Unit	Parameter Description	Value
lb-s^2/in.	Carbody mass	302
lb-s^2/in.	Truck bolster mass	5.18
lb-s^2/in.	Truck frame mass	12.69
lb-s^2/in.	Equalizer beam mass	1.10
lb-s^2/in.	Wheelset mass	11
in.	Truck wheelbase	102
in.	Truck center spacing	714
in.	Wheel radius	18
in.	Carbody center of gravity from top of rail	88.9
in.	Bolster center of gravity from top of rail	26.5
in.	Truck frame center of gravity from top of rail	27.89
in.	Equalizer beam center of gravity from top of rail	14.84
in.	Wheelset center of gravity from top of rail	18
in.	Transverse secondary spring spacing	86.04
in.	Transverse secondary damper spacing	107.04
in.	Transverse bolster anchor rod spacing	107.04
in.	Transverse primary spring spacing	86.04
in.	Center of bolster anchor rod height from top of rail	18.96
lb-s^2-in.	Carbody roll moment of inertia	1.40E+06
lb-s^2-in.	Carbody pitch moment of inertia	3.28E+07
lb-s^2-in.	Carbody yaw moment of inertia	3.28E+07
lb-s^2-in.	Truck bolster roll moment of inertia	4.40E+03
lb-s^2-in.	Truck bolster pitch moment of inertia	2.49E+02
lb-s^2-in.	Truck bolster yaw moment of inertia	4.54E+03
lb-s^2-in.	Truck frame roll moment of inertia	1.35E+04
lb-s^2-in.	Truck frame pitch moment of inertia	1.12E+04
lb-s^2-in.	Truck frame yaw moment of inertia	2.38E+04
lb-s^2-in.	Wheelset roll moment of inertia	8.33E+03
lb-s^2-in.	Wheelset pitch moment of inertia	1.16E+02
lb-s^2-in.	Wheelset yaw moment of inertia	8.33E+03
lb/in.	Primary longitudinal stiffness (per wheel)	6.45E+03
lb/in.	Primary lateral stiffness (per wheel)	6.45E+03
lb/in.	Primary vertical stiffness (per wheel)	1.00E+04
lb/in.	Secondary suspension lateral stiffness (per spingset)	4.91E+03
lb/in.	Secondary suspension vertical stiffness (per spingset)	4.13E+03
lb-s/in.	Secondary lateral damping (per truck)	5.60E+02
lb-s/in.	Secondary vertical damping (per truck)	2.85E+02

4. INSTRUMENTATION

4.1 Data Acquisition System

The following list is a general description of the data acquisition system used during the static and dynamic tests:

1. TTC Instrumentation railcar (T-5).
2. IBM RS 6000 Computer.
3. HP Printer.
4. I/O-tech 16 Channel A/D Converter.
5. Instrum Signal Conditioners.
6. Ten-x Optical Storage Drive.
7. TTCI Digital Data Acquisition and Analysis Software.
8. IBM Linux Data Analysis Computer.
9. Rail /Wheel Profilometer.

Table 3 shows a list of the measurements for this test program. Channel 0 was used for the train speed and Channel 1 for the automatic detection locator of the instrumentation car. Channels 2 through 17 were used for the static tests and 18 through 39 were added for the dynamic tests for the specific parameters indicated in the table.

4.2 Data Reduction

4.2.1 Recording Techniques

All measurements were recorded digitally at a rate of 500 samples per second using a four pole Bessel analog filter and a low-pass cutoff of 30 Hz.

4.2.2 Data Analysis

Data analysis consisted of individual channel time histories and statistics plotted after each test run. In addition, a data analysis routine was pre-programmed using P-V Wave software to perform typical data analysis during testing. This analysis was used to quantify measured data regarding the safe operating criteria of the vehicle. Dynamic instability and the generation of excessive forces in curves were also analyzed.

Table 3. Static and dynamic test instrumentation list

Channel	Name	Description	Range
0	TSPD	Train speed	0 to 100 mph
1	ALD	Automatic Location Detector - Instr Car	0 to 10V
2	VFL	Vertical Load Left Side	10 kips
3	VFR	Vertical Load Right Side	10 kips
4	SD1	Secondary Suspension Displacement	0 to 10 in.
5	SD2	Secondary Suspension Displacement	0 to 10 in.
6	PD1	Primary Suspension Displacement	0 to 10 in.
7	PD2	Primary Suspension Displacement	0 to 10 in.
8	PD3	Primary Suspension Displacement	0 to 10 in.
9	PD4	Primary Suspension Displacement	0 to 10 in.
10	CBY	Carbody b-end lateral acceleration	0 to 5g
11	CBZ	Carbody b-end vertical acceleration	0 to 5g
12	CTY	Carbody top lateral acceleration	0 to 5g
13	CTZ	Carbody top vertical acceleration	0 to 5g
14	CBY	Carbody bottom lateral acceleration	0 to 5g
15	CBZ	Carbody bottom vertical acceleration	0 to 5g
16	CAY	Carbody a-end lateral acceleration	0 to 5g
17	CAZ	Carbody a-end vertical acceleration	0 to 5g
18	V1L	Axle 1 Vertical Force Left	0 to 25 kips
19	L1L	Axle 1 Lateral Force Left	0 to 12.5 kips
20	LV1L	Axle 1 L/V Ratio Left	0 to 1
21	V1R	Axle 1 Vertical Force Right	0 to 25 kips
22	L1R	Axle 1 Lateral Force Right	0 to 12.5 kips
23	LV1R	Axle 1 L/V Ratio Right	0 to 1
24	V2L	Axle 2 Vertical Force Left	0 to 25 kips
25	L2L	Axle 2 Lateral Force Left	0 to 12.5 kips
26	LV2L	Axle 2 L/V Ratio Left	0 to 1
27	V2R	Axle 2 Vertical Force Right	0 to 25 kips
28	L2R	Axle 2 Lateral Force Right	0 to 12.5 kips
29	LV2R	Axle 2 L/V Ratio Right	0 to 1
30	SPARE		
31	SPARE		

4.3 Instrumented Wheelsets

The TTCI instrumented wheelsets (IWS) are multi-axial, multi-load-point load cells capable of measuring vertical, lateral, and longitudinal wheel/rail contact forces across the range of the wheel tread and flange. These wheelsets make use of many strain gage based Wheatstone bridge circuits laid out on the wheel plate and axle. Finite element modeling is first used to identify areas of high strain under specific load cases. The gages are then laid on the wheel set in a manner that optimizes sensitivity while keeping cross talk to a minimum. An example of cross talk is any output due to lateral force in a circuit intended to measure vertical force.

Calibration of the IWS is performed on a specially designed loading fixture. This highly accurate method of calibration combined with exact strain gage placement allows the IWS to maintain the following specifications:

- Vertical wheel load measurements are with ±5 percent or 250 lb (whichever is greater) of the actual vertical load.

- Lateral wheel load measurements are within ±5 percent or 100 lb (whichever is greater) of the actual lateral load.

5. PARAMETER CHARACTERIZATION

To construct the models, input data describing the car and track characteristics are required in the simulation runs. The data collected included:

- Track lateral and vertical stiffness.
- Vehicle static suspension characterization.
- Vehicle rigid body modal characterization.
- Track and wheel profile measurements.

5.1 Track Lateral and Vertical Stiffness

The lateral resistance of the ties was measured using the Single Tie Push Test (STPT) fixtures for wood and concrete ties. The measurements were made on the test tracks in various locations. The vertical track stiffness was also measured at various locations along the test track. The lateral resistance and vertical stiffness are used in the OMNISIM vehicle/track model.

5.2 Static Suspension System Characterization

The purpose of this test was to measure the load-displacement characteristics for the primary and secondary suspensions. Load measuring instrumented rails combined with displacement transducers were used to obtain stiffness data (force versus displacement) for each suspension element. The method typically used to measure the vertical suspension characteristics is shown in Figure 4, where the carbody is unloaded and deflections are measured on the primary and secondary suspension elements. Unloading of the wheels was achieved using pneumatic floor jacks and overhead cranes. Load cells mounted in-line with the applied force, and displacement transducers mounted across each suspension element will be used to obtain stiffness data (force versus displacement). Prior to the execution of the truck characterization tests, all dampers (vertical and lateral) were removed from both trucks. Additional truck modifications were also required to secure movement of the spring plank on the truck under test. The physical characteristics are as shown in Tables 1 and 2.

5.3 Rigid Body Modal Characteristics

The modal characterization tests were conducted to obtain rigid body modal frequencies and damping for each dynamic vehicle mode. Excitation for all modes was performed manually at selected locations, collecting data from strategically placed accelerometers. Carbody mass moments of inertia and the center of gravity height were calculated using the measured natural frequencies and a parameter identification algorithm.

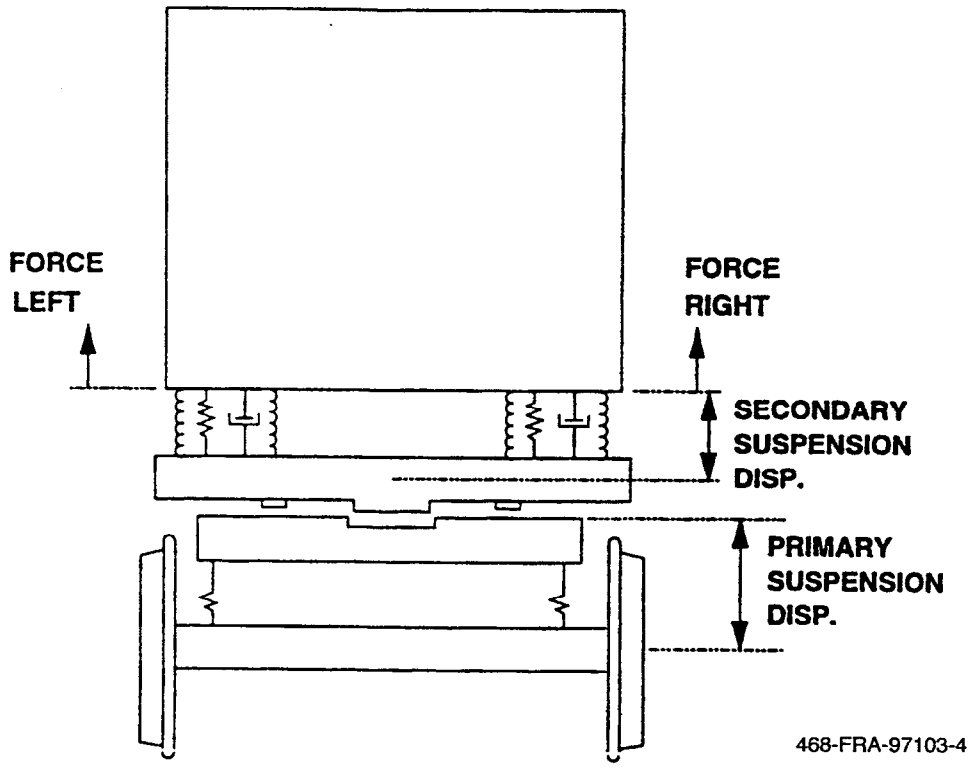

Figure 4. Vertical suspension characterization test

These values are used in the OMNISIM vehicle model. The primary dynamic modes of vibration tested are shown in Figure 5. By exciting the carbody at selected locations, these vibration modes were generated and the frequency response was measured. The damping coefficients are evaluated by measuring the hysteresis of force-versus-displacement plots for each suspension element. The measured values of frequency for the rigid body modes are summarized in Table 4. The calculated frequencies from the manufacturer's data on the non-equalized truck car are also shown. The agreement between the test and manufacturer's data seems to be reasonable.

5.4 Track and Wheel Profile Measurements

For accurate inputs to OMNISIM, representative wheel and rail profiles were recorded using a portable profilometer.

The wheel profilometer was magnetically attached to the wheel while a digitization probe rolls over the wheel surface. Data was obtained using a notebook PC for graphical display and data processing for modeling requirements. Wheel profile processing also included measurements of wheel diameter. Rail profile measurements were obtained using similar instrumentation. Each rail was measured with reference to the opposite rail for measurements of relative cant and gage. The rolling radius difference versus the wheelset lateral displacement for

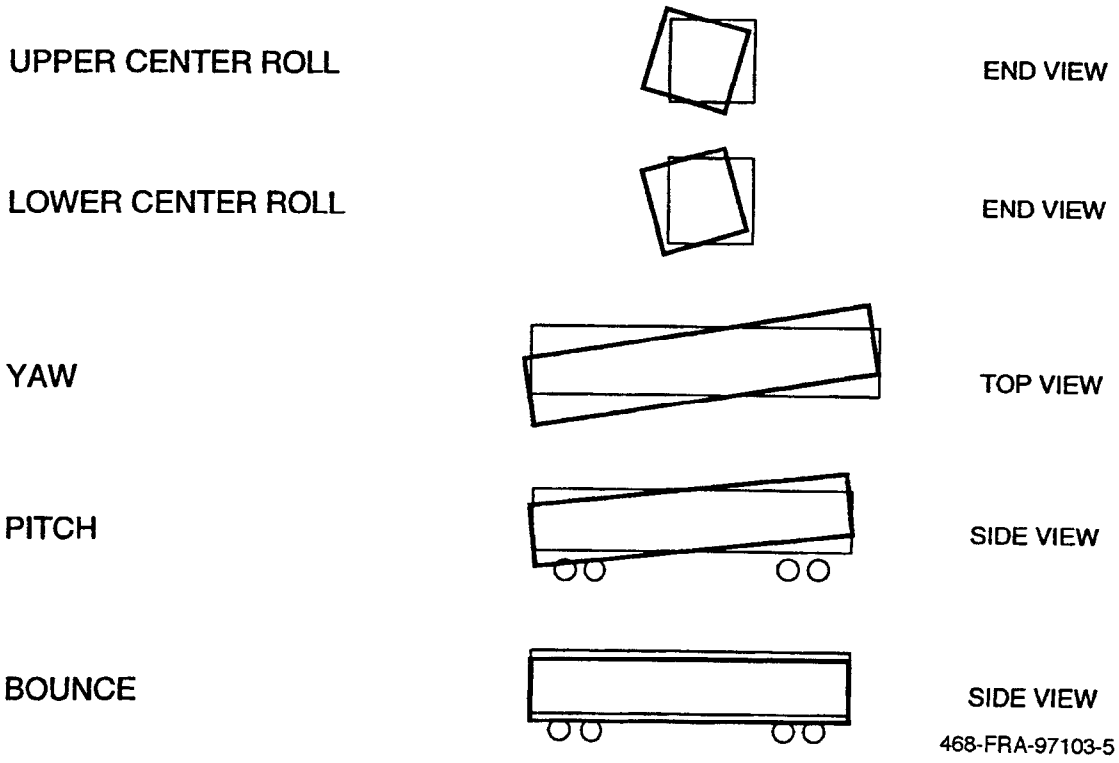

Figure 5. Rigid body modes

the vehicle with non-equalized trucks is shown in Figure 6. For the vehicle with equalized trucks, the instrumented wheelset (see Figure 7) differed from the non-instrumented wheelset (see Figure 8), therefore different wheel/rail profiles were used for the wheelsets. A rail tribometer was also used to measure the rail coefficient of friction.

Table 4. Rigid body modal characterization

Mode	Frequency (Hz)	
	Non-Equalized Trucks	Equalized Trucks
Bounce	1.17 (1.03)	1.17
Lower Center Roll	0.40	0.49
Upper Center Roll	1.25	1.22
Pitch	1.17 (1.03)	1.27
Yaw	1.08 (1.05)	0.98

Note:
Numbers in parentheses represent calculated frequencies from the manufacturer's data. No manufacturer's data was available for the equalized truck car.

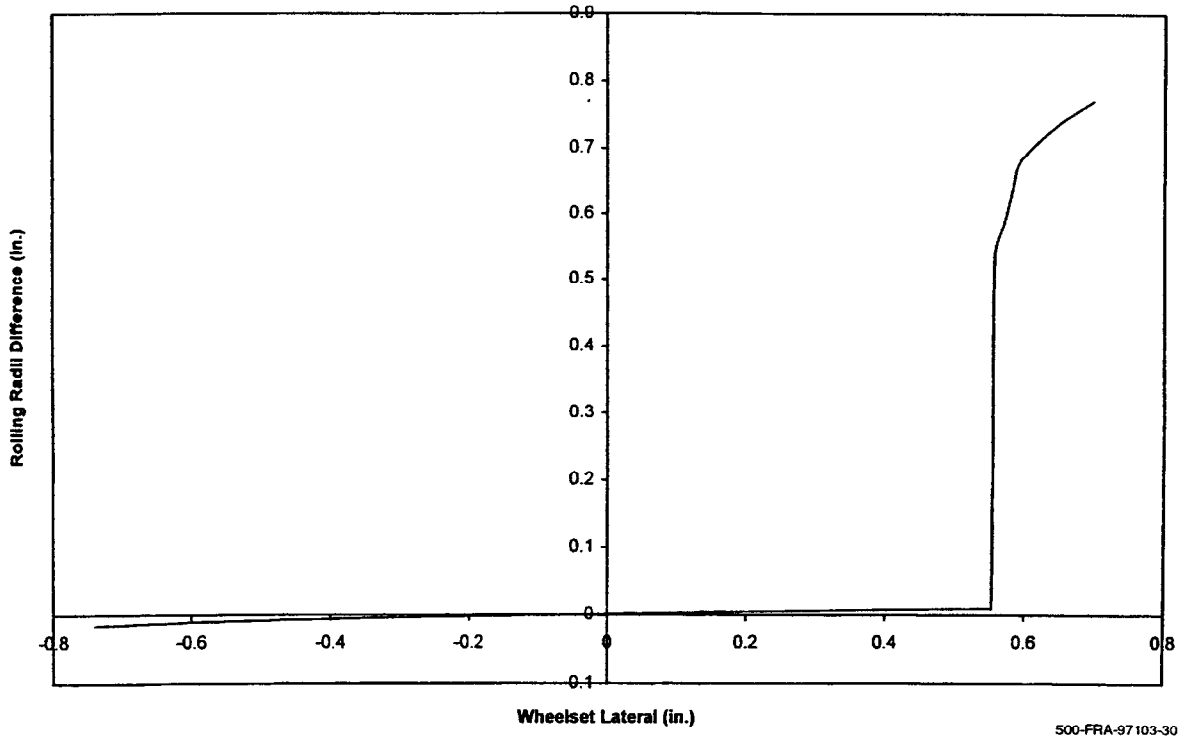

Figure 6. Rolling radius difference (non-equalized trucks)

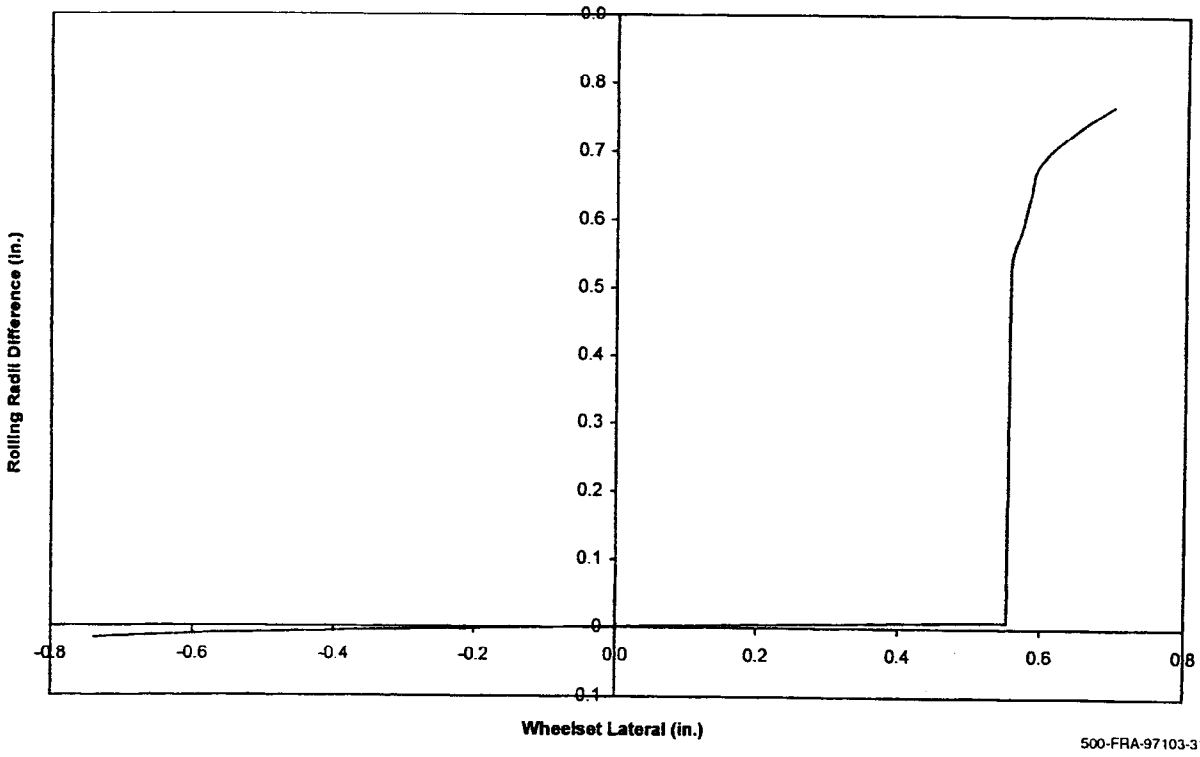

Figure 7. Rolling radius difference (instrumented wheelset, equalized trucks)

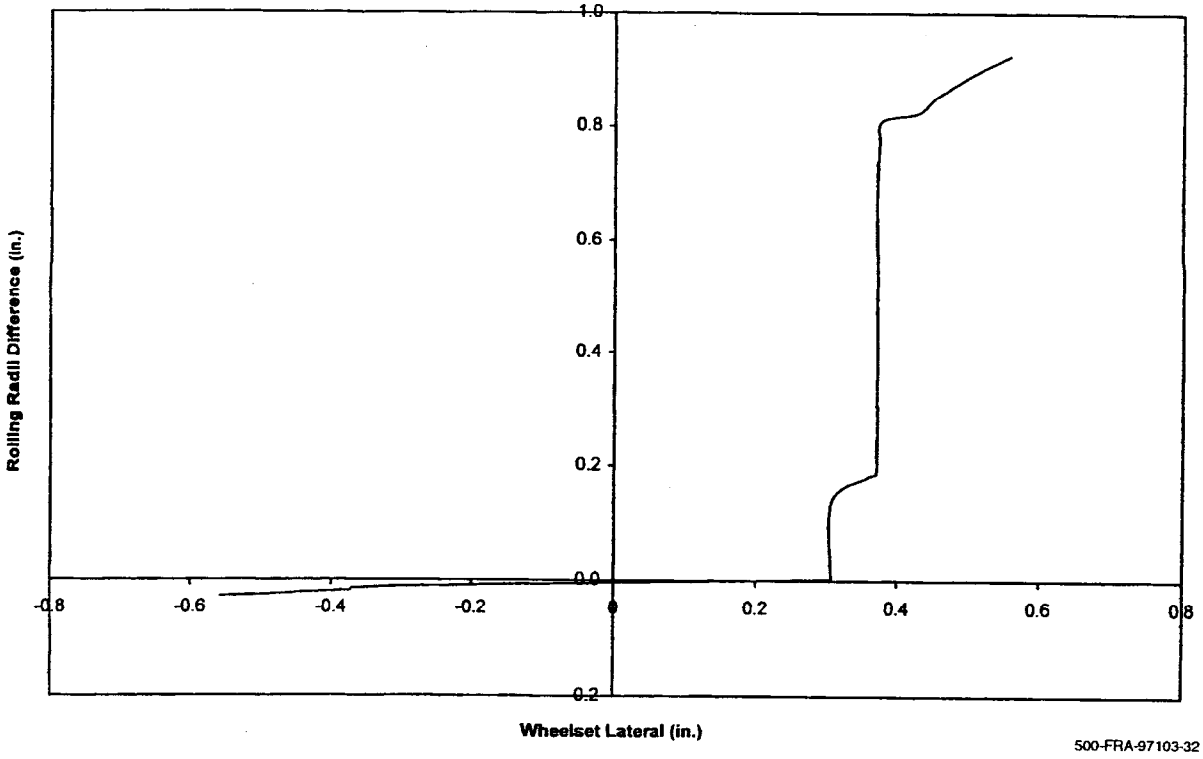

Figure 8. Rolling radius difference (non-instrumented wheelset, equalized trucks)

6. TEST SCENARIOS AND PROCEDURES

The dynamic tests discussed in the following sections were performed on various test tracks located at TTC. The track configurations are shown in Figure 9. Simulations were run using the computer program OMNISIM on a Pentium PC. The track scenarios were modeled and the program was exercised to produce lateral and vertical forces. Time history plots were developed for the simulation and compared to time histories of the test data. Comparisons were made for the maximum lateral force and the minimum vertical force. These were chosen because the maximum lateral force coupled with the minimum vertical force produce the largest L/V ratio. Also maximum carbody lateral acceleration was calculated for the range of test speeds.

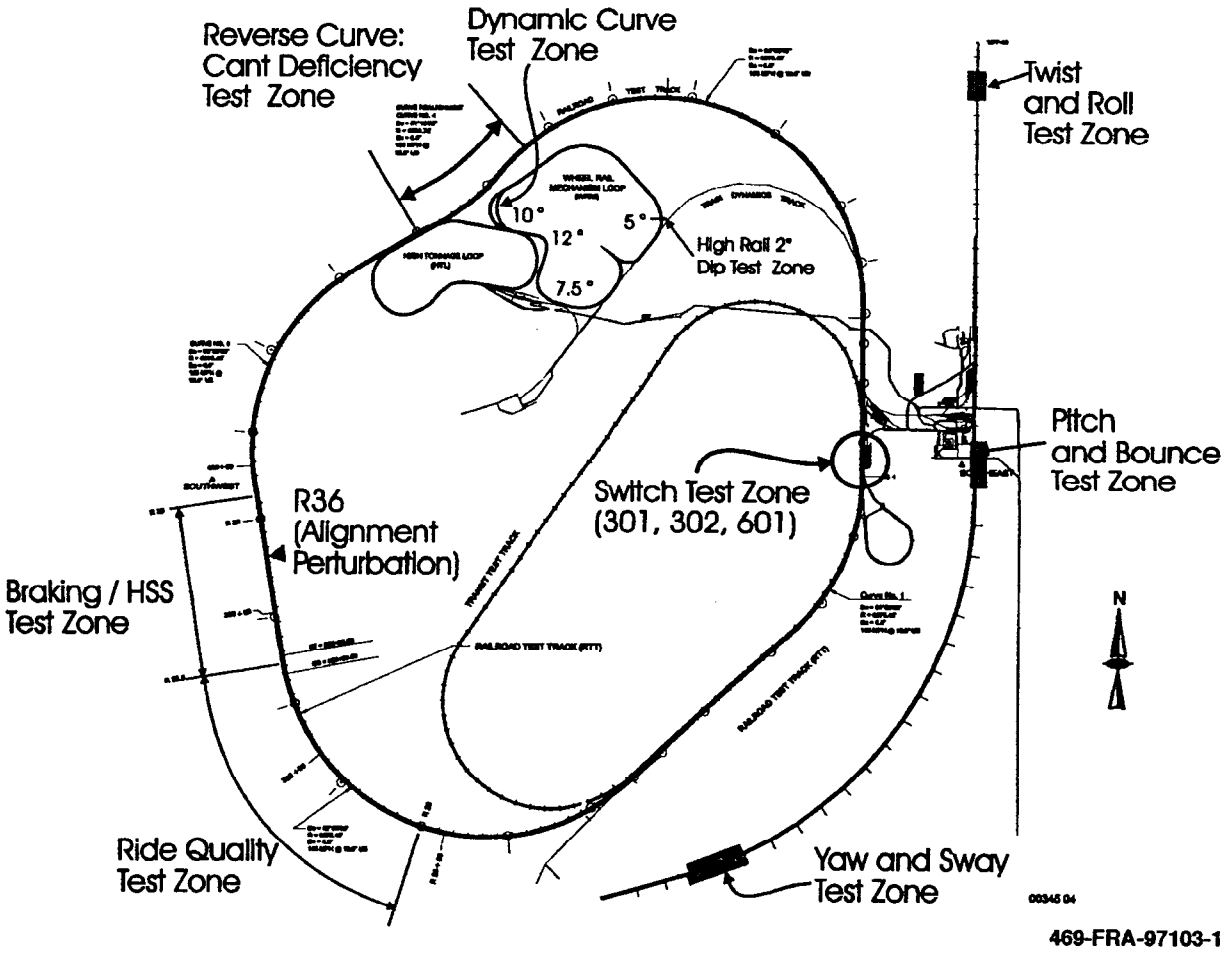

Figure 9. TTC test tracks

6.1 Dynamic Test Scenarios (Vehicle with Non-Equalized Trucks)

The car tested was the cab car in a three car consist. The car was tested in both pull and push modes. When the car was pulled the instrumented wheelset was trailing and conversely when the test car was pushed the instrumented wheelset was leading. Data including wheel vertical and lateral forces were measured on each of the two AAR instrumented wheelsets.

6.1.1 Vehicle Response to Variations in Vertical Alignment

Tests with variations in curved track vertical alignment were conducted to measure the capability of the car to operate safely in low speed curves at permissible speeds and to predict the potential of wheel lift. This test is also referred to as the vertical dip test. Test runs were performed on the 5 deg portion of the Wheel Rail Mechanisms (WRM) loop. The 5 deg curve has a 20 mph balance speed and has concrete ties on granite ballast. A vertical perturbation of 2 in. on the outer rail was installed on the track. Figure 10 shows the vertical dip that was installed in the 5 deg curve. The test was run for a range of speeds (5 to 22 mph) in forward and reverse directions. A video camera was also deployed on the carbody focussing on the primary suspension to capture its movement under potential wheel lift situations.

6.1.2 Steady Curving with Spirals

Steady curving tests were conducted to measure the test car capability to operate safely on high speed curves. The test consist was operated at speeds from the balance speed up to an

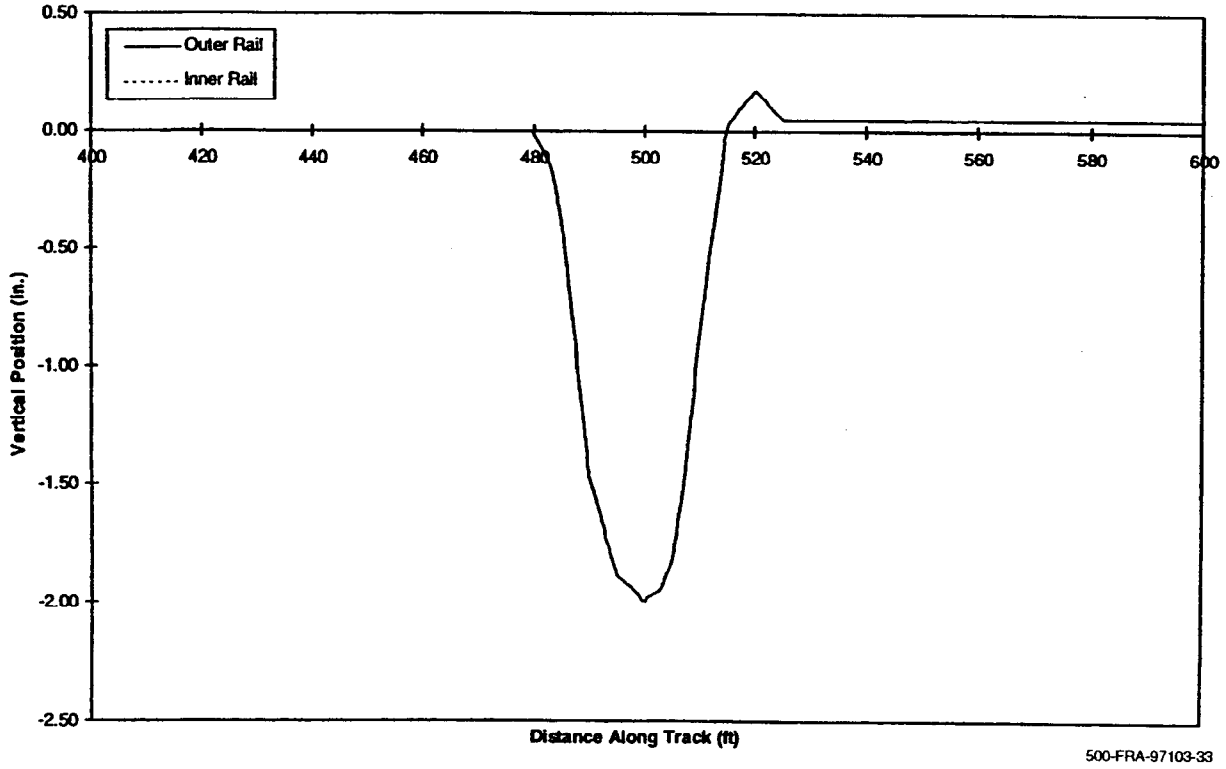

Figure 10. Vertical dip in the 5 deg curve

unbalanced (cant deficiency) condition of ~7 in. Unbalance is defined as the additional height in inches, which if added to the rail in a curve at a certain car speed would provide a single resultant force, (combined effect of weight and centrifugal force on the car) in a direction perpendicular to the plane of the track. A constant 1 deg 15 min reverse curve with 6 in. superelevation, on the Railroad Test Track (RTT) was used for all tests. Test runs were performed over Class 5 through 6 track, at speeds of 84 mph (balance speed) to 124 mph (~7 in. unbalance) on the RTT. The tracks have AREA 136 rail and wood ties with cut spike construction on slag ballast.

6.1.3 Dynamic Curving

The test for dynamic curving was designed to evaluate safety of the car as it negotiates combinations of vertical profile irregularities and crosslevel in jointed tracks. The resulting forces between the wheel and rail should have an adequate margin of safety against any tendency of the wheel to climb. The 10 deg curved track for dynamic curving consists of five staggered vertical perturbations over a wavelength of 39 ft, with a crosslevel of 0.5 in. (see Figure 11). The latter was achieved by appropriately shimming the rails, which also creates combined gage and alignment variations. The maximum gage of 57.5 in. corresponds to the low points of the outer rail. The minimum gage of 56.5 in. corresponds to the low points on the inner rail. This is shown in Figure 12. The tests were performed at speeds in the range of 10 to 32 mph.

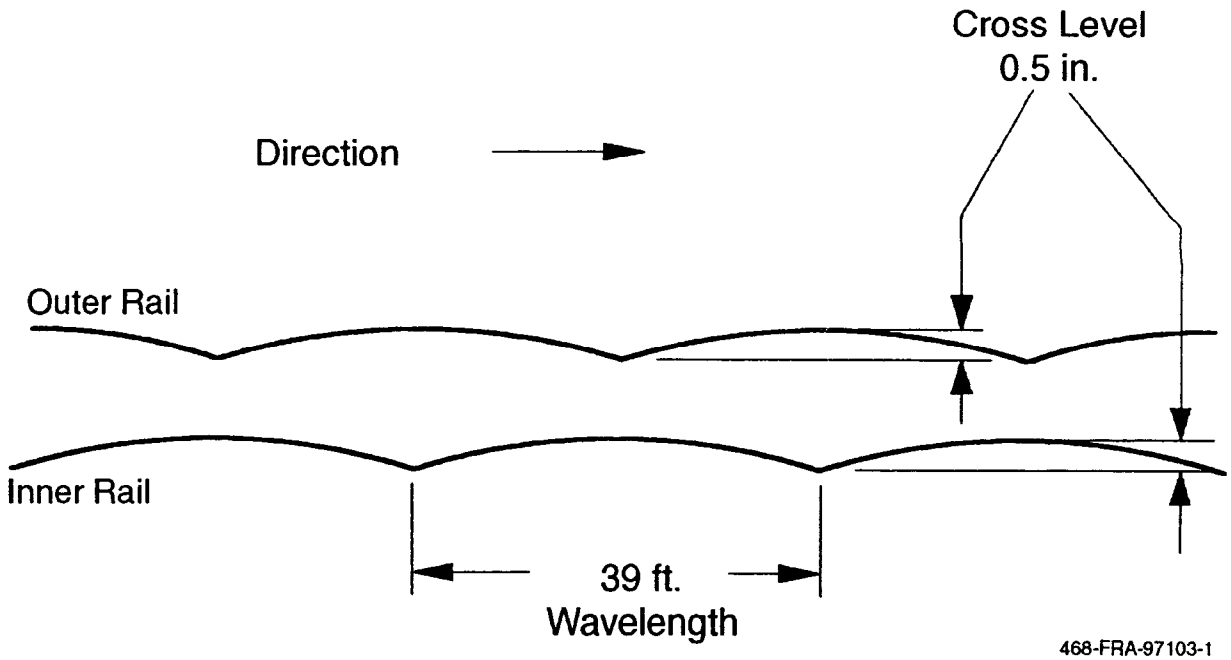

Figure 11. Crosslevel variation for dynamic curving

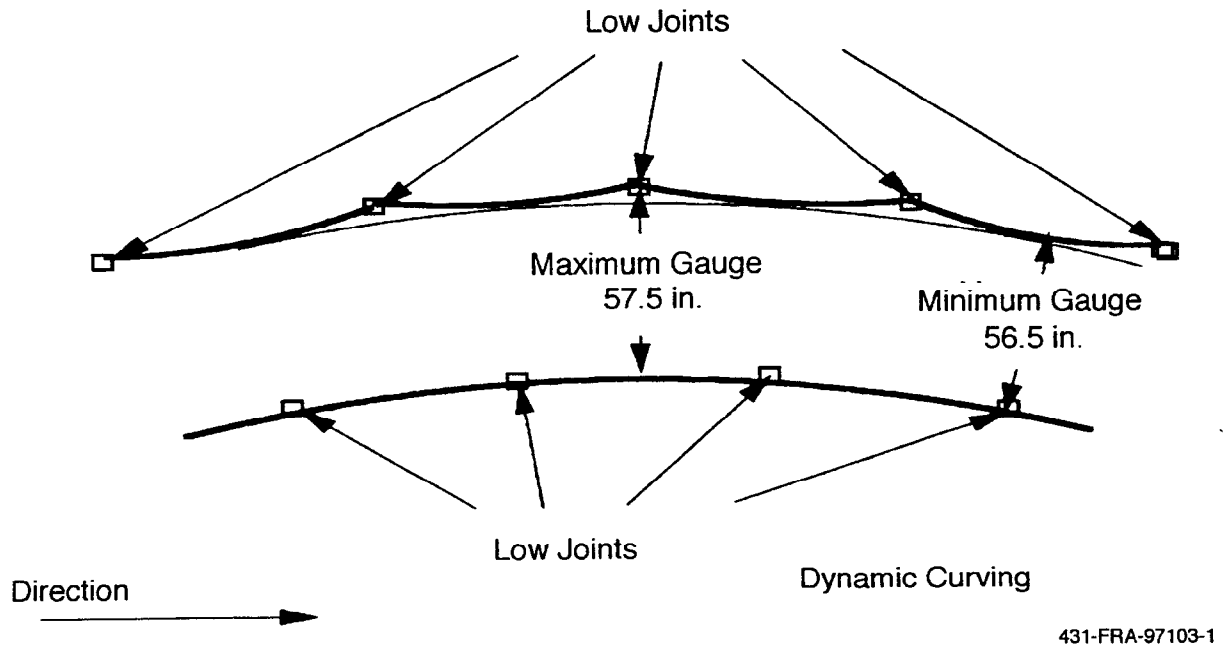

Figure 12. Gage and alignment variation for dynamic curving

6.1.4 Yaw and Sway

This test was designed to evaluate vehicle safety in its negotiation of track perturbations that generate yaw and sway oscillations. The resulting forces between the wheel and rail should have an adequate margin of safety against any tendency for the car to derail. The car was excited by a symmetric, sinusoidal track alignment deviation with a wavelength of 39 ft on tangent track. Each simulation included 5 parallel, lateral perturbations with a sinusoidal double amplitude of 1.25 in. peak to peak on both rails and a constant wide gage (see Figure 13). The tests were performed at speeds in the range of 15 to 90 mph, with the intent to capture the resonant speed.

6.1.5 Twist and Roll

Successive crosslevel excitation of cars may lead to large car roll and twist amplitudes, which should be limited for car safety assurance. The analyses and tests are required to evaluate the margin of safety against derailment. The test and simulation track sections included 10 vertical perturbations 39 ft apart, staggered each with an amplitude of 0.75 in. (see Figure 14). The cusp shaped perturbations were located on each rail to generate the lower and upper roll and twist resonance modes. The tests were performed at speeds in the range of 10 to 70 mph.

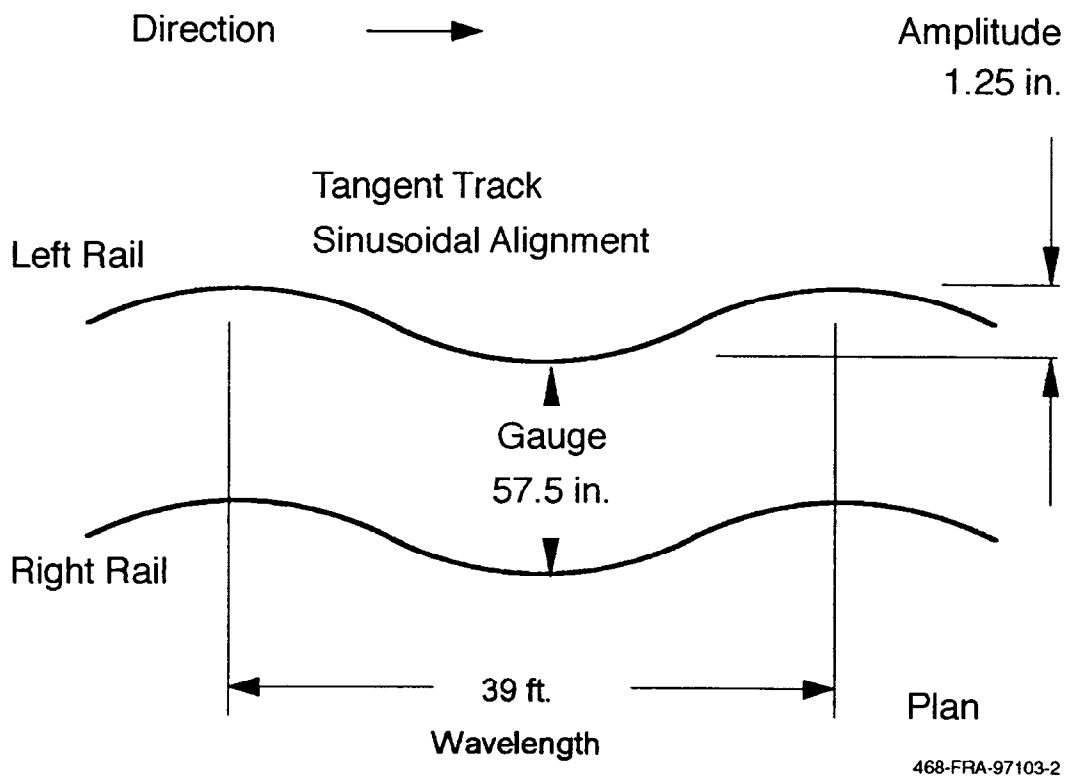

Figure 13. Track alignment variation for yaw and sway

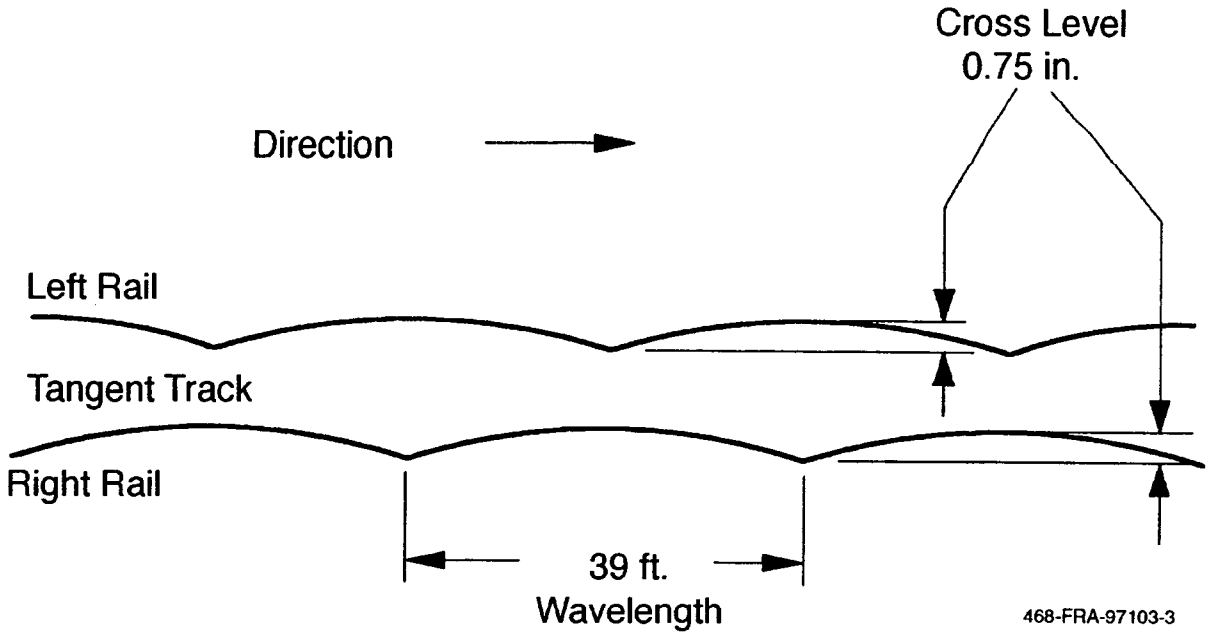

Figure 14. Crosslevel variation for twist and roll

6.1.6 Pitch and Bounce

This test was designed to evaluate the car safety as it negotiates track perturbations which generate pitch and bounce oscillations. An example is a track constructed with parallel joints and/or track structure with changes in the vertical track stiffness. The analyses and tests show the margin of safety in the wheel-rail forces against any tendency for the car to derail. The track included 10 parallel, vertical perturbations, 39 ft apart, with amplitude of 0.75 in. (see Figure 15). The tests were performed at speeds in the range of 10 to 70 mph, ensuring the capture of the resonant speed.

6.1.7 Hunting Test with Initial Alignment Defects

The hunting test was conducted to provide information on lateral vehicle stability at various operating speeds on tangent track. Tests were conducted on the Railroad Test Track (RTT) during dry conditions while recording carbody accelerations and wheel/rail forces. The tests were performed at speeds in the range of 80 to 130 mph. The test vehicle was operated over the test track through a single lateral perturbation of 9/16 in. with a 22 ft wavelength to initiate a lateral dynamic response. The installed lateral perturbation is equal on both rails and is shown in Figure 16.

6.2 Dynamic Test Scenarios (Vehicle with Equalized Trucks)

For the curving tests (vertical bump, constant curving and dynamic curving) the car tested was the cab car in a four car consist. For the remaining tests (yaw and sway, twist and roll, and pitch and bounce tests) the same car was tested but in a three car consist. The car was tested in both pull and push modes. When the car was pulled the instrumented wheelset was leading and

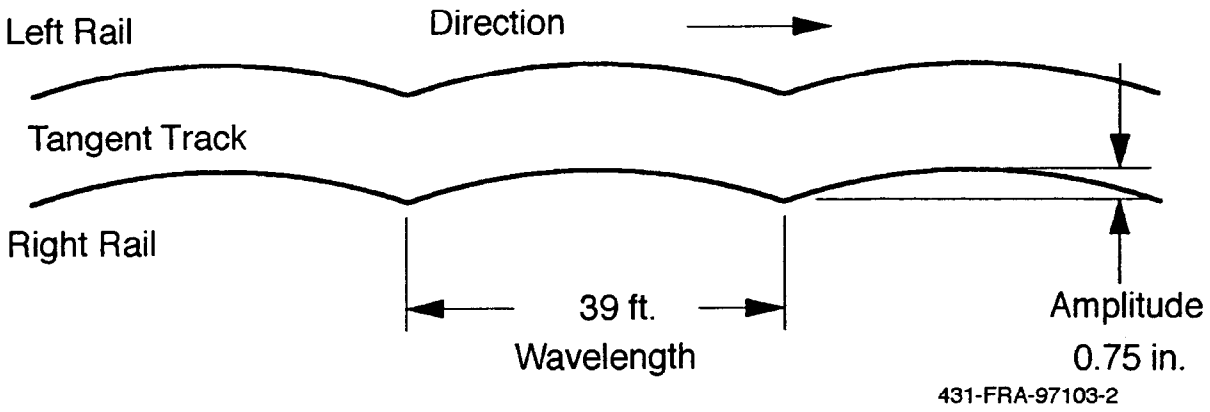

Figure 15. Track surface variation for pitch and bounce

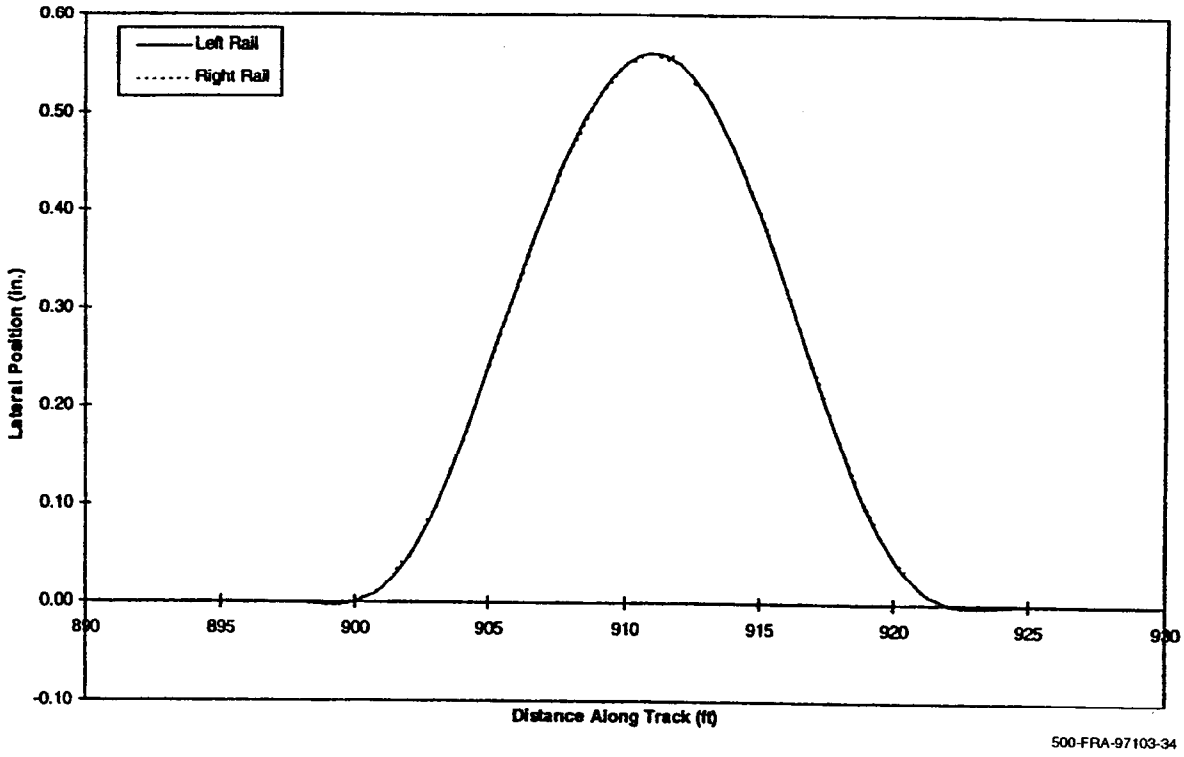

Figure 16. Lateral perturbation for hunting test

conversely when the test car was pushed the instrumented wheelset was trailing. Data including wheel vertical and lateral forces were measured on each of the two AAR instrumented wheelsets.

6.2.1 Vehicle Response to Variations in Vertical Alignment

A test with variations in curved track vertical alignment was conducted to measure the test car capability to operate safely in low speed curves at permissible speeds and to predict the potential of wheel lift. This test is also referred to as the vertical bump test. Test runs were performed on the 7.5 deg curve of the Wheel Rail Mechanisms (WRM) loop. The 7.5 deg curve has a 24 mph balance speed and has concrete ties on granite ballast. A vertical perturbation of 2 in. amplitude (bump) on the inner rail was installed on the track. Figure 17 shows the vertical bump that was installed in the 7.5 deg curve. The test was run for a range of speeds (10 to 24 mph) in forward and reverse directions. A video camera was also deployed on the carbody focussing on the primary suspension to capture its movement under potential wheel lift situations. A wayside video camera was deployed to capture the occurrence or potential of wheel lift.

6.2.2 Constant Curving with Spirals

Constant curving tests were conducted to measure the test car capability to operate safely on tight curves. The test consist was operated at speeds from below balance speed up to an

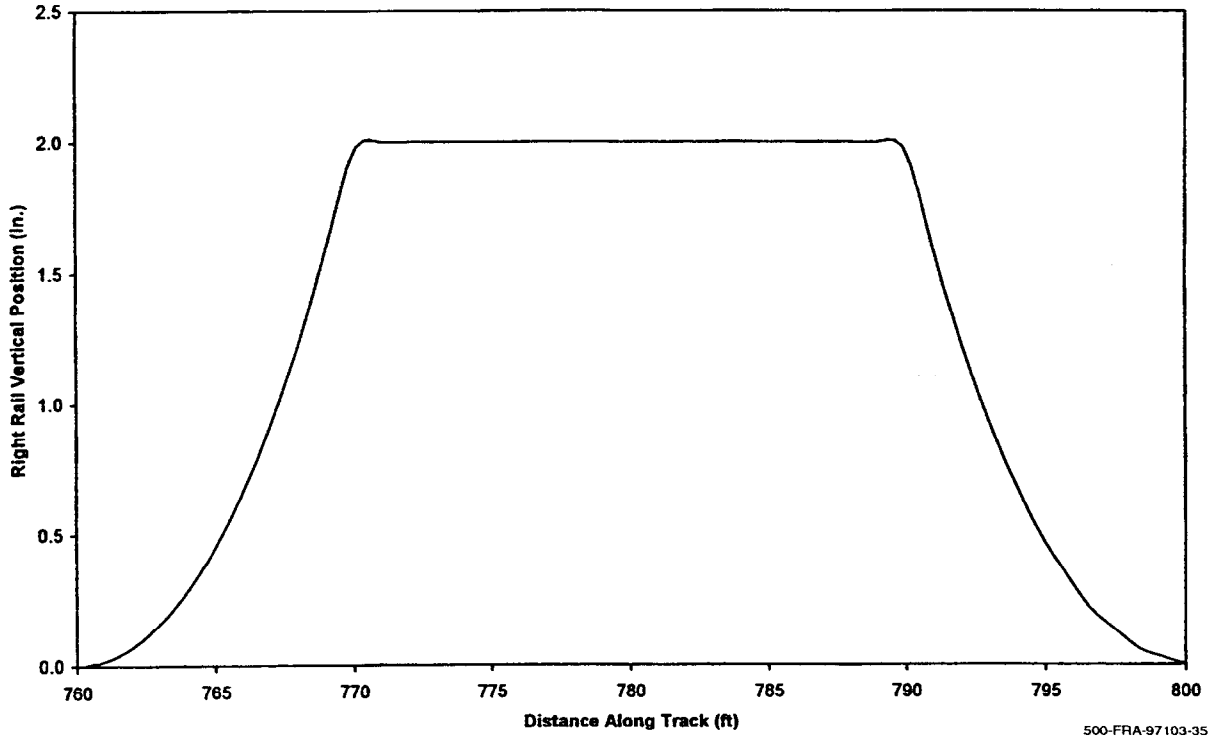

Figure 17. Vertical bump in the 7.5 deg curve

unbalanced (cant deficiency) condition of ~3 in. The tests were run on the WRM loop and consisted of a 7.5 deg curve, a 12 deg curve and a 10 deg curve. All curves have a balance speed of 24 mph. The 7.5 deg curve has 3 in. superelevation, the 12 deg curve has 5 in. superelevation and the 10 deg curve has 4 in. superelevation. Test runs were performed at speeds of 12 mph (except the 12 deg, which was performed at 15 mph), 24 mph (balance speed) and 32 mph (~3 in. unbalance) on the WRM. The tracks have AREA 136 rail and concrete ties on granite ballast.

6.2.3 Other Scenarios

Dynamic Curving

This is the same test as in the car with non-equalized trucks (see subsection 6.1.3).

Yaw and Sway

This is the same test as in the car with non-equalized trucks (see subsection 6.1.4).

Twist and Roll

This is the same test as in the car with non-equalized trucks (see subsection 6.1.5).

Pitch and Bounce

This is the same test as in the car with non-equalized trucks (see subsection 6.1.6).

7. CORRELATIONS SUMMARY

Detailed correlations of OMNISIM simulation results with the test data are presented in the appendices. The dynamic response characteristics are correlated for both types of rail car and for all the track scenarios in the tests. These include:

- Maximum vertical wheel forces.
- Maximum lateral wheel forces.
- Minimum vertical wheel forces.
- RMS values for the vertical and lateral forces in the zone of track irregularity.
- Maximum carbody accelerations.

The maximum vertical and lateral wheel forces are often used as a measure of quantitative validation of the model. The maximum lateral force is also a measure of potential unsafe behavior of the car. The minimum vertical wheel force is a measure of potential unsafe wheel lift behavior of the car. The RMS value over the zone of interest represents the overall agreement between simulation and test data. The carbody acceleration is important for ride comfort assessment and is also useful for quantitative validation of the model.

7.1 Maximum Absolute Forces

The maximum absolute forces are summarized in Tables 5 and 6 for the vehicle with non-equalized trucks and the vehicle with equalized trucks, respectively. The summary results are in the form of maximum absolute vertical and lateral forces of the lead outer wheel for a few speeds in each dynamic scenario. The lateral force levels in pitch and bounce are too small to be of any practical significance and are not shown.

The results in Tables 5 and 6 show good correlation (under 10 percent) in a majority of the test scenarios, especially for the vertical force. In every case but the lateral force in the dynamic curving scenarios, the simulation is conservative in its prediction.

7.2 Minimum Vertical Forces

Tables 7 and 8 show the theoretical and test data for the vehicle with non-equalized trucks and the vehicle with equalized trucks, respectively. Wheel lift is clearly seen in the case of the non-equalized truck car at a speed of 20 mph. The simulation showed that the dynamic wheel

Table 5. Lead outer wheel maximum absolute forces (non-equalized trucks)

Test	Speed (mph)	Curve (deg)	Vertical Force (kips)		Lateral Force (kips)	
			Test	Simulation	Test	Simulation
Vertical Dip	10	5	21.17	19.50	10.15	7.86
Vertical Dip	15	5	23.82	21.49	11.65	7.98
Vertical Dip	20	5	24.57	22.55	13.59	8.11
Vertical Dip	22	5	24.58	22.25	13.29	8.17
Steady Curving	84	1.25	20.67	17.41	7.22	4.32
Steady Curving	90	1.25	21.85	18.03	7.50	4.65
Steady Curving	114	1.25	26.20	21.13	7.37	5.85
Steady Curving	124	1.25	29.86	23.07	7.32	6.63
Dynamic Curving	20	10	19.10	19.31	6.94	13.95
Dynamic Curving	28	10	22.96	21.18	11.12	17.12
Twist and Roll	18.8	tangent	21.40	20.39	1.74	1.24
Twist and Roll	60	tangent	22.04	20.82	2.42	1.97
Pitch and Bounce	20	tangent	17.95	17.62		
Pitch and Bounce	60	tangent	19.19	17.91		
Yaw and Sway	20	tangent	20.73	20.33	5.09	1.26
Yaw and Sway	60	tangent	21.66	17.32	6.74	0.46
Hunting	80	tangent	18.85	17.25	0.92	0.12
Hunting	100	tangent	19.26	17.27	1.90	0.19
Hunting	130	tangent	19.55	17.28	3.79	0.31

load is reduced by about 63 percent, compared to that of the static case and is clearly considered to be unsafe per existing FRA standards.

7.3 RMS Forces

The RMS results are summarized in Tables 9 and 10 for the vehicle with non-equalized trucks and the vehicle with equalized trucks, respectively. The summary results are in the form of RMS vertical and lateral forces of the lead outer wheel for a few speeds in each dynamic scenario. As in the maximum absolute force tables of subsection 7.1, the lateral force levels in pitch and bounce are too small to be of any practical significance and are not shown.

Table 6. Lead outer wheel maximum absolute forces (equalized trucks)

Test	Speed (mph)	Curve (deg)	Vertical Force (kips) Test	Vertical Force (kips) Simulation	Lateral Force (kips) Test	Lateral Force (kips) Simulation
Vertical Bump	10	7.5	23.50	20.09	10.46	9.12
Vertical Bump	18	7.5	25.87	22.99	11.14	9.57
Vertical Bump	24	7.5	28.48	23.25	12.73	10.04
Steady Curving	12	7.5	22.67	19.65	8.17	8.42
Steady Curving	24	7.5	23.66	20.72	9.51	9.31
Steady Curving	32	7.5	25.41	22.49	10.68	10.20
Steady Curving	12	10	22.63	20.33	9.27	8.47
Steady Curving	24	10	24.50	21.64	11.51	9.82
Steady Curving	32	10	27.19	23.78	13.38	11.01
Steady Curving	15	12	21.71	20.39	7.82	8.59
Steady Curving	24	12	23.08	21.44	9.79	9.94
Steady Curving	32	12	25.93	24.15	13.08	11.36
Dynamic Curving	18.6	10	24.08	20.88	13.93	17.61
Dynamic Curving	28	10	28.01	26.85	16.84	24.85
Twist and Roll	19.2	tangent	24.08	21.95	3.53	1.32
Twist and Roll	60	tangent	24.66	22.42	4.21	2.02
Pitch and Bounce	30	tangent	22.00	20.57		
Pitch and Bounce	60	tangent	22.08	19.87		
Yaw and Sway	20	tangent	21.31	19.31	4.15	0.36
Yaw and Sway	60	tangent	22.07	19.45	4.33	0.50

7.4 Summary

The simulation tool, OMNISIM has been exercised to predict the dynamic response of a vehicle negotiating various track scenarios including transient response to vertical and lateral perturbations in the track alignment, steady-state curving, dynamic curving, and truck hunting. The Appendices present detailed simulation and test correlations.

7.4.1 Vehicle with Non-Equalized Trucks

For the vehicle with non-equalized trucks the following conclusions are reached with respect to correlations between test and computer simulation data:

1. The vehicle response to a variation in vertical alignment shows that simulation results for vertical forces agree closely with test data at all speeds. The simulation predicts wheel unloading in close agreement with test data.

Table 7. Lead outer wheel minimum vertical forces (non-equalized trucks)

Test	Speed (mph)	Curve (deg)	Vertical Force (kips) Test	Vertical Force (kips) Simulation
Vertical Dip	10	5	8.78	11.16
Vertical Dip	15	5	7.35	9.37
Vertical Dip	20	5	0.00	6.27
Vertical Dip	22	5	0.00	6.07
Steady Curving	84	1.25	12.97	15.44
Steady Curving	90	1.25	12.68	15.61
Steady Curving	114	1.25	12.97	15.48
Steady Curving	124	1.25	11.52	15.25
Dynamic Curving	20	10	12.51	13.84
Dynamic Curving	28	10	14.85	15.83
Twist and Roll	18.8	tangent	12.98	13.93
Twist and Roll	60	tangent	12.42	13.53
Pitch and Bounce	20	tangent	15.83	16.61
Pitch and Bounce	60	tangent	15.10	16.43
Yaw and Sway	20	tangent	14.01	13.87
Yaw and Sway	60	tangent	15.35	16.76
Hunting	80	tangent	14.78	16.86
Hunting	100	tangent	14.35	16.86
Hunting	130	tangent	13.66	16.83

2. In the steady curving tests with spirals the simulation has good correlation with the measured vertical forces at all speeds. The correlation for the lateral force on individual wheels is not as good, however, the lateral net axle forces are in relatively good agreement between simulation and test results both at balance and over balance speeds.

3. In the dynamic curving tests the simulation is able to accurately predict the shape and amplitude of the vertical forces. The simulation has very good correlation for the vertical forces at all speeds. The correlation for the lateral force is not as good. The distribution of predicted lateral forces have the same shape as test lateral forces but are larger in amplitude, at all test speeds. Both the simulation and test data indicate that a wheel climb condition is not approached for the conditions studied.

4. In yaw and sway tests, the simulation has very good correlation with test data for the vertical force at all speeds. The correlation for the lateral force is not as good. The simulation is able to predict the shape and amplitude of the vertical forces. The

Table 8. Lead outer wheel minimum vertical forces (equalized trucks)

Test	Speed (mph)	Curve (deg)	Vertical Force (kips) Test	Vertical Force (kips) Simulation
Vertical Bump	10	7.5	14.18	15.06
Vertical Bump	18	7.5	14.49	15.02
Vertical Bump	24	7.5	16.44	16.12
Steady Curving	12	7.5	15.22	16.29
Steady Curving	24	7.5	16.42	17.61
Steady Curving	32	7.5	17.06	18.04
Steady Curving	12	10	14.83	16.51
Steady Curving	24	10	16.24	18.17
Steady Curving	32	10	17.46	18.56
Steady Curving	15	12	13.32	15.28
Steady Curving	24	12	14.41	16.94
Steady Curving	32	12	16.14	17.65
Dynamic Curving	18.6	10	13.56	14.67
Dynamic Curving	28	10	16.10	16.03
Twist and Roll	19.2	tangent	15.40	15.71
Twist and Roll	60	tangent	15.24	15.53
Pitch and Bounce	30	tangent	17.80	17.14
Pitch and Bounce	60	tangent	17.43	18.02
Yaw and Sway	20	tangent	17.56	18.48
Yaw and Sway	60	tangent	16.97	18.26

predicted lateral force distributions have similar shape as in test lateral forces but the simulation under predicts the amplitude. The lateral forces had poor agreement believed primarily due to lateral force "spikes."

5. In twist and roll tests the simulation has very good correlation with test data for the amplitude of the vertical and lateral forces at all speeds.

6. In pitch and bounce tests the simulation has good correlation with test data for the vertical force throughout the speed range. The simulation predicts the shape and amplitude of the vertical forces. The predicted lateral forces are small, as are the test results.

7. The vehicle did not show any truck or body hunting oscillations up to the speed limits achieved in the test program (130 mph). This is consistent with the theory, which predicted a hunting speed of well over 200 mph.

Table 9. Lead outer wheel RMS forces (non-equalized trucks)

Test	Speed (mph)	Curve (deg)	Vertical Force (kips) Test	Vertical Force (kips) Simulation	Lateral Force (kips) Test	Lateral Force (kips) Simulation
Vertical Dip	10	5	14.09	15.50	4.88	5.03
Vertical Dip	15	5	14.55	15.75	4.93	5.14
Vertical Dip	20	5	14.55	16.09	7.01	5.28
Vertical Dip	22	5	15.00	16.24	5.80	5.31
Steady Curving	84	1.25	16.95	16.45	1.64	2.59
Steady Curving	90	1.25	17.56	16.80	1.35	2.78
Steady Curving	114	1.25	18.67	18.29	1.61	3.51
Steady Curving	124	1.25	17.35	19.05	1.80	3.91
Dynamic Curving	20	10	16.38	17.04	3.74	7.18
Dynamic Curving	28	10	19.68	18.39	6.04	7.86
Twist and Roll	18.8	tangent	17.26	17.14	0.59	0.50
Twist and Roll	60	tangent	17.10	17.18	0.84	0.82
Pitch and Bounce	20	tangent	17.08	17.10		
Pitch and Bounce	60	tangent	17.12	17.10		
Yaw and Sway	20	tangent	17.62	17.10	0.67	0.18
Yaw and Sway	60	tangent	17.48	17.10	0.72	0.14
Hunting	80	tangent	16.58	17.10	0.26	0.05
Hunting	100	tangent	16.92	17.10	0.35	0.05
Hunting	130	tangent	16.58	17.10	0.50	0.06

7.4.2 Vehicle with Equalized Trucks

For the vehicle with equalized trucks, the following conclusions are reached with respect to correlations between test and computer simulation data:

1. The simulation shows very good correlation of the vertical force for negotiation of the vertical bump at all speeds; however, the correlation for the lateral force is not as good. The simulation tool predicts wheel unloading and no wheel lift at any of the test speeds, consistent with tests.

2. In the steady curving tests with spirals the simulation has good correlation with the measured vertical forces at all speeds. The correlation for the lateral force on individual wheels is not as good, however, the lateral net axle forces are in relatively good agreement between simulation and test results both at balance and over balance speeds.

Table 10. Lead outer wheel RMS forces (equalized trucks)

Test	Speed (mph)	Curve (deg)	Vertical Force (kips) Test	Vertical Force (kips) Simulation	Lateral Force (kips) Test	Lateral Force (kips) Simulation
Vertical Bump	10	7.5	18.75	17.78	6.28	6.97
Vertical Bump	18	7.5	19.36	18.61	6.75	7.46
Vertical Bump	24	7.5	20.42	19.52	6.94	7.83
Steady Curving	12	7.5	18.72	17.94	4.95	7.72
Steady Curving	24	7.5	20.48	19.62	5.50	8.38
Steady Curving	32	7.5	22.36	21.33	6.08	9.06
Steady Curving	12	10	18.51	17.47	6.21	7.81
Steady Curving	24	10	20.92	19.83	7.07	9.00
Steady Curving	32	10	23.56	22.24	7.92	10.05
Steady Curving	15	12	17.86	17.66	5.15	7.49
Steady Curving	24	12	19.61	19.58	6.31	8.45
Steady Curving	32	12	22.30	21.99	7.30	9.52
Dynamic Curving	18.6	10	18.69	18.50	8.45	6.38
Dynamic Curving	28	10	21.73	19.93	9.37	7.03
Twist and Roll	19.2	tangent	19.99	18.90	1.47	0.47
Twist and Roll	60	tangent	19.83	18.92	1.49	0.60
Pitch and Bounce	30	tangent	19.97	18.88		
Pitch and Bounce	60	tangent	19.55	18.86		
Yaw and Sway	20	tangent	19.57	18.86	1.27	0.11
Yaw and Sway	60	tangent	19.27	18.86	1.22	0.11

3. In the dynamic curving tests the simulation is able to accurately predict the shape and amplitude of the vertical forces. The simulation has very good correlation for the vertical forces at all speeds. The correlation for the lateral force is not as good. The distribution of predicted lateral forces have the same shape as test lateral forces but are larger in amplitude, at all test speeds. Both the simulation and test data indicate that a wheel climb condition is not approached for the conditions studied.

4. In yaw and sway tests, the simulation has very good correlation with test data for the vertical force at all speeds. The correlation for the lateral force is not as good. The simulation is able to predict the shape and amplitude of the vertical forces. The predicted lateral force distributions have similar shape as in test lateral forces but the simulation under predicts the amplitude. The lateral forces had poor agreement believed primarily due to lateral force "spikes."

5. In twist and roll tests, the simulation has relatively good correlation for the amplitude of the vertical force at all speeds at all speeds. Simulation predictions for the vertical

and in the twist and roll tests are reasonable. The simulation predictions for the lateral force have the same shape as the test data but the simulation underestimates the values.

6. In pitch and bounce tests the simulation has good correlation with test data for the vertical force throughout the speed range. The simulation predicts the shape and amplitude of the vertical forces. The predicted lateral forces are small, as are the test results.

8. CONCLUSIONS

1. Critical to the safety methodology are the car suspension parameters, track conditions and the critical operating scenarios. The simulation code is a valuable tool in the safety evaluations along with key tests. The mass, inertial properties, suspension stiffness and damping properties of the car are generally available in the manufacturer data. Whereas mass and inertial properties do not significantly change with the age of the car, the suspension parameters can degrade with age and service life of the car. Hence, testing for car suspension parameters may be required on older cars, or cars with no apparent data from the manufacturer.

   The equalized truck car tested has no manufacturer's data; hence testing was performed to characterize its parameters.

   The non-equalized truck car was new, but tests for parameter characterization were still performed to establish the methodology for test characterization. Small differences were found between the manufacturer's data and the test data, although these did not significantly affect the simulation results.

2. The vehicle with equalized trucks had misaligned axles which made the vehicle behave as if it was on a curve when it was on a tangent. There is a lateral force in the test data that ranges from -0.5 kips to 1 kip when it should be zero lateral force. This was not modeled in OMNISIM.

3. The critical track scenarios were based on past studies in the literature. Although there is no proof that these cover all potentially unsafe track conditions, a car which can negotiate these conditions can be expected to show safe dynamic behavior by and large in revenue service. It must be stated that testing of cars under each of the scenarios is not necessary for a track worthiness assessment of the car. Only those scenarios, for which the anticipated behavior of the car is unsafe, need to be simulated for confirmation and redesign.

4. OMNISIM has all the important features and attributes of a modern vehicle-track interaction simulation code. The code has a reasonably accurate predictive capability for the wheel rail forces as well as the potential failure modes of the car, such as wheel lift.

5. Instead of OMNISIM, simpler specialized models can also be used to analyze track scenarios. Different specialized models will be required for different track scenarios. It is more convenient and computer efficient to have one simulation code being used for all the established as well as any potential new track scenario. With OMNISIM, it is possible to build an expert computer code in which the track scenarios are built-in and the safety evaluation of any car can be automated using Windows type interface.

6. In considering the cases where safety related limits were approached, the simulations and tests both identified in a similar manner the presence or absence of such conditions. In cases where wheel lift occurred, the simulation and test results were similar. Throughout the correlation study, good agreement was achieved between vertical force test data and simulation data.

7. Although agreement in the predicted and test data on the lateral force is not good in certain cases (dynamic curving and yaw and sway), the levels of forces are small and no unsafe condition is predicted by OMNISIM and witnessed in the tests.

9. REFERENCES

1. Samavedam, G., et al., "Conventional Passenger Rail Vehicle Safety, Volume I: Summary of Safe Performance Limits," DOT/FRA/ORD-97, Final Report, October 1997.
2. Samavedam, G., et al., "Conventional Passenger Rail Vehicle Safety, Technical Report Volume II: Detailed Analyses and Simulation Results," DOT/FRA/ORD-97, Final Report, November 1997.
3. Samavedam, G., et al., "Analyses of Track Shift Under High-Speed Vehicle-Track Interaction – Safety of High-Speed Ground Transportation," DOT Report No. DOT/FRA/ ORD-97/02, June 1997.
4. Cooperrider, N. K., and Heller, R., "User's Manual for the Asymmetric Wheel/Rail Contact Characterization Program," Federal Railroad Administration Report FRA/ORD-78/05, December 1977.
5. Kalker, J. J., "The Computation of Three Dimensional Rolling Contact with Dry Friction," International Journal for Numerical Methods in Engineering, Vol. 14, pp.1293-1307, 1979.

APPENDIX A

COMPARISON OF TESTS TO SIMULATIONS (PASSENGER RAIL VEHICLE WITH NON-EQUALIZED TRUCKS)

Simulations were run using the computer program OMNISIM on a Pentium PC. The track scenarios were modeled and the program was exercised to produce lateral and vertical forces. Time history plots were developed for the simulation and compared to time histories of the test data. Comparisons were made for the maximum lateral force and the minimum vertical force. These were chosen because the maximum lateral force coupled with the minimum vertical force produce the largest L/V ratio. Also maximum carbody lateral acceleration is presented for the range of test speeds. The following sections give a description of each test, a comparison of the test data to the simulation results, and conclusions.

A.1 Vehicle Response to Variations in Vertical Alignment

Test data and simulation results for the wheel vertical and lateral forces resulting from the traverse of the vertical dip are displayed in Figures A-1 and A-2 for 20 mph operation and in Figures A-3 and A-4 for 15 mph. The test data indicates a wheel lift condition (zero vertical force) occurring at 20 mph, whereas the simulation result indicated a wheel unloading (37 percent of the vertical static force). At the point where wheel lift occurs, the simulation is discontinued. For both 15 and 20 mph cases, good agreement is found between the predicted and measured vertical forces at all four wheels of the instrumented truck.

At 20 mph, the outer wheel of the lead axle vertical force increases to a value of approximately 17 to 18 kips just prior to reducing to zero (wheel lift condition). At 15 mph, the outer wheel of the lead axle vertical force similarly increases to a value of approximately 17 kips, decreases to a minimum of approximately 7 kips and then increases again to approximately 24 kips with good correspondence between the test data and simulation.

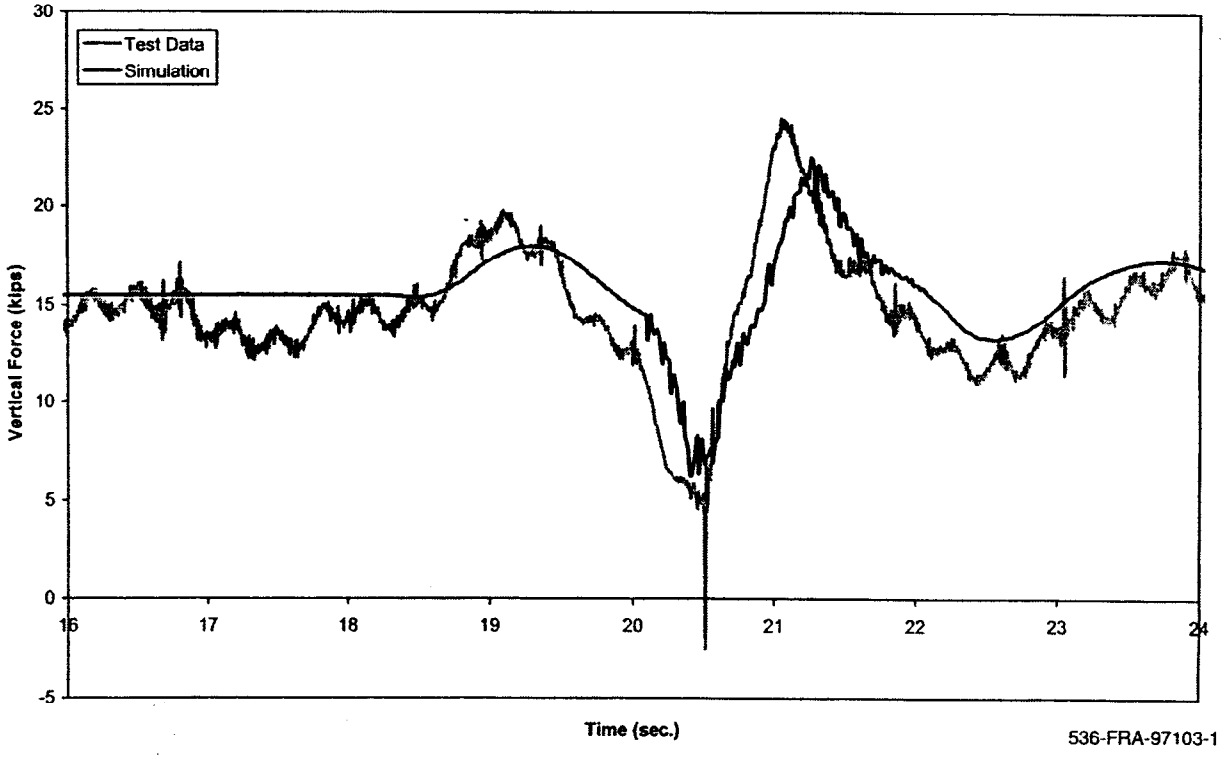

Figure A-1(a). Vertical dip test - vertical force time history, 20 mph (lead outer wheel)

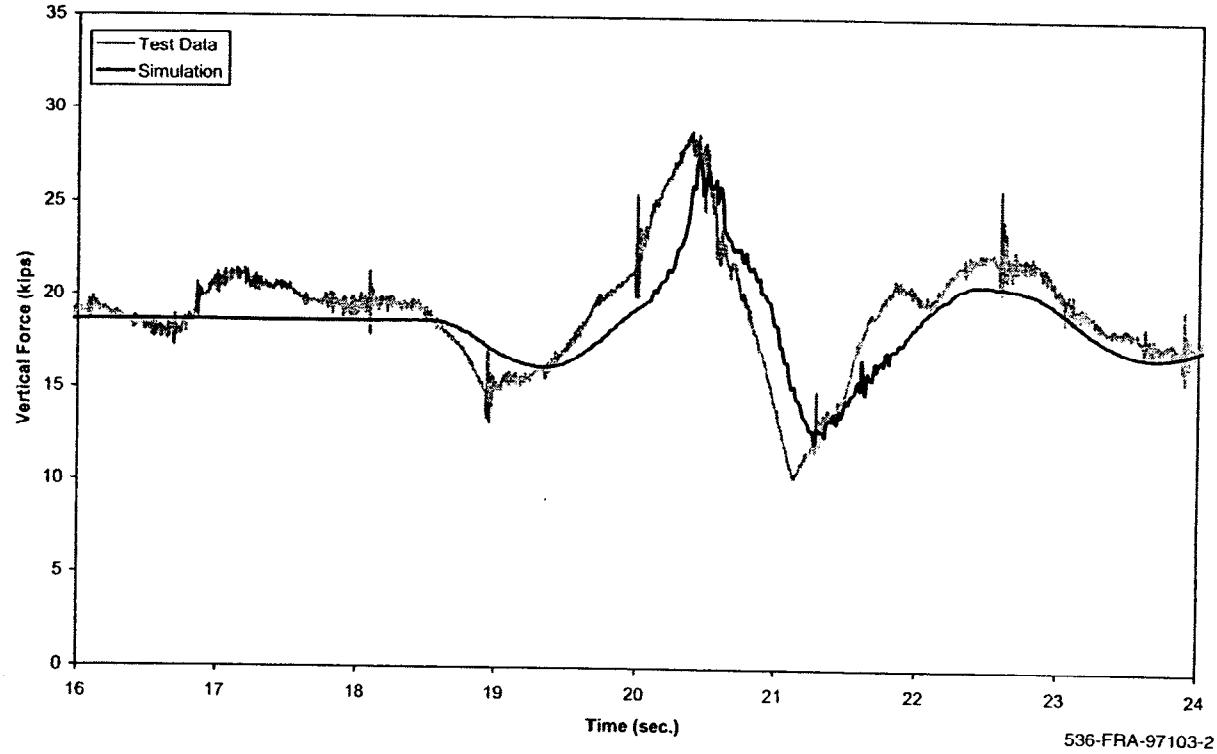

Figure A-1(b). Vertical dip test - vertical force time history, 20 mph (lead inner wheel)

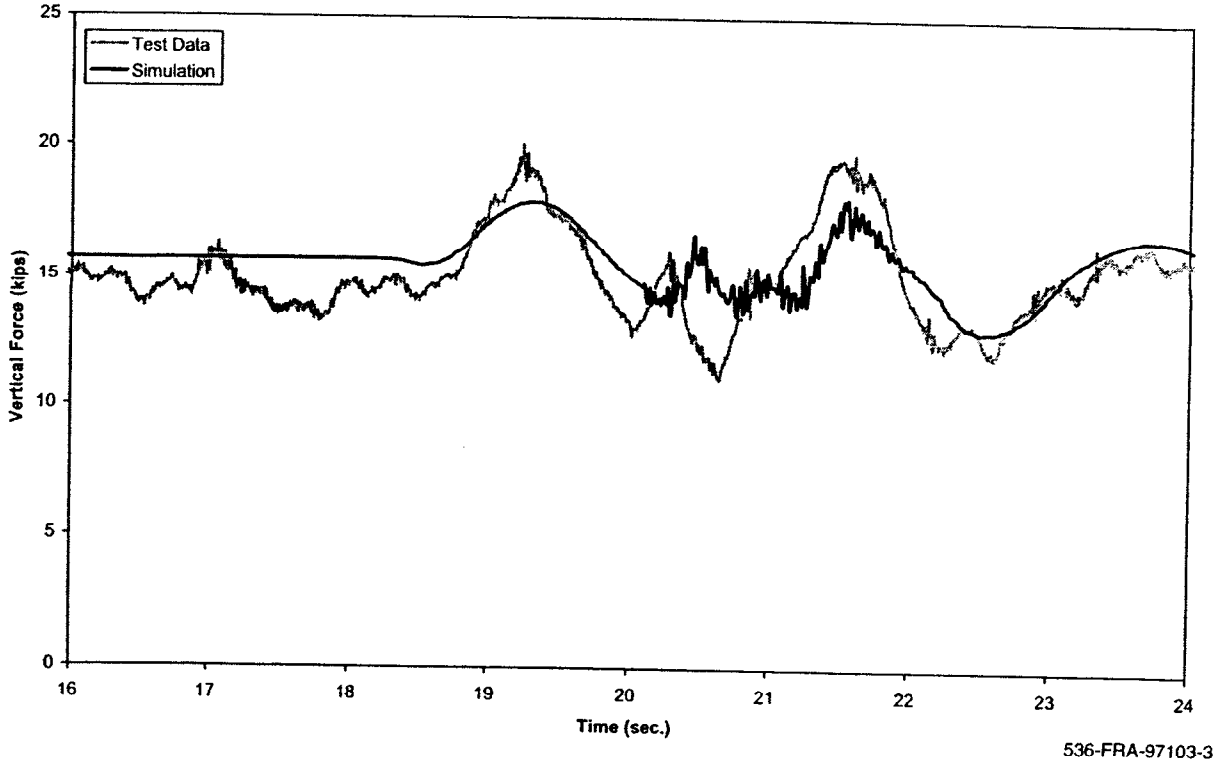

Figure A-1(c). Vertical dip test - vertical force time history, 20 mph (trailing outer wheel)

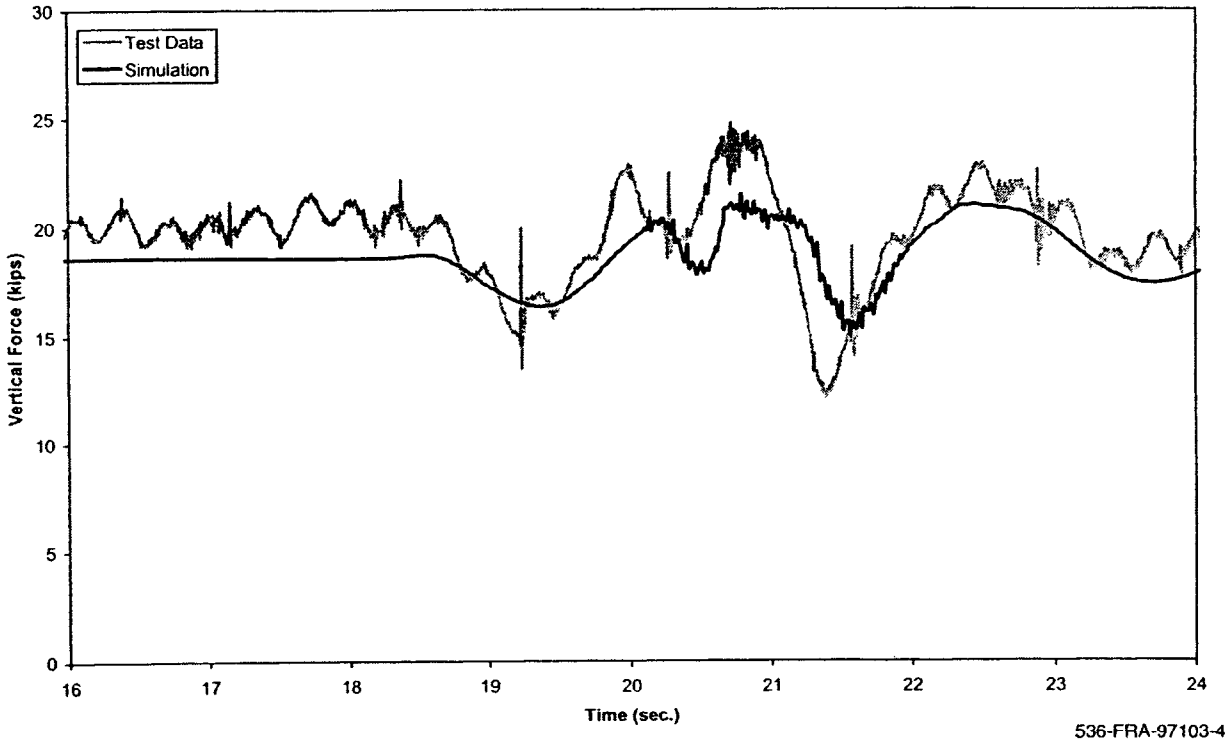

Figure A-1(d). Vertical dip test - vertical force time history, 20 mph (trailing inner wheel)

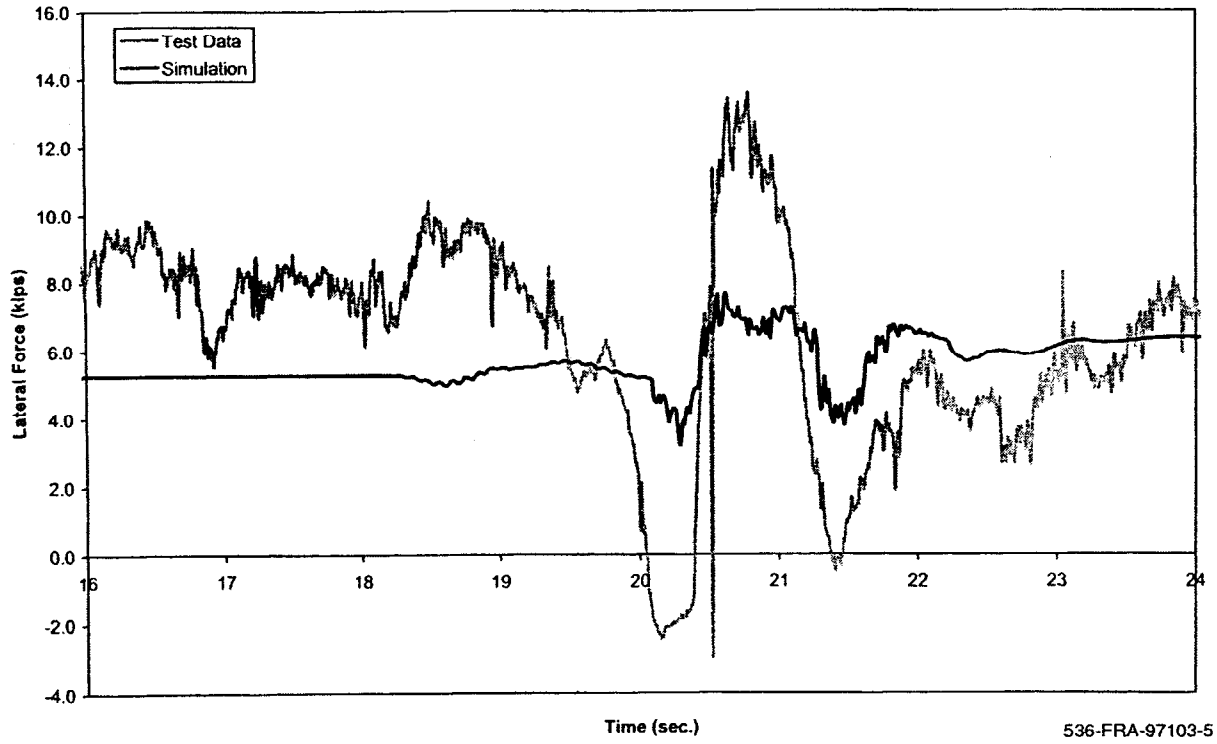

Figure A-2(a). Vertical dip test - lateral force time history, 20 mph (lead outer wheel)

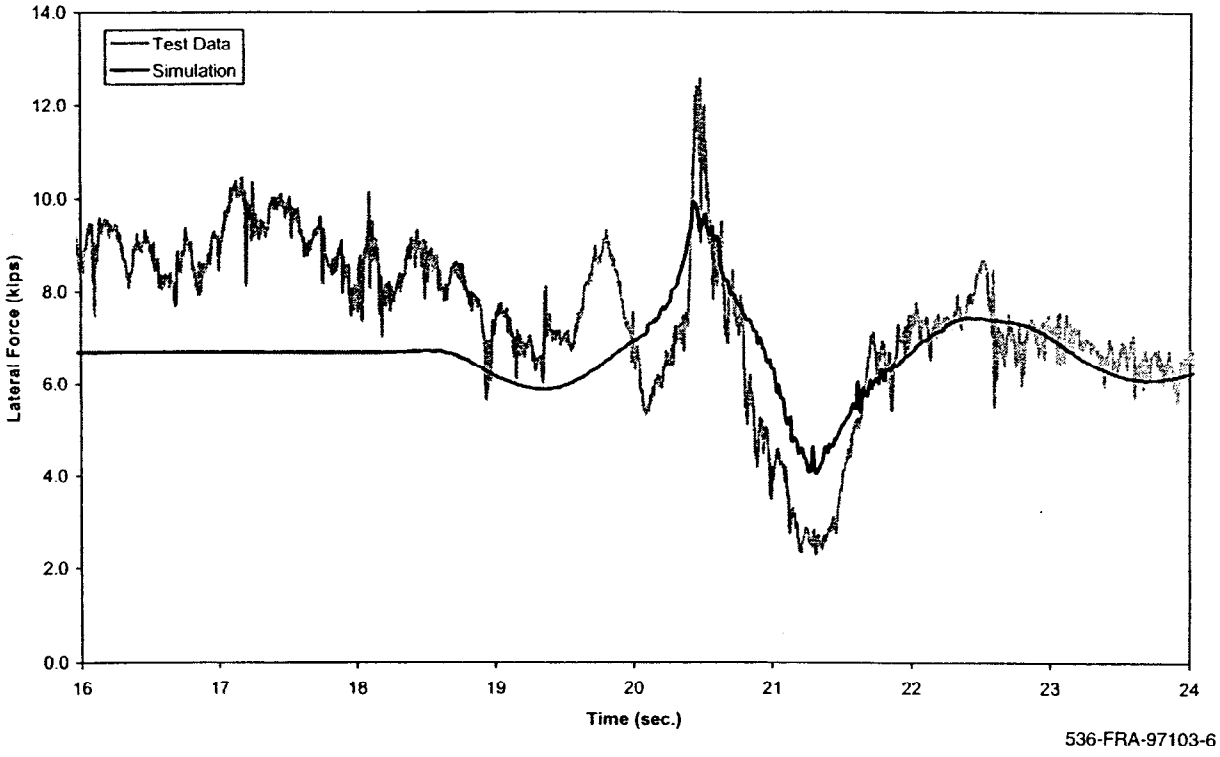

Figure A-2(b). Vertical dip test - lateral force time history, 20 mph (lead inner wheel)

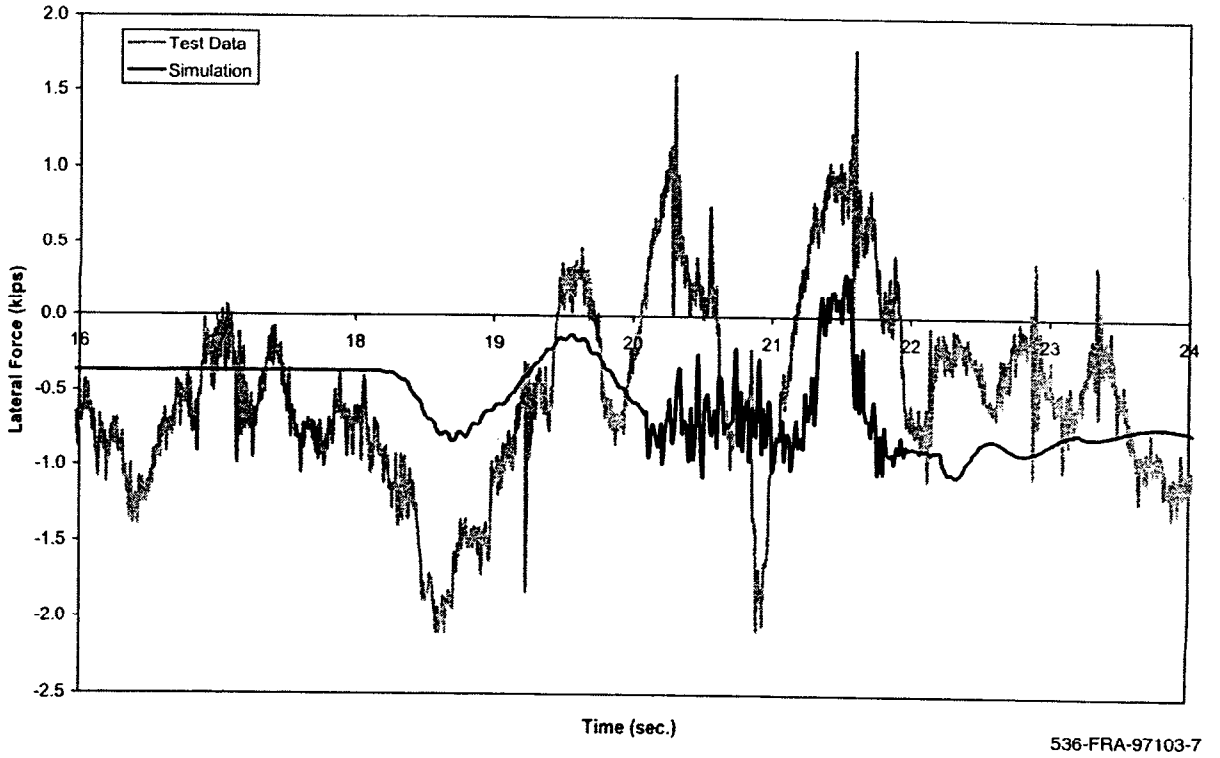

Figure A-2(c). Vertical dip test - lateral force time history, 20 mph (trailing outer wheel)

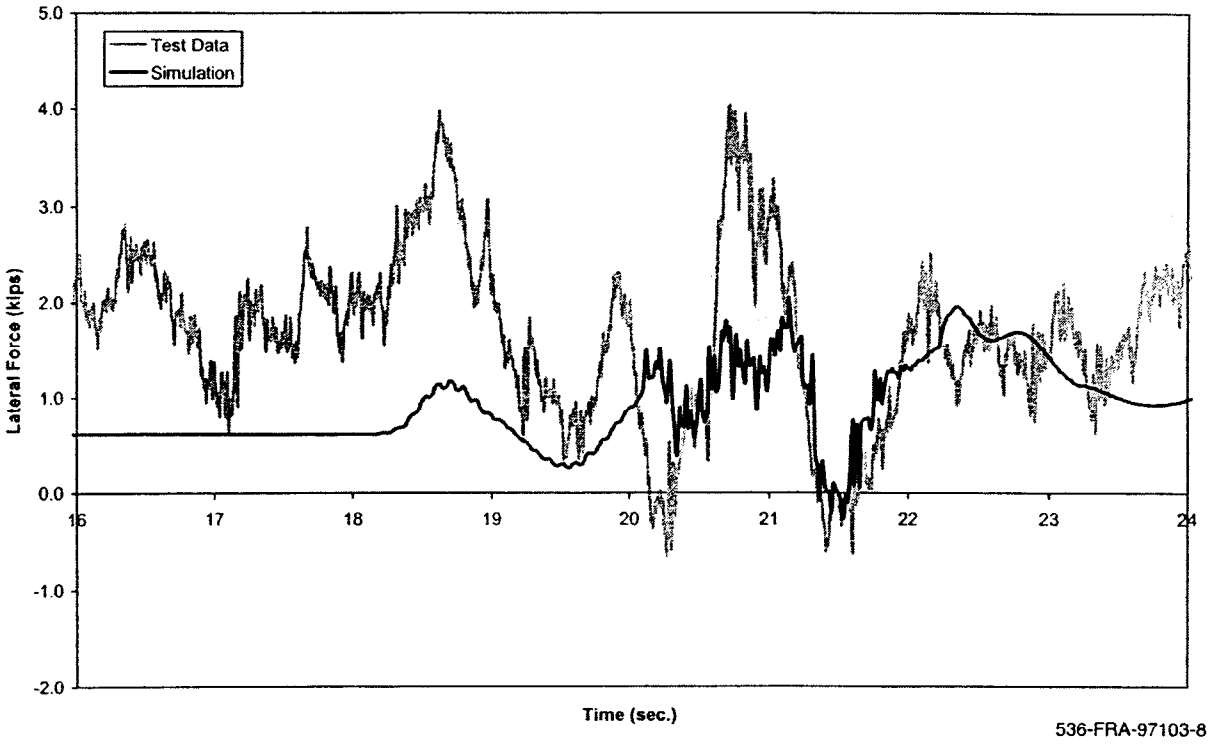

Figure A-2(d). Vertical dip test - lateral force time history, 20 mph (trailing inner wheel)

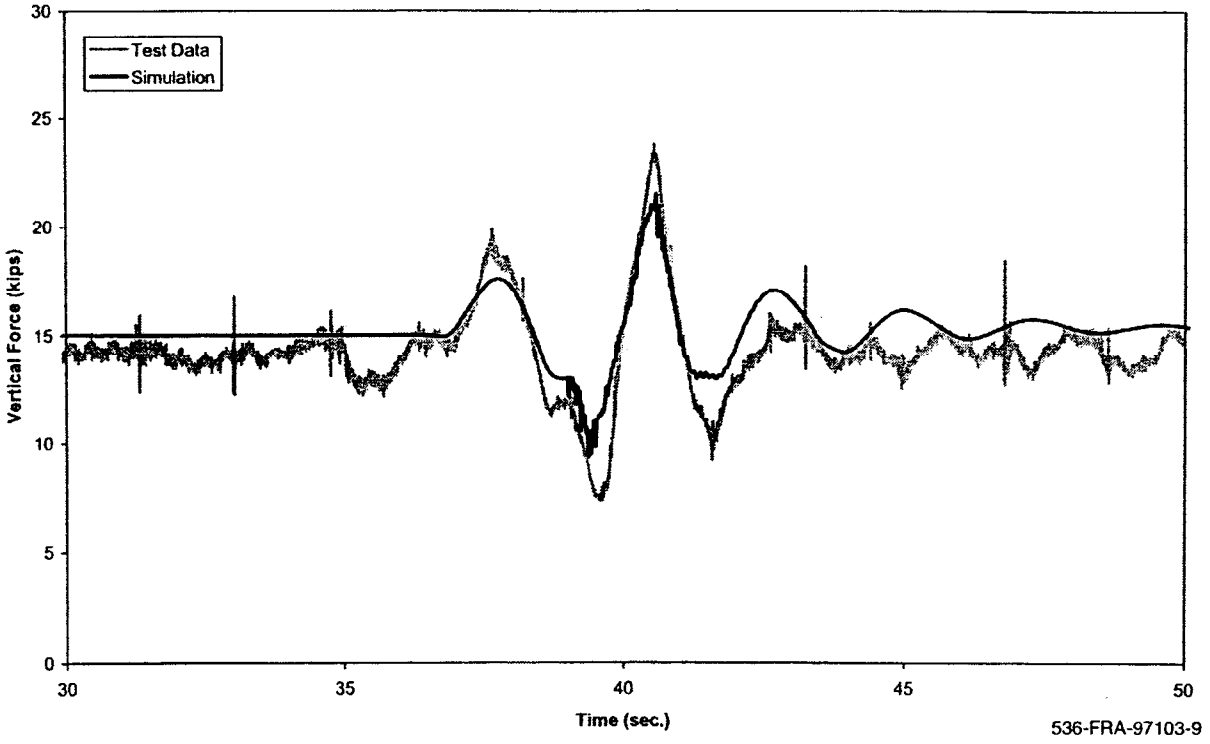

Figure A-3(a). Vertical dip test - vertical force time history, 15 mph (lead outer wheel)

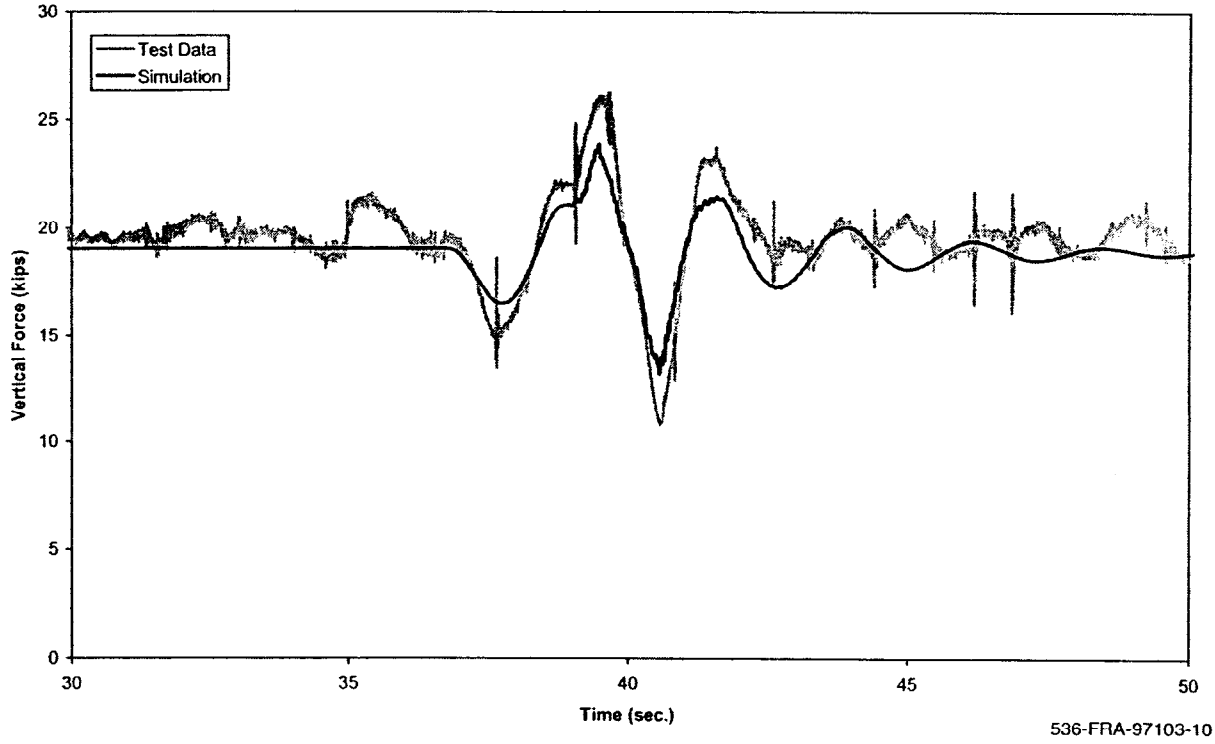

Figure A-3(b). Vertical dip test - vertical force time history, 15 mph (lead inner wheel)

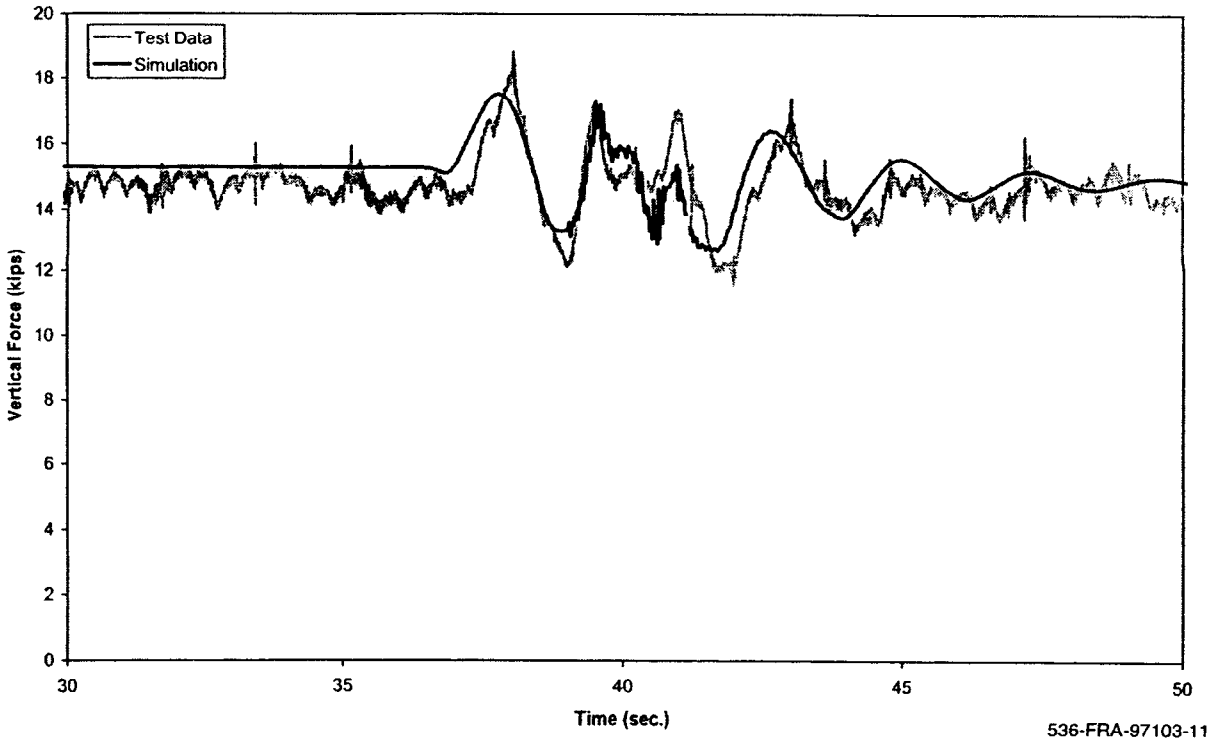

Figure A-3(c). Vertical dip test - vertical force time history, 15 mph (trailing outer wheel)

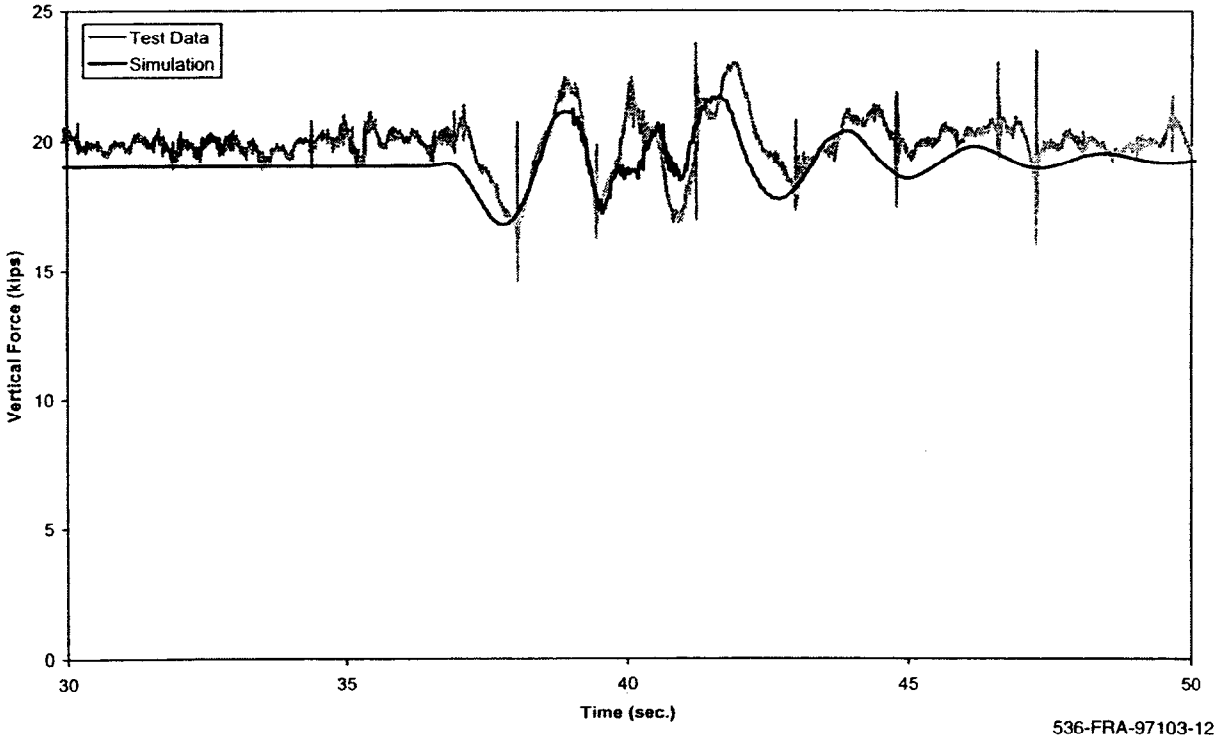

Figure A-3(d). Vertical dip test - vertical force time history, 15 mph (trailing inner wheel)

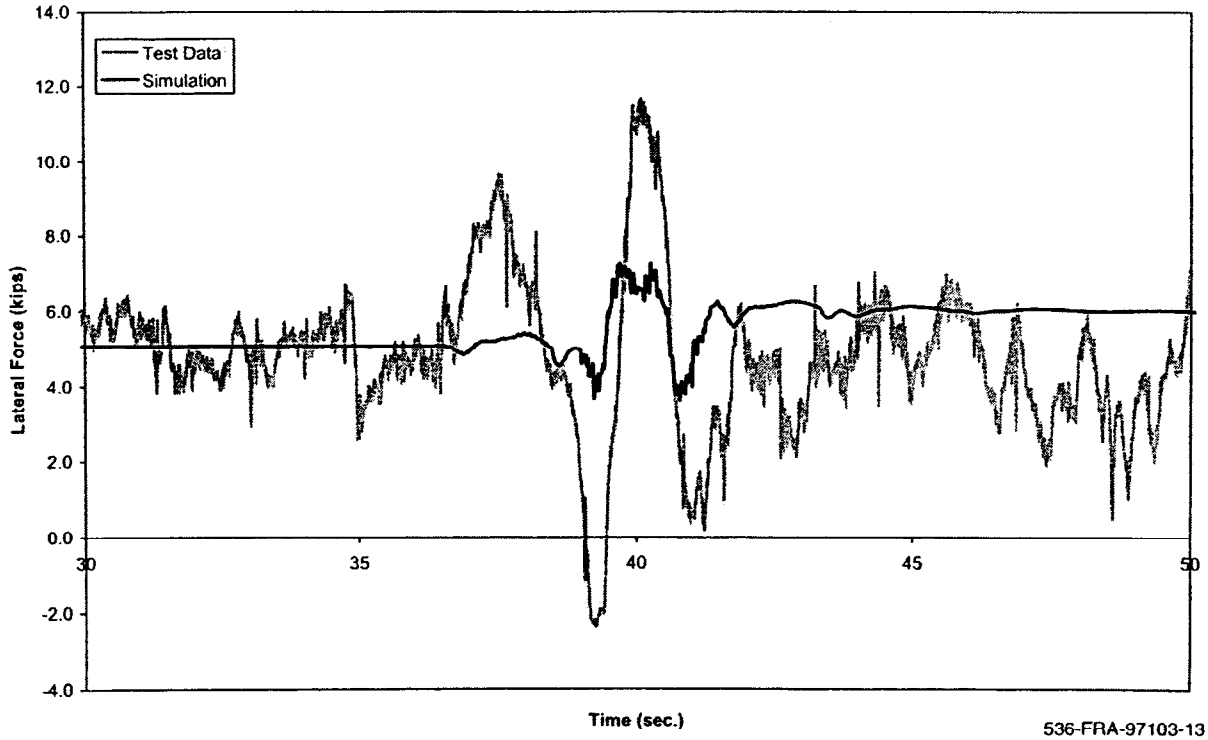

Figure A-4(a). Vertical dip test - lateral force time history, 15 mph (lead outer wheel)

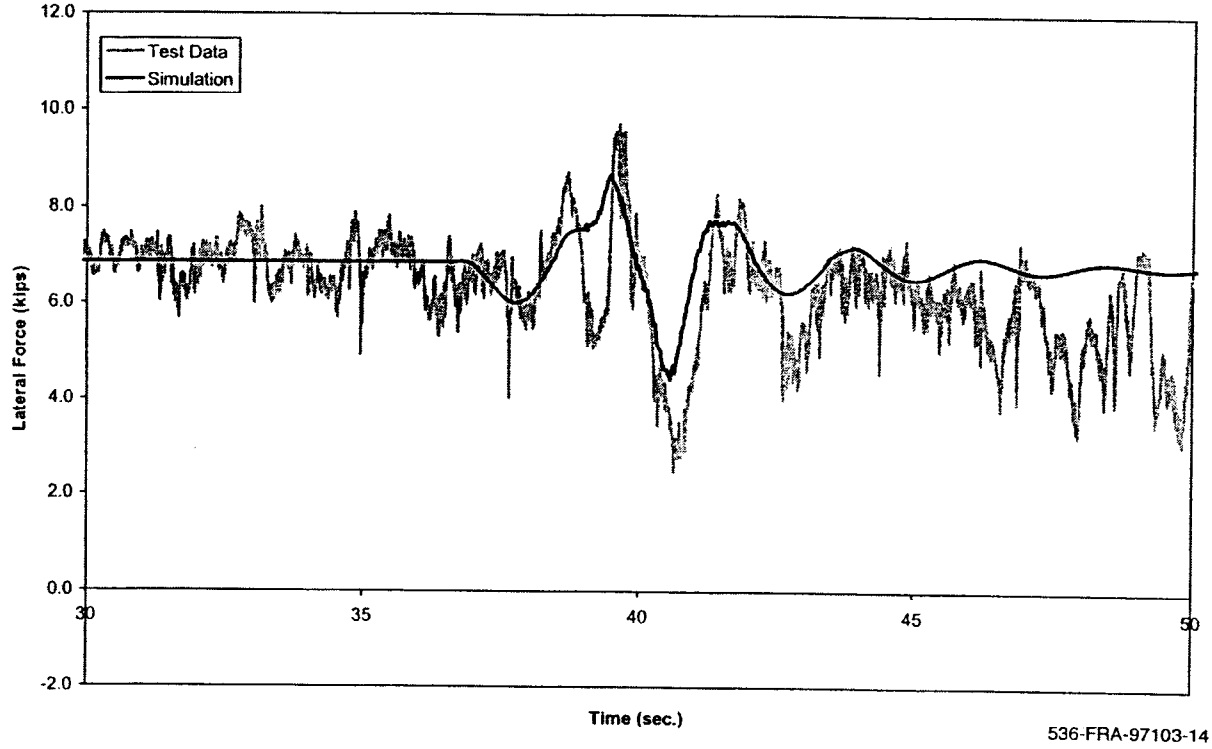

Figure A-4(b). Vertical dip test - lateral force time history, 15 mph (lead inner wheel)

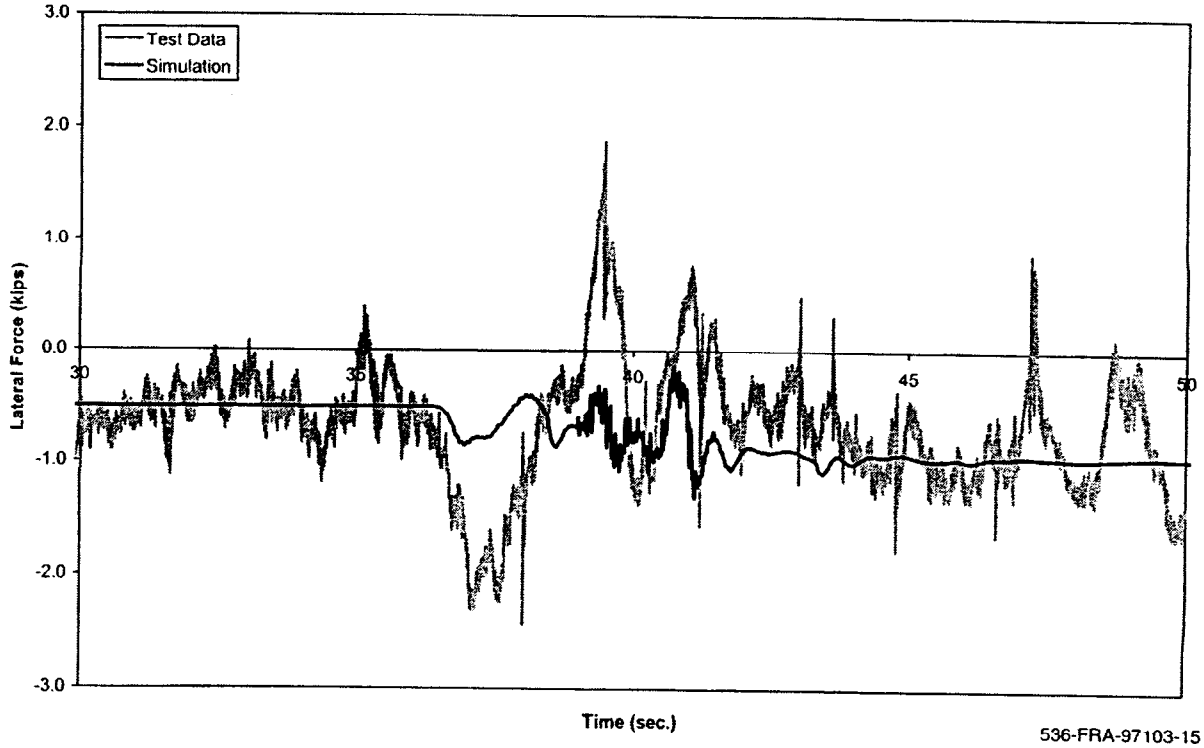

Figure A-4(c). Vertical dip test - lateral force time history, 15 mph (trailing outer wheel)

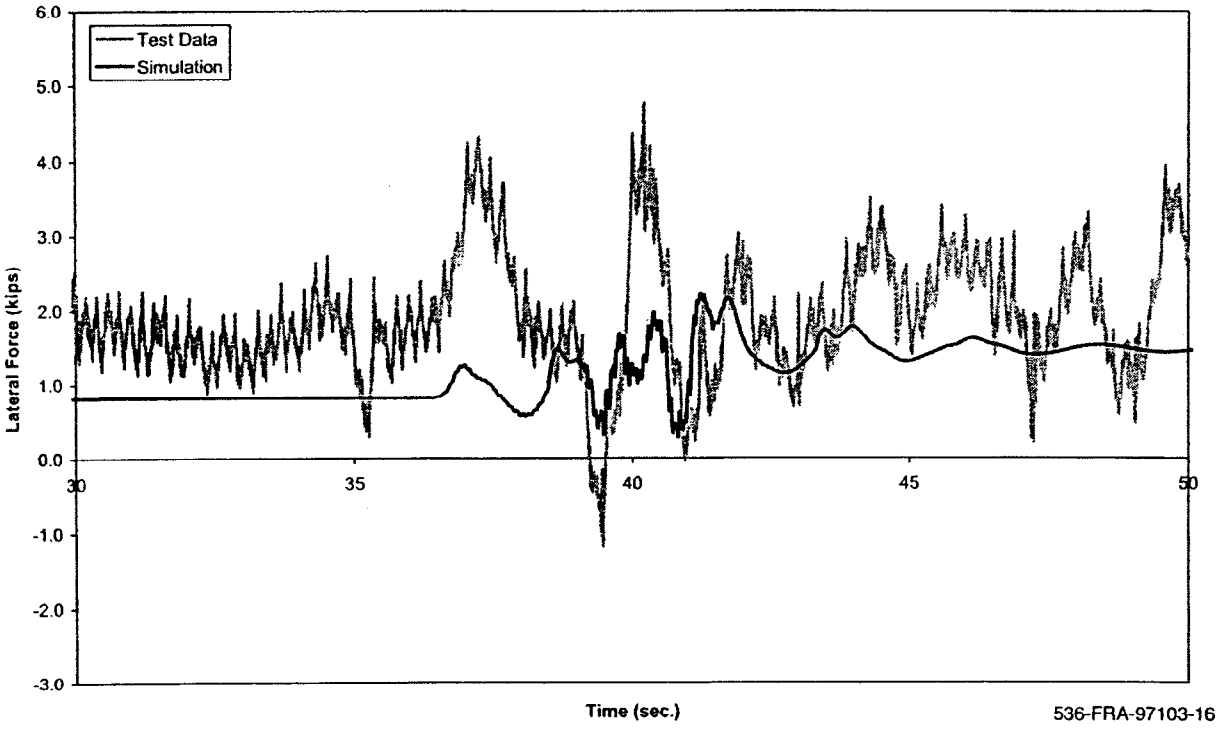

Figure A-4(d). Vertical dip test - lateral force time history, 15 mph (trailing inner wheel)

The measured and predicted lateral forces have similar shapes and levels of magnitude, however, the correlations are not as good as found for the vertical force. For the 20 mph case, the lateral force on the lead axle prior to entering the dip is approximately 5.5 kips (simulation) and 7.5 kips (test) for the outer wheel and 6.75 kips (simulation) and 9 kips (test) for the inner wheel. The lateral forces for both the simulation and test data on the outer and inner wheel change abruptly at the point of wheel lift. The trailing axle lateral forces test data are in the approximately ±2.0 kips range for the outer wheel and –0.5 to 4 kips range for the inner wheel. The simulation results have similar waveforms but at reduced levels with the outer wheel lateral forces varying from –0.75 to 0.25 kips and the inner wheel lateral force a maximum of 1.25 kips.

At 15 mph the lateral force test data have relatively good agreement with the simulation data for the initial lateral force values prior to entering the dip. The waveforms of the simulations are similar to the test data during passage through the dip, but have smaller amplitudes than the test data by 4 to 5 kips for the lead axle outer wheel, and 2 kips for the trailing axle outer wheel.

A plot of the minimum vertical force occurring during negotiation of the dip for a range of speeds is shown in Figure A-5 for the outer wheel on the lead axle of the trailing truck. Good correlation is shown over the speed range for the vertical force.

A.2 Steady Curving with Spirals

Test data and simulation results for passage through the curve are presented in Figures A-6, A-7 and A-8 for operation at 84 mph and in Figures A-9, A-10 and A-11 for operation at

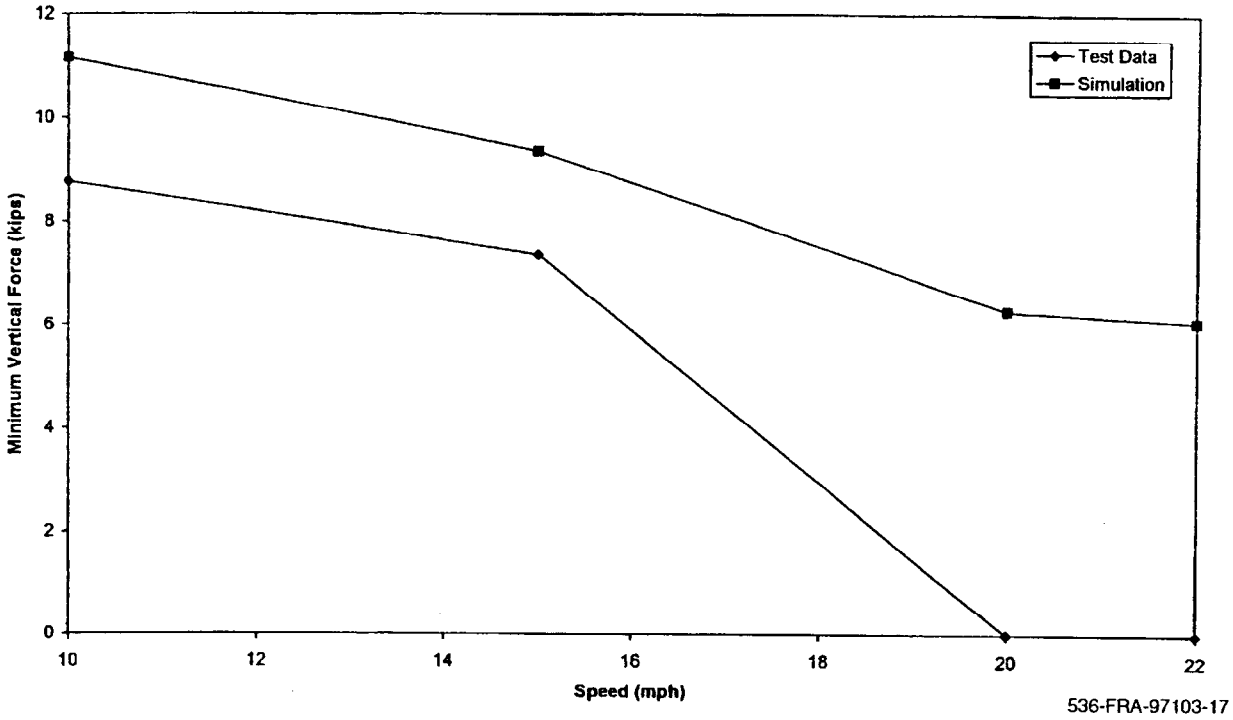

Figure A-5. Vertical dip test - minimum vertical force (lead outer wheel)

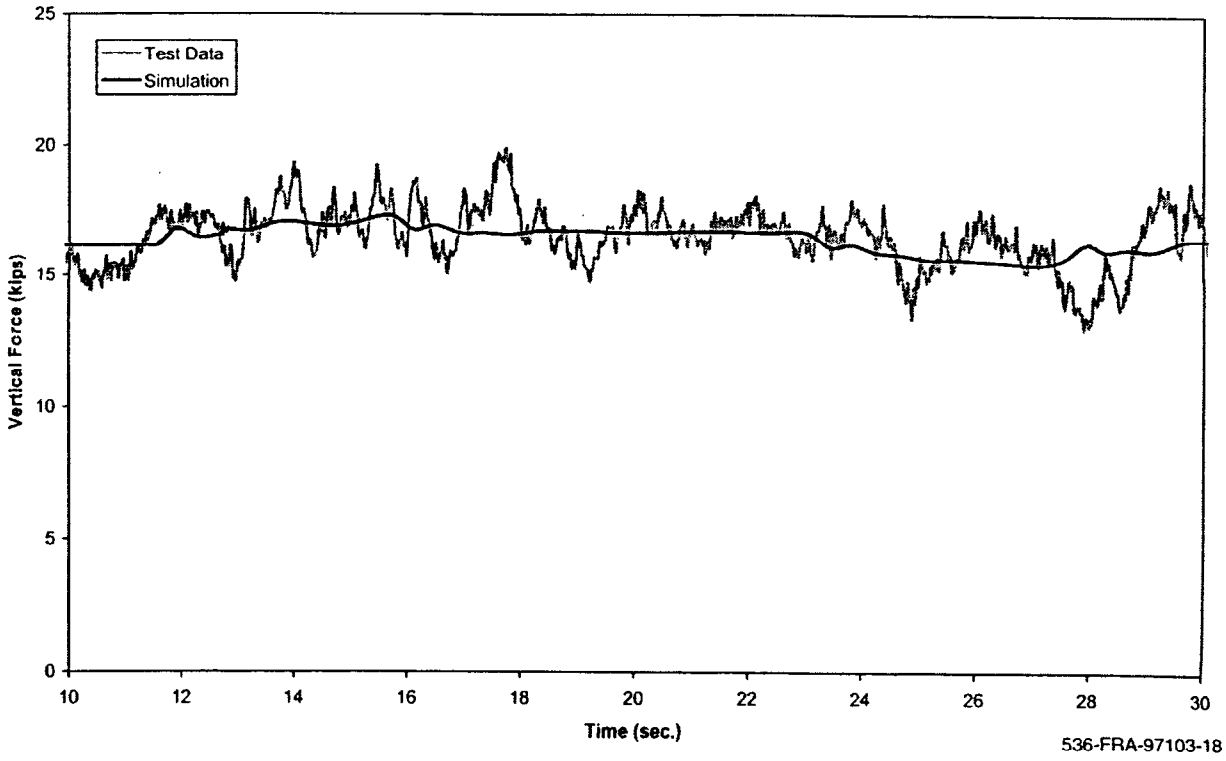

Figure A-6(a). Steady curving - vertical force time history, 84 mph (lead outer wheel)

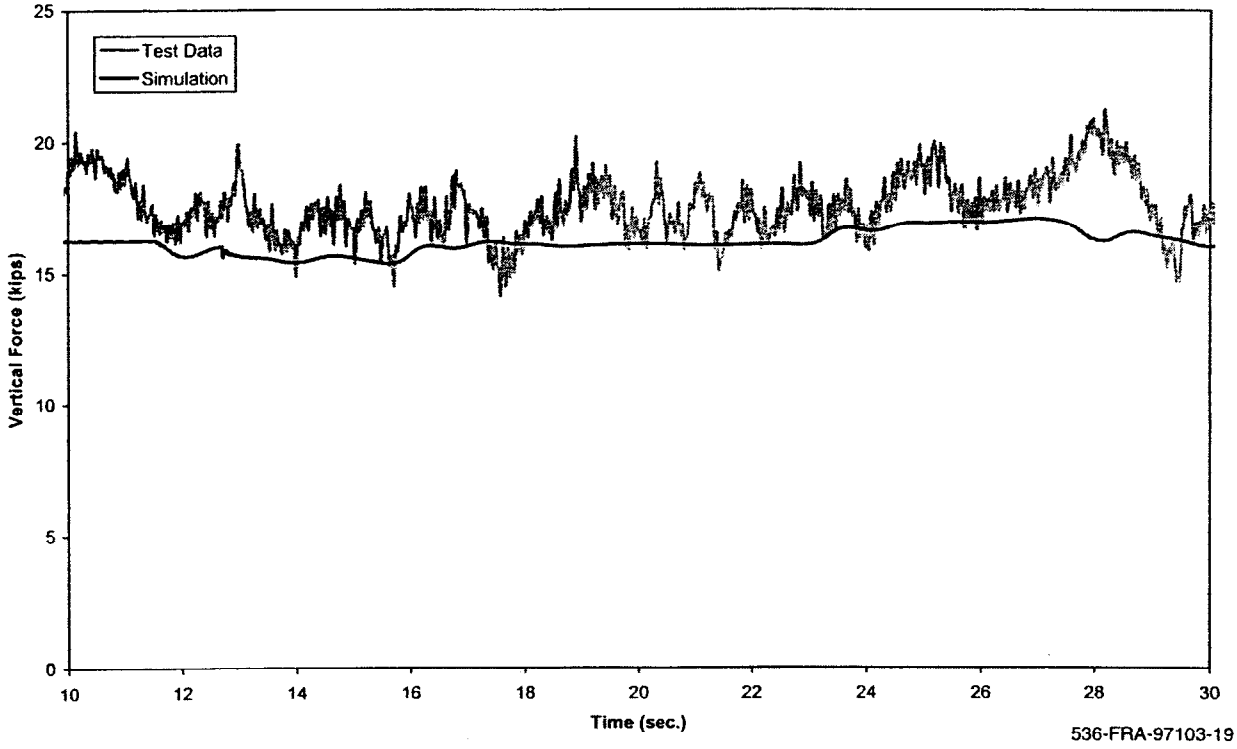

Figure A-6(b). Steady curving - vertical force time history, 84 mph (lead inner wheel)

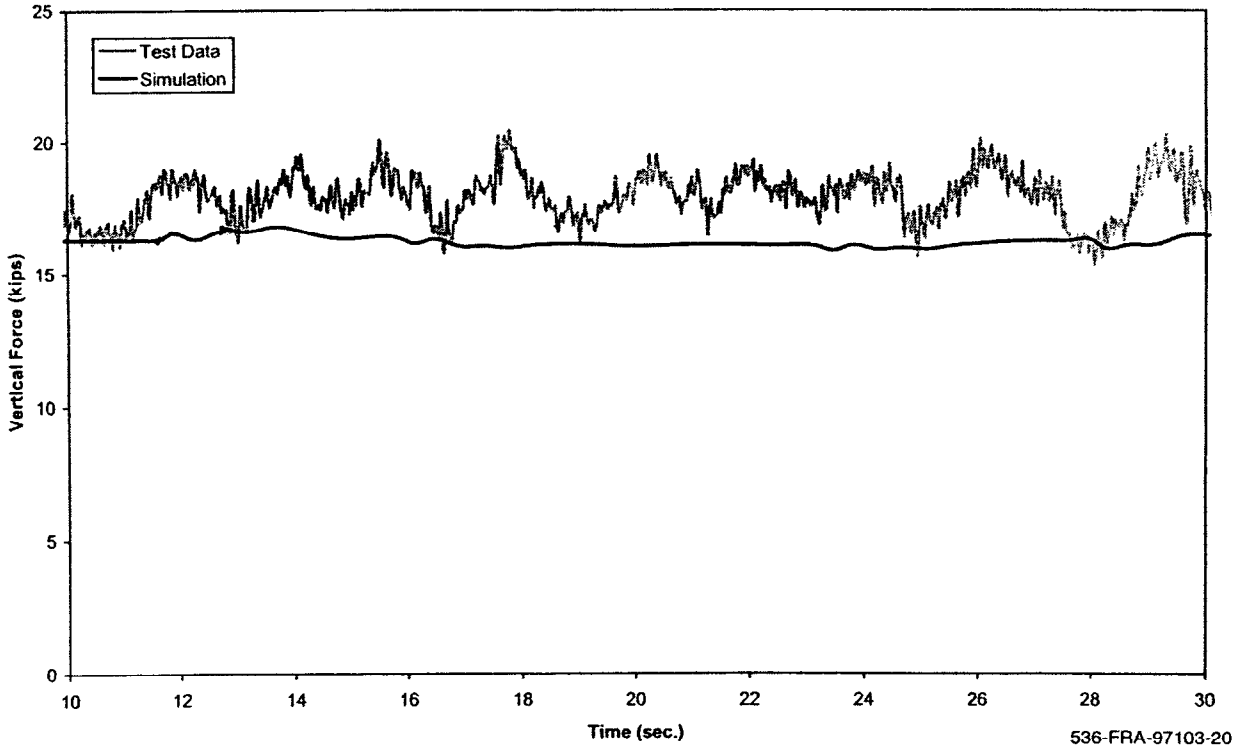

Figure A-6(c). Steady curving - vertical force time history, 84 mph (trailing outer wheel)

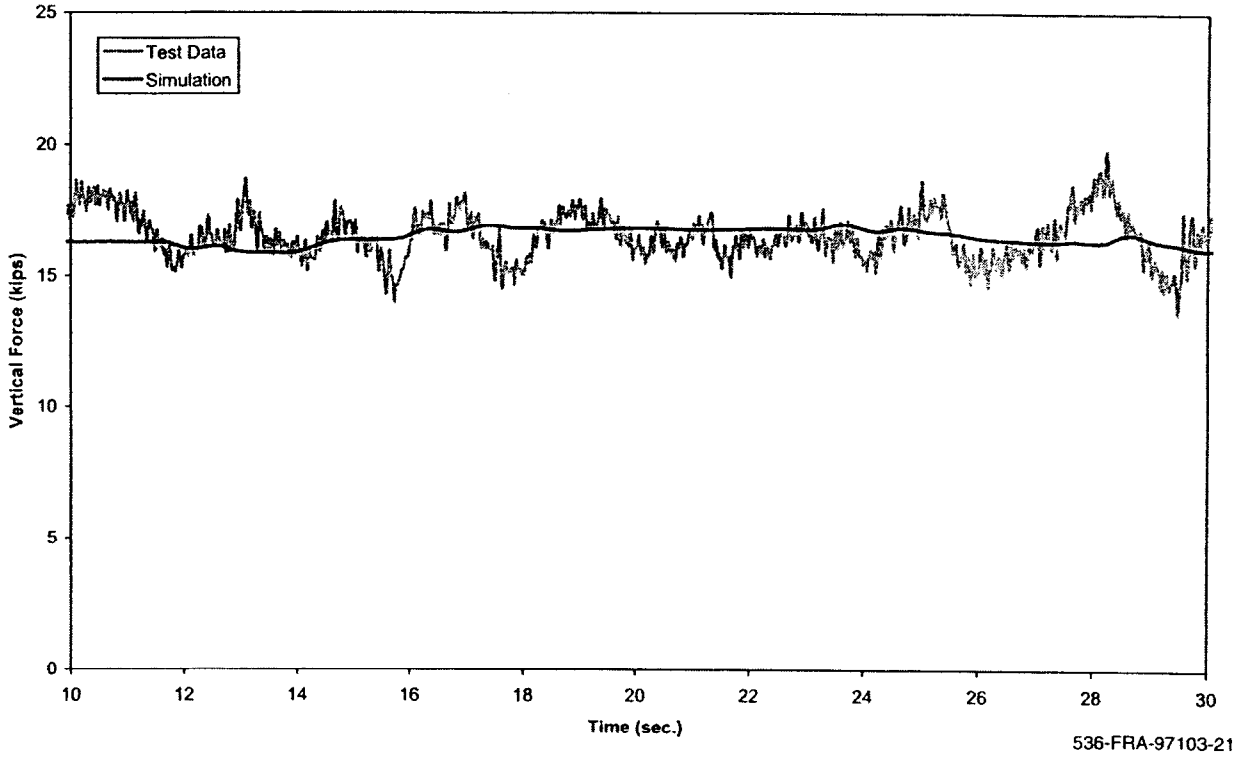

Figure A-6(d). Steady curving - vertical force time history, 84 mph (trailing inner wheel)

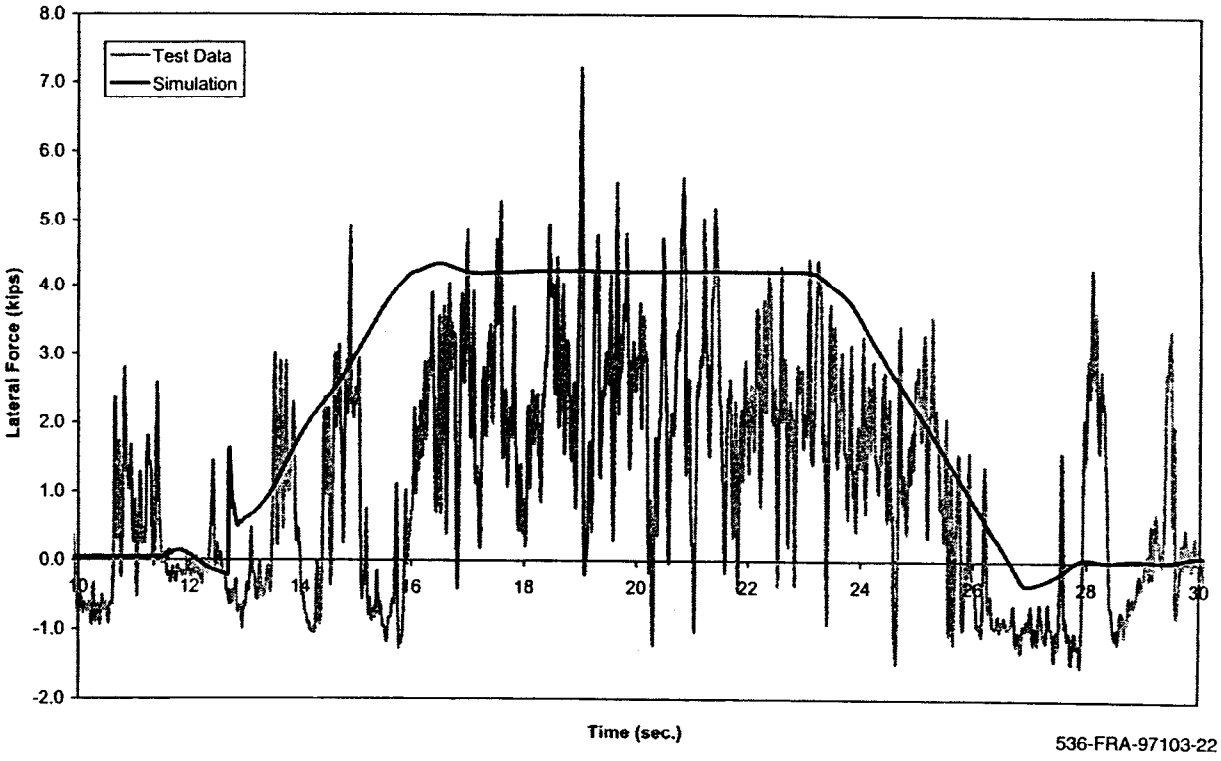

Figure A-7(a). Steady curving - lateral force time history, 84 mph (lead outer wheel)

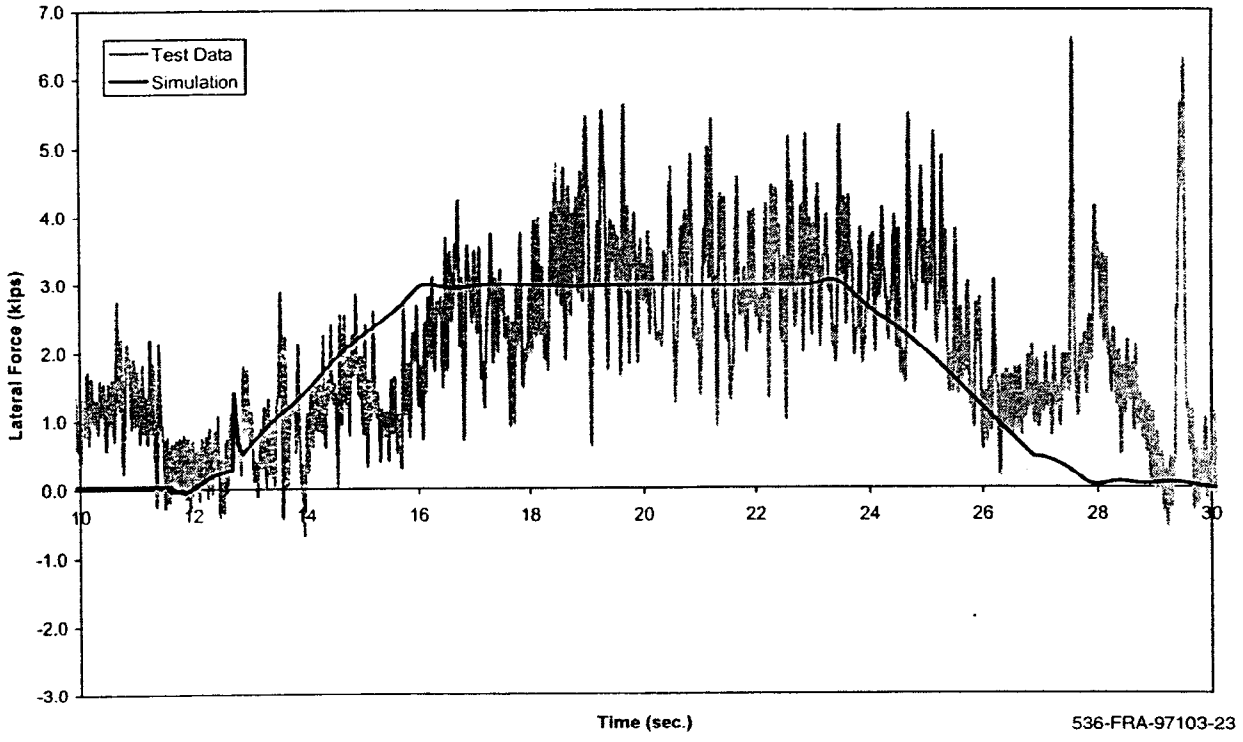

Figure A-7(b). Steady curving - lateral force time history, 84 mph (lead inner wheel)

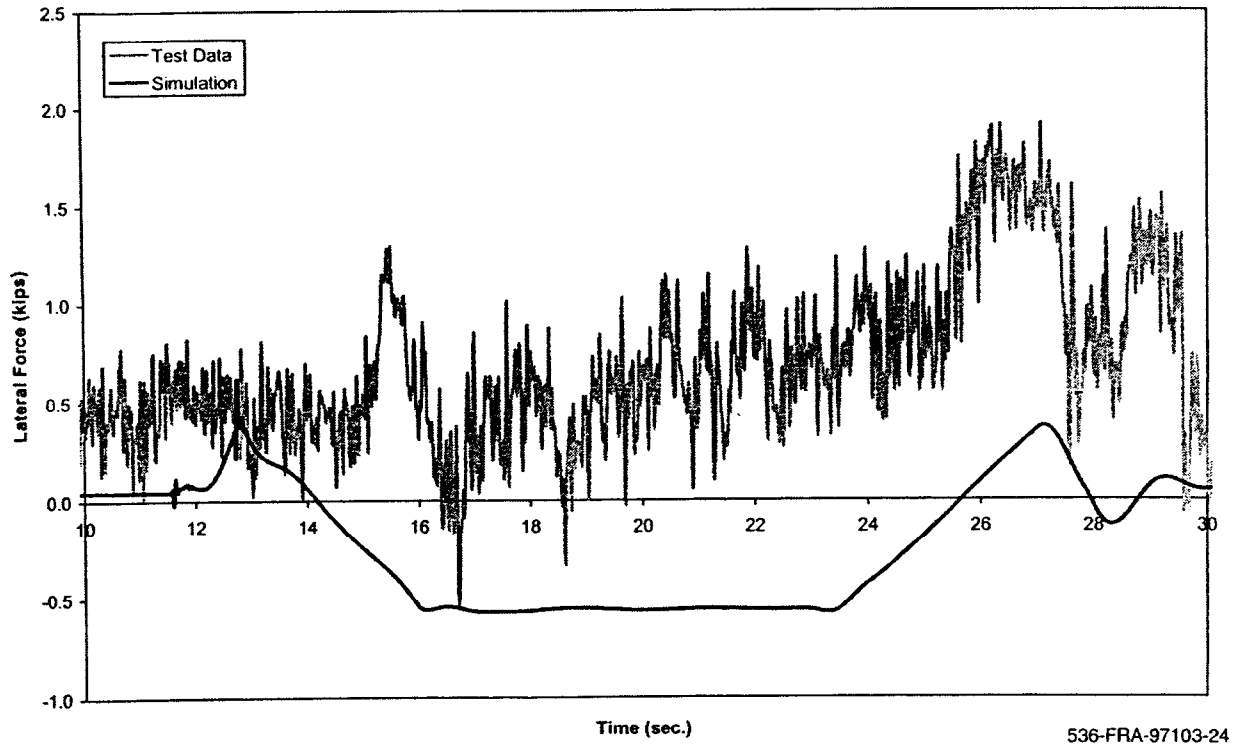

Figure A-7(c). Steady curving - lateral force time history, 84 mph (trailing outer wheel)

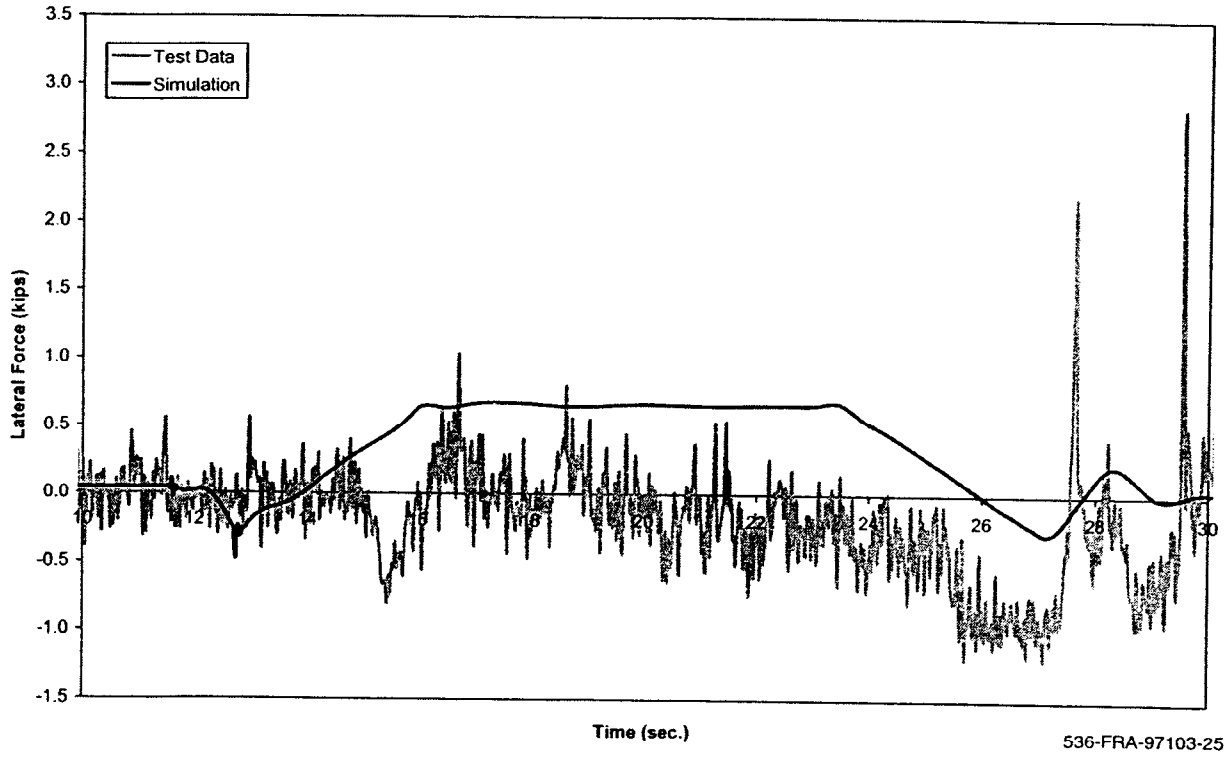

Figure A-7(d). Steady curving - lateral force time history, 84 mph (trailing inner wheel)

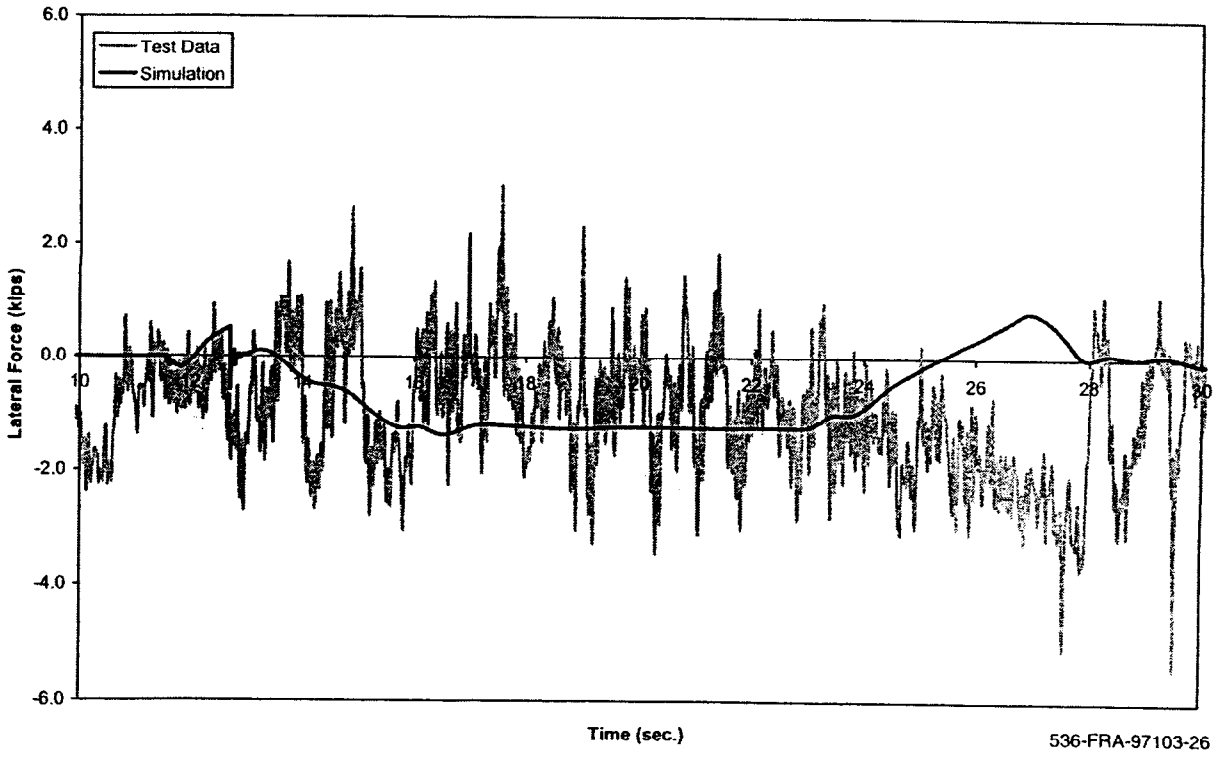

Figure A-8(a). Steady curving - net axle lateral force time history, 84 mph (lead axle)

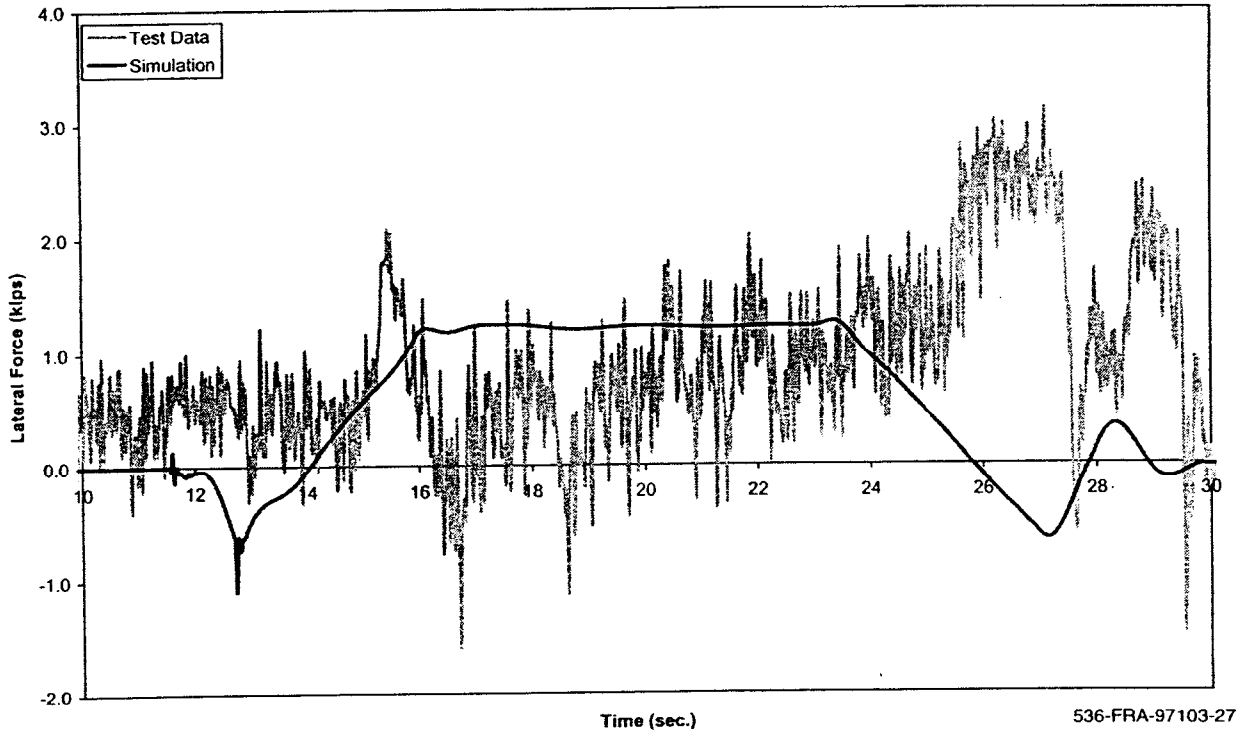

Figure A-8(b). Steady curving - net axle lateral force time history, 84 mph (trailing axle)

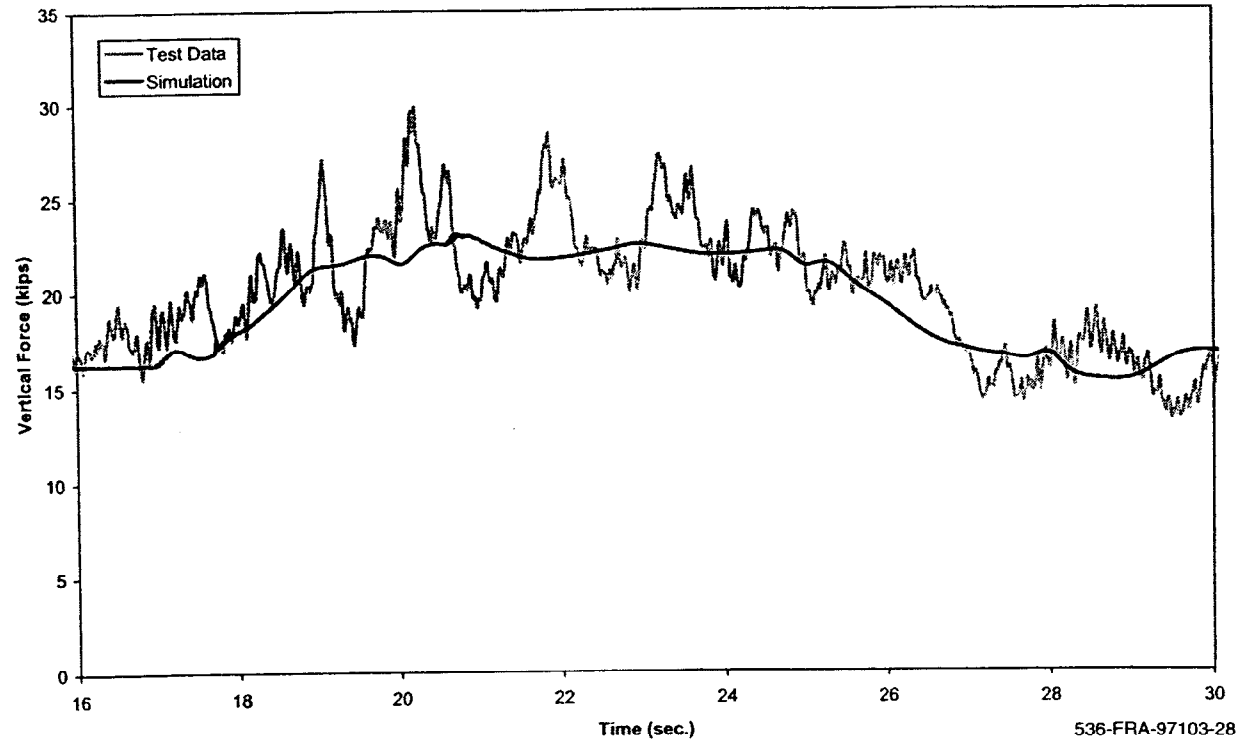

Figure A-9(a). Steady curving - vertical force time history, 124 mph (lead outer wheel)

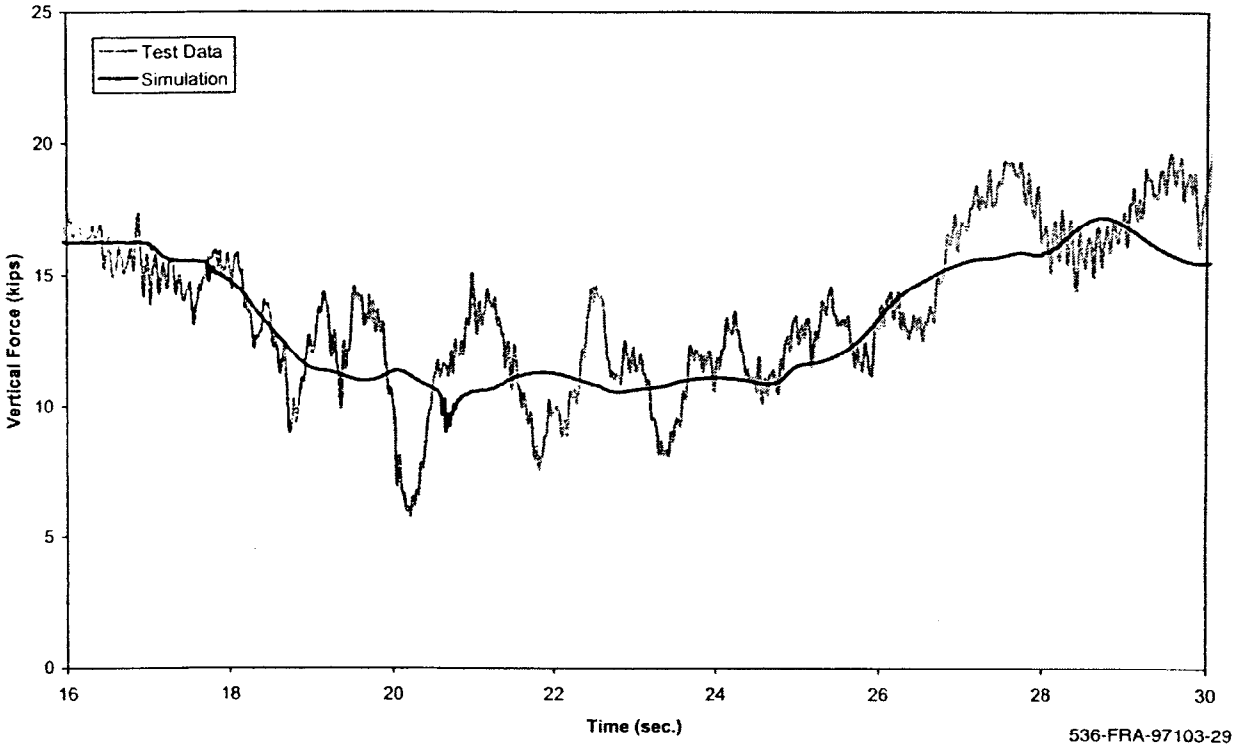

Figure A-9(b). Steady curving - vertical force time history, 124 mph (lead inner wheel)

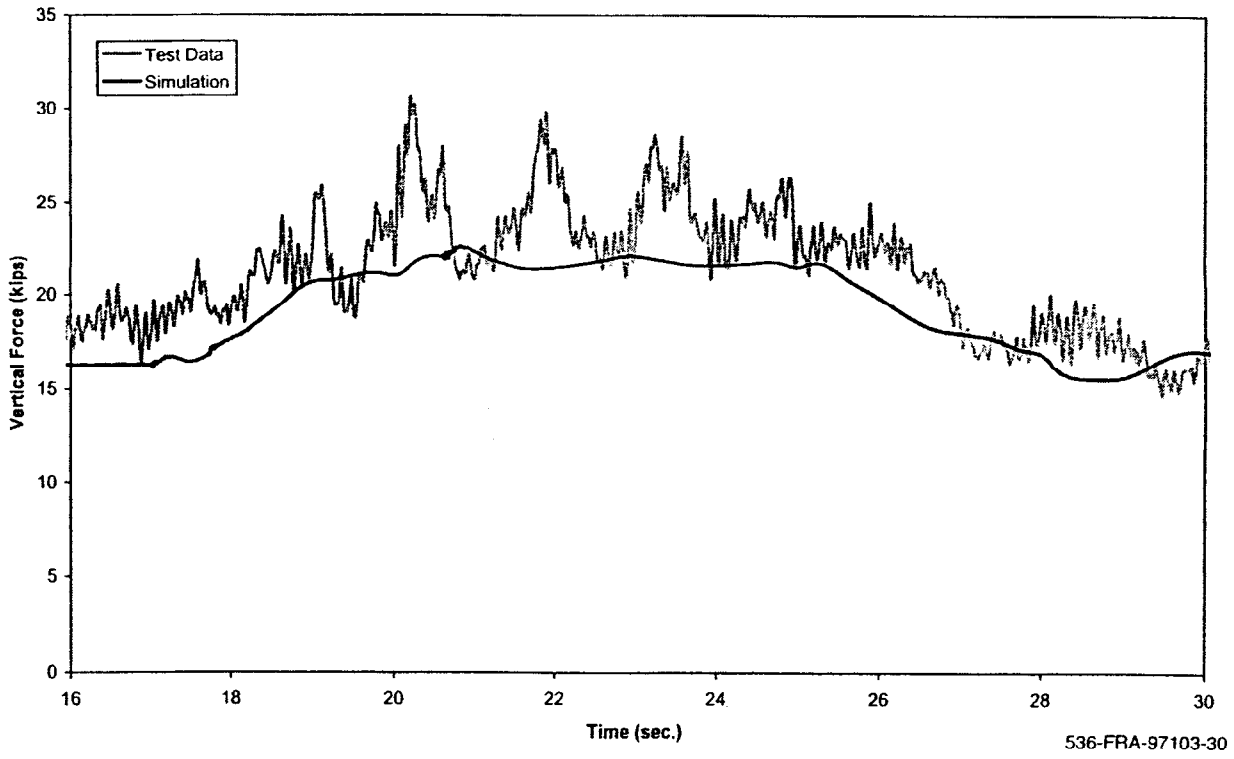

Figure A-9(c). Steady curving - vertical force time history, 124 mph (trailing outer wheel)

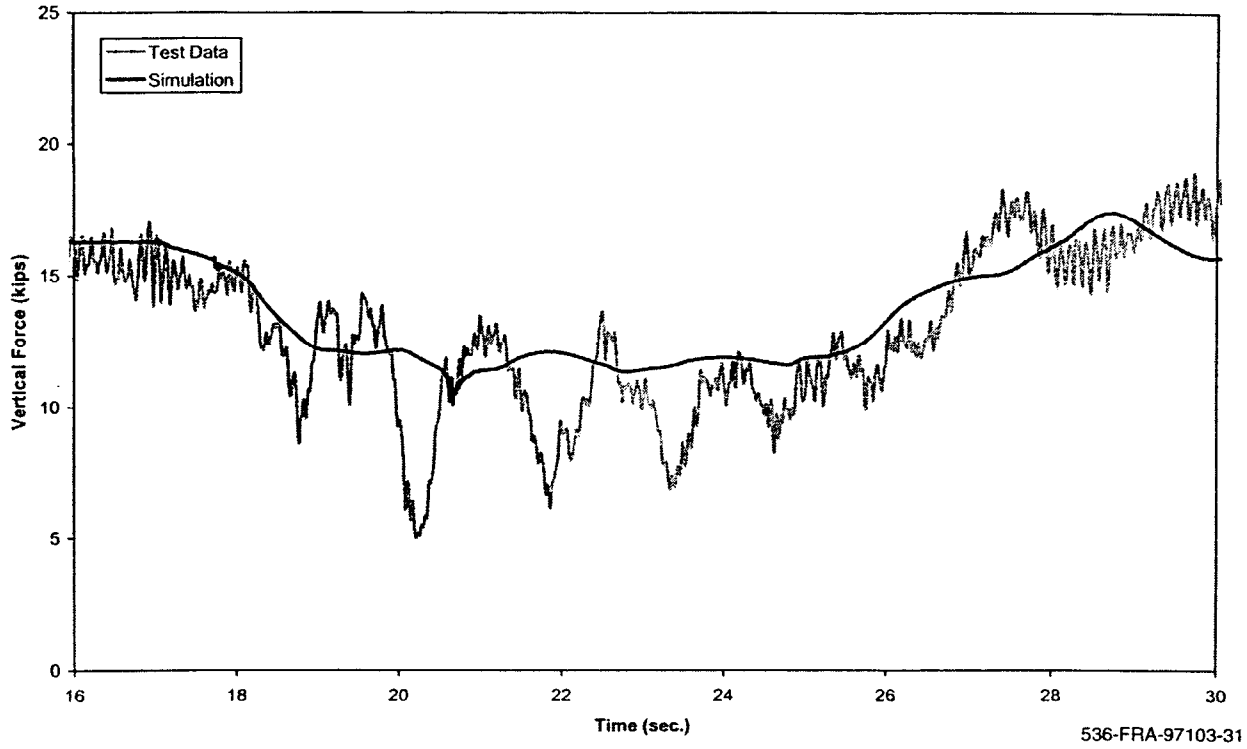

Figure A-9(d). Steady curving - vertical force time history, 124 mph (trailing inner wheel)

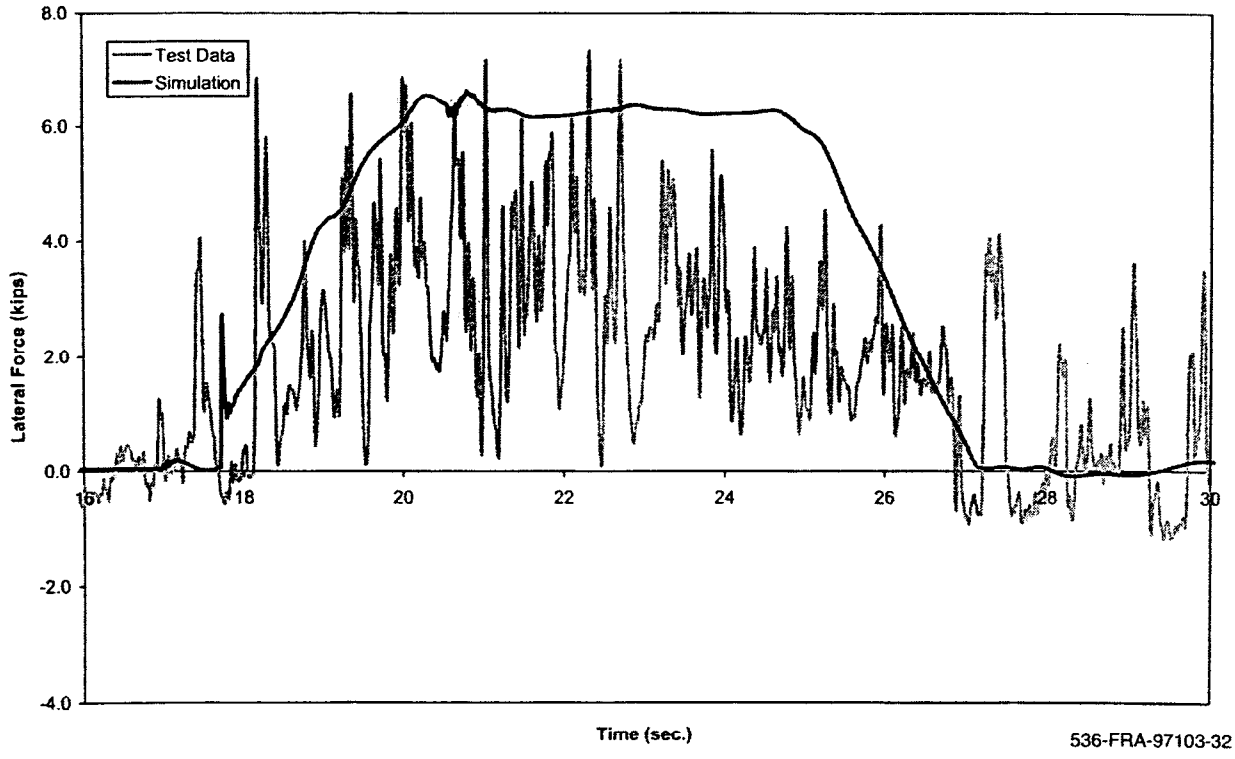

Figure A-10(a). Steady curving - lateral force time history, 124 mph (lead outer wheel)

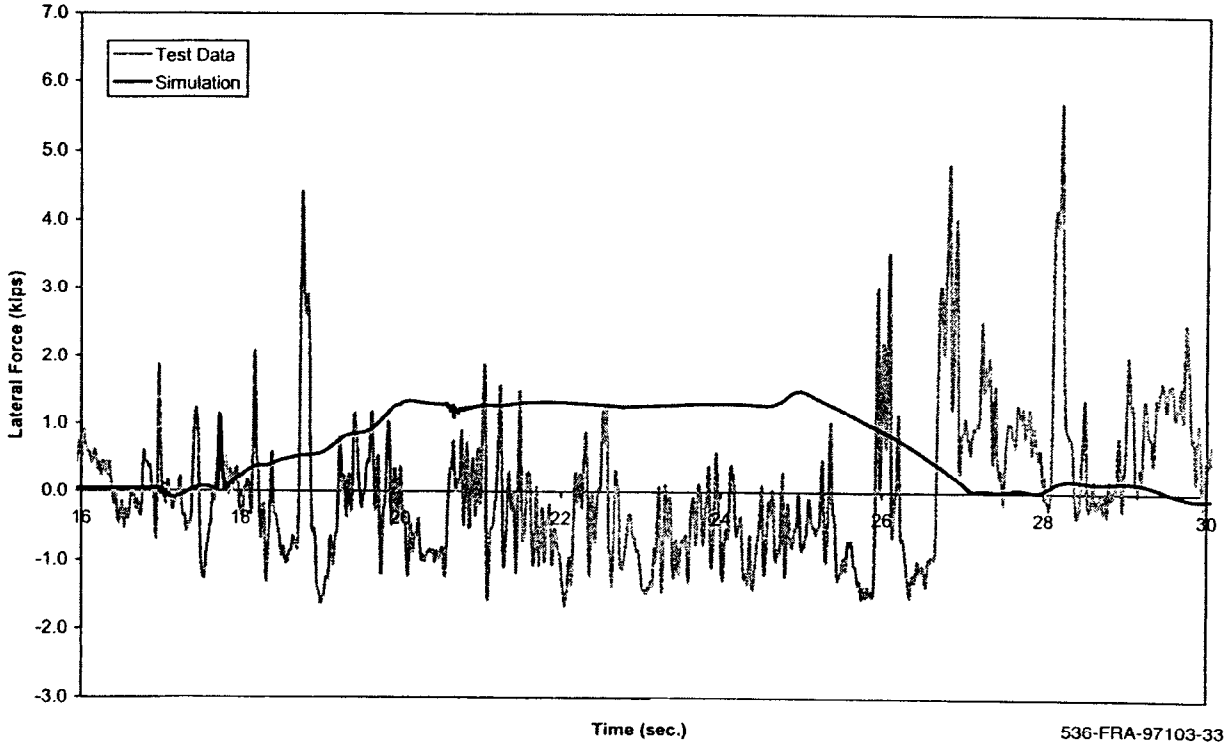

Figure A-10(b). Steady curving - lateral force time history, 124 mph (lead inner wheel)

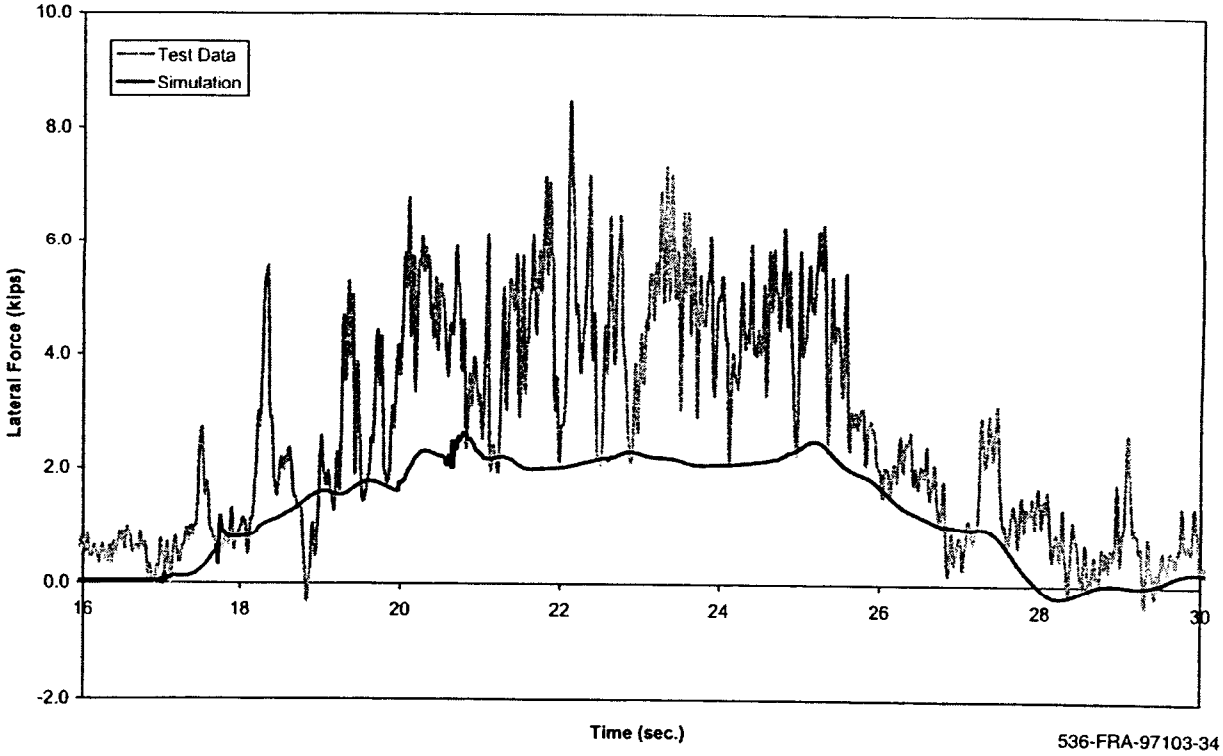

Figure A-10(c). Steady curving - lateral force time history, 124 mph (trailing outer wheel)

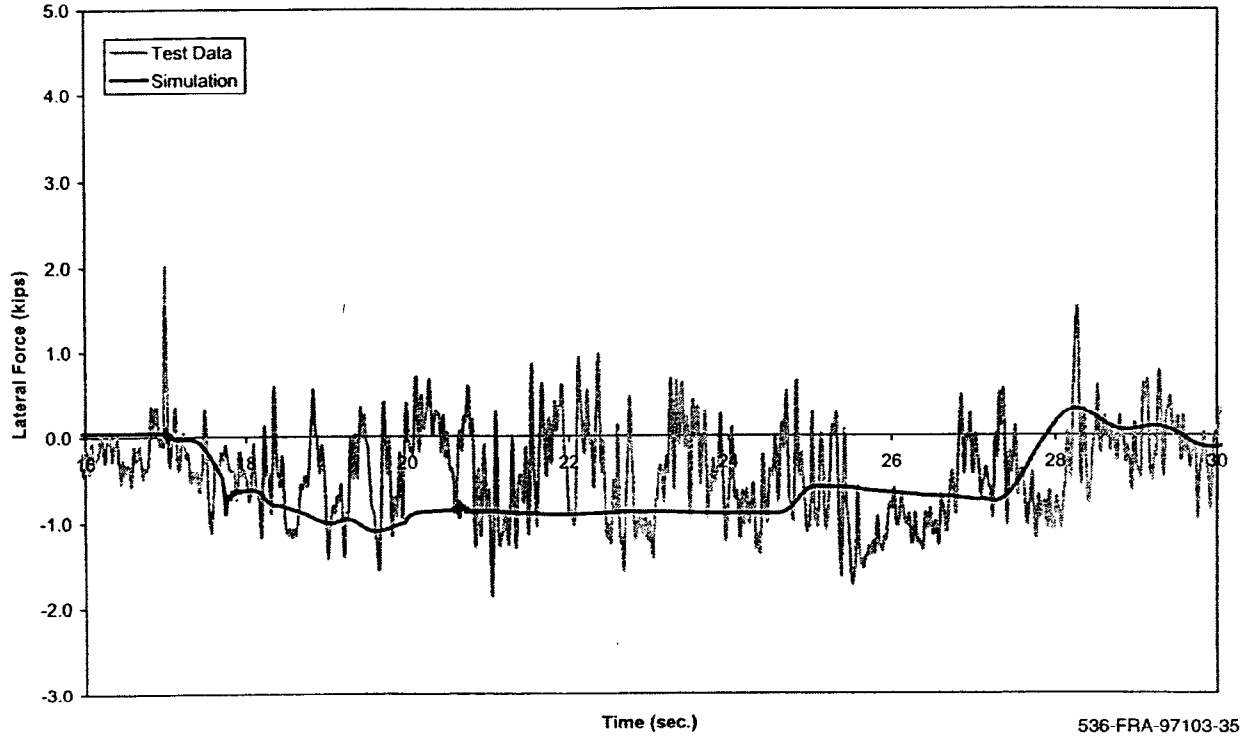

Figure A-10(d). Steady curving - lateral force time history, 124 mph (trailing inner wheel)

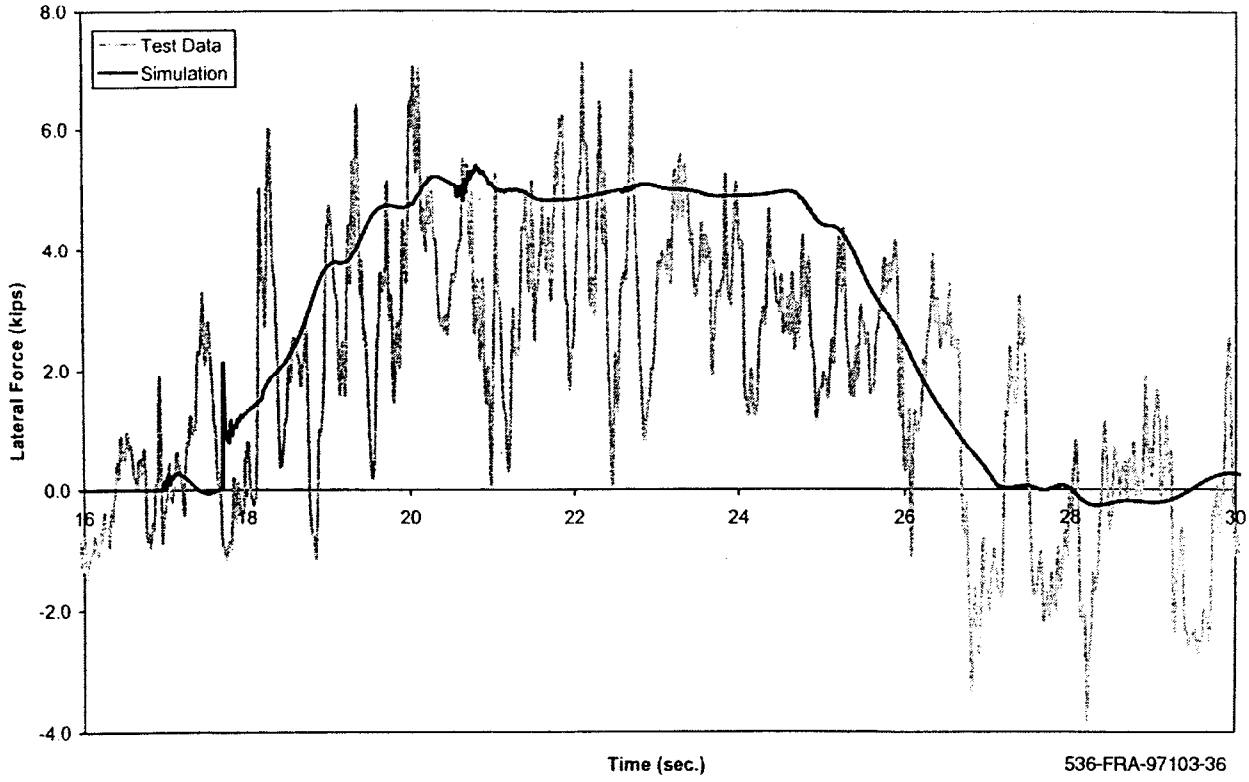

Figure A-11(a). Steady curving - net axle lateral force time history, 124 mph (lead axle)

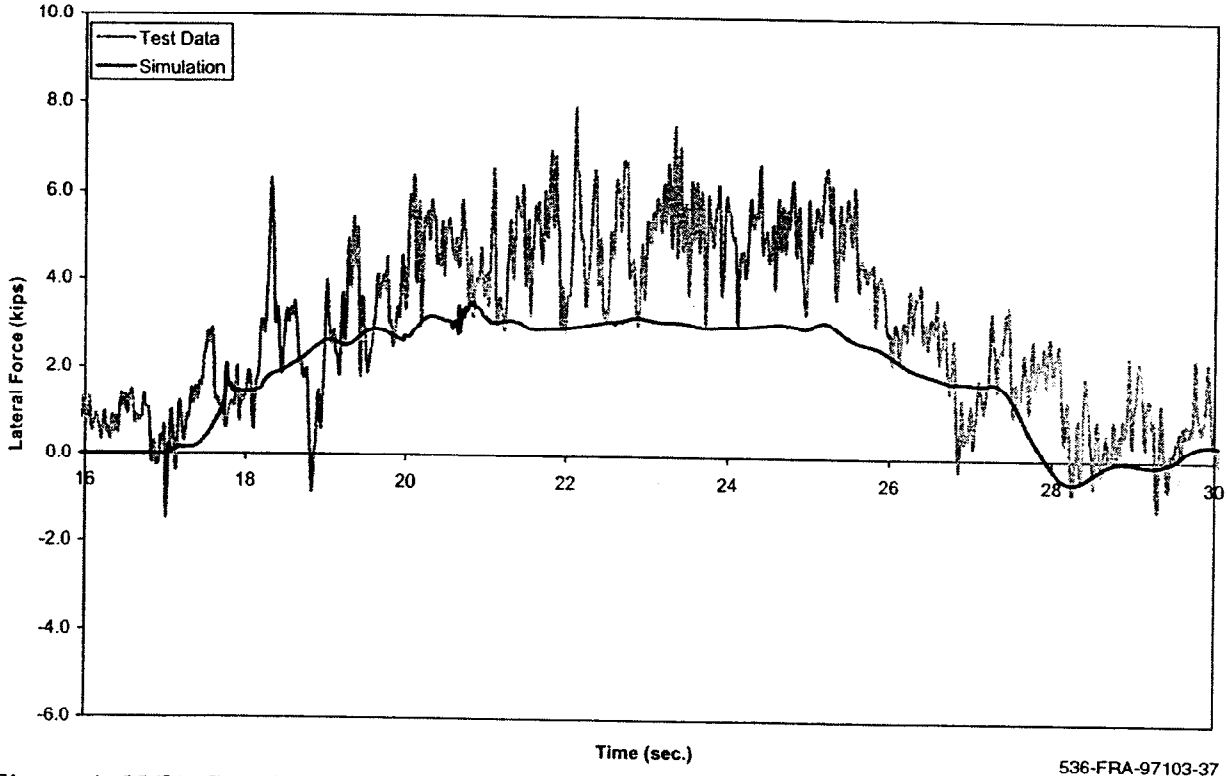

Figure A-11(b). Steady curving - net axle lateral force time history, 124 mph (trailing axle)

124 mph. Vertical force data in Figure A-8 for operation at balance speed show that both the test data and simulation indicate that the vertical forces remain very close to their nominal values for all four wheels during the curve negotiation. The variations in the test data (Figure A-6) from the nominal value are believed due to local track perturbations. The lateral force data (Figure A-7) for the individual wheels have close agreement between the simulation and the test data. Comparison of the simulation and test data for the net lateral force on the lead and trailing axles, summarized in Figure A-8, also has close correlations. For the lead axle, simulation gives -1.0 kip compared with test data of approximately 0.75 kip. For the trailing axle, simulation gives 1.0 kip, which is almost the same value as the test data. Both the individual wheel lateral loads and the net axle lateral loads from the simulation and test agree. The sum of the two net axle loads is approximately zero for operation at balance speed in both the simulation and test data, as one would expect.

The vertical force data, presented in Figure A-9, shows that at 124 mph, the outer wheel vertical force increases to approximately 22 to 23 kips and the inner wheel value decreases to approximately 10 kips for both axles. The test and simulation data are close. Lead axle lateral force data (Figure A-10) shows that the outer wheel is approximately 6 kips for the simulation in comparison to 4 kips for the test data, whereas the inner wheel is 1.0 kip for the simulation and approximately -0.5 kip for the test data. The trailing axle lateral force for the outer wheel is 2 kips in the simulation and approximately 4 kips in the test data and for the inner wheel is -1.0 kip for the simulation in comparison to approximately -0.75 kips for the test data.

The net axle lateral force for both axles is presented in Figure A-11. The lead axle net lateral force is approximately 5 kips with close agreement between the simulation and test data while the trailing axle lateral force is 3 kips for the simulation and approximately 3.5 kips for the test data. The net axle lateral forces are in relatively good agreement between the simulation and test data and reflect a net truck lateral force of approximately 8 to 8.5 kips for the over balance speed of approximately 7 in. The theoretical value is 8.0 kips and is calculated as the difference between centripetal force and the horizontal component of the weight.

A.3 Dynamic Curving

The vertical and lateral forces for the trailing truck wheels are shown in Figures A-12 and A-13, respectively for operation at 20 mph. The vertical force simulation and test data are in good agreement. The vertical forces vary from 14 to 20 kips as the perturbations are negotiated. The lateral force waveforms for the simulation and test data are similar for the trailing axle wheels, and the amplitudes are in good agreement. For the lead axle, simulation data shows higher (by approximately 4 kips) average values of force on both the outer and inner wheels.

Data for operation at 28 mph, illustrated in Figure A-14, also indicate good correlation between the vertical forces predicted and measured for all four wheels. The lateral force data of Figure A-15 for the trailing axle are also in reasonable agreement. The lead axle simulation has an average value of approximately 3 to 4 kips greater than the test data for the inner and outer wheels.

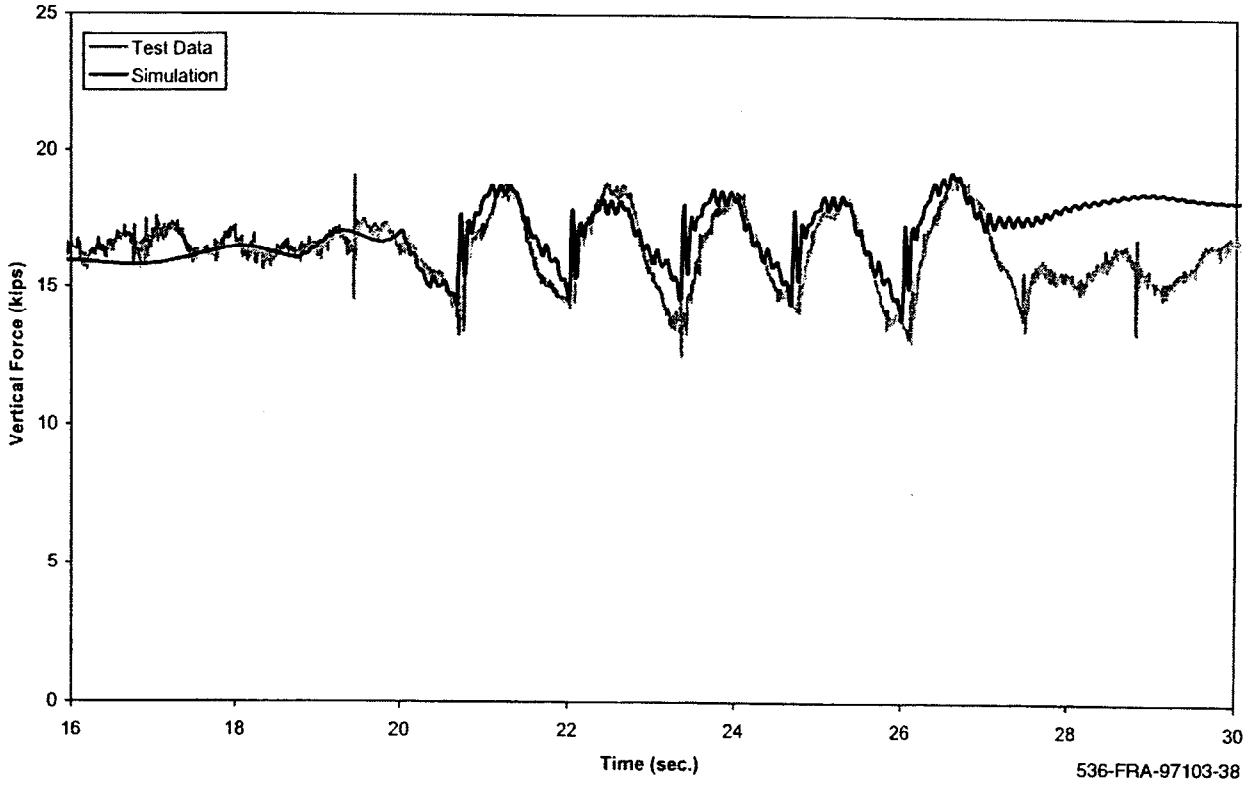

Figure A-12(a). Dynamic curving - vertical force time history, 20 mph (lead outer wheel)

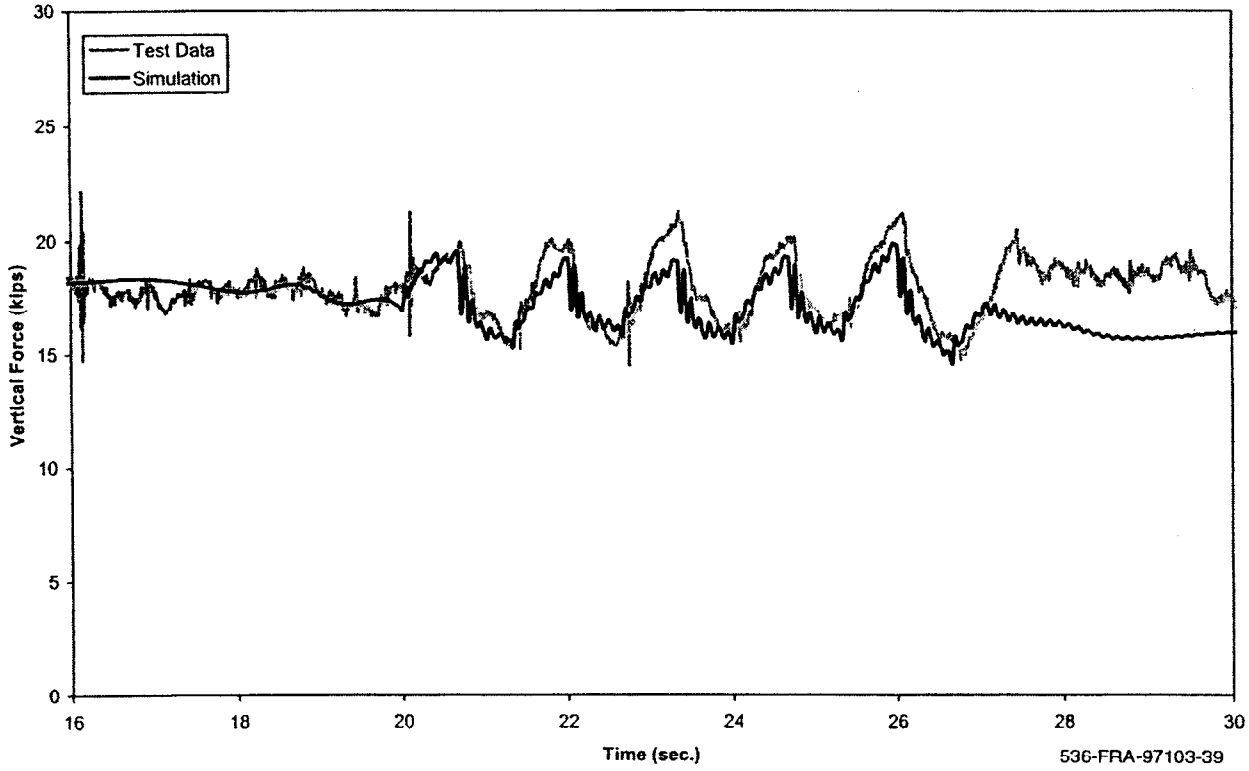

Figure A-12(b). Dynamic curving - vertical force time history, 20 mph (lead inner wheel)

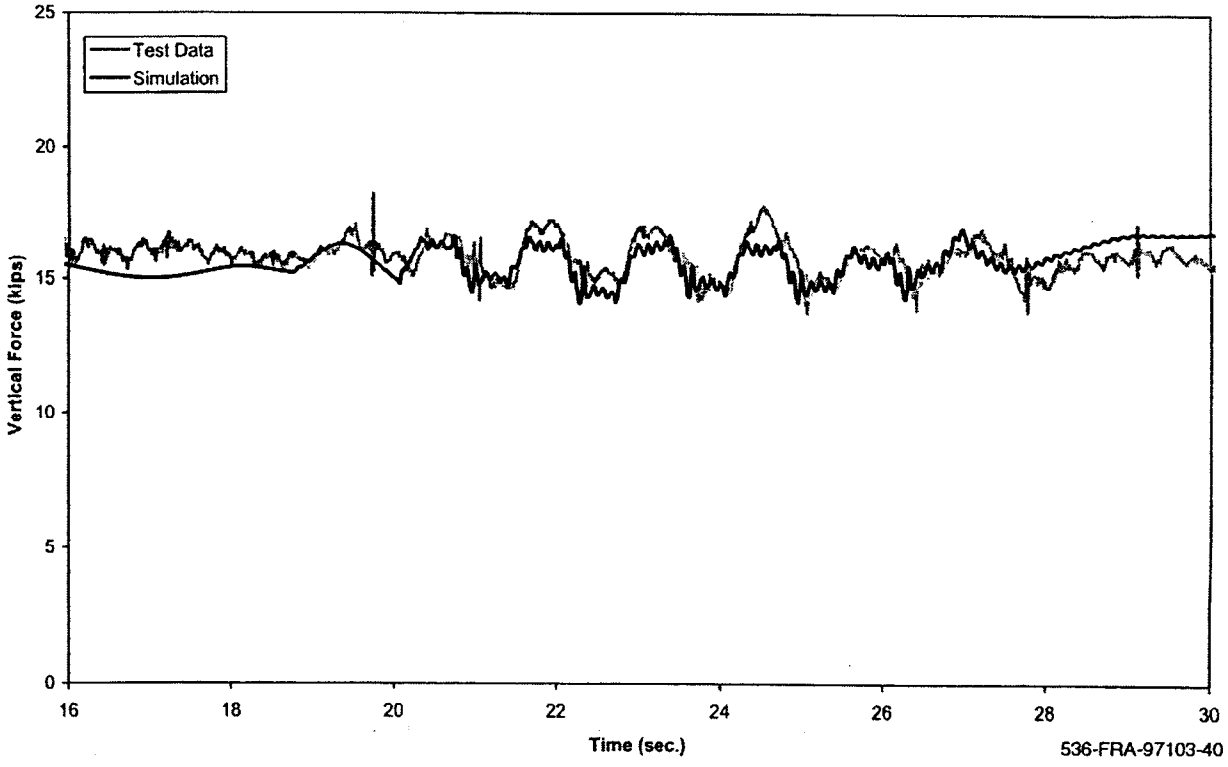

Figure A-12(c). Dynamic curving - vertical force time history, 20 mph (trailing outer wheel)

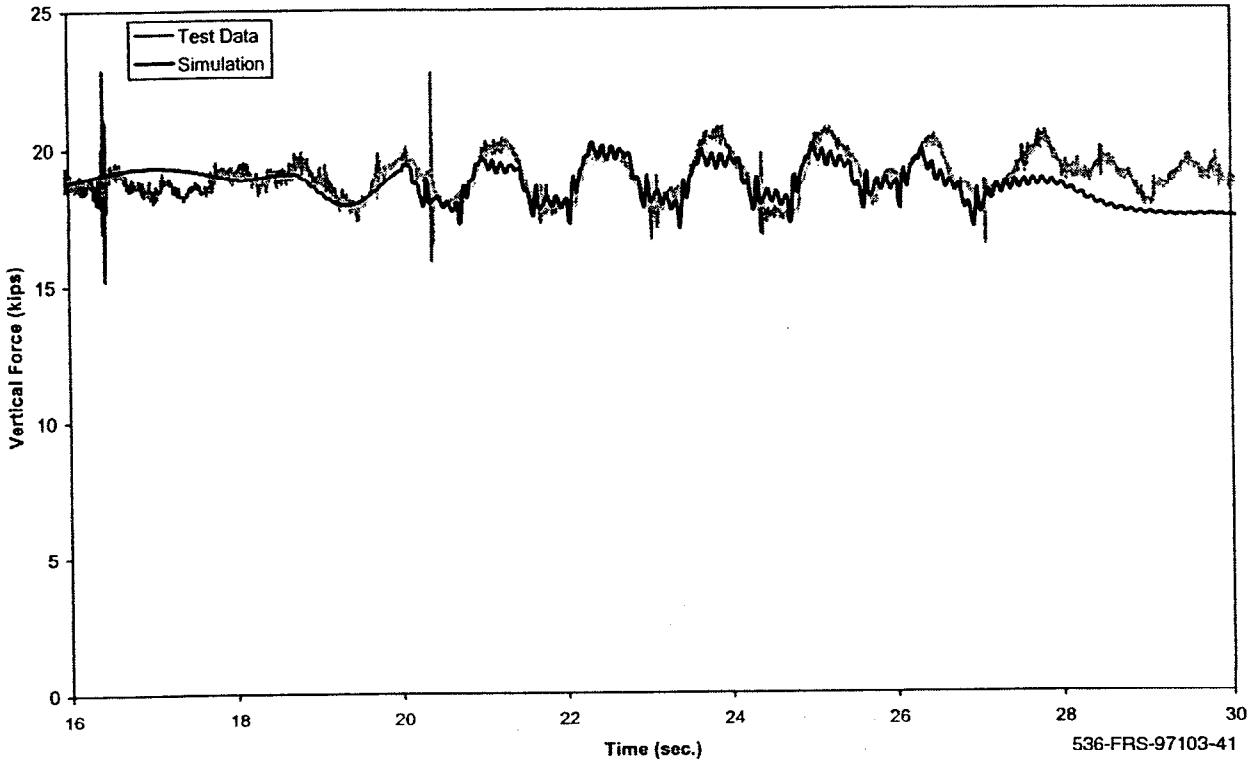

Figure A-12(d). Dynamic curving - vertical force time history, 20 mph (trailing inner wheel)

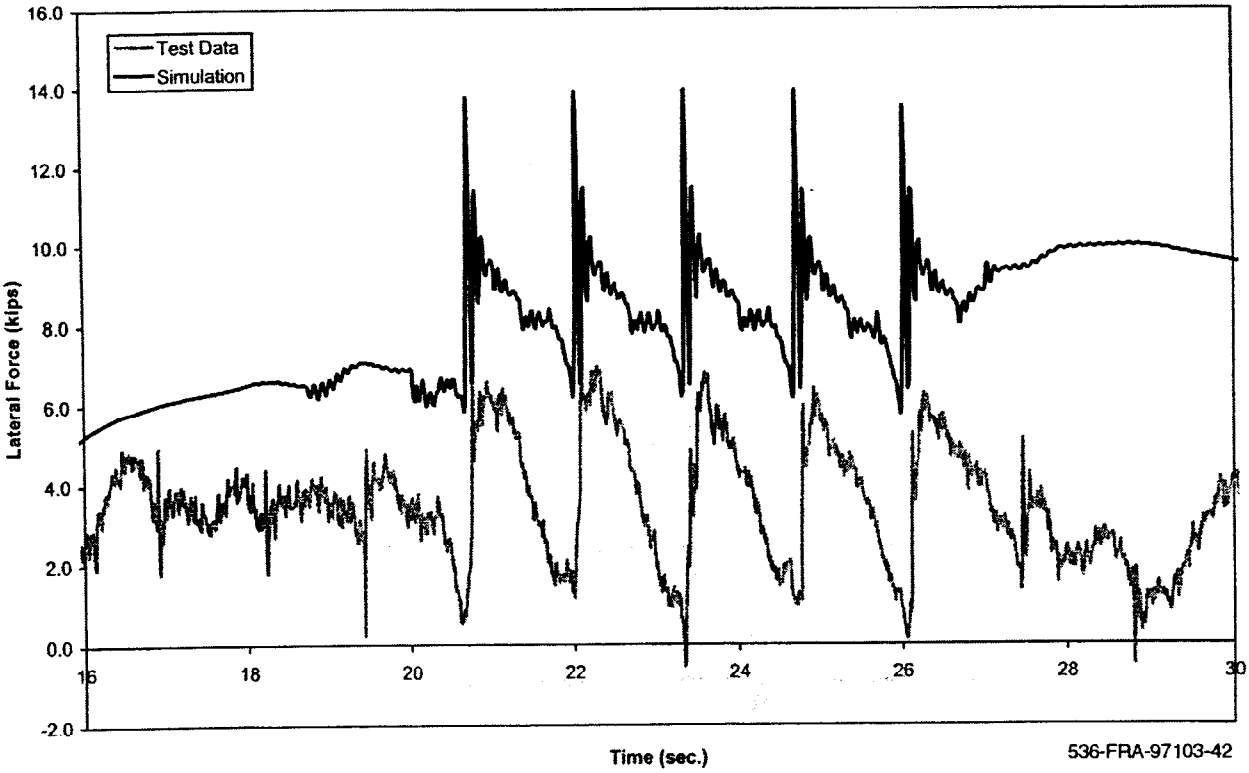

Figure A-13(a). Dynamic curving - lateral force time history, 20 mph (lead outer wheel)

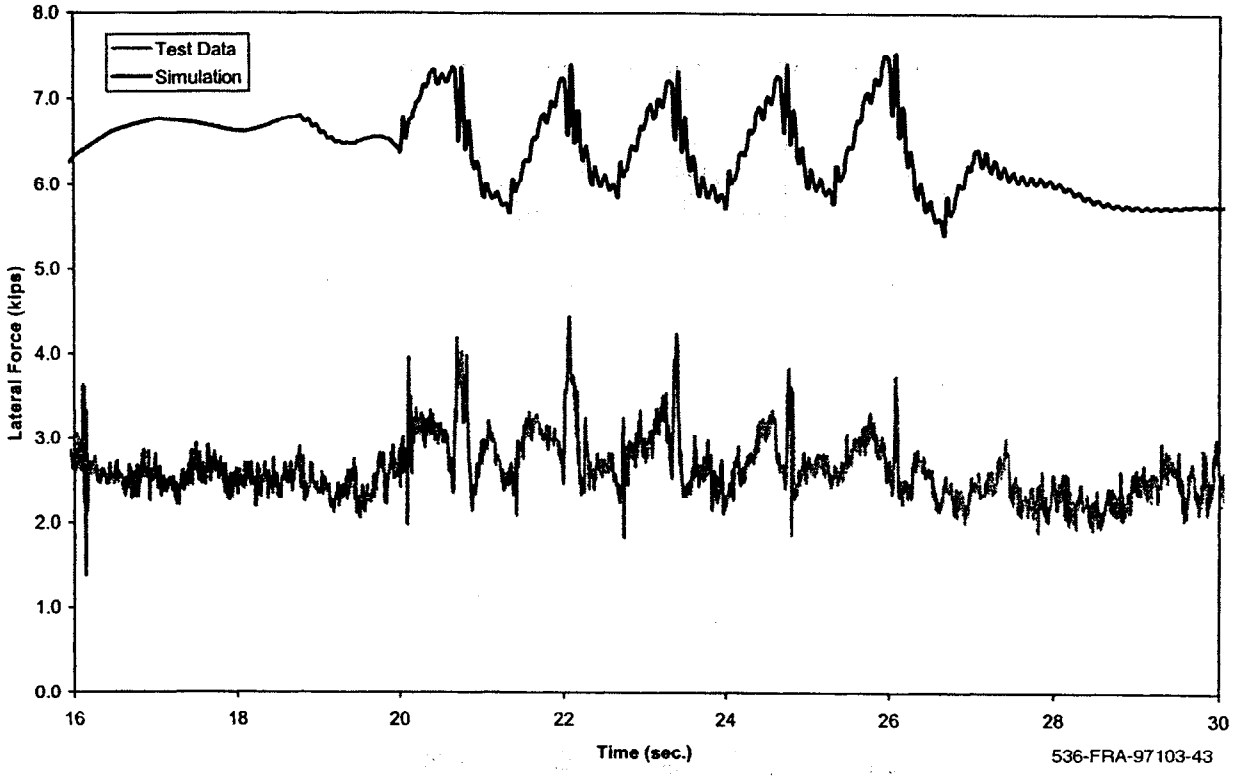

Figure A-13(b). Dynamic curving - lateral force time history, 20 mph (lead inner wheel)

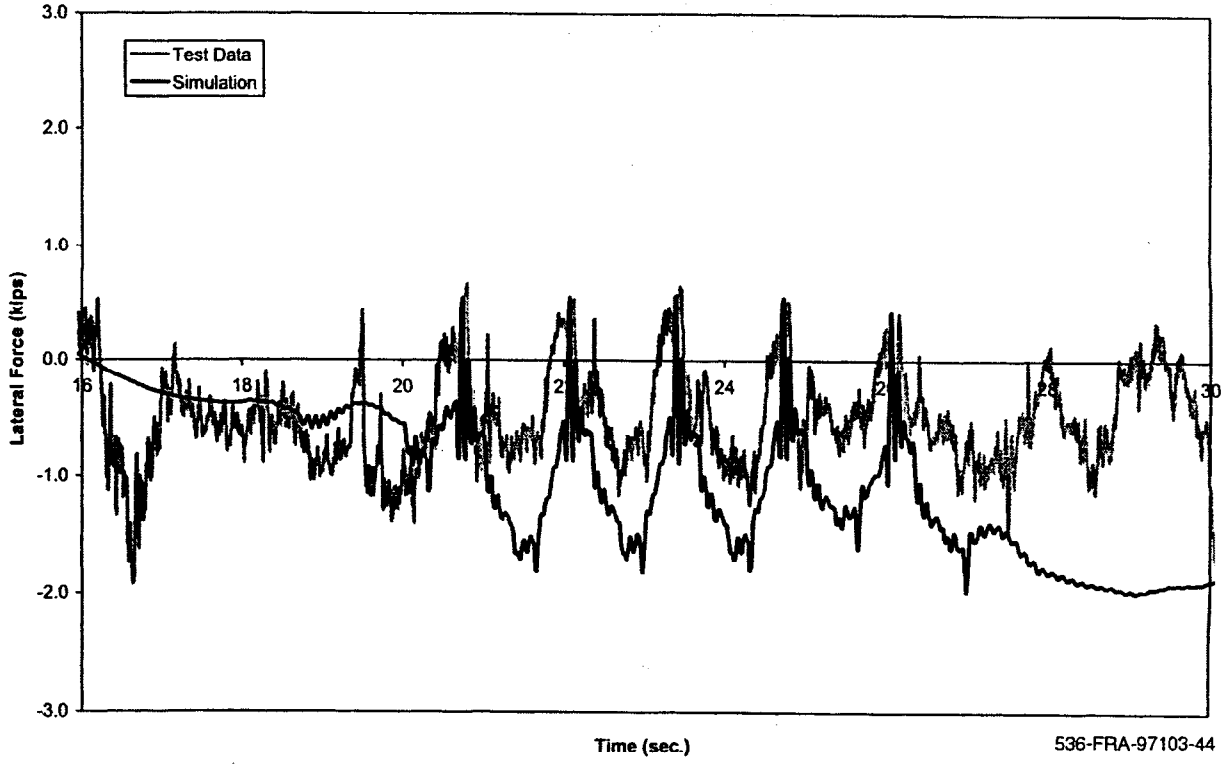

Figure A-13(c). Dynamic curving - lateral force time history, 20 mph (trailing outer wheel)

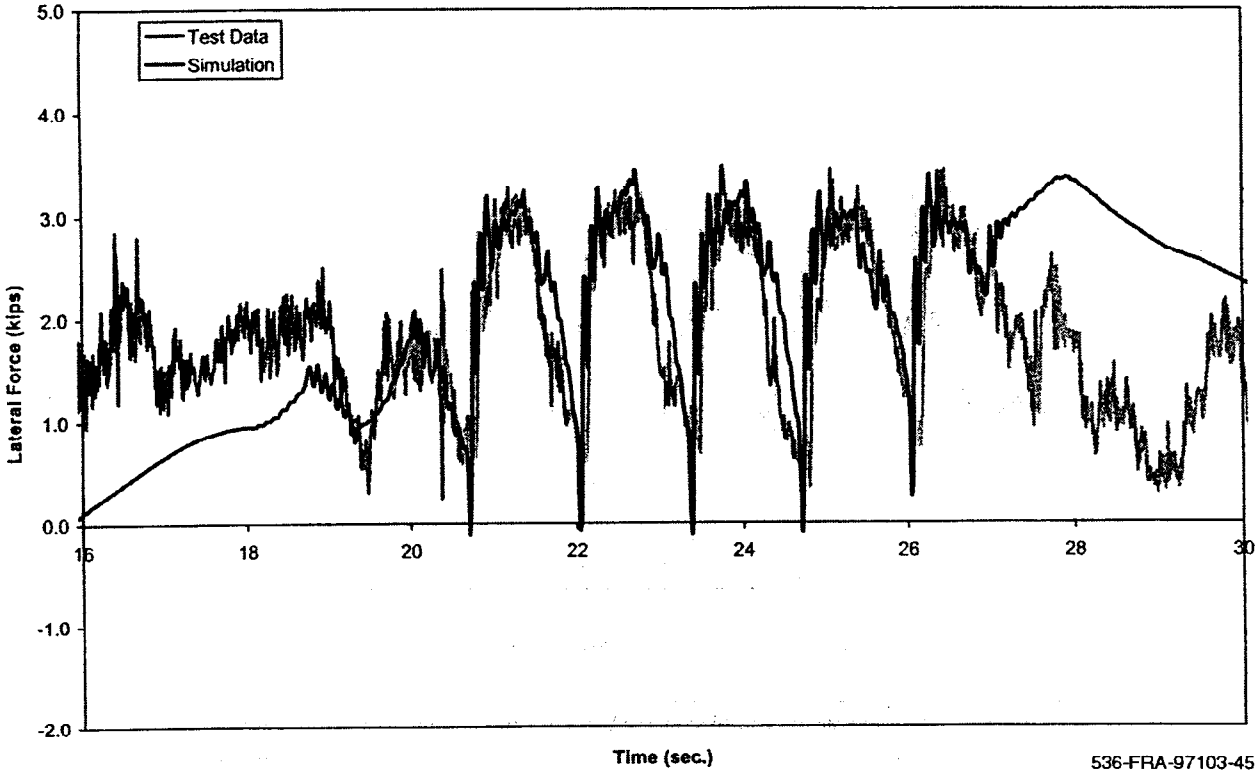

Figure A-13(d). Dynamic curving - lateral force time history, 20 mph (trailing inner wheel)

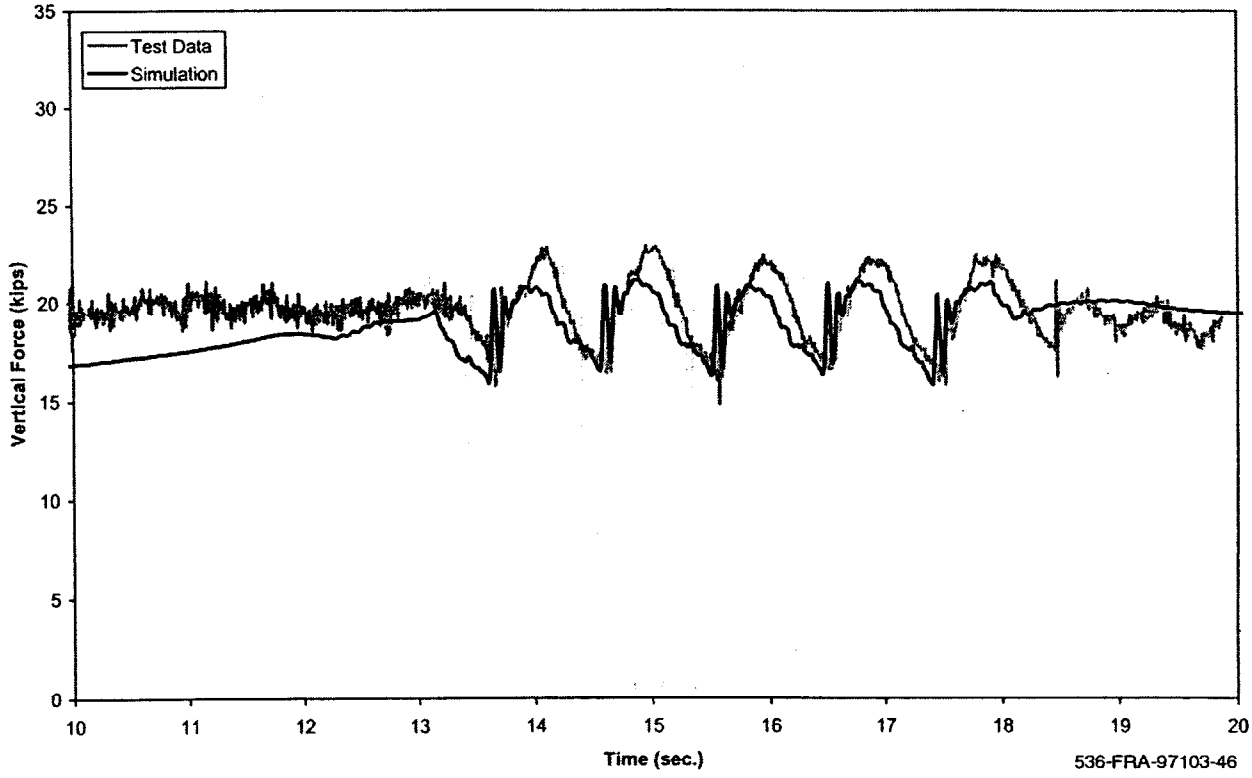

Figure A-14(a). Dynamic curving - vertical force time history, 28 mph (lead outer wheel)

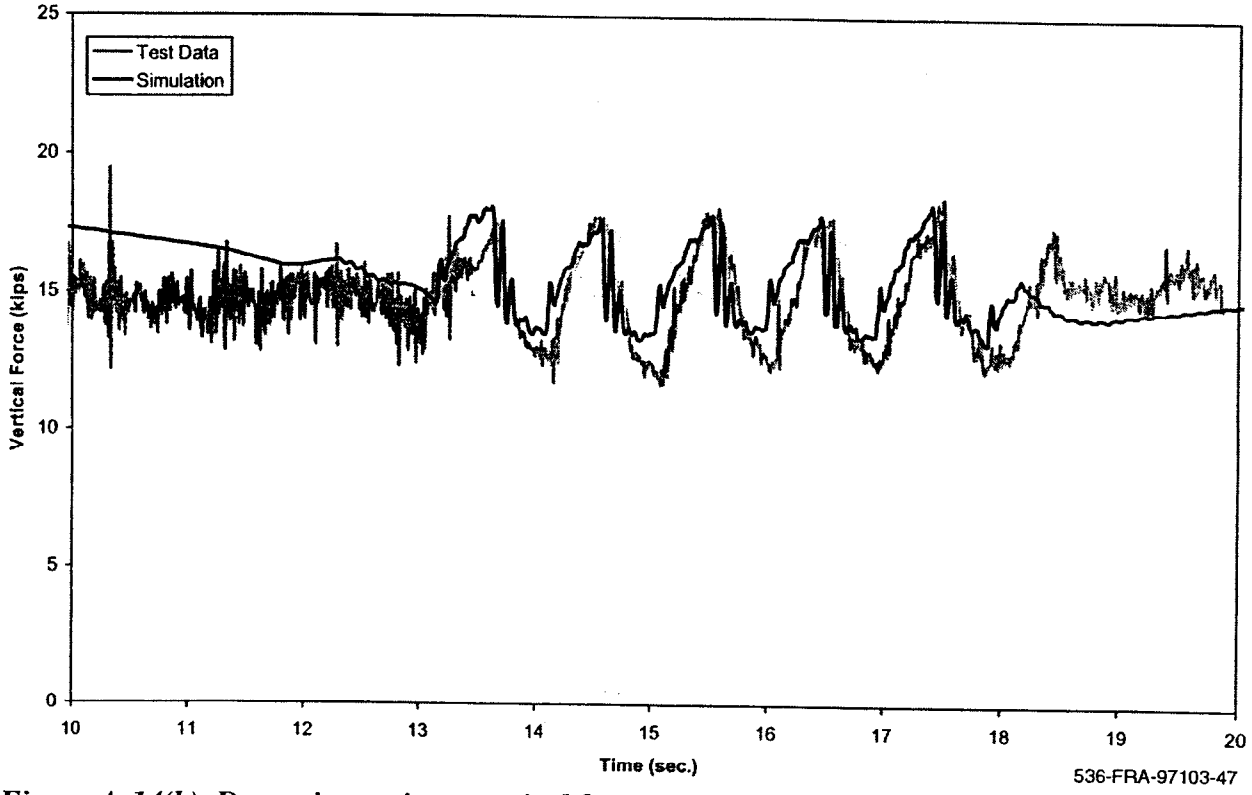

Figure A-14(b). Dynamic curving - vertical force time history, 28 mph (lead inner wheel)

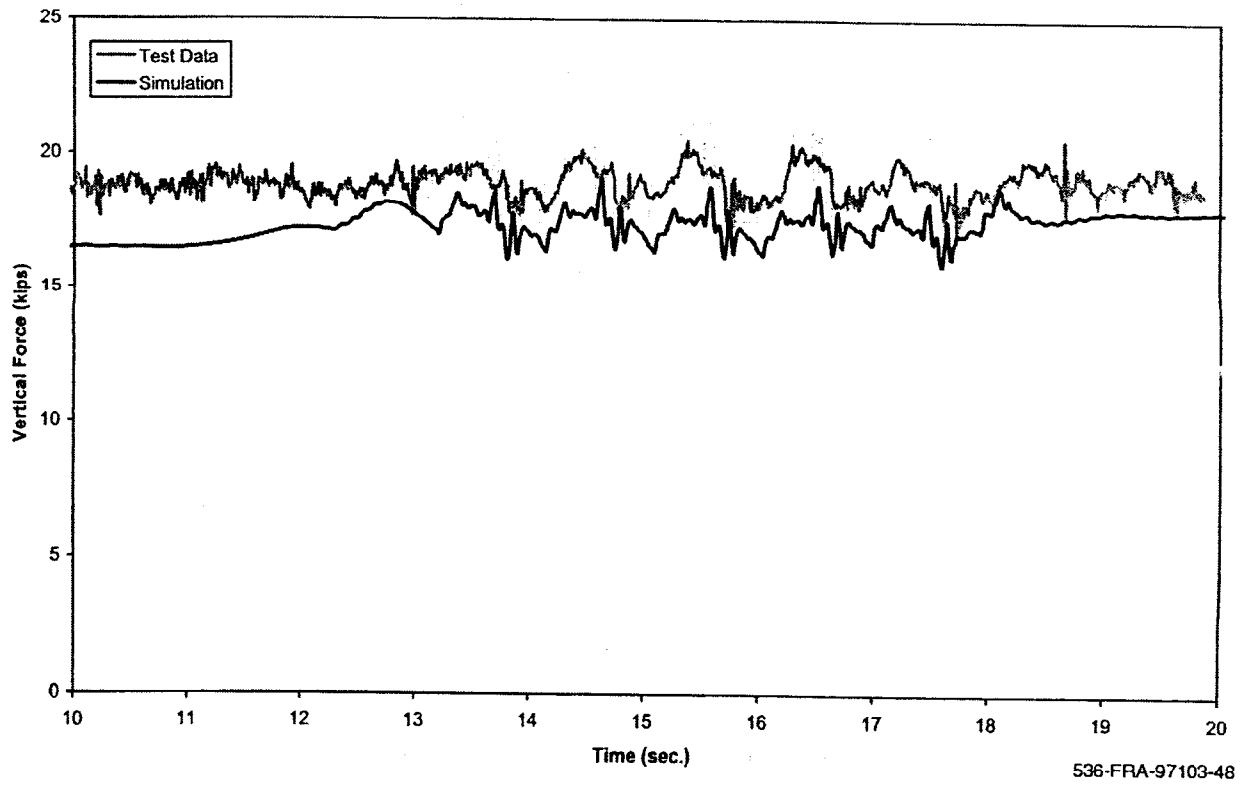

Figure A-14(c). Dynamic curving - vertical force time history, 28 mph (trailing outer wheel)

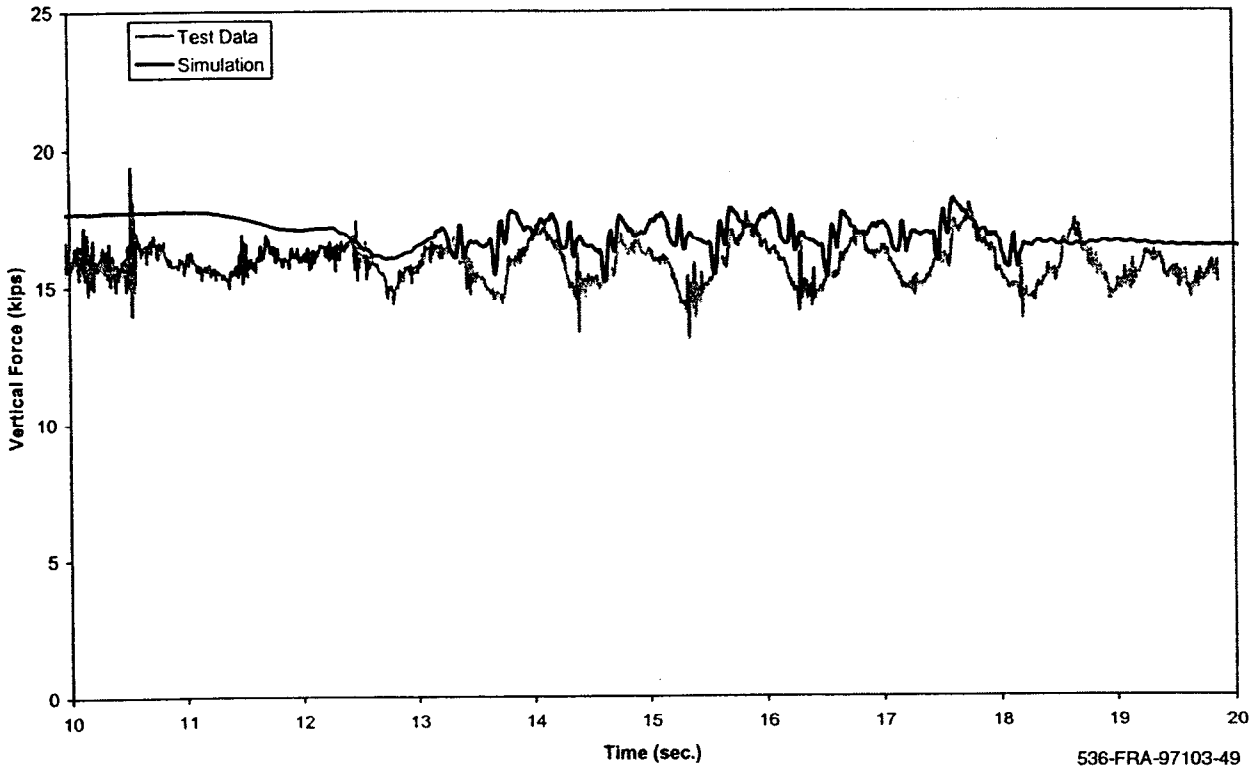

Figure A-14(d). Dynamic curving - vertical force time history, 28 mph (trailing inner wheel)

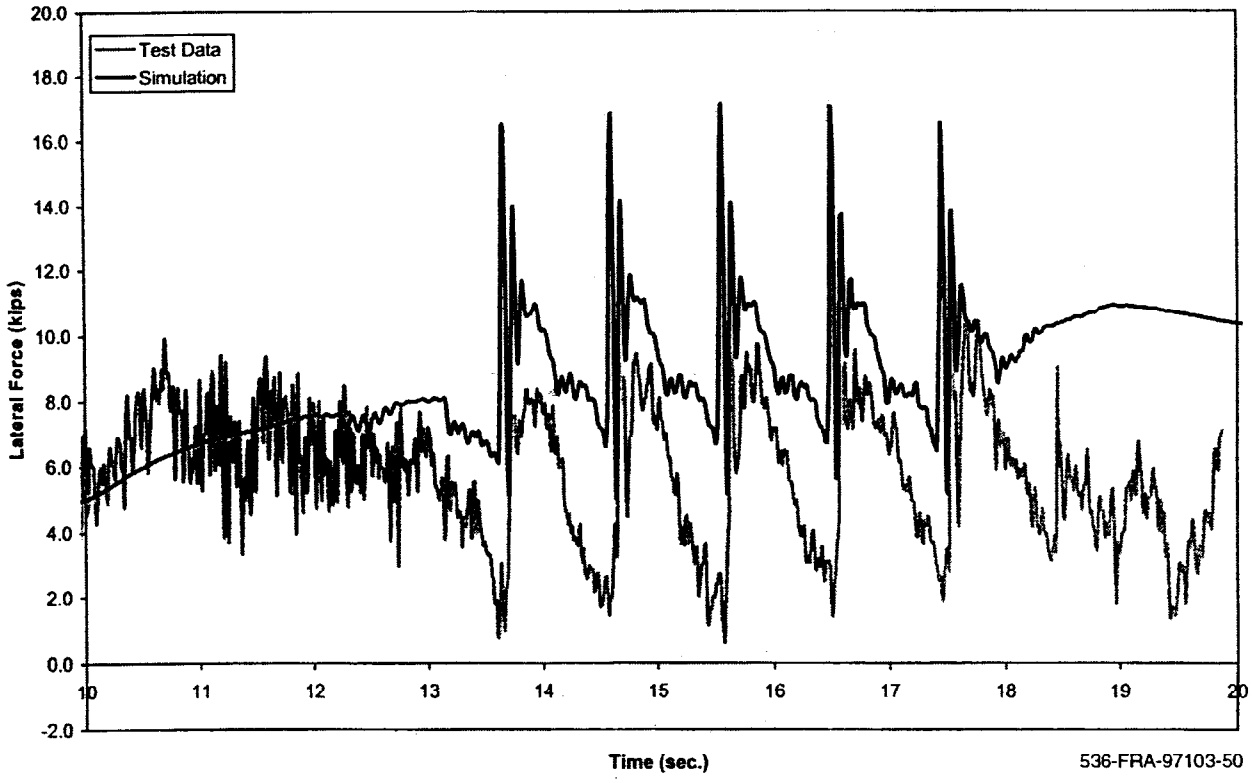

Figure A-15(a). Dynamic curving - lateral force time history, 28 mph (lead outer wheel)

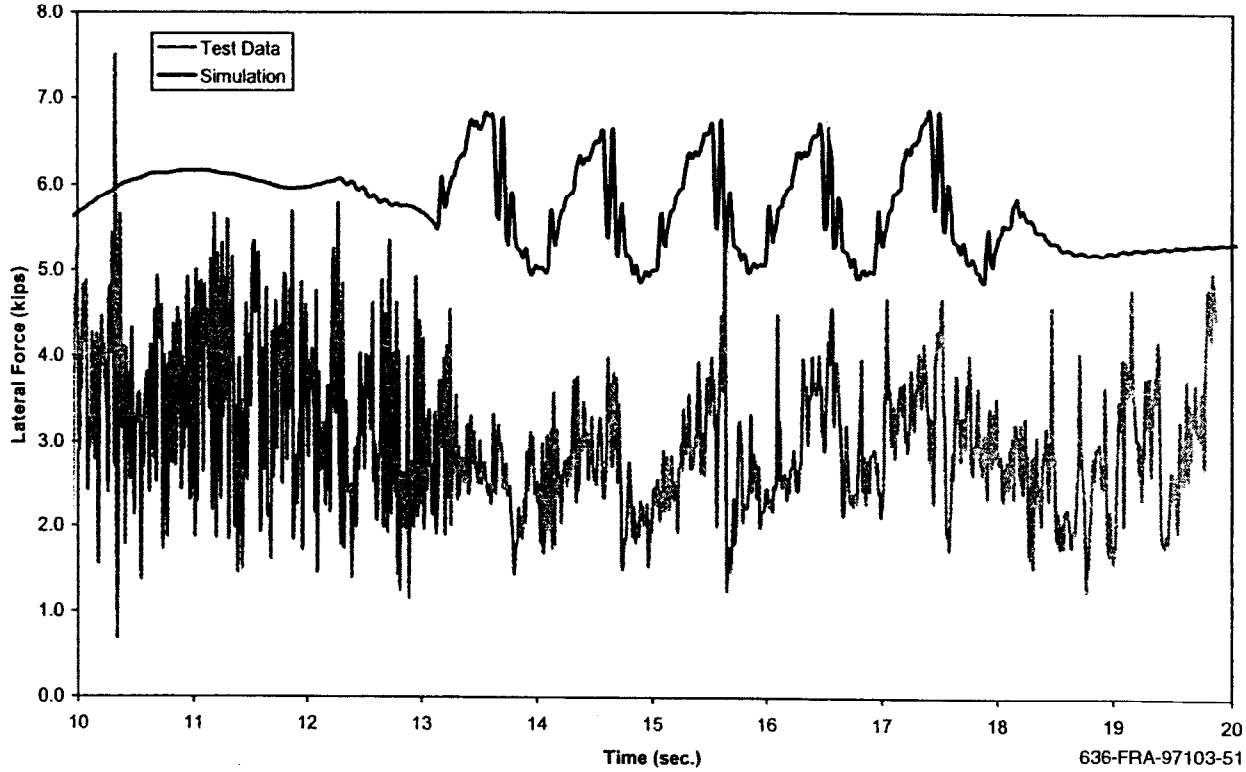

Figure A-15(b). Dynamic curving - lateral force time history, 28 mph (lead inner wheel)

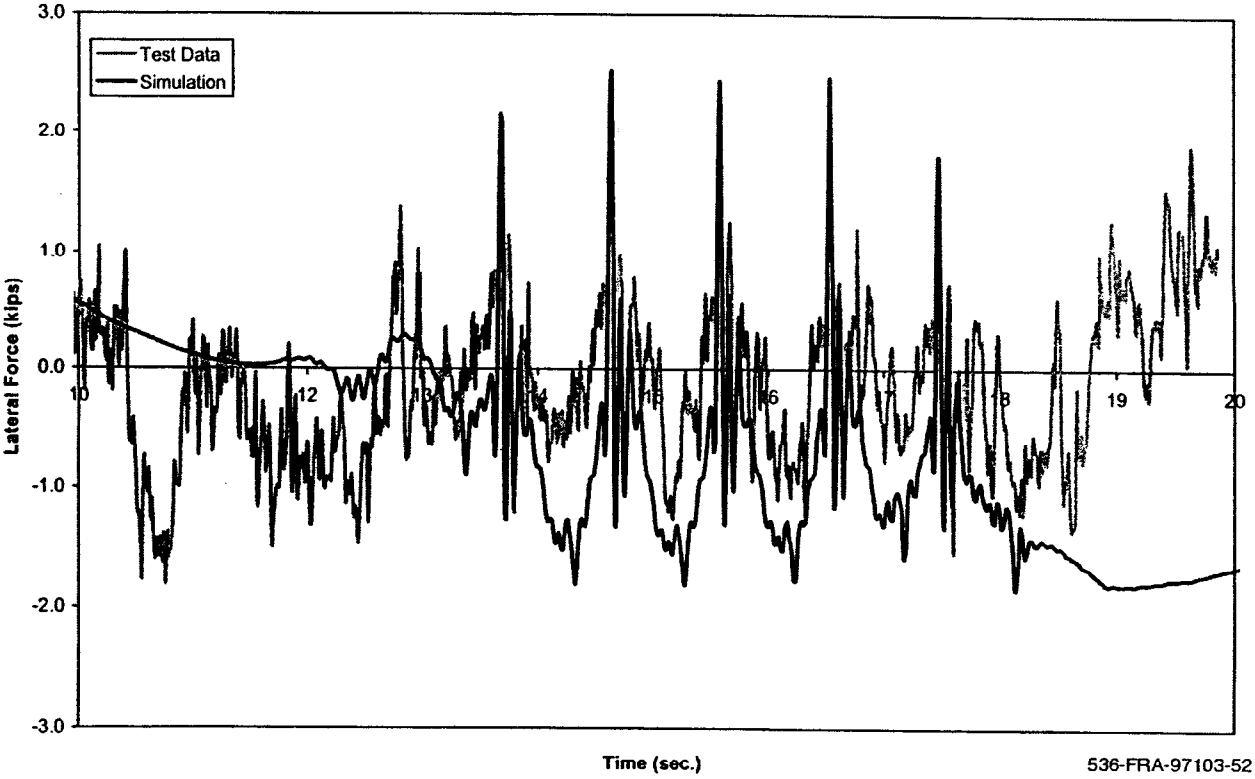

Figure A-15(c). Dynamic curving - lateral force time history, 28 mph (trailing outer wheel)

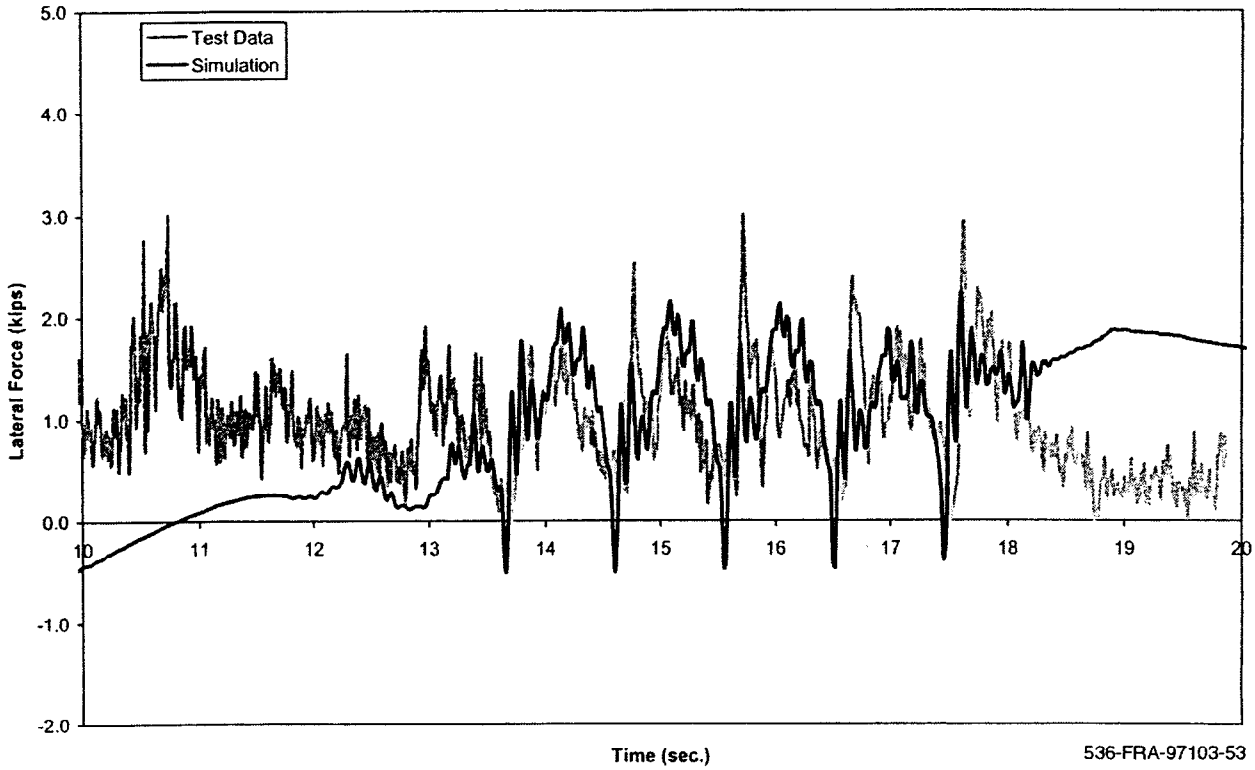

Figure A-15(d). Dynamic curving - lateral force time history, 28 mph (trailing inner wheel)

A plot of the minimum vertical force and maximum lateral force occurring during the tests is shown in Figures A-16 and A-17. Good correlation is shown through the speed range for the vertical force. The lateral force correlation is not as good. The maximum absolute lateral carbody acceleration at the "B" end is shown in Figure A-18. The test data have lower values of acceleration than the simulation over the speed range.

A.4 Yaw and Sway

Comparisons of the test and simulation data are shown in Figures A-19 and A-20 for vertical and lateral forces, respectively for 20 mph and in Figures A-21 and A-22 for 60 mph. For the tests at both speeds, the vertical data have relatively small variations on the order of ±1 kip from the nominal value of vertical load of 17 kips. While the lead axle test data indicates nominally equal loads on each wheel, the trailing axle test data shows a nominal load of 15.5 kips on the left wheel and 18.5 kips on the right wheel. The five cycle variation in vertical load illustrated in the simulation is also reflected in the test data. The lateral test data on all four wheels at both speeds have a series of sharp "spikes" of lateral force with amplitudes typically of 3 to 7 kips. These spikes occur at 39 ft intervals.

The minimum vertical force over the speed range of 15 to 90 mph occurring during a test run is plotted in Figure A-23 for the left front axle wheel. The maximum lateral force and maximum lateral carbody acceleration at the B end are plotted respectively in Figures A-24 and A-25. The lateral maximum wheel force and carbody acceleration data exceed the simulation data

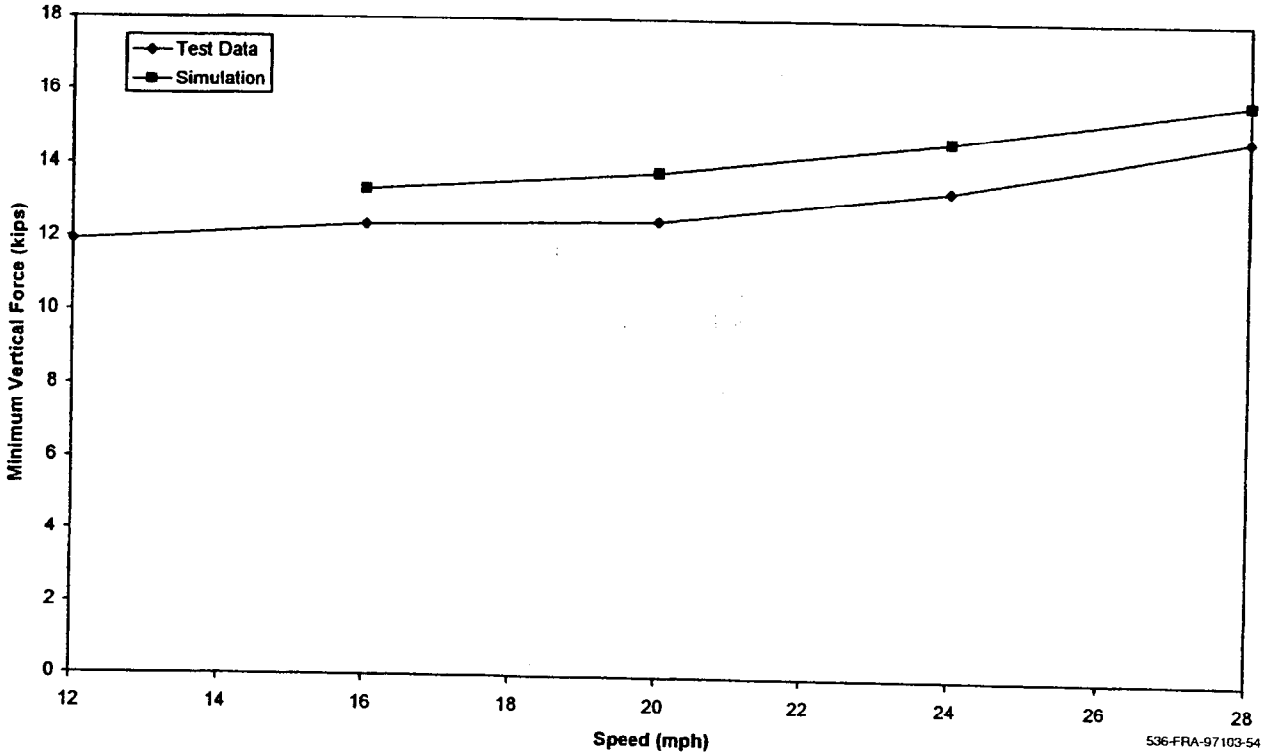

Figure A-16. Dynamic curving - minimum vertical force (lead outer wheel)

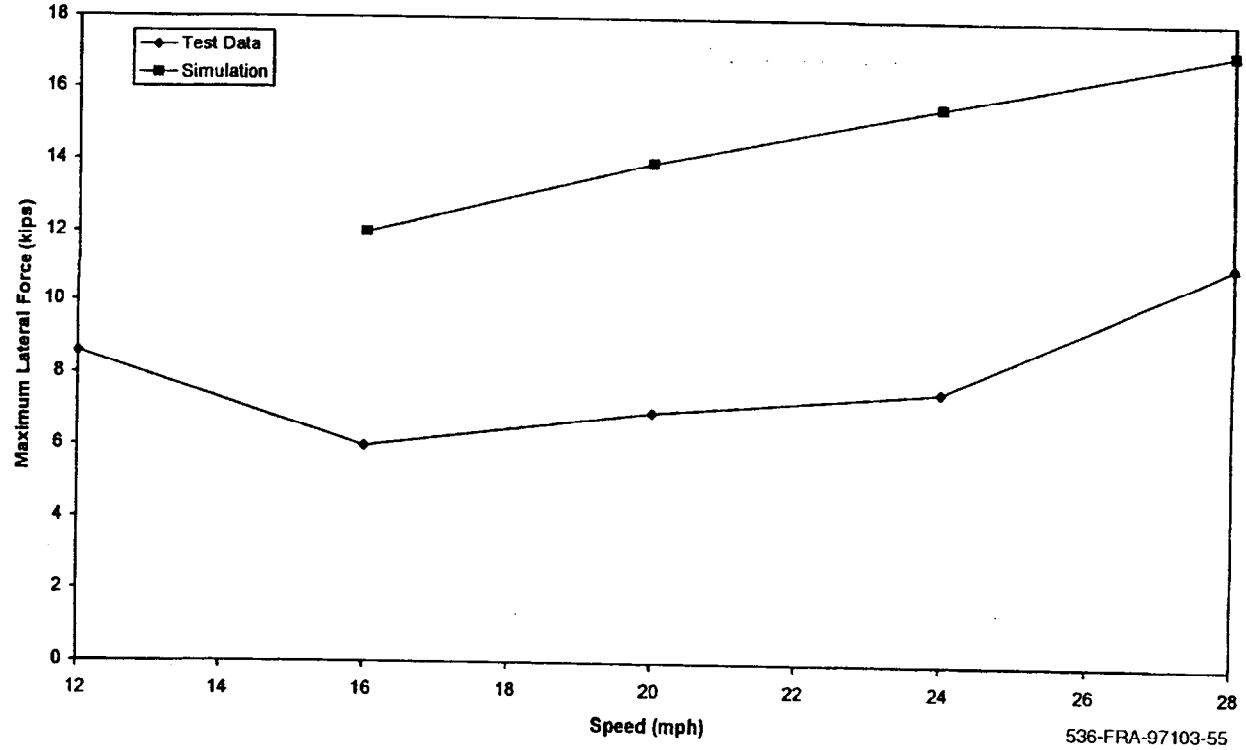

Figure A-17. Dynamic curving - maximum lateral force (lead outer wheel)

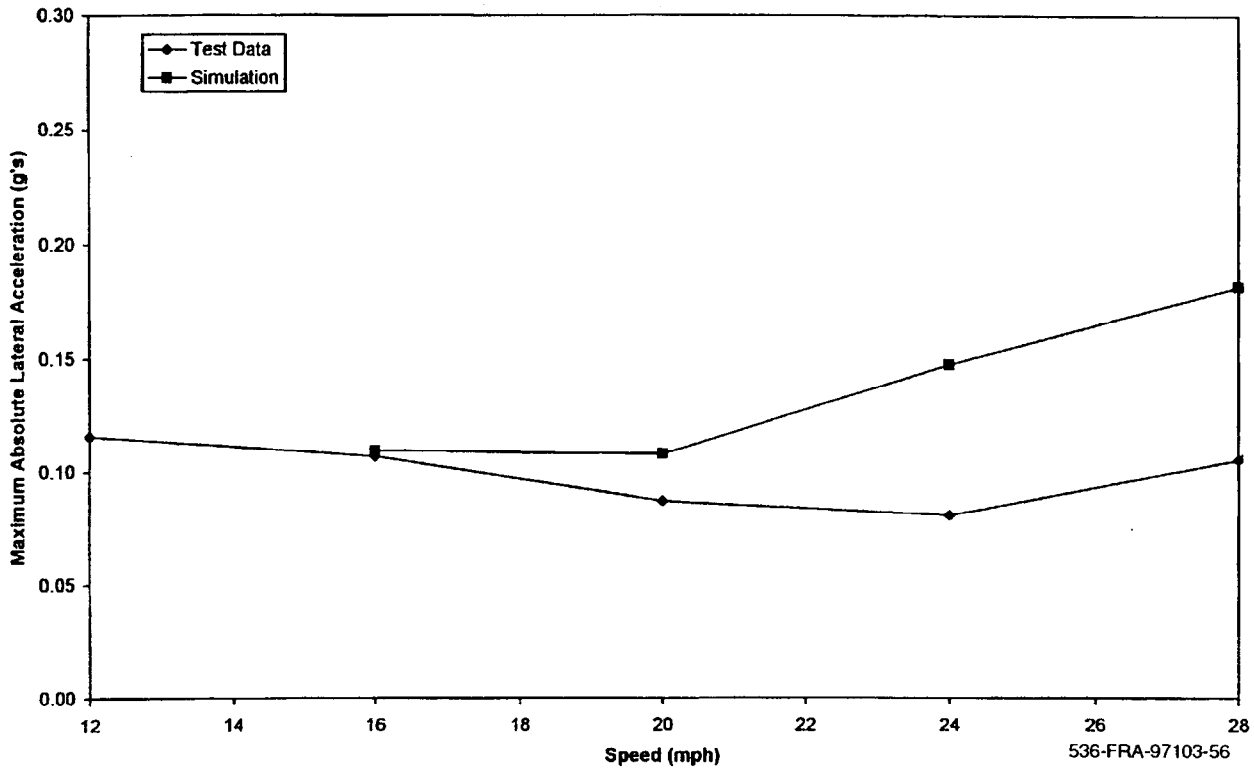

Figure A-18. Dynamic curving - maximum absolute lateral car body acceleration ("B" end)

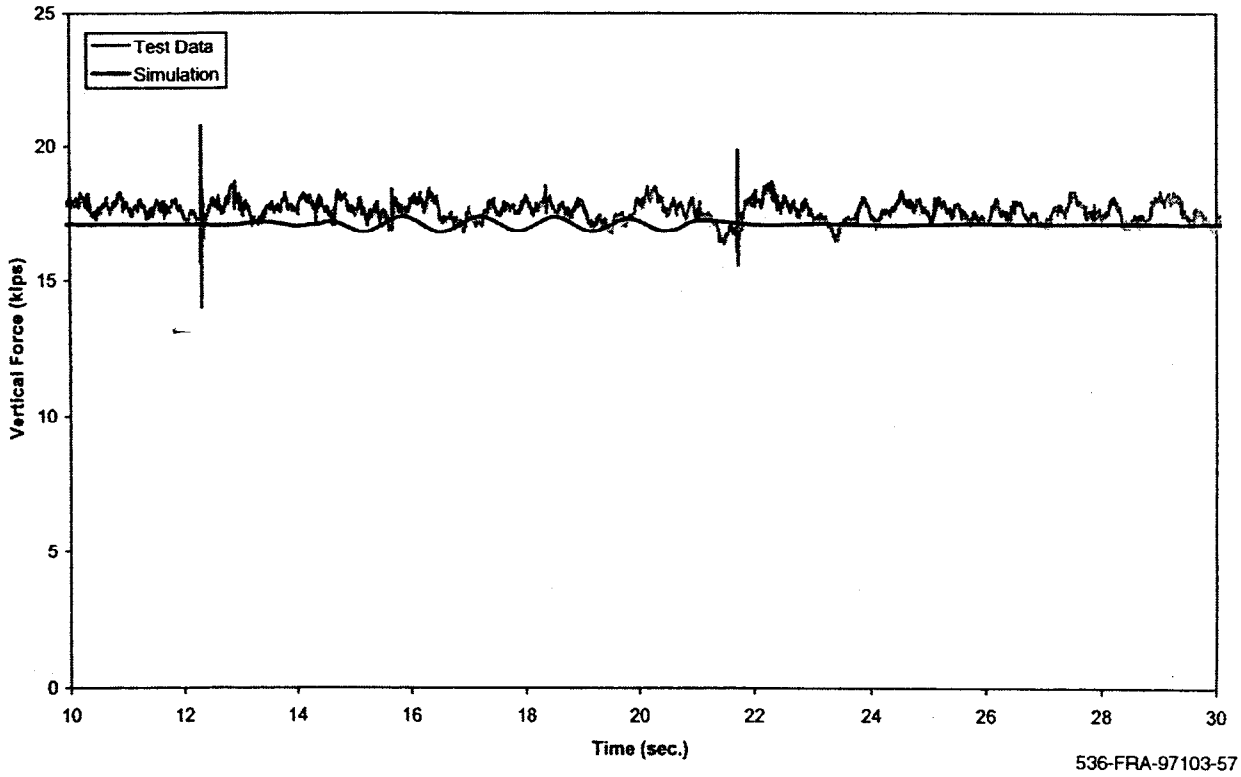

Figure A-19(a). Yaw and sway - vertical force time history, 20 mph (lead left wheel)

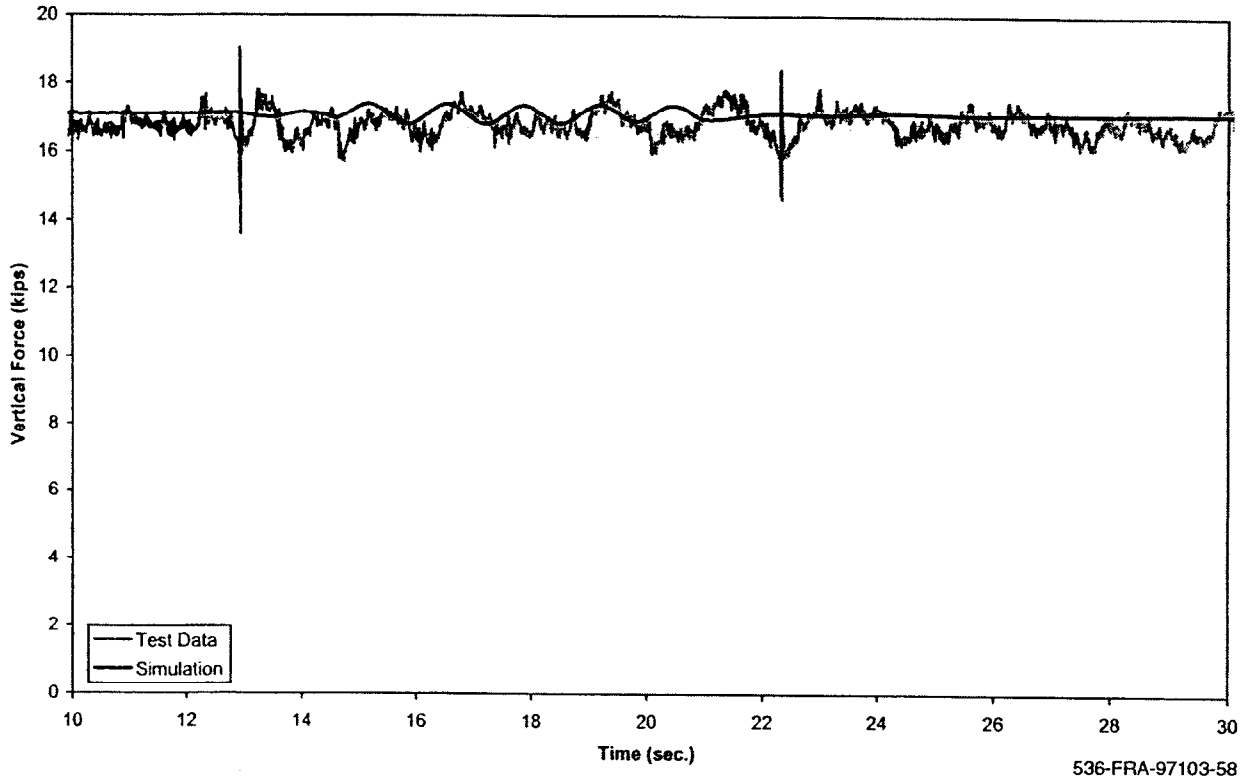

Figure A-19(b). Yaw and sway - vertical force time history, 20 mph (lead right wheel)

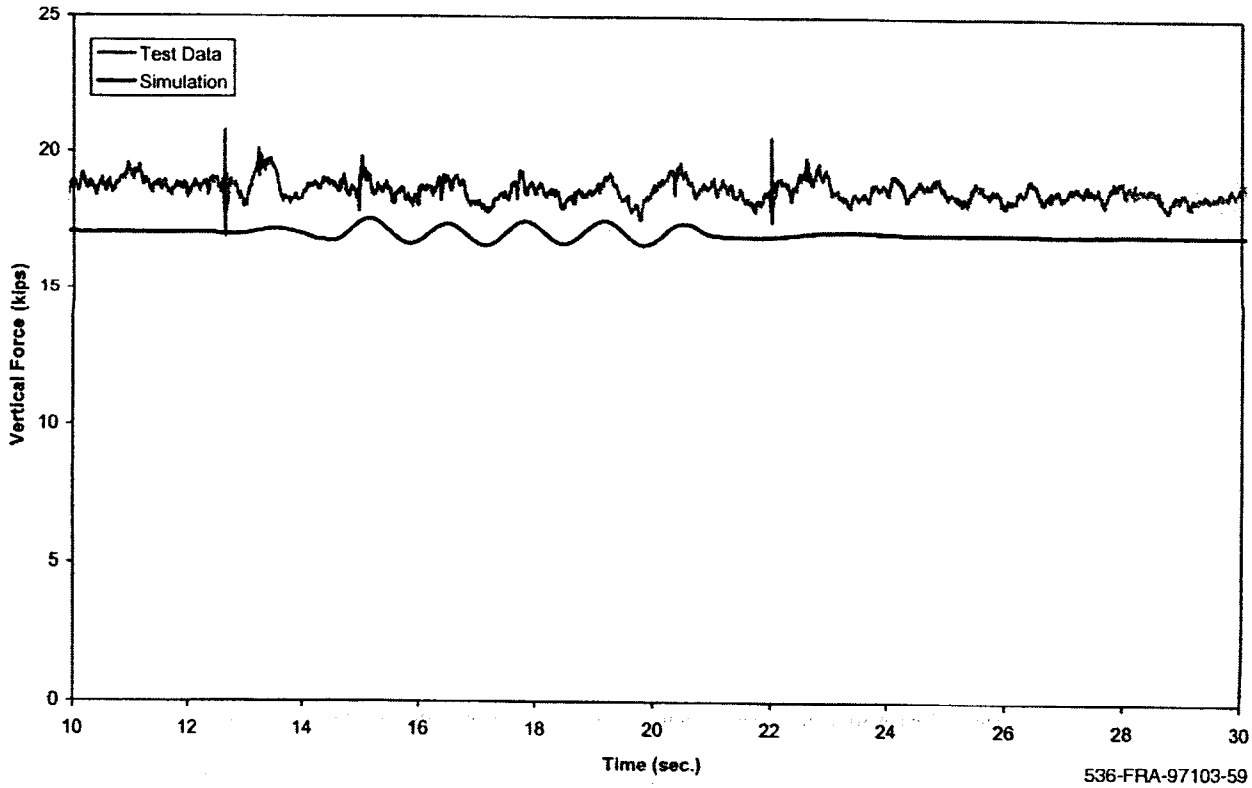

Figure A-19(c). Yaw and sway - vertical force time history, 20 mph (trailing left wheel)

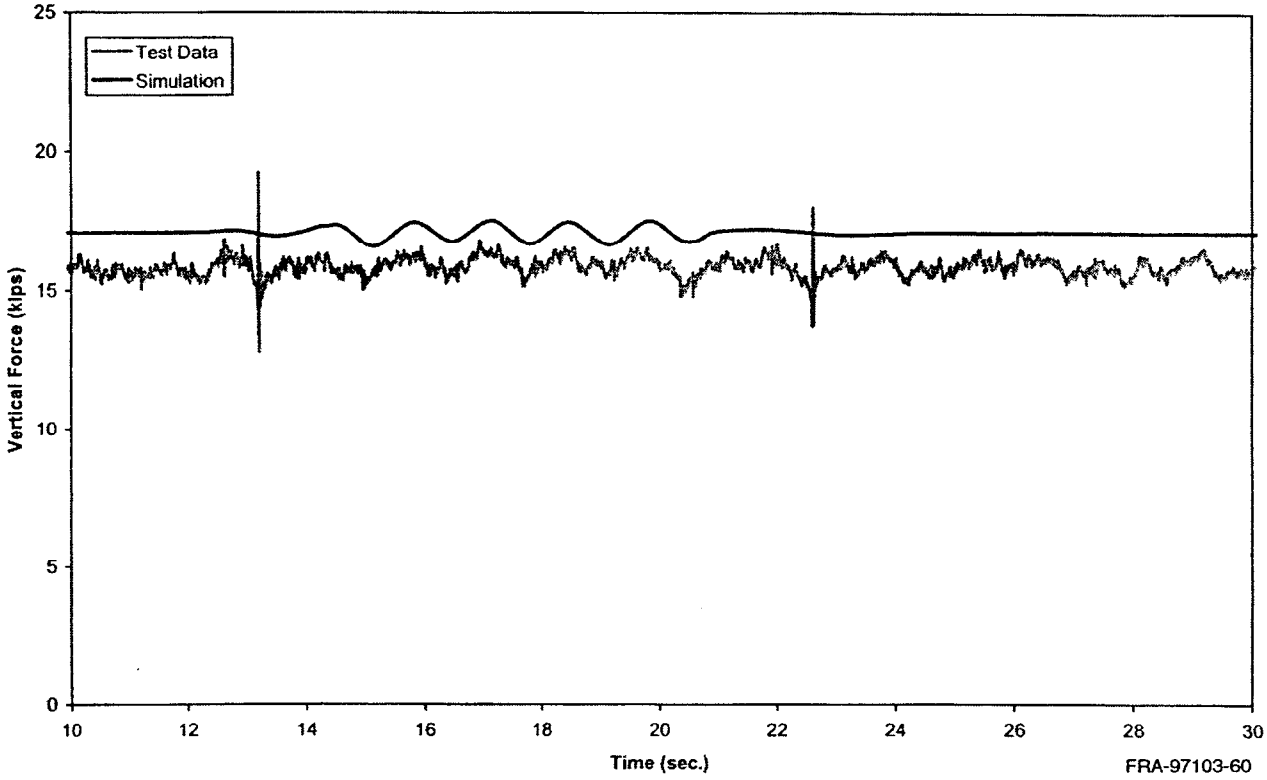

Figure A-19(d). Yaw and sway - vertical force time history, 20 mph (trailing right wheel)

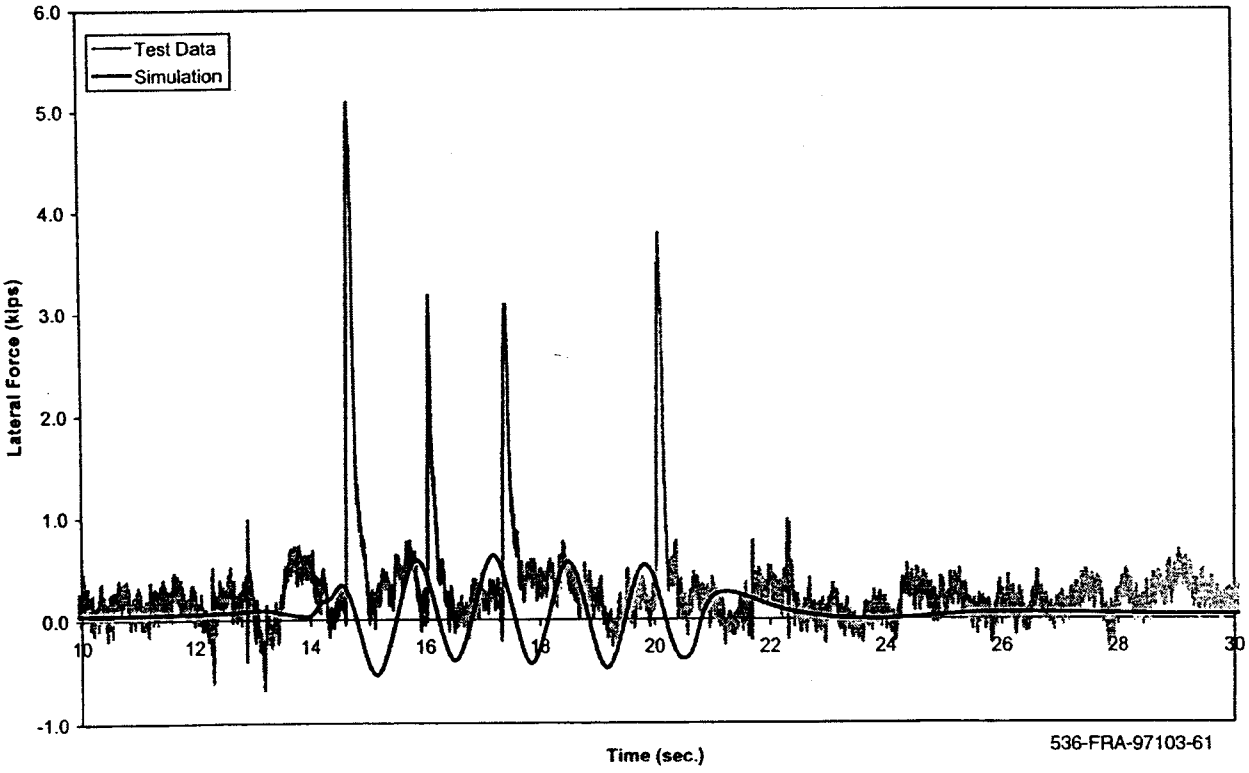

Figure A-20(a). Yaw and sway - lateral force time history, 20 mph (lead left wheel)

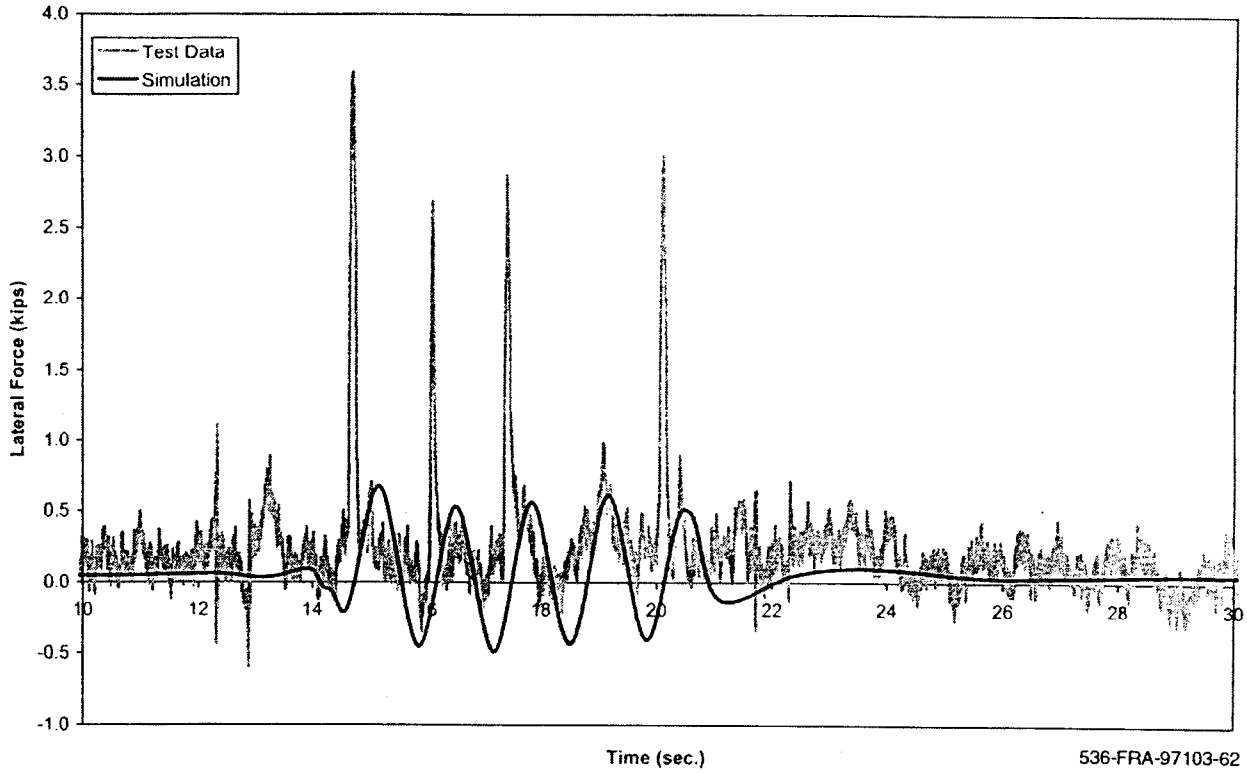

Figure A-20(b). Yaw and sway - lateral force time history, 20 mph (lead right wheel)

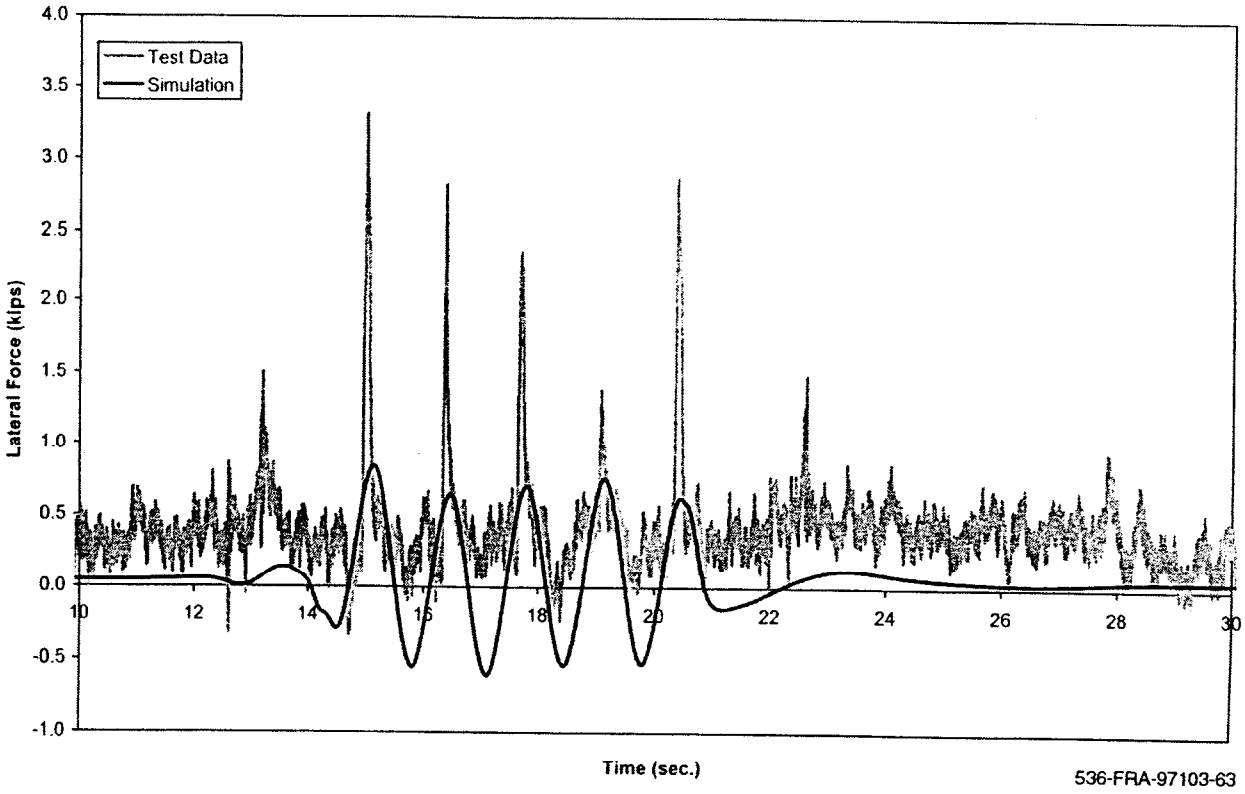

Figure A-20(c). Yaw and sway - lateral force time history, 20 mph (trailing left wheel)

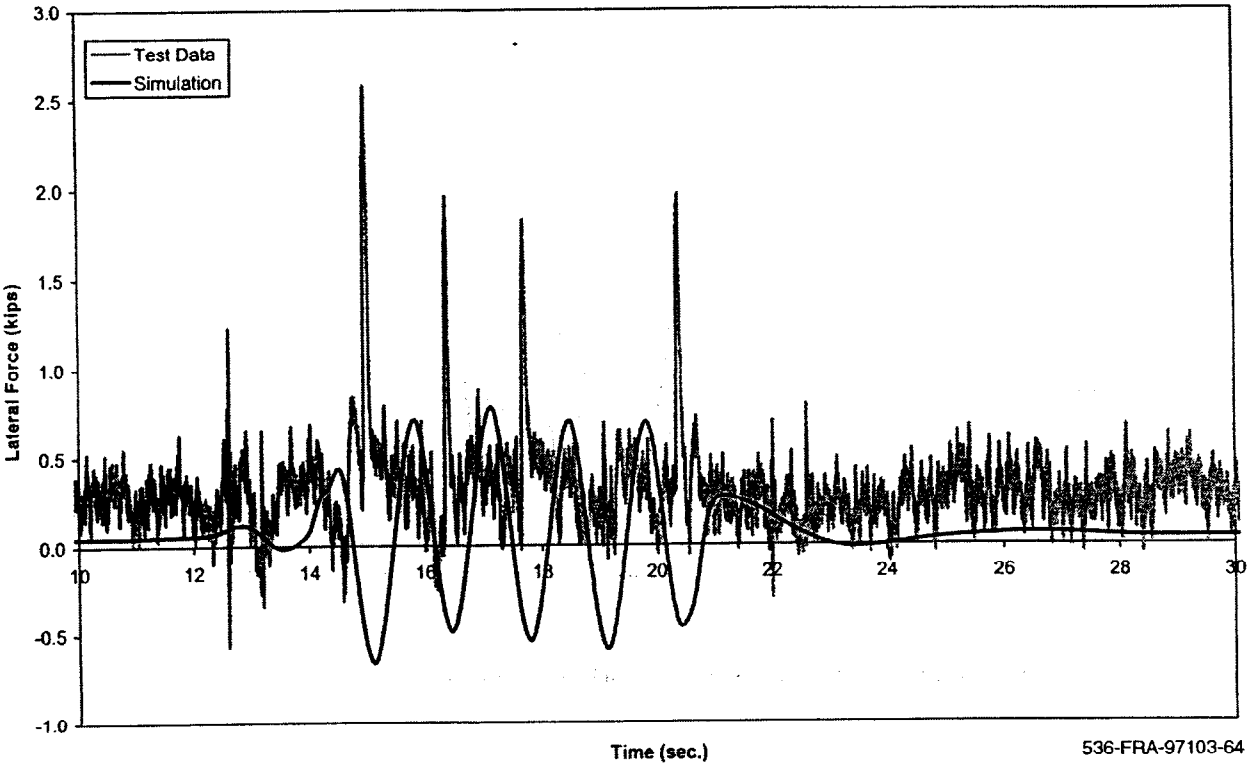

Figure A-20(d). Yaw and sway - lateral force time history, 20 mph (trailing right wheel)

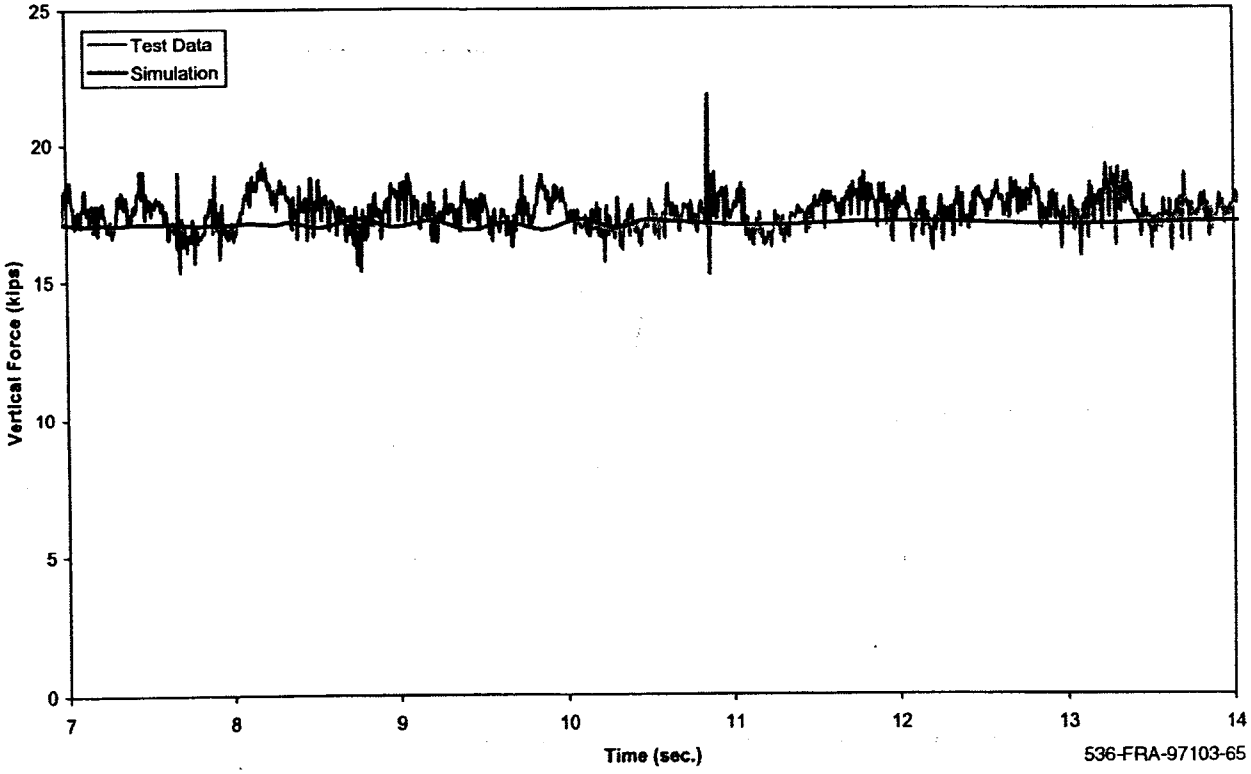

Figure A-21(a). Yaw and sway - vertical force time history, 60 mph (lead left wheel)

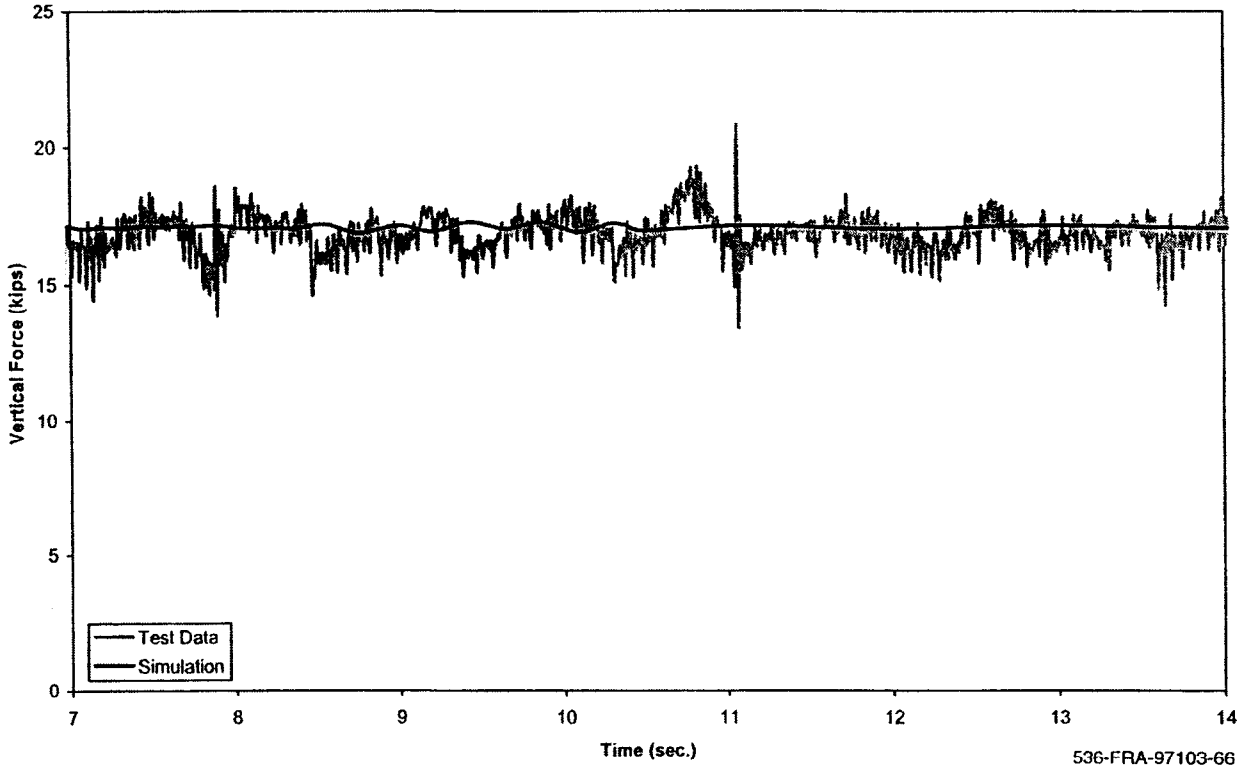

Figure A-21(b). Yaw and sway - vertical force time history, 60 mph (lead right wheel)

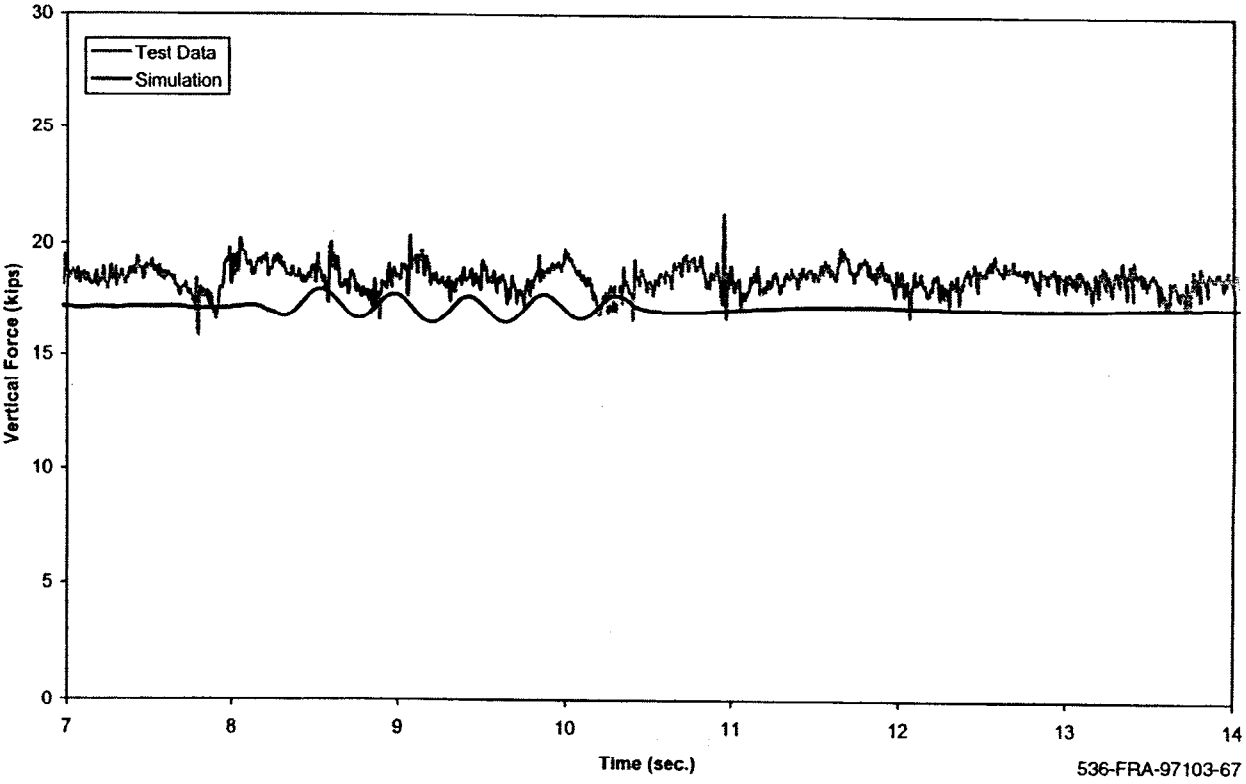

Figure A-21(c). Yaw and sway - vertical force time history, 60 mph (trailing left wheel)

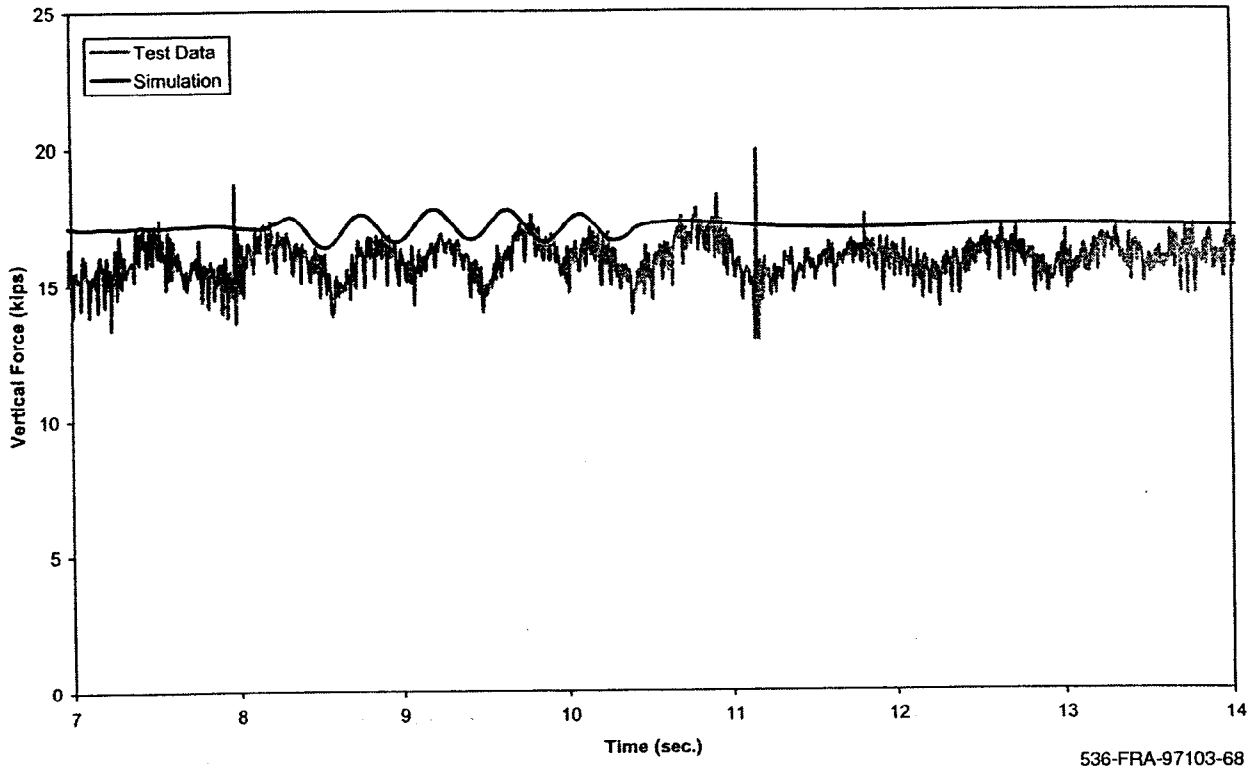

Figure A-21(d). Yaw and sway - vertical force time history, 60 mph (trailing right wheel)

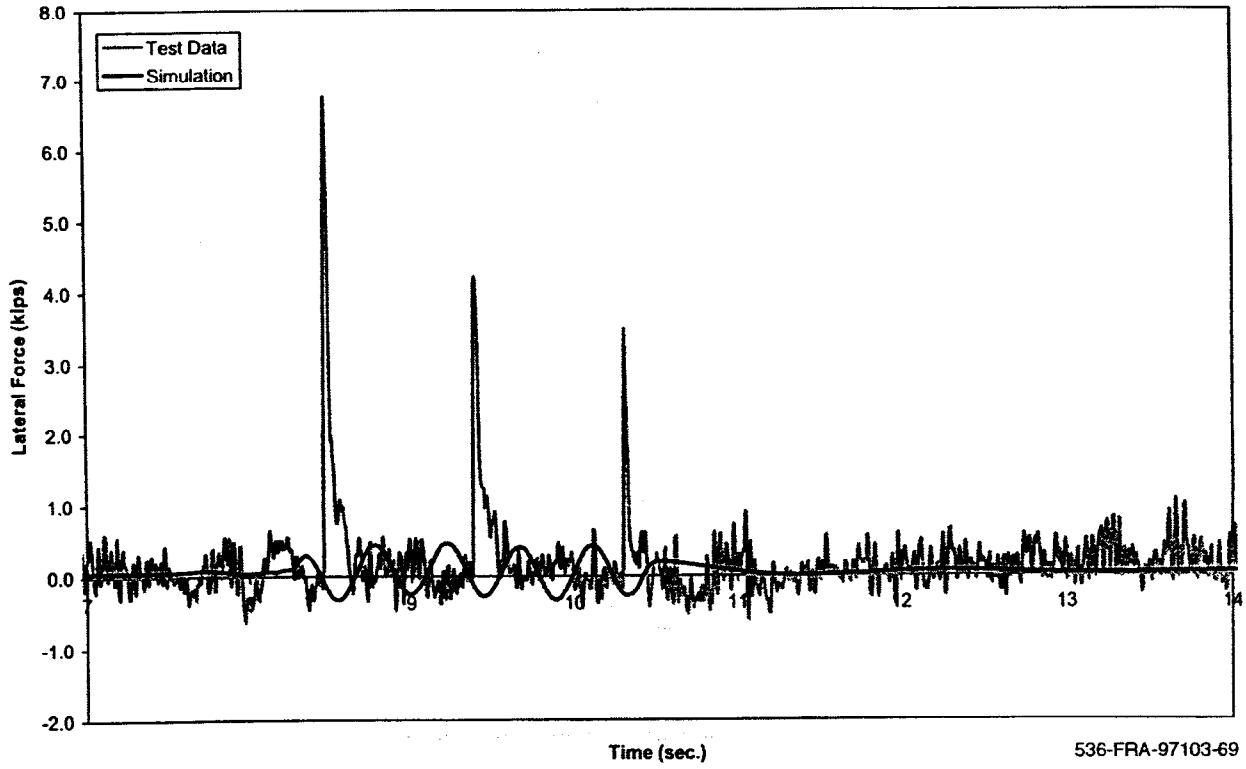

Figure A-22(a). Yaw and sway - lateral force time history, 60 mph (lead left wheel)

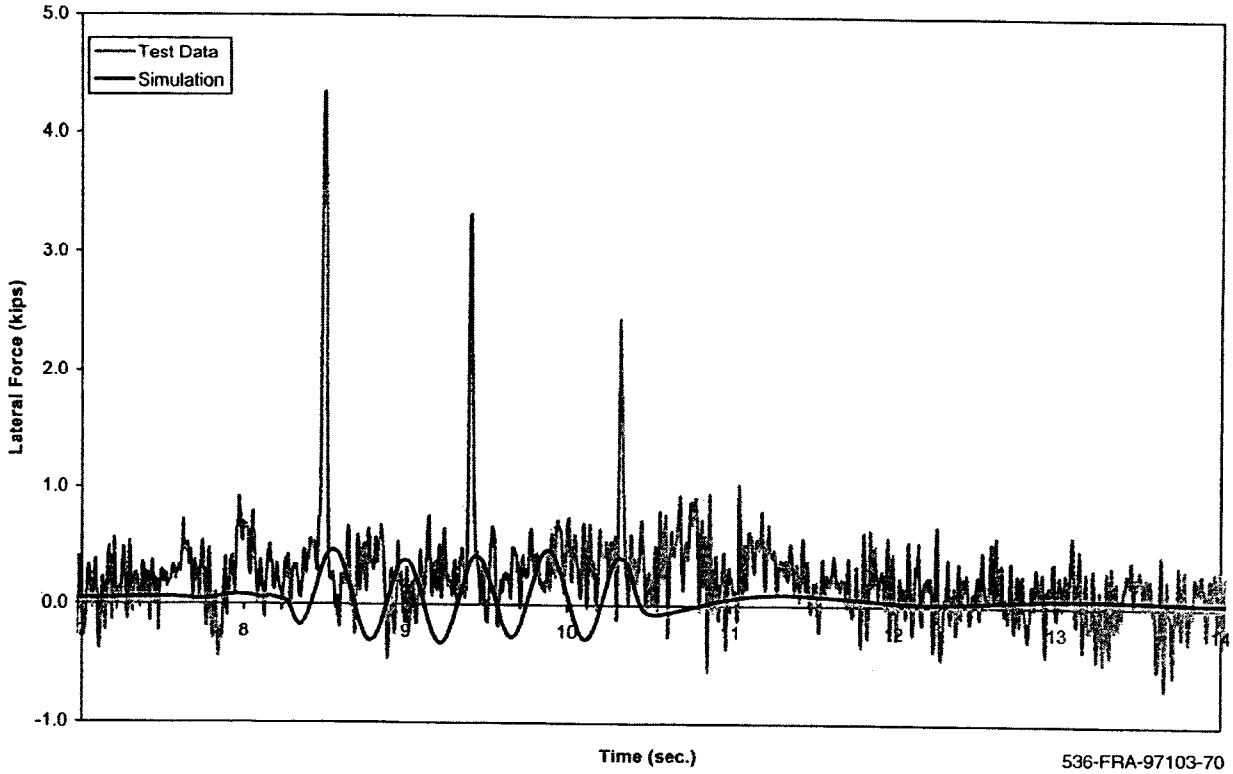

Figure A-22(b). Yaw and sway - lateral force time history, 60 mph (lead right wheel)

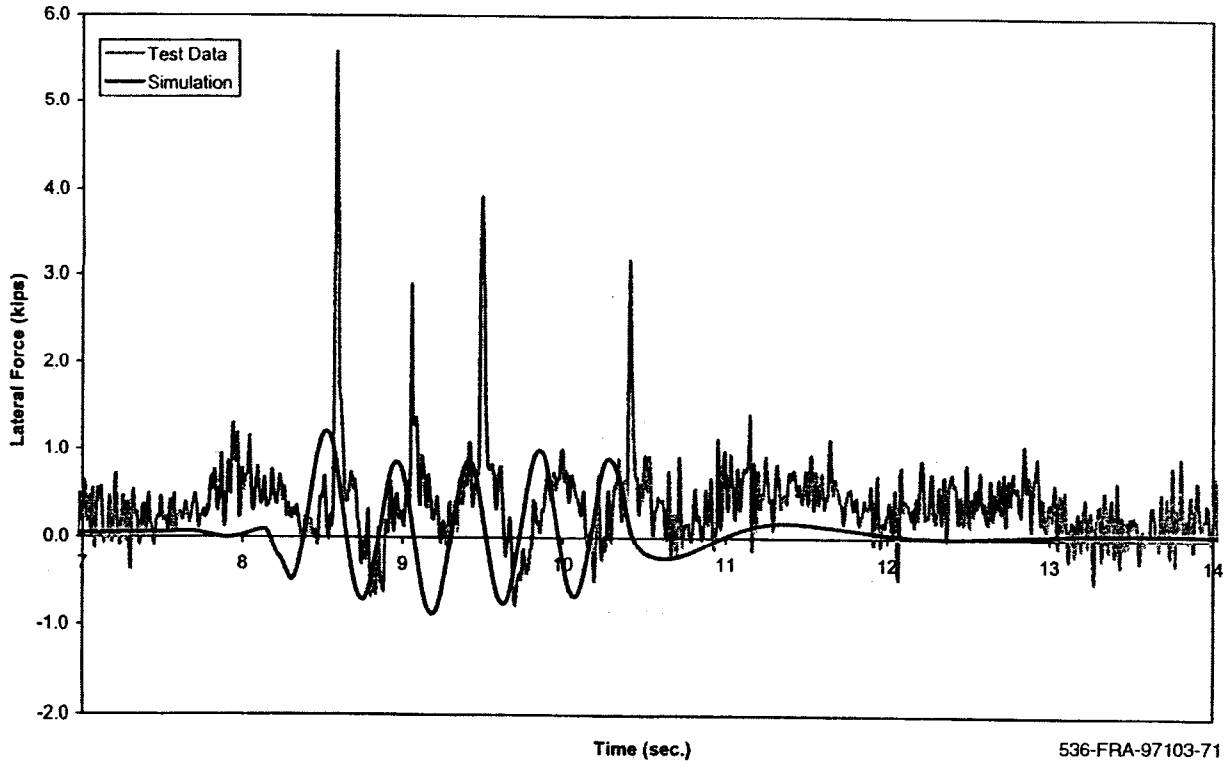

Figure A-22(c). Yaw and sway - lateral force time history, 60 mph (trailing left wheel)

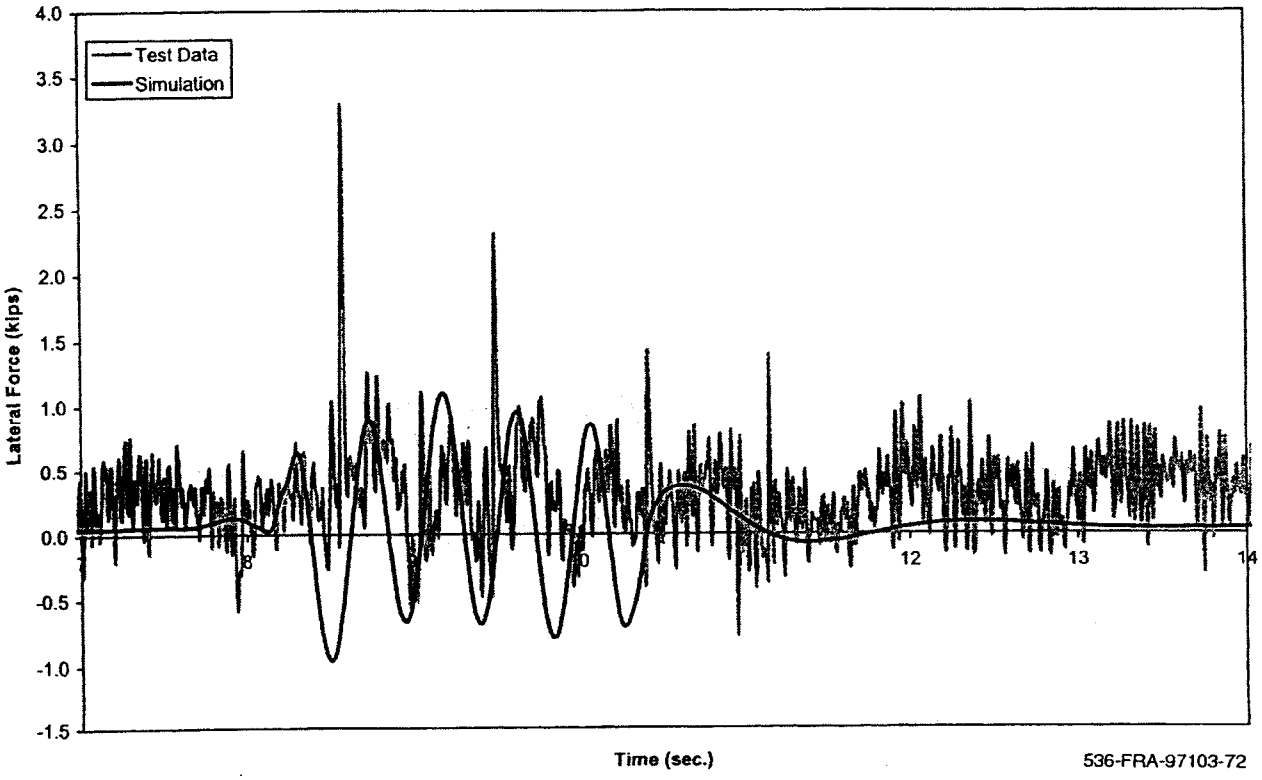

Figure A-22(d). Yaw and sway - lateral force time history, 60 mph (trailing right wheel)

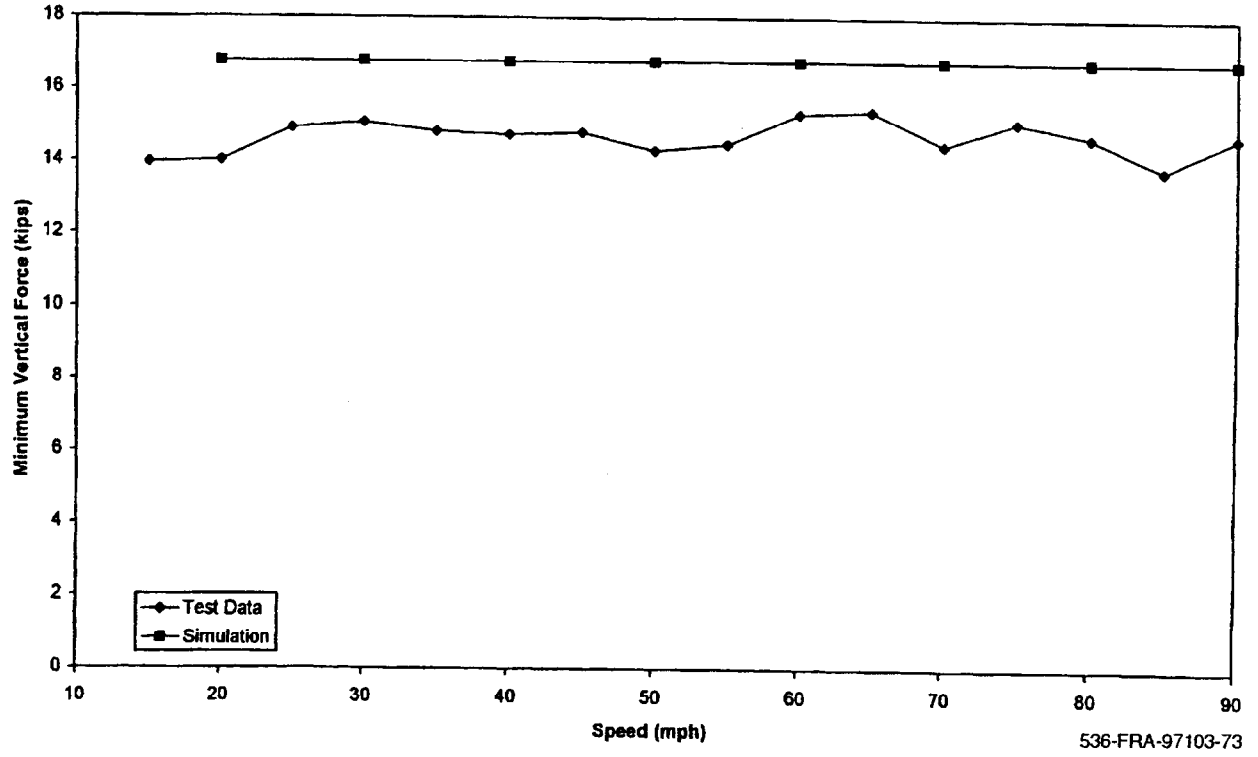

Figure A-23. Yaw and sway - minimum vertical force (lead left wheel)

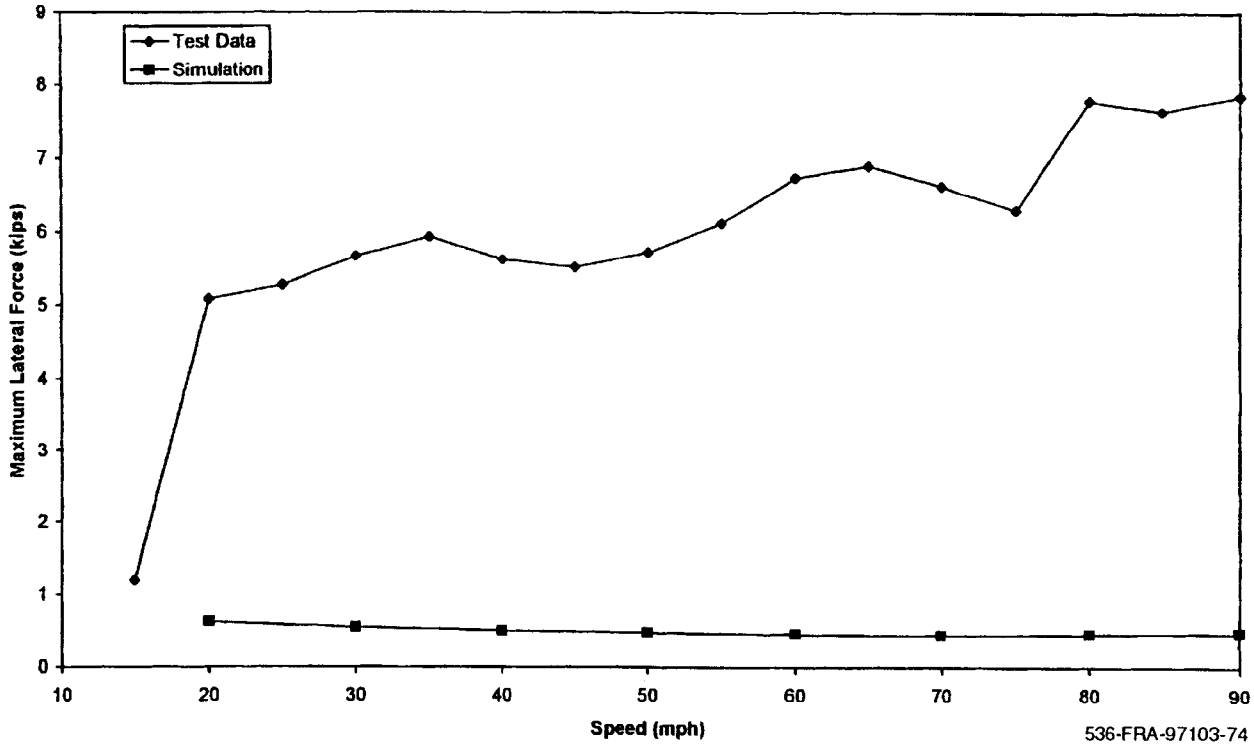

Figure A-24. Yaw and sway - maximum lateral force (lead left wheel)

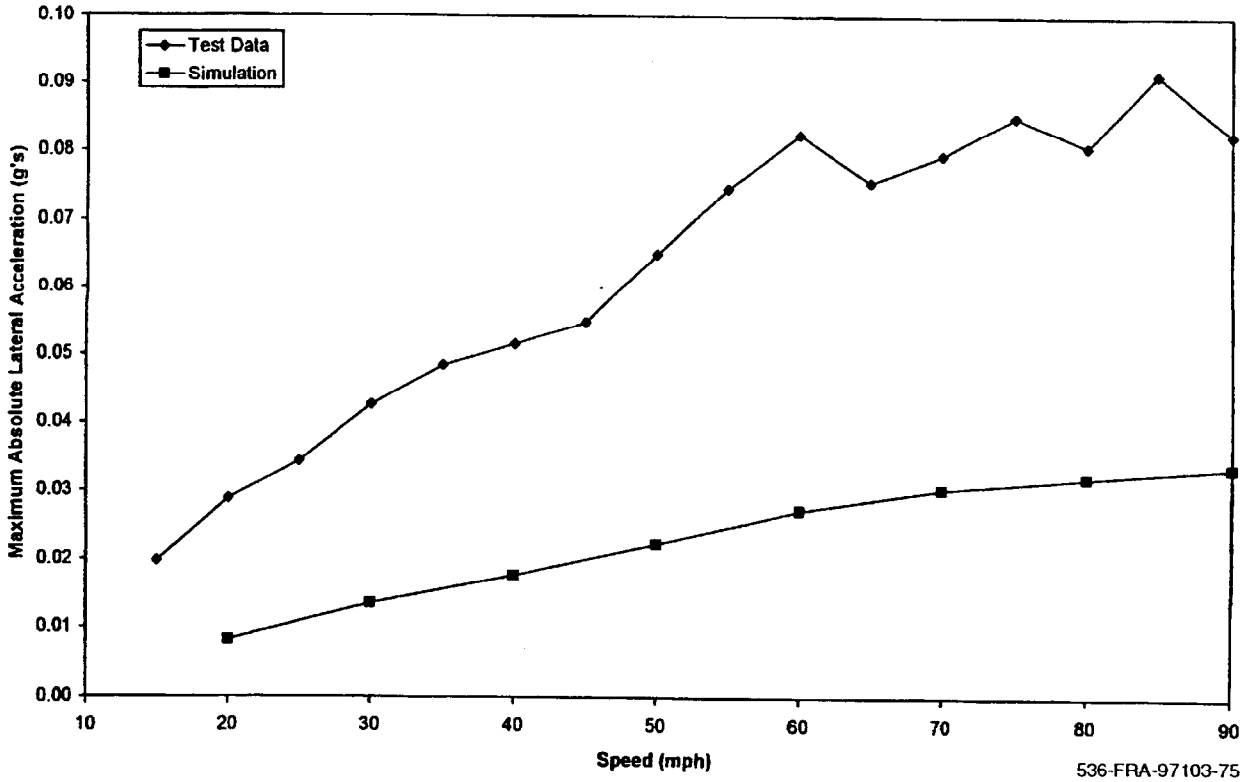

Figure A-25. Yaw and sway - maximum absolute lateral car body acceleration ("B" end)

significantly if the "spikes" in the test data due to the joints are included. The resonant condition is not obvious from the test data possibly due to large damping in the system.

A.5 Twist and Roll

Comparisons of the test data for all four wheels of the trailing truck vertical and lateral forces are summarized in Figures A-26 and A-27 for 18.8 mph and Figures A-28 and A-29 for 60 mph tests. The comparisons illustrate good agreement in vertical force waveforms and amplitudes.

The vertical force amplitude of the four wheels varies between approximately 13 and 22 kips and shows good agreement between the test and simulation. The lateral force data for the lead axle vary between about –1.0 to +1.7 kips and also show good agreement between the test and simulation. The lateral force data for the trailing axle vary from –0.5 to +1.5 kips for the tests and ±0.5 kips in the simulation and are considered to be approaching values small enough to represent the test accuracy limits. The vertical force test and simulation data at 60 mph vary from approximately 12.5 to 22 kips and are in excellent agreement. The test and lateral force simulation data for the lead axle vary from approximately –1.5 to +2.5 kips and are in relatively good agreement. The lateral test and simulation force data for the trailing axle vary from –1.0 to +1.5 kips with the general levels in agreement.

Plots of the test and simulation of minimum vertical force and maximum lateral force are shown in Figures A-30 and A-31 for the lead axle left wheel of the trailing truck. Good correlation is seen for the vertical force in the speed range while the lateral force test data is approximately 25 percent greater than the simulation. The maximum absolute lateral carbody

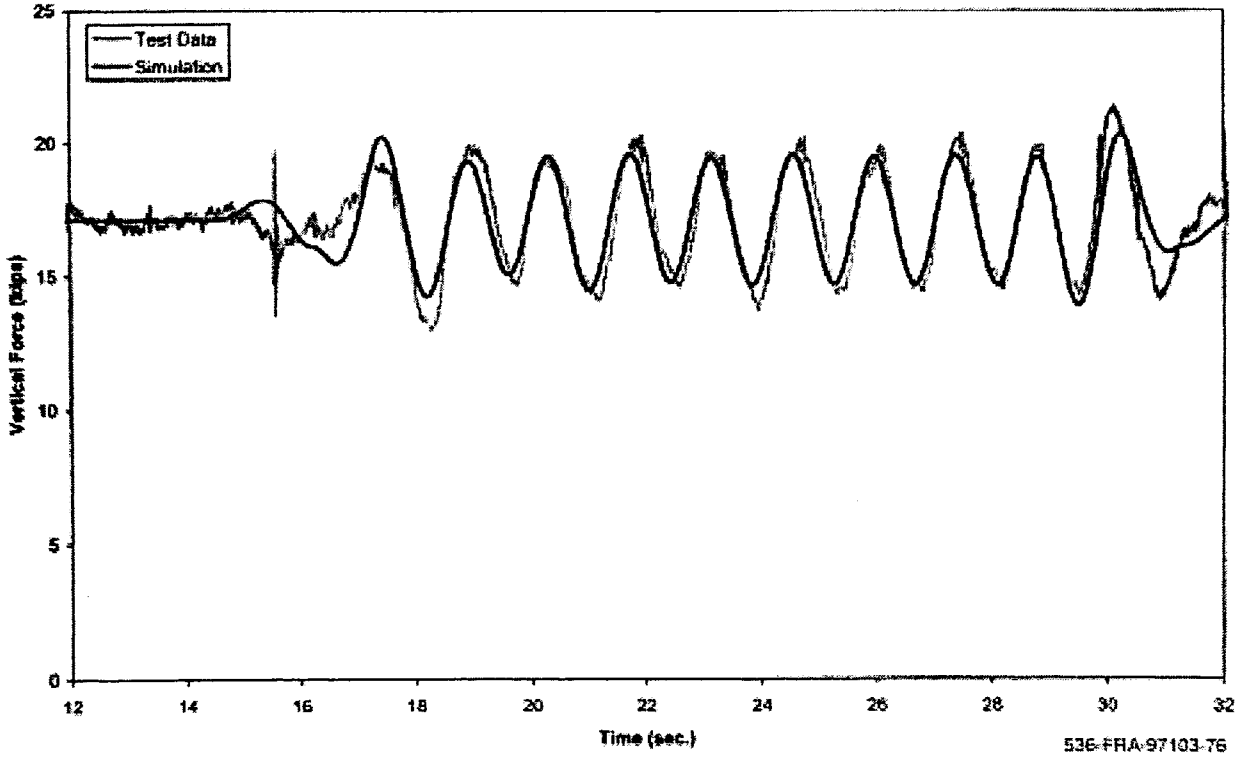

Figure A-26(a). Twist and roll - vertical force time history, 18.8 mph (lead left wheel)

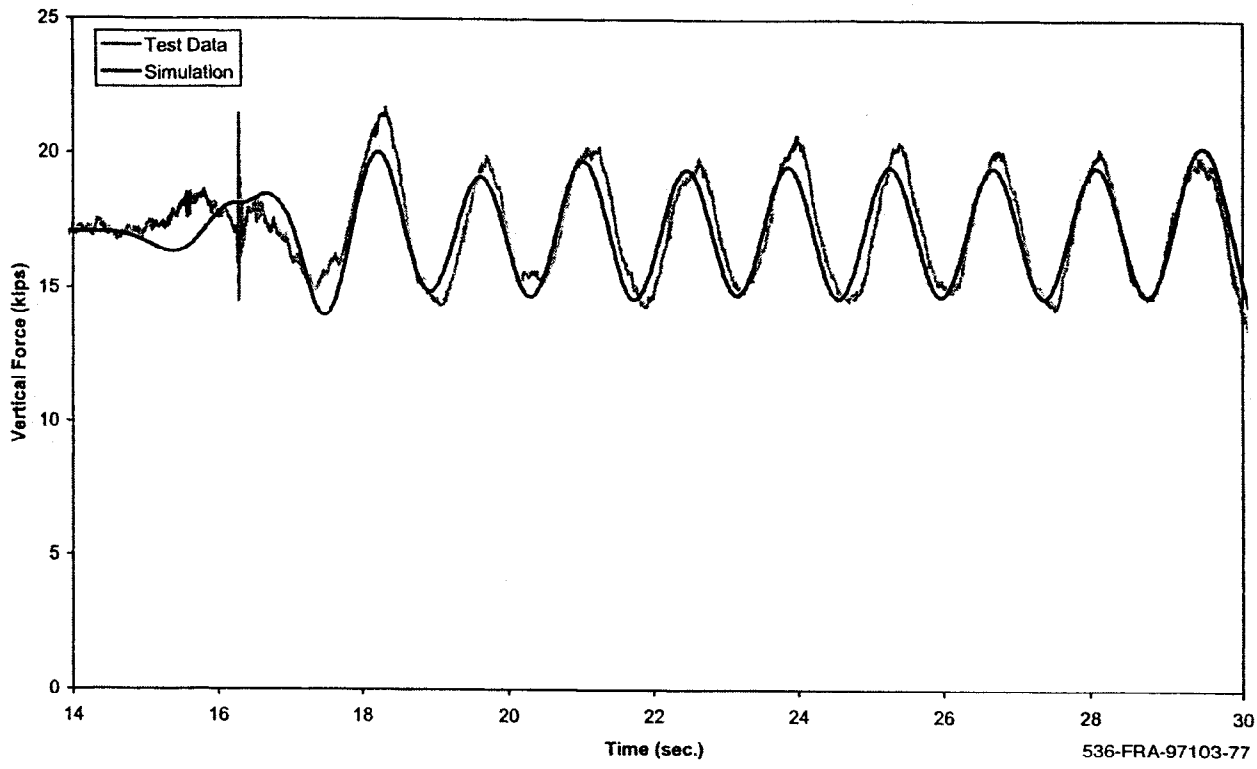

Figure A-26(b). Twist and roll - vertical force time history, 18.8 mph (lead right wheel)

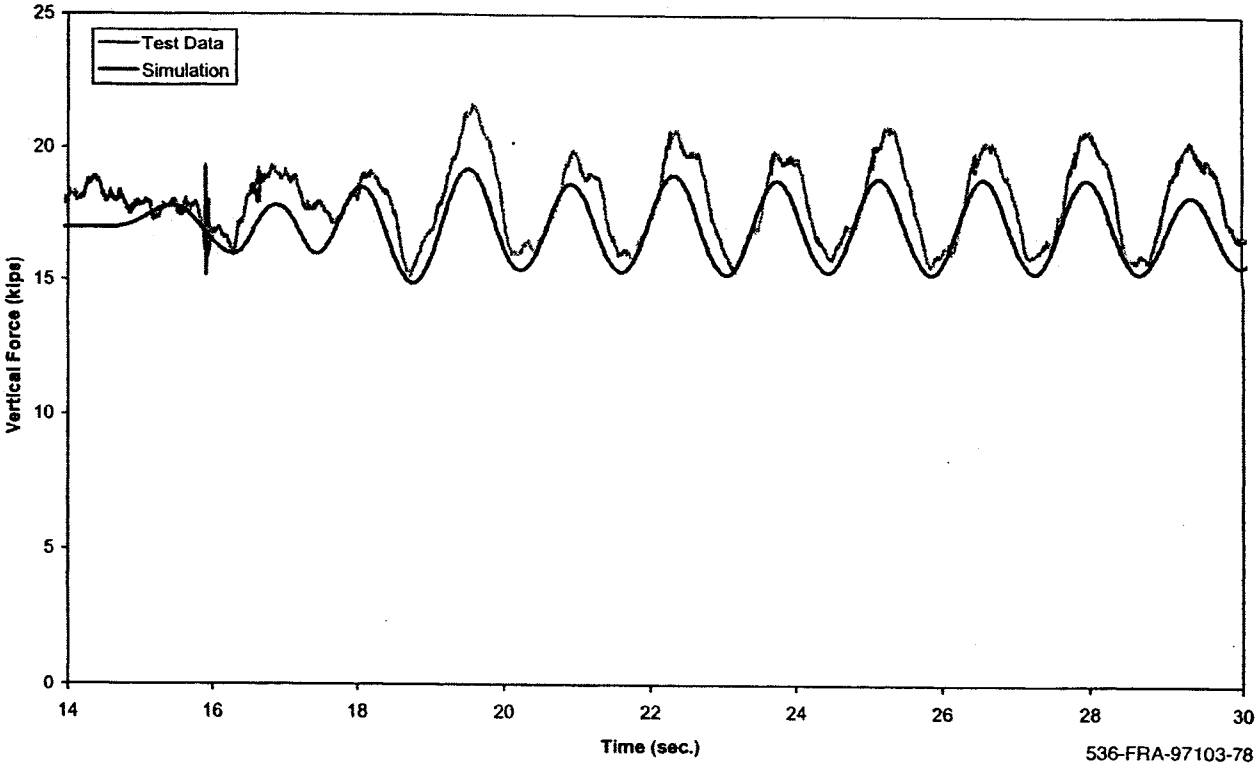

Figure A-26(c). Twist and roll - vertical force time history, 18.8 mph (trailing left wheel)

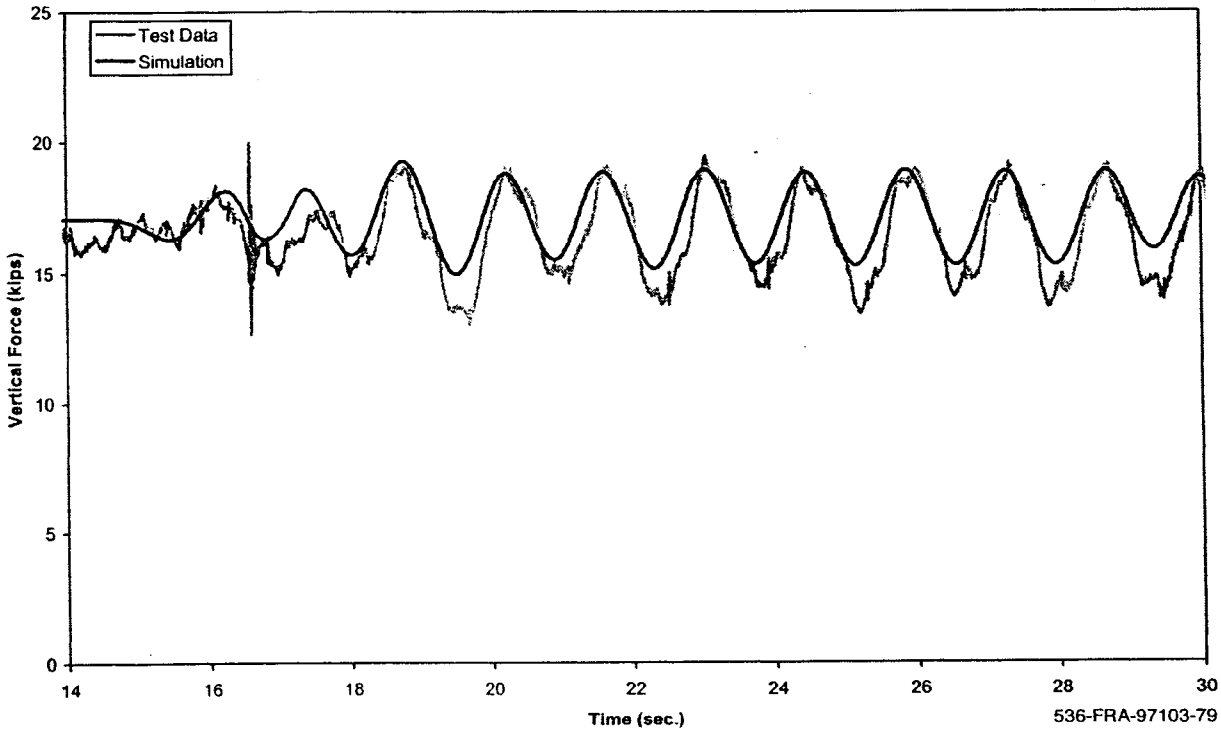

Figure A-26(d). Twist and roll - vertical force time history, 18.8 mph (trailing right wheel)

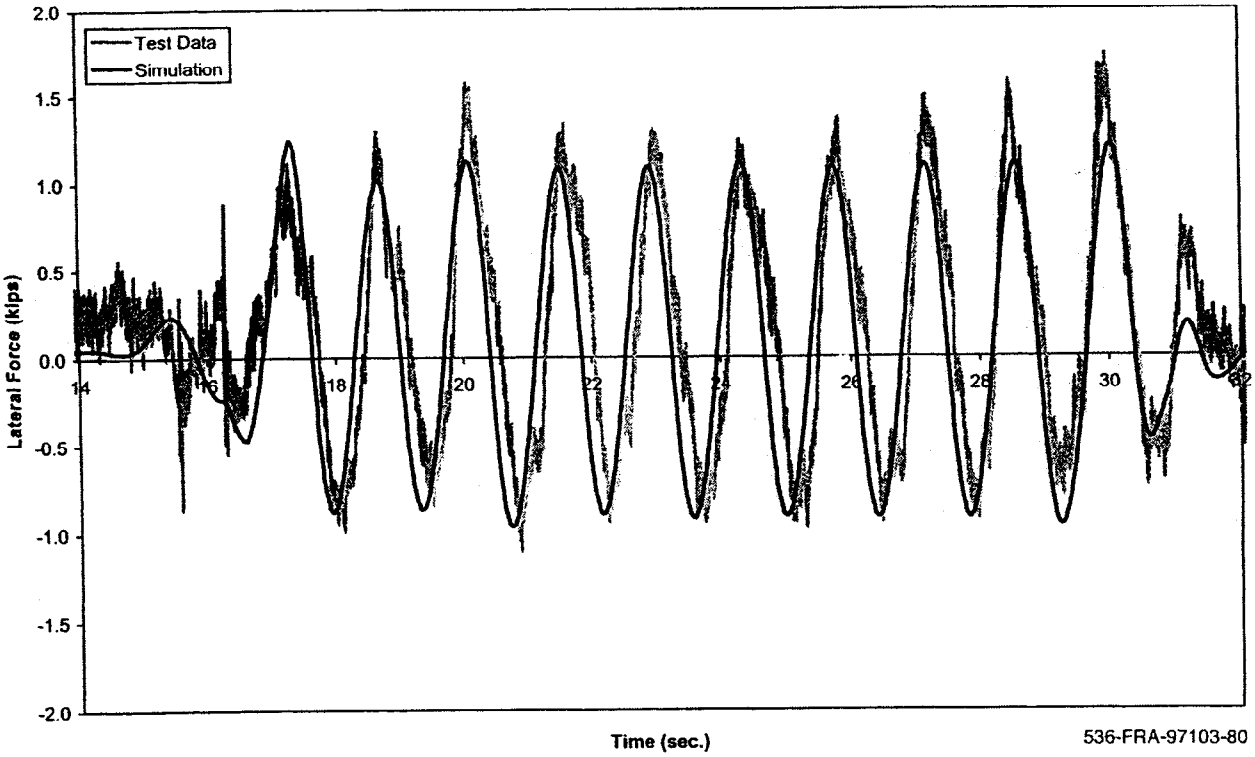

Figure A-27(a). Twist and roll - lateral force time history, 18.8 mph (lead left wheel)

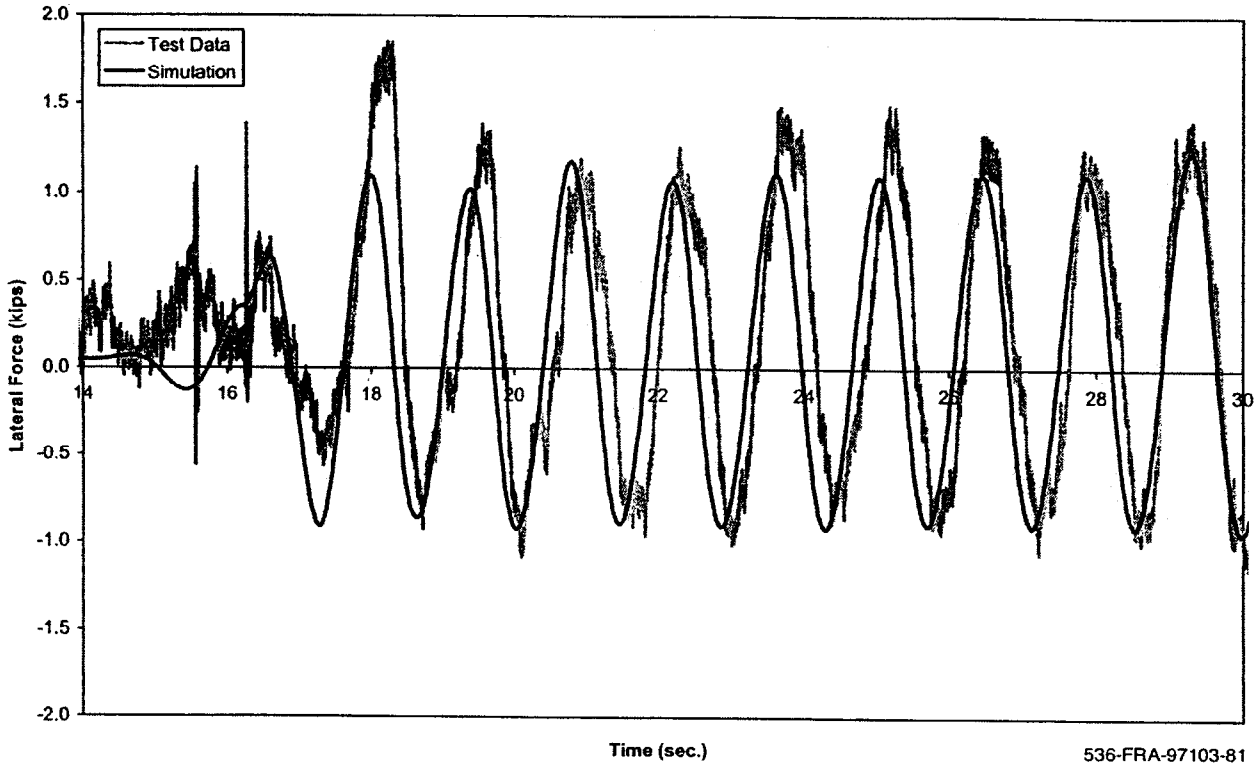

Figure A-27(b). Twist and roll - lateral force time history, 18.8 mph (lead right wheel)

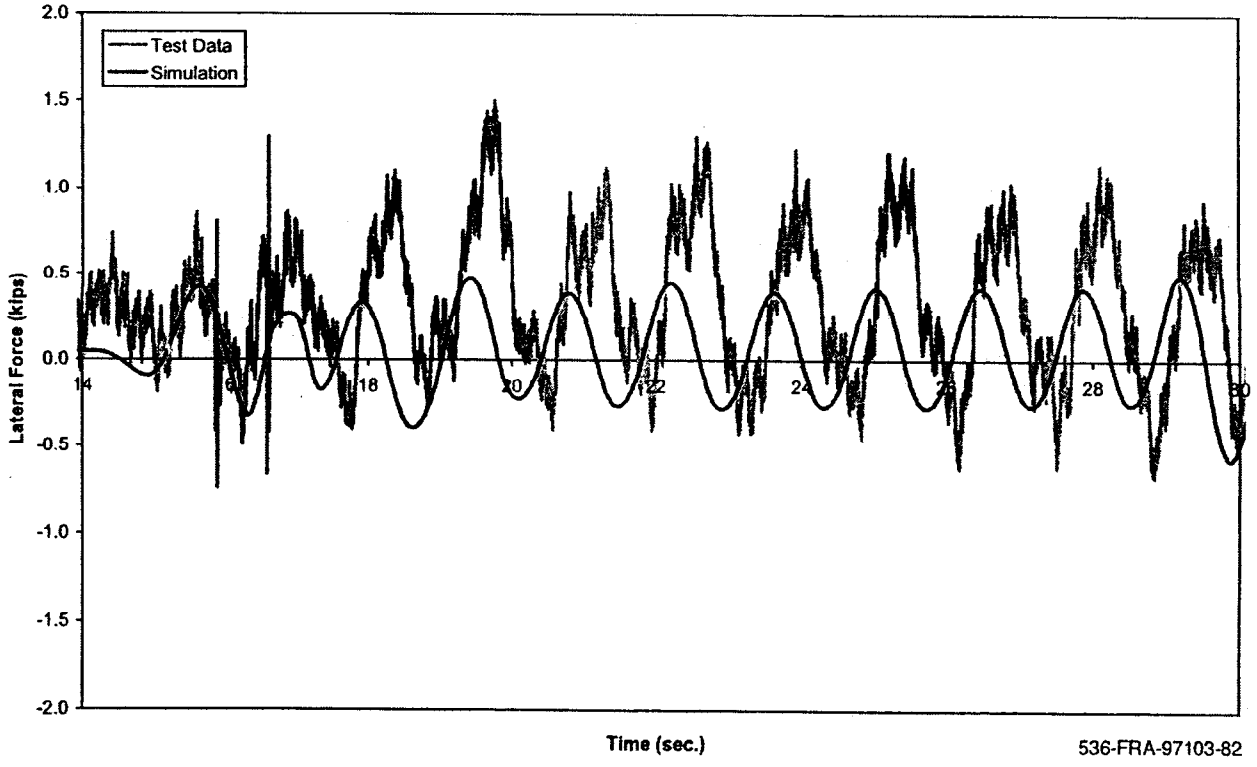

Figure A-27(c). Twist and roll - lateral force time history, 18.8 mph (trailing left wheel)

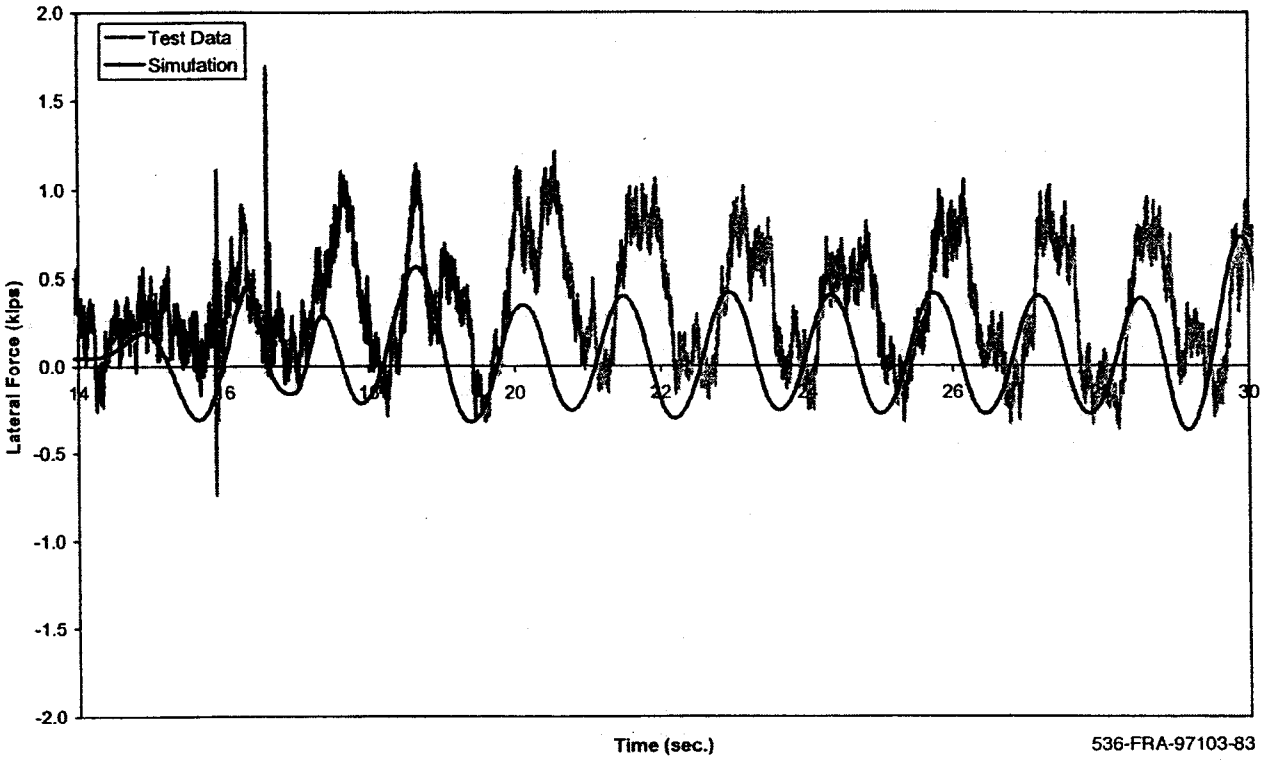

Figure A-27(d). Twist and roll - lateral force time history, 18.8 mph (trailing right wheel)

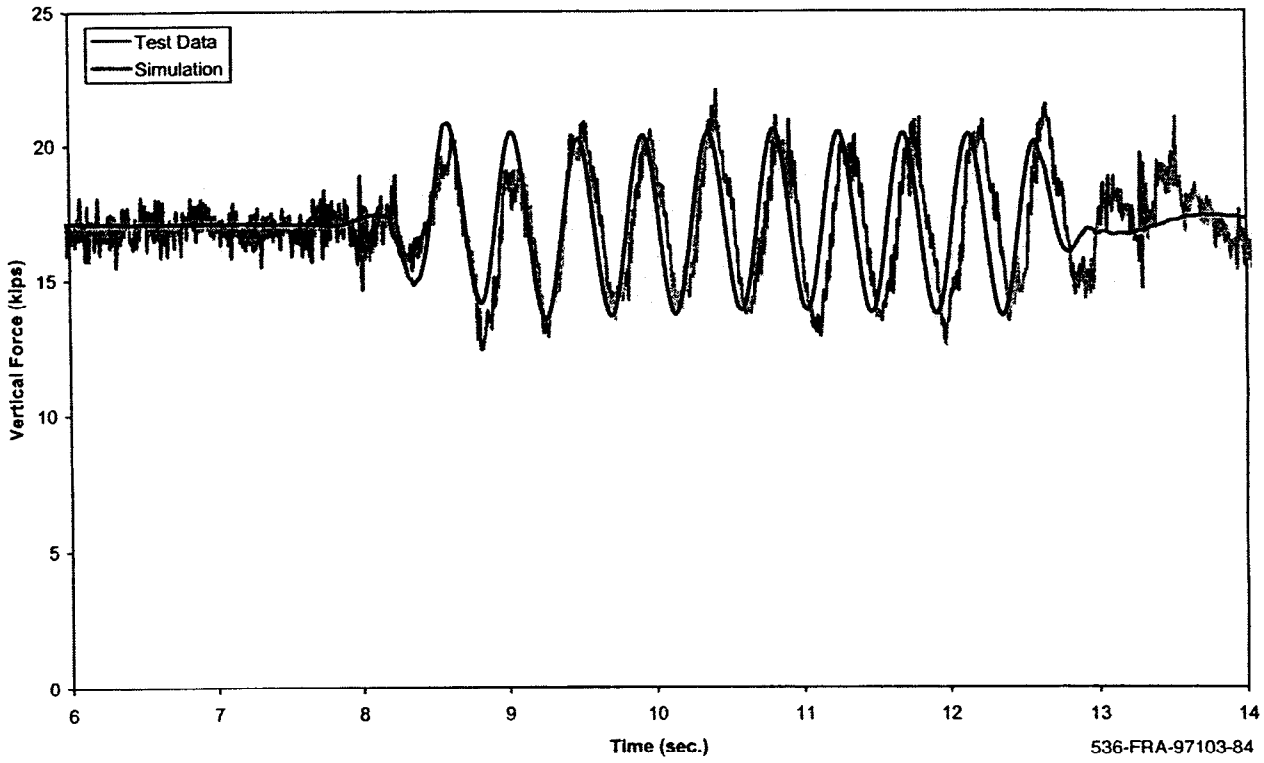

Figure A-28(a). Twist and roll - vertical force time history, 60 mph (lead left wheel)

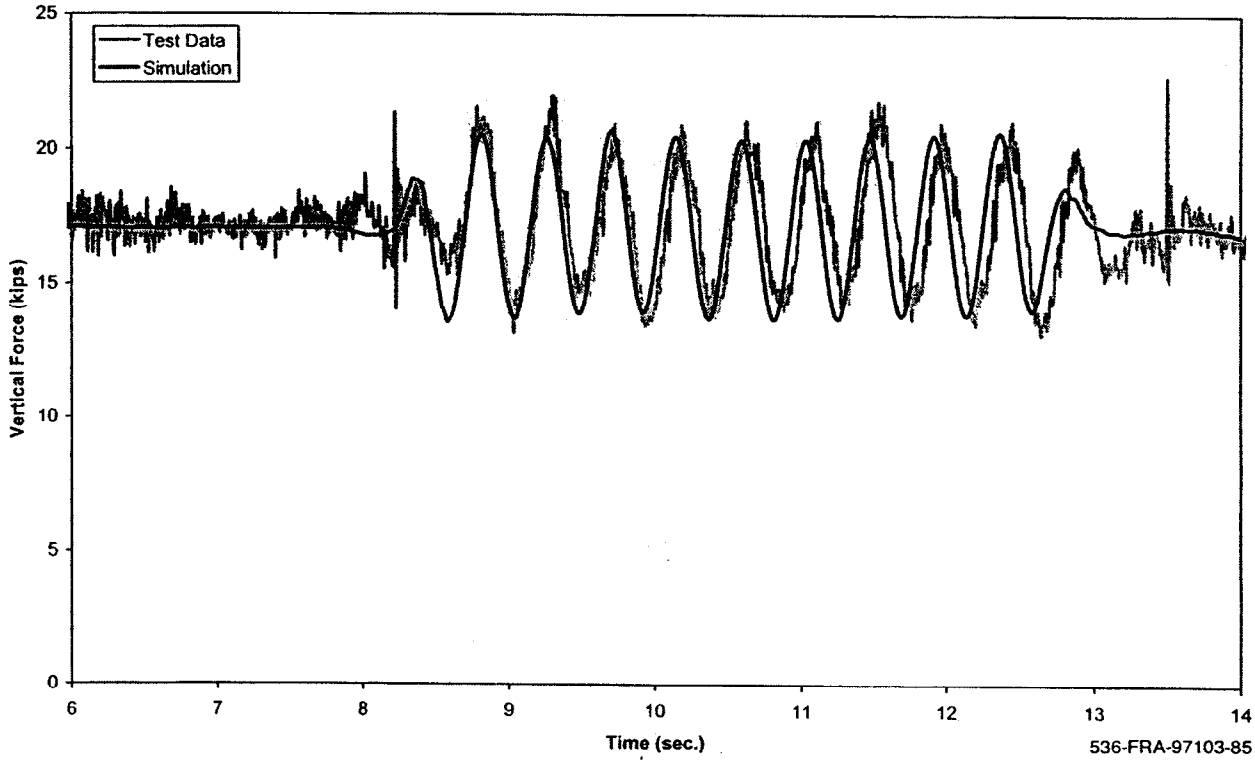

Figure A-28(b). Twist and roll - vertical force time history, 60 mph (lead right wheel)

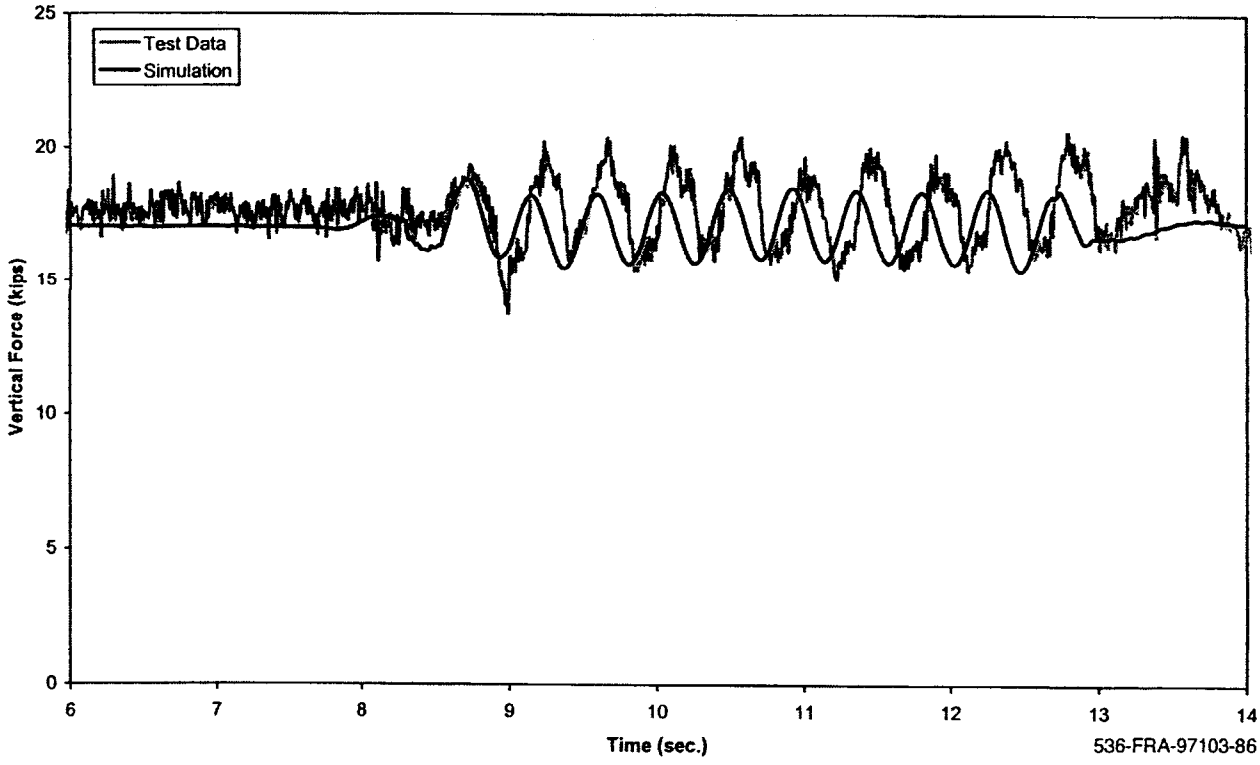

Figure A-28(c). Twist and roll - vertical force time history, 60 mph (trailing left wheel)

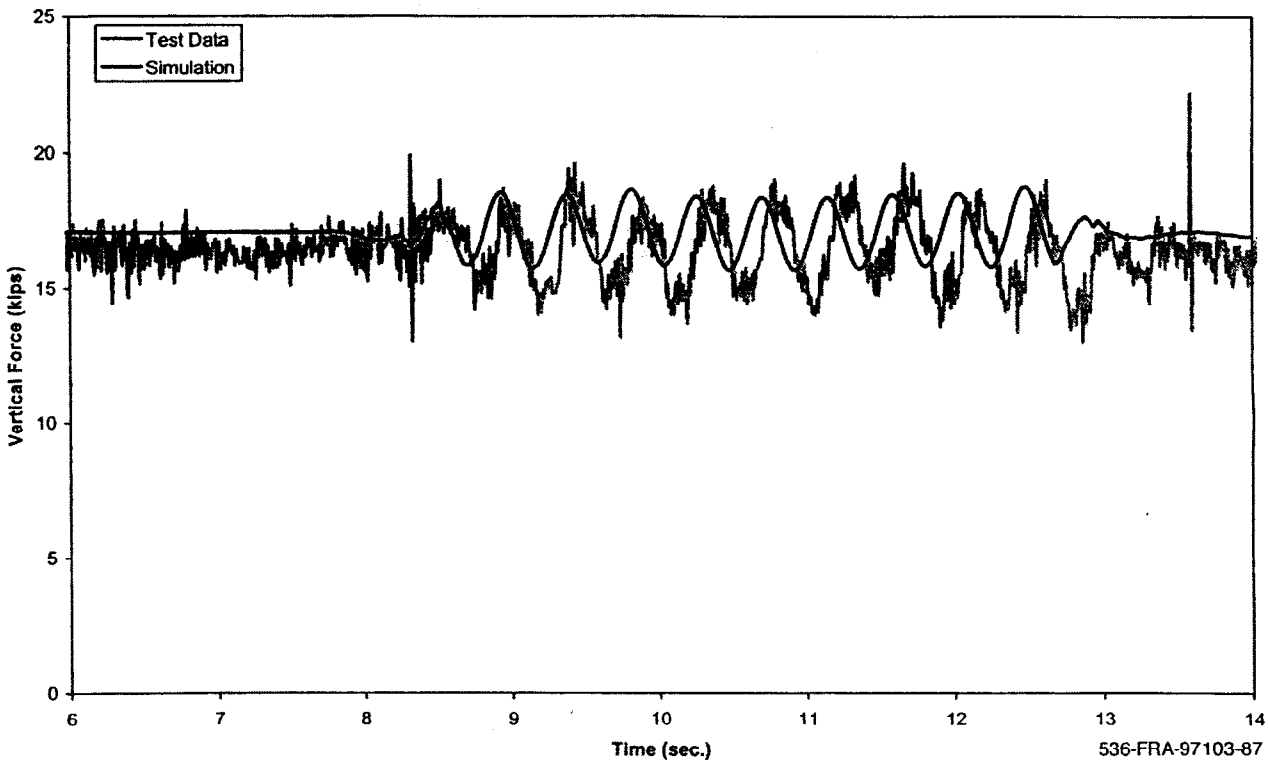

Figure A-28(d). Twist and roll - vertical force time history, 60 mph (trailing right wheel)

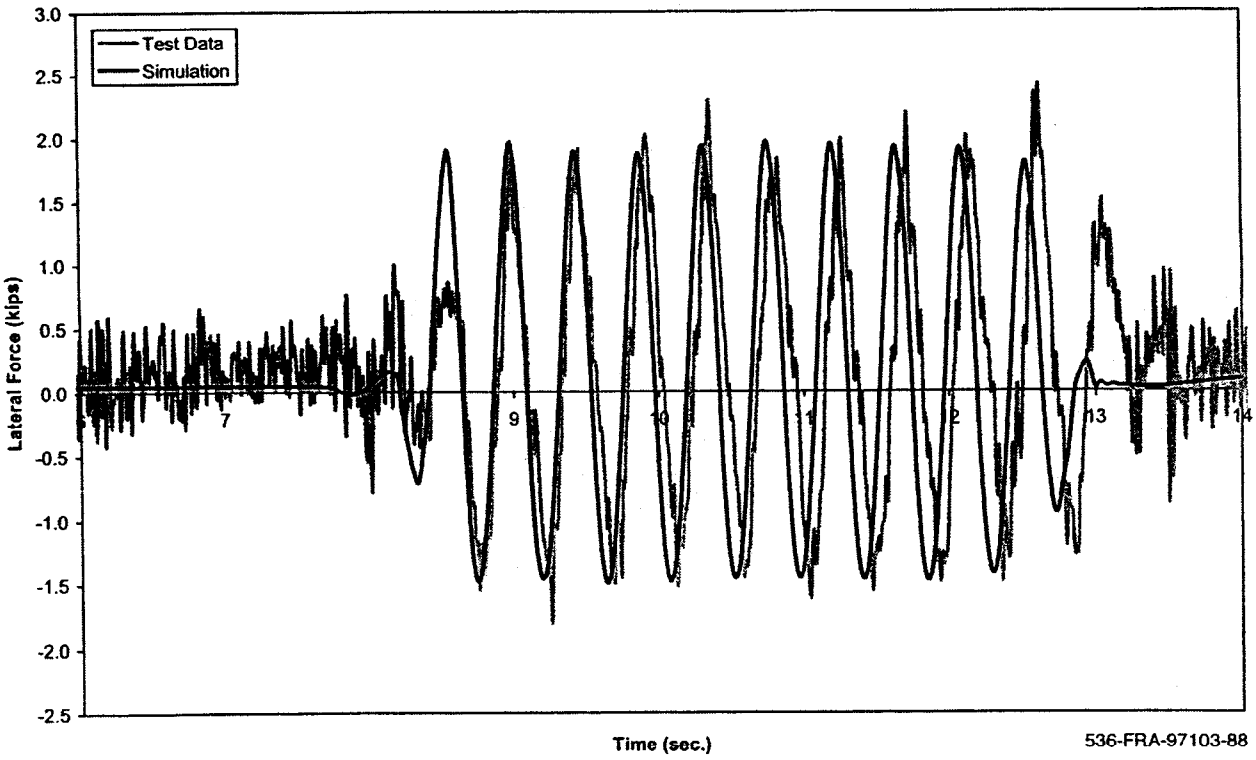

Figure A-29(a). Twist and roll - lateral force time history, 60 mph (lead left wheel)

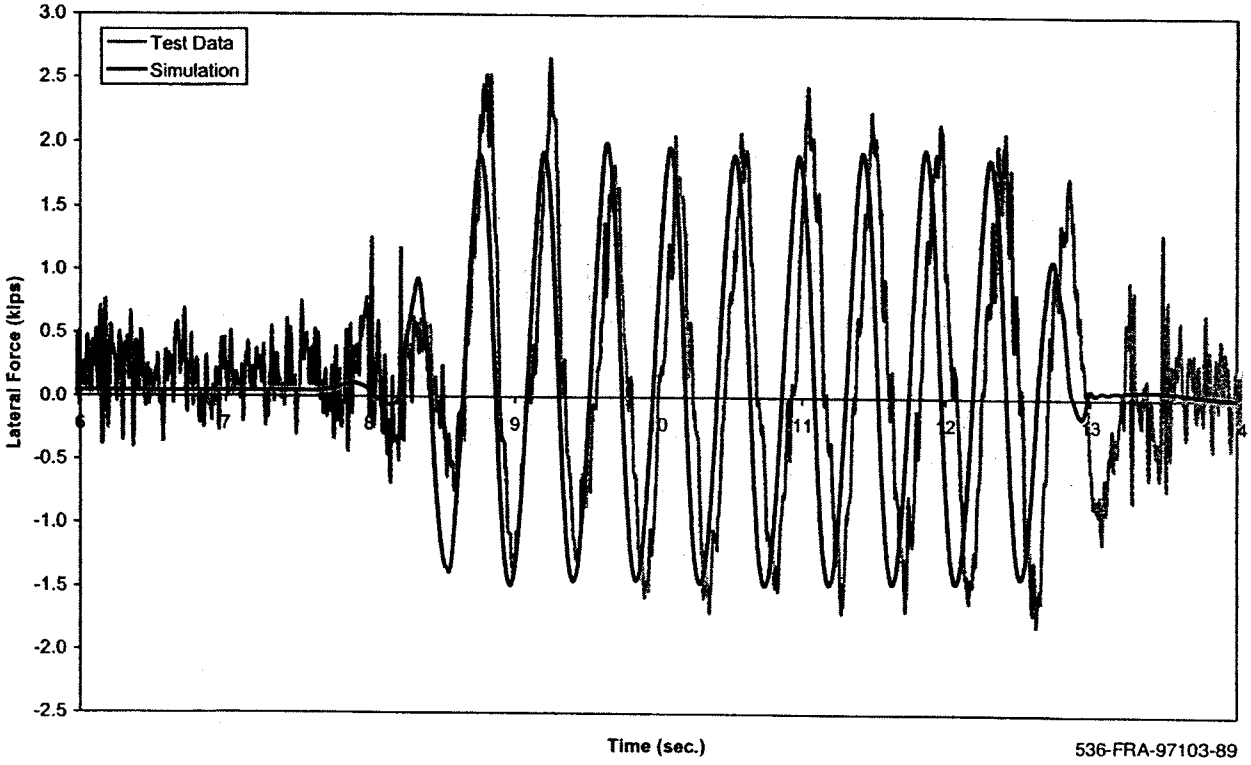

Figure A-29(b). Twist and roll - lateral force time history, 60 mph (lead right wheel)

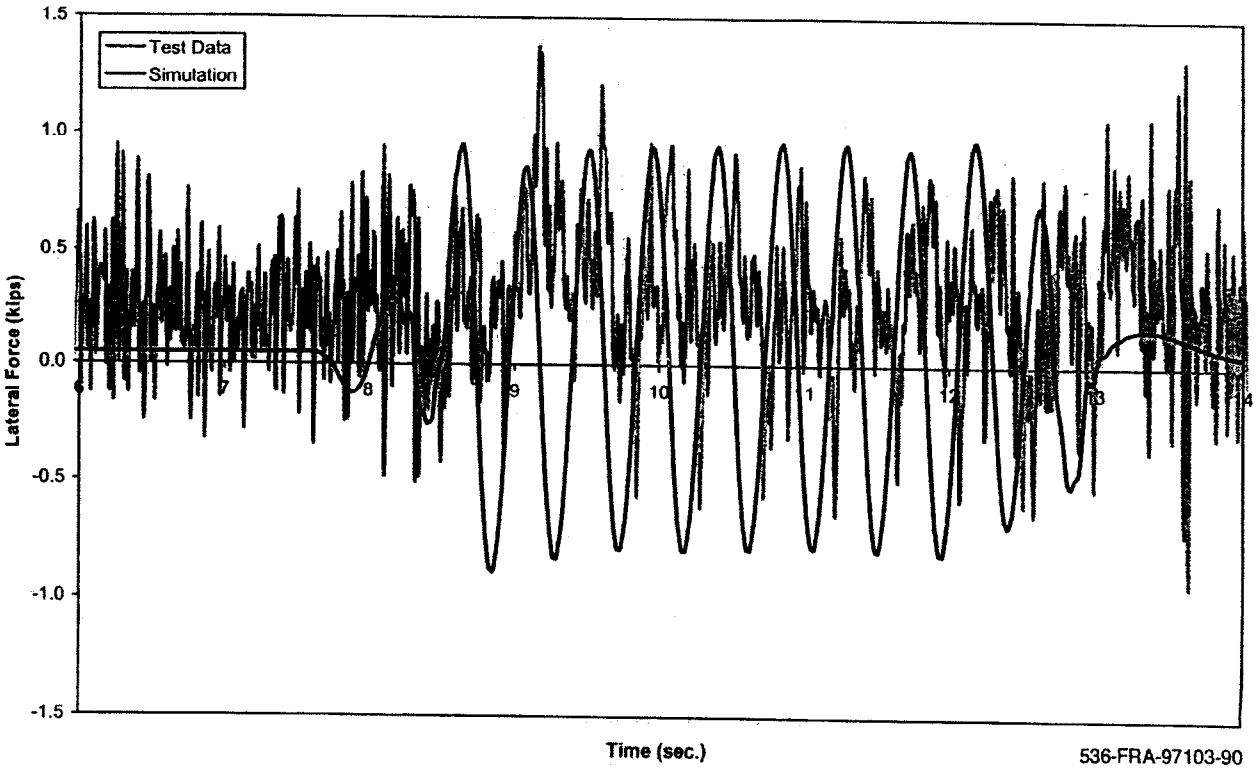

Figure A-29(c). Twist and roll - lateral force time history, 60 mph (trailing left wheel)

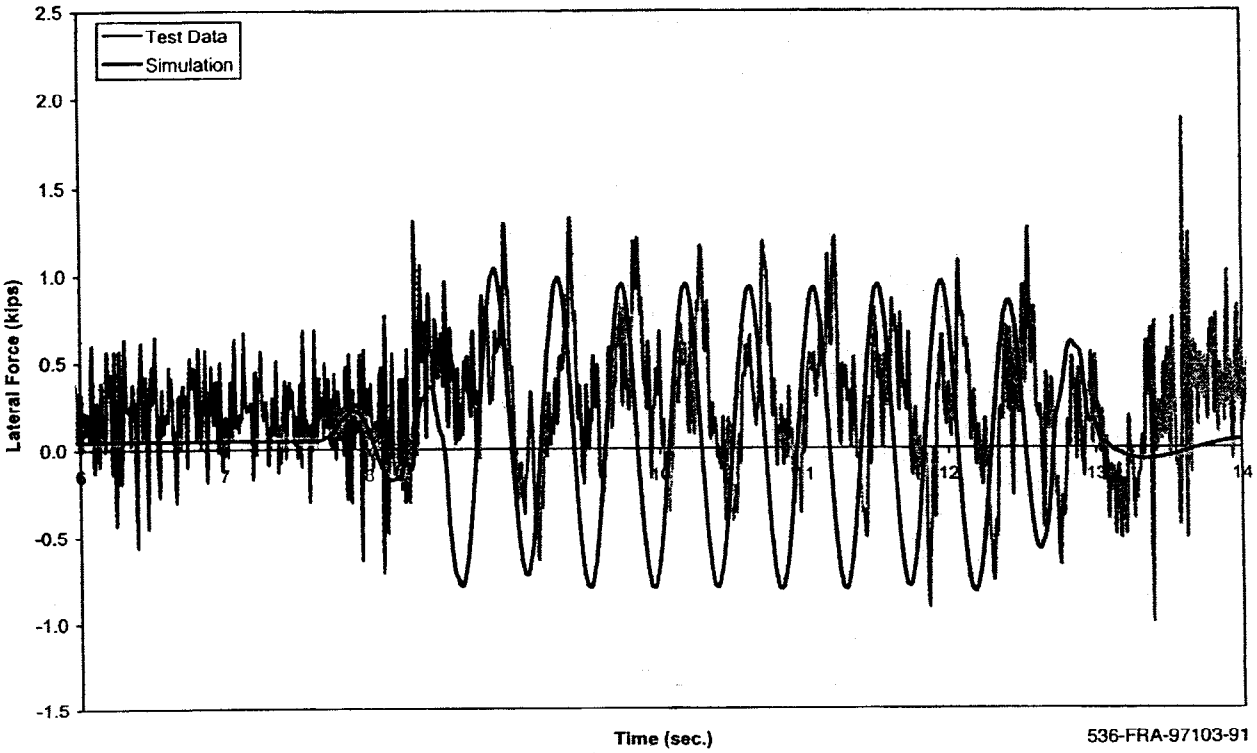

Figure A-29(d). Twist and roll - lateral force time history, 60 mph (trailing right wheel)

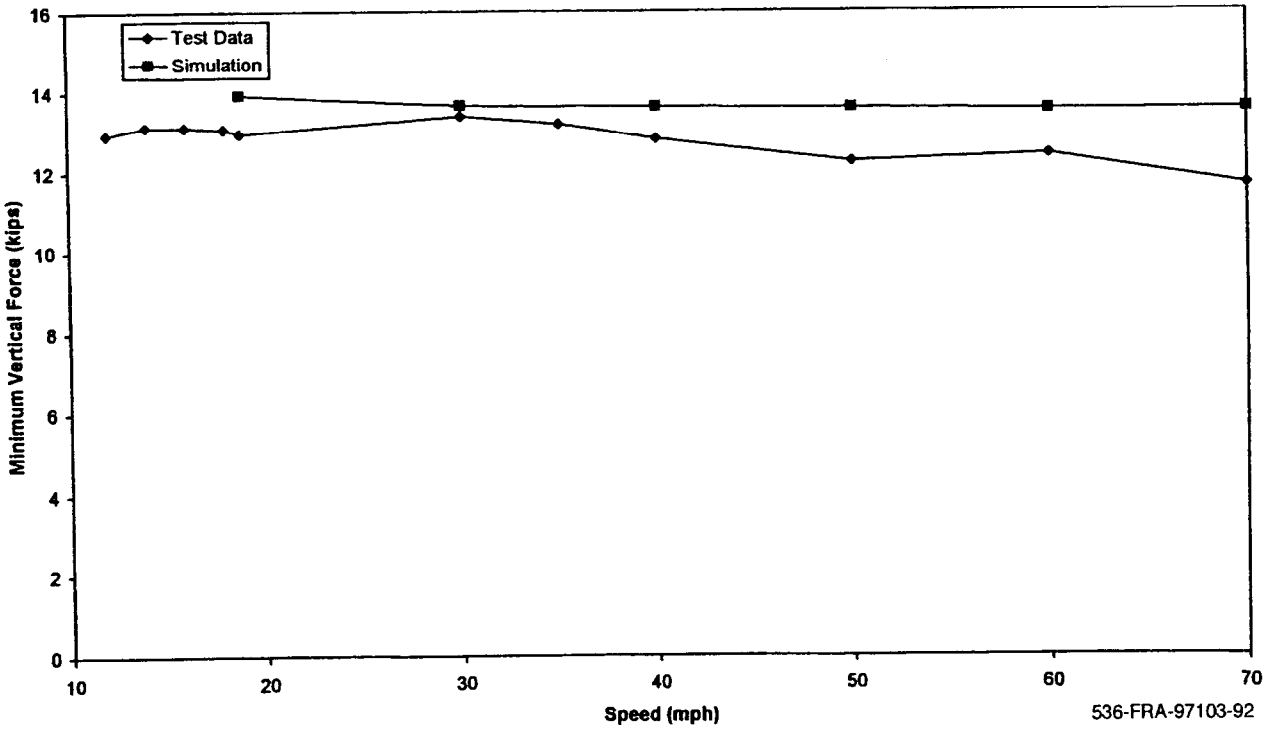

Figure A-30. Twist and sway - minimum vertical force (lead left wheel)

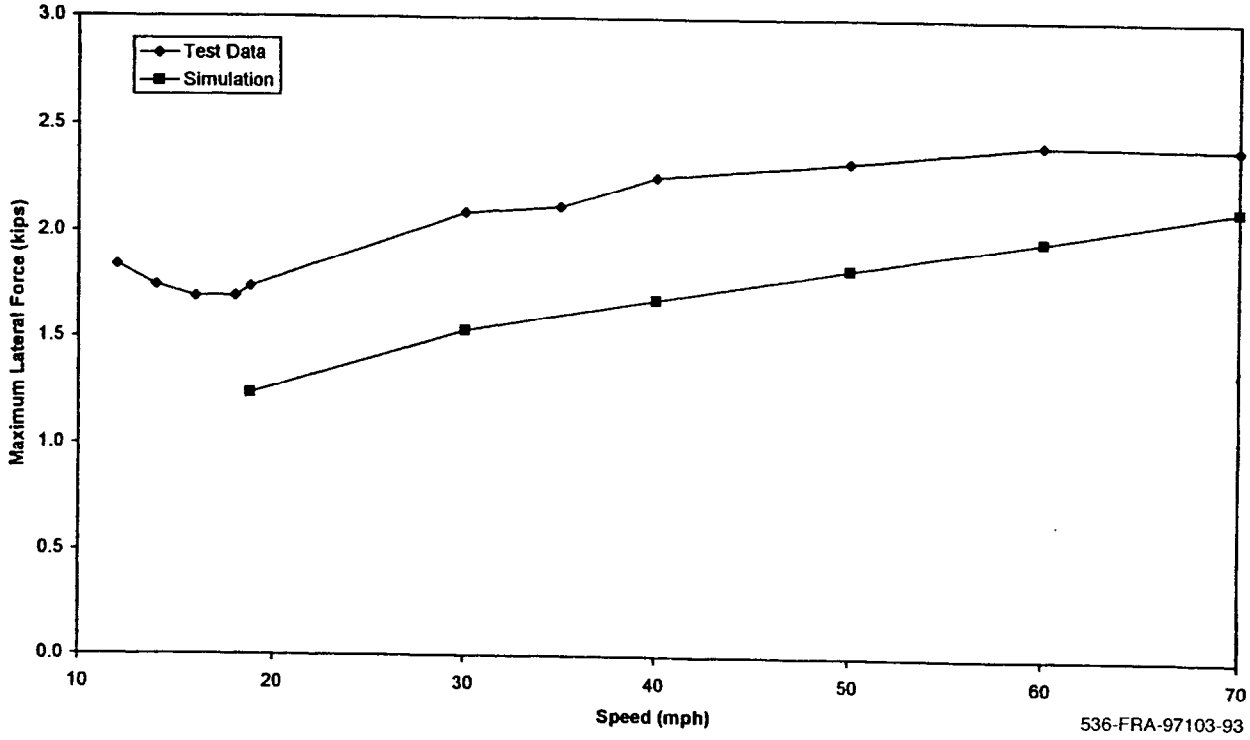

Figure A-31. Twist and sway - maximum lateral force (lead left wheel)

acceleration at the "B" end is shown in Figure A-32. The simulation underestimates the values by 0.04g, though the general trend of the car body acceleration with speed is well predicted by the simulation.

A.6 Pitch and Bounce

Figure A-33 illustrates the case of a pitch and bounce correlation of the vertical force for the four wheels of the trailing truck at a speed of 20 mph. Good correlation is seen between the test data and simulation results. The small fluctuations in the test data are attributed to the inherent variations in the rail vertical profile data, not modeled in the simulation. The lateral force levels are too small to be of any practical significance and are not shown. Similar results were obtained for other speeds.

Figure A-34 shows the vertical forces for the four wheels for a pitch and bounce test conducted at 60 mph. The correlation for the vertical force levels is good for all wheels.

A plot of the correlation of test and simulation data of minimum vertical force is shown in Figure A-35 for the left wheel on the lead axle of the trailing truck. Good correlation is shown through the speed range for the vertical force. The minimum vertical force is about 31 mph in both the test data and simulation. This occurs at the resonance speeds. The resonant condition is not noticeably strong.

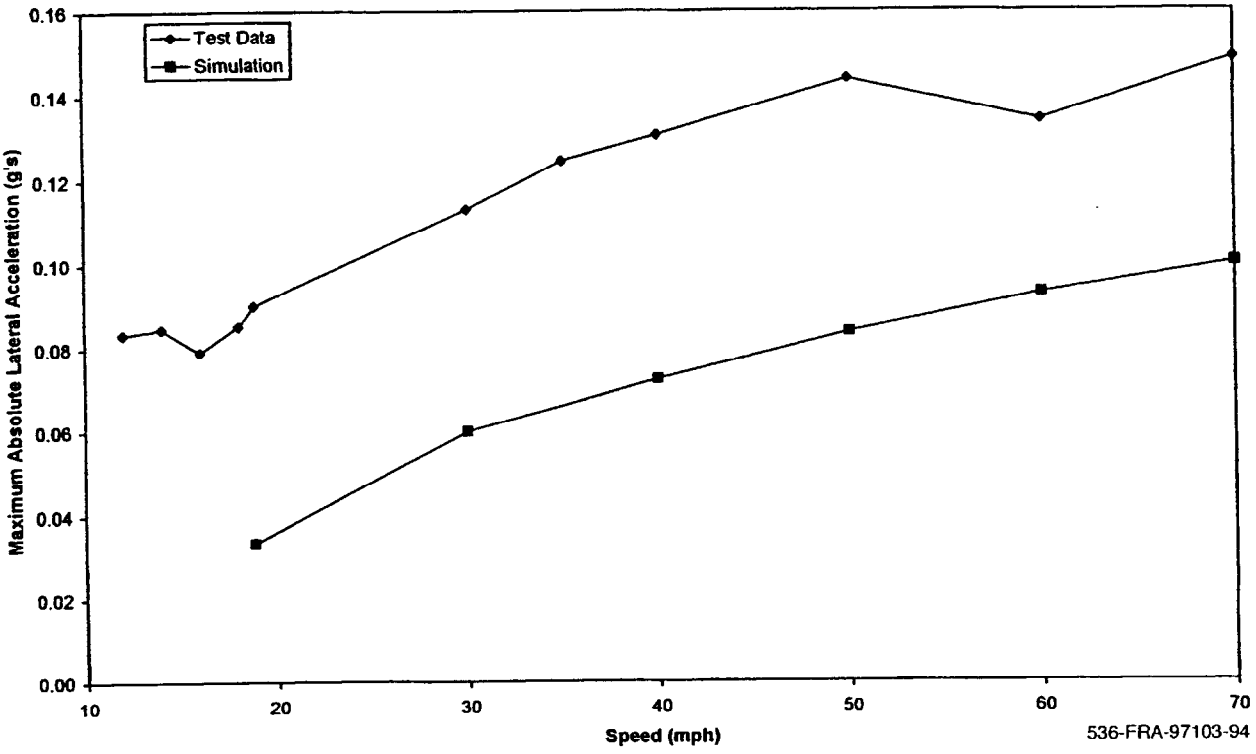

Figure A-32. Twist and sway - maximum absolute lateral car body acceleration ("B" end)

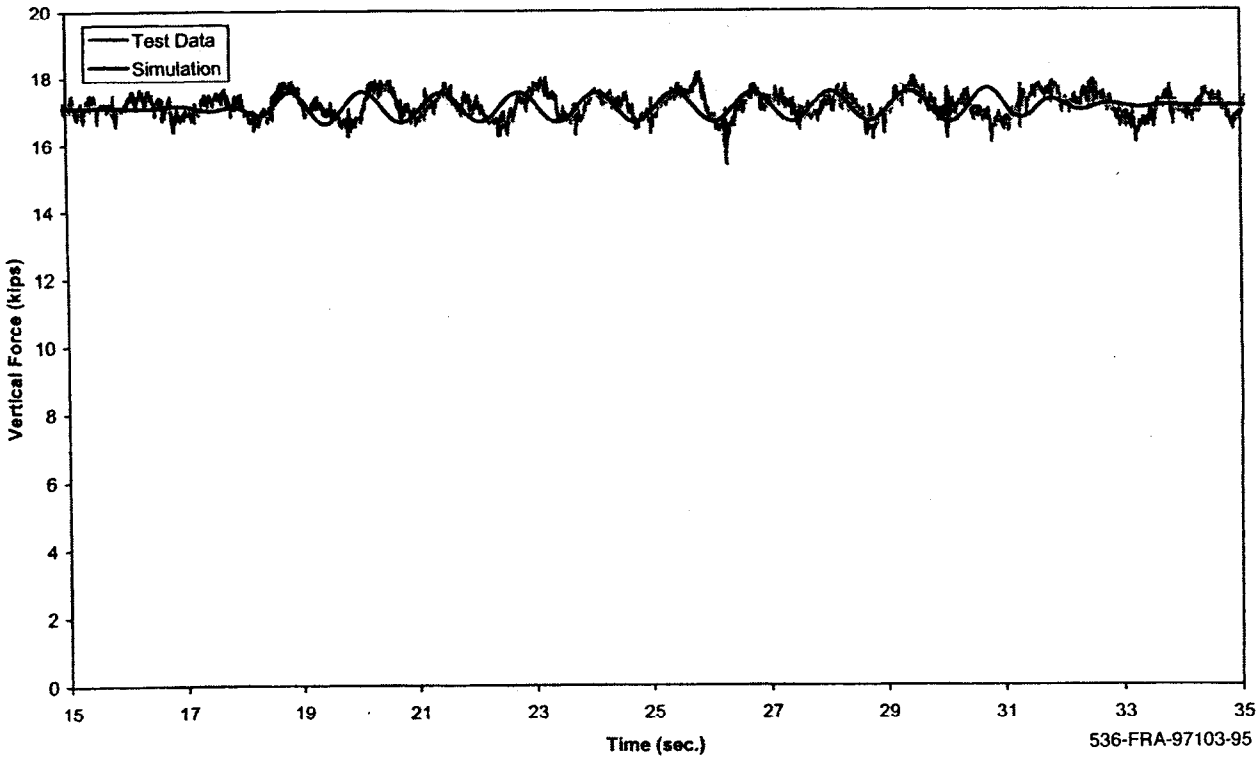

Figure A-33(a). Pitch and bounce - vertical force time history, 20 mph (lead left wheel)

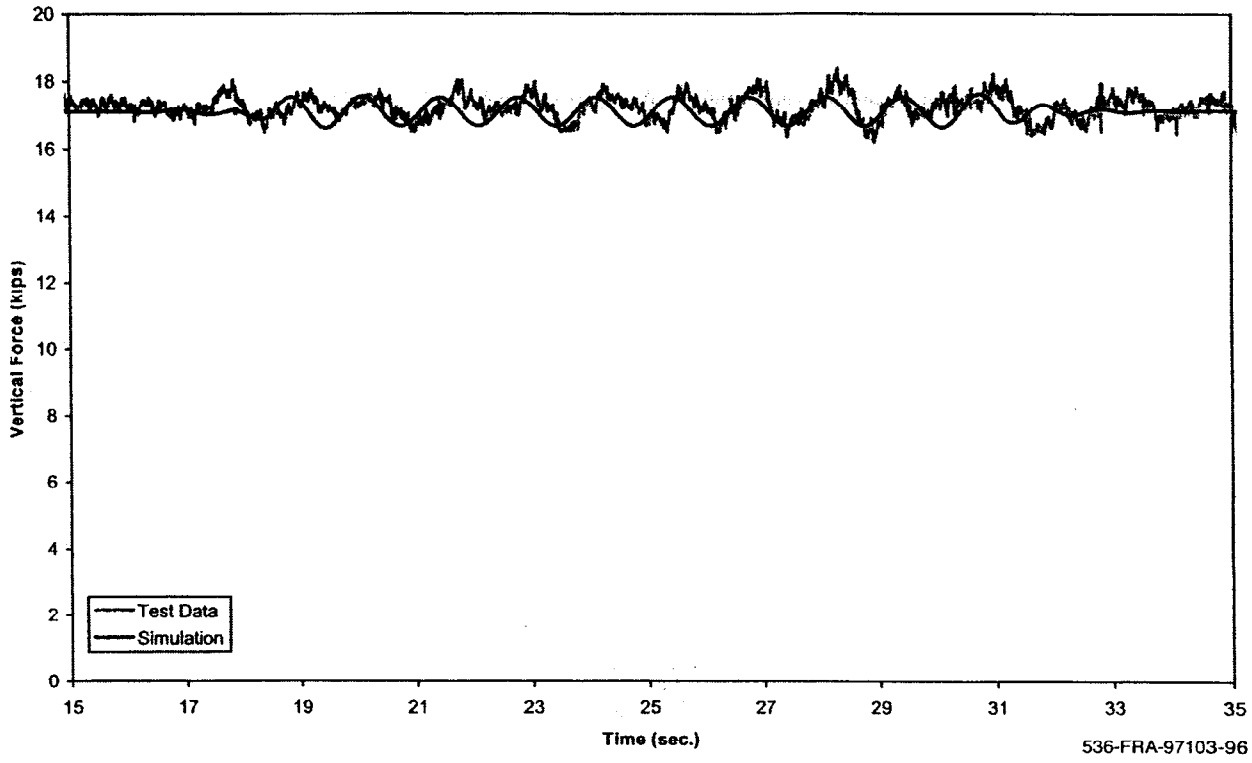

Figure A-33(b). Pitch and bounce - vertical force time history, 20 mph (lead right wheel)

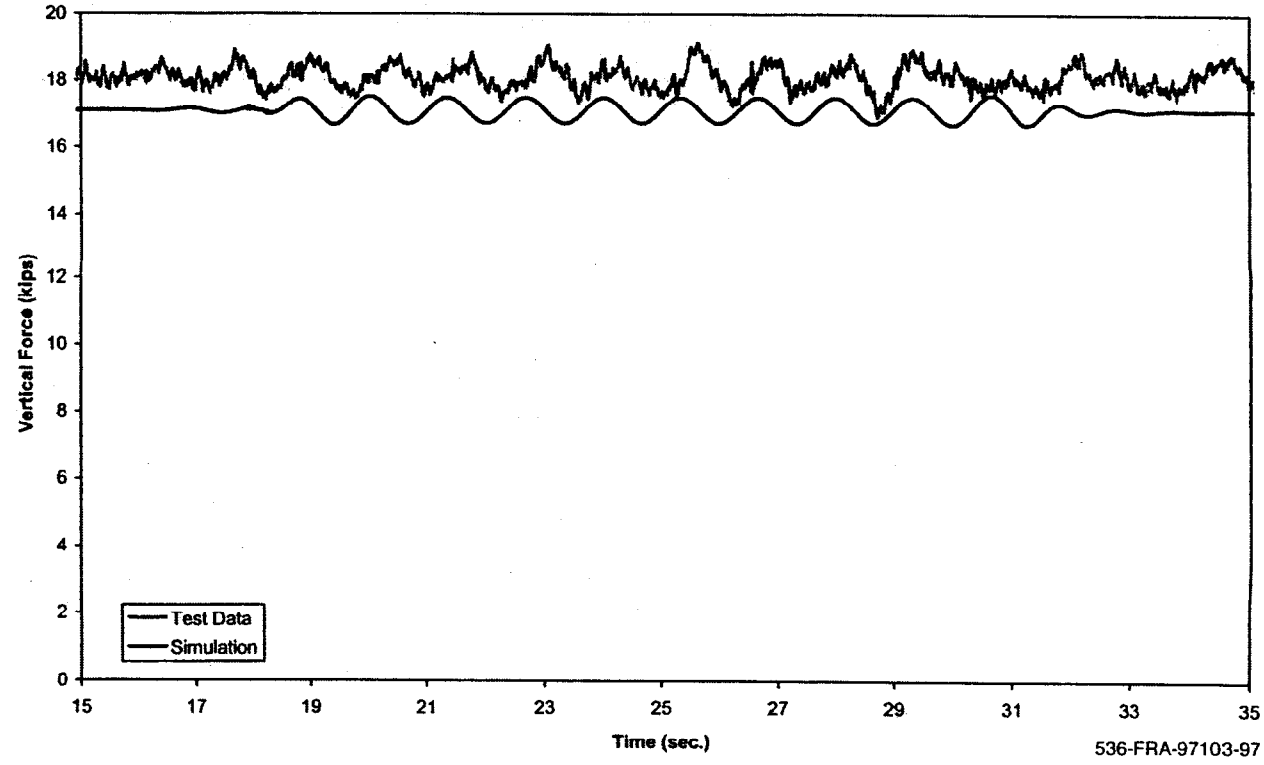

Figure A-33(c). Pitch and bounce - vertical force time history, 20 mph (trailing left wheel)

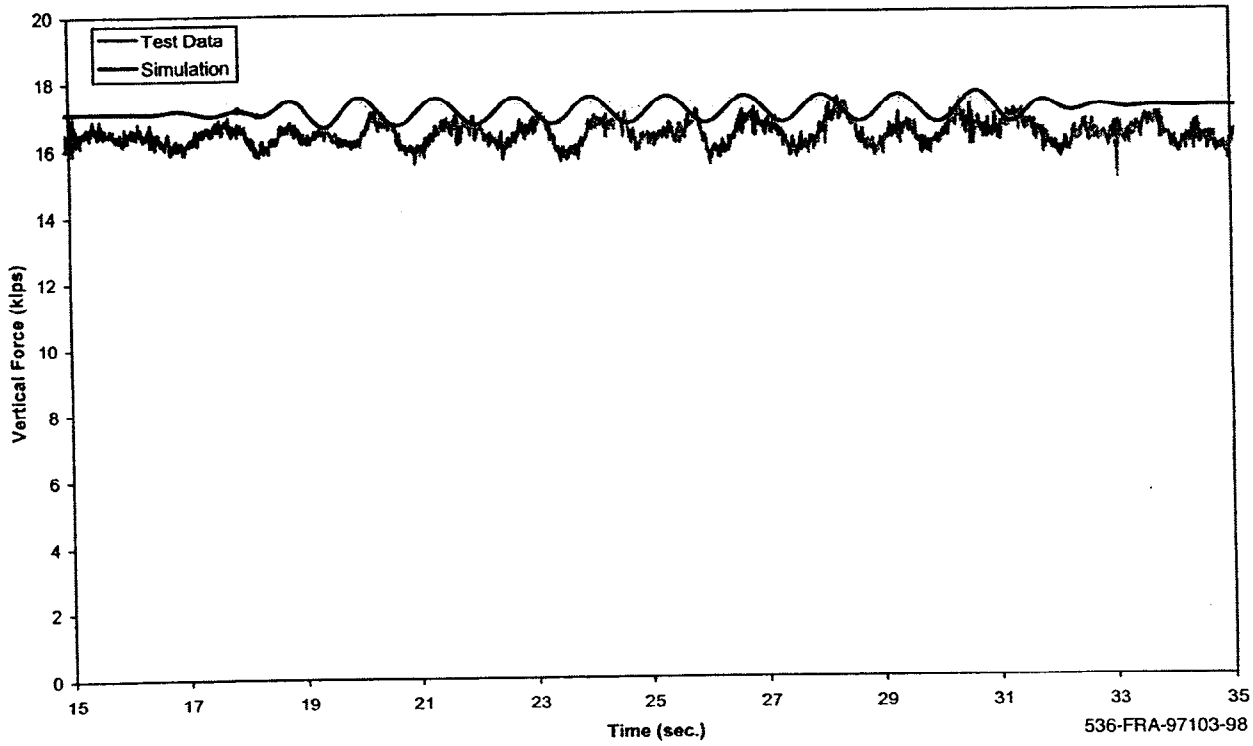

Figure A-33(d). Pitch and bounce - vertical force time history, 20 mph (trailing right wheel)

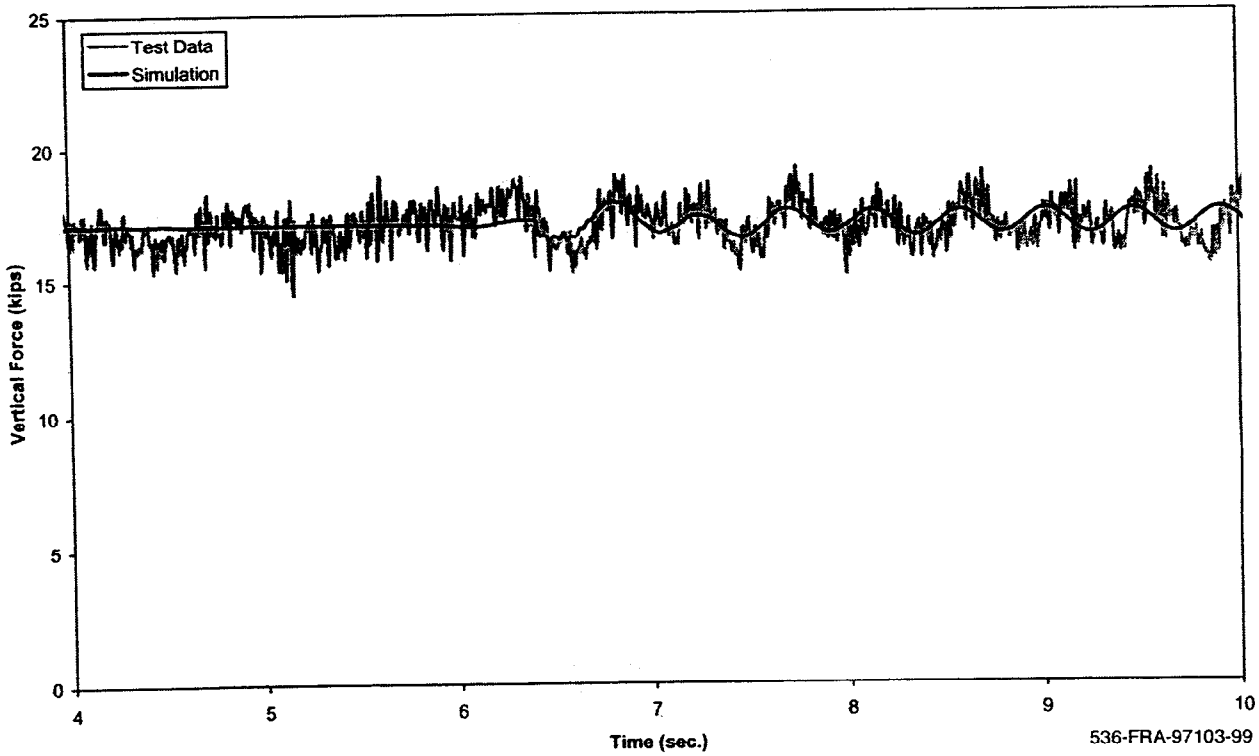

Figure A-34(a). Pitch and bounce - lateral force time history, 60 mph (lead left wheel)

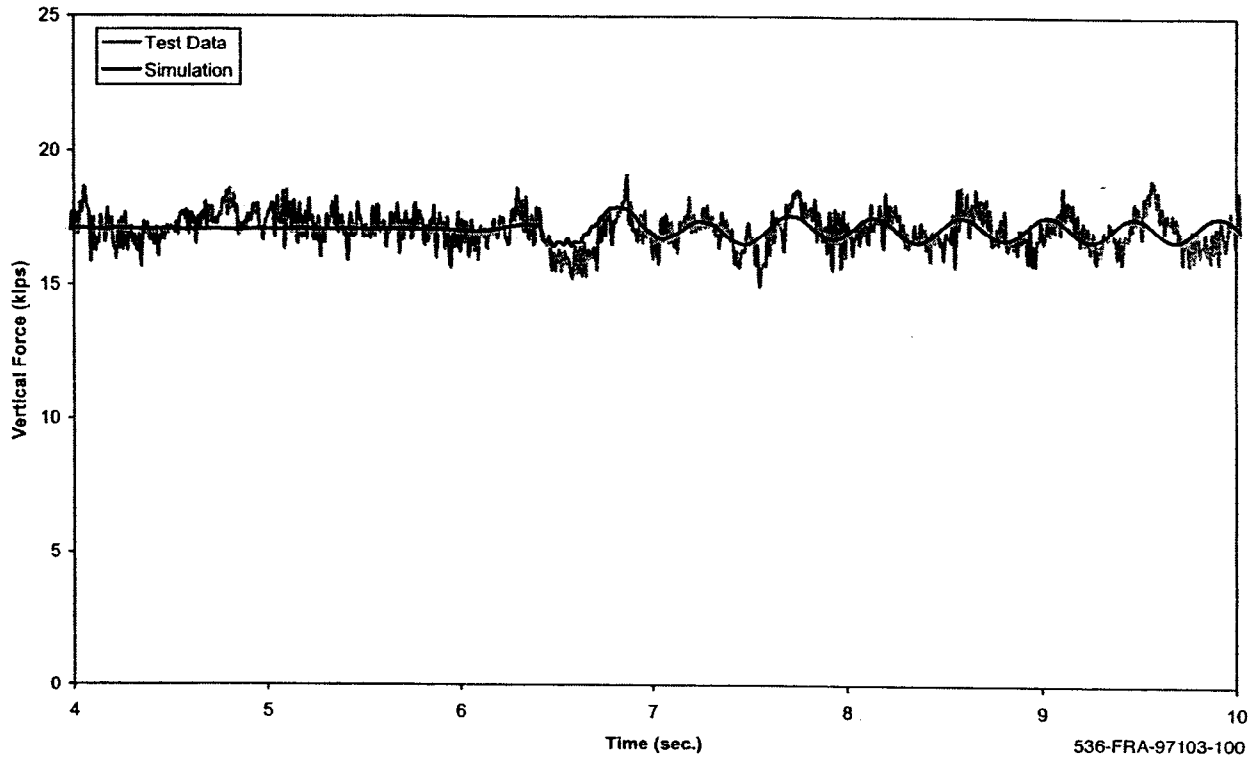

Figure A-34(b). Pitch and bounce - lateral force time history, 60 mph (lead right wheel)

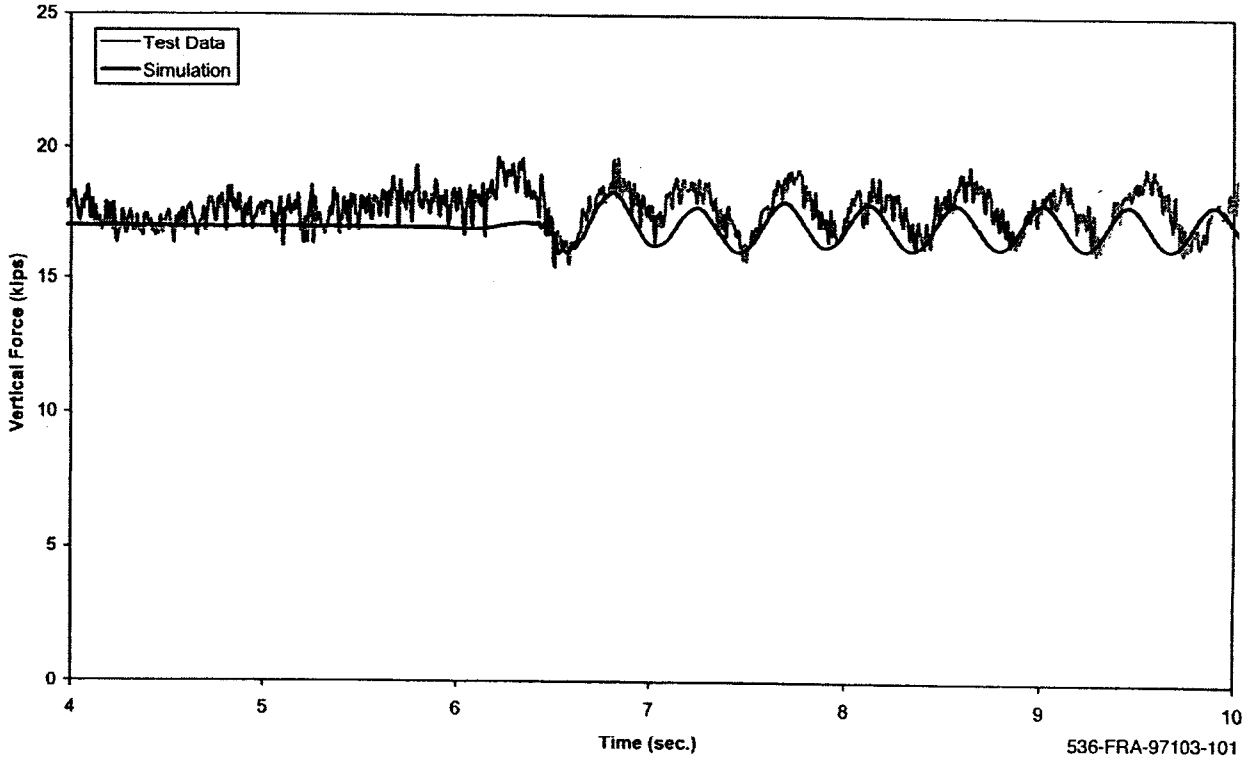

Figure A-34(c). Pitch and bounce - lateral force time history, 60 mph (trailing left wheel)

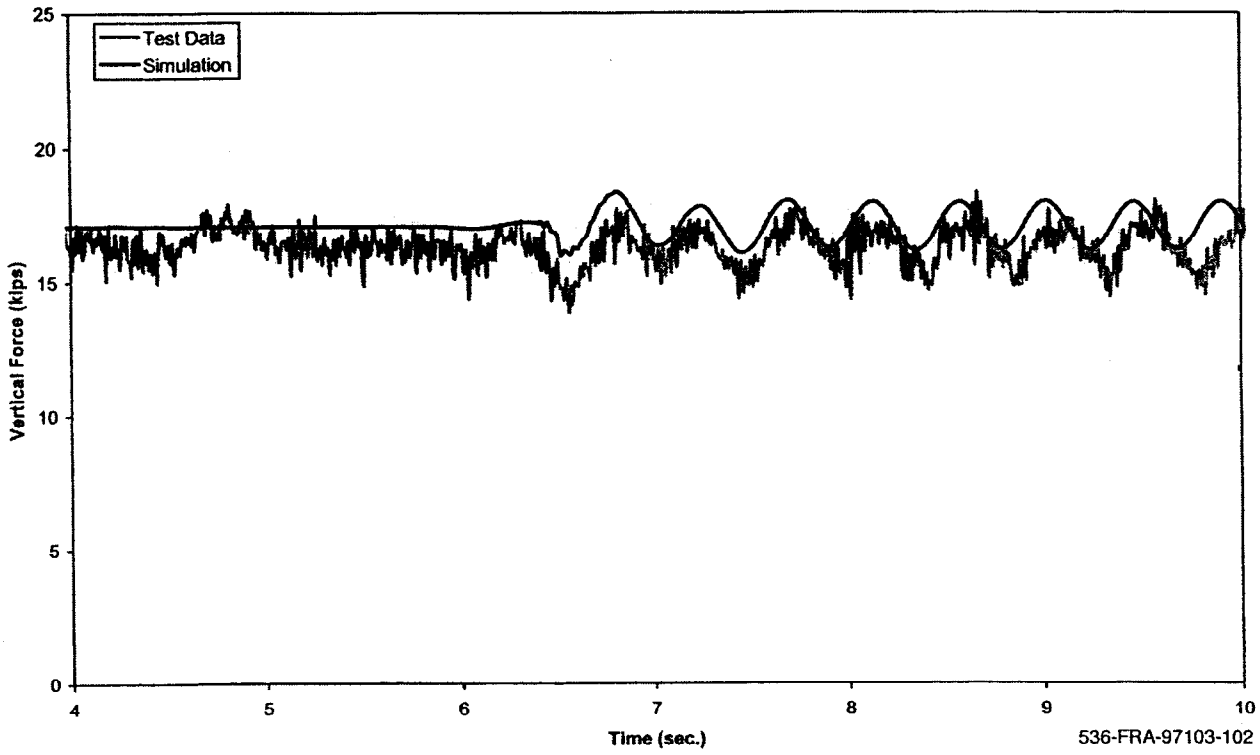

Figure A-34(d). Pitch and bounce - lateral force time history, 60 mph (trailing right wheel)

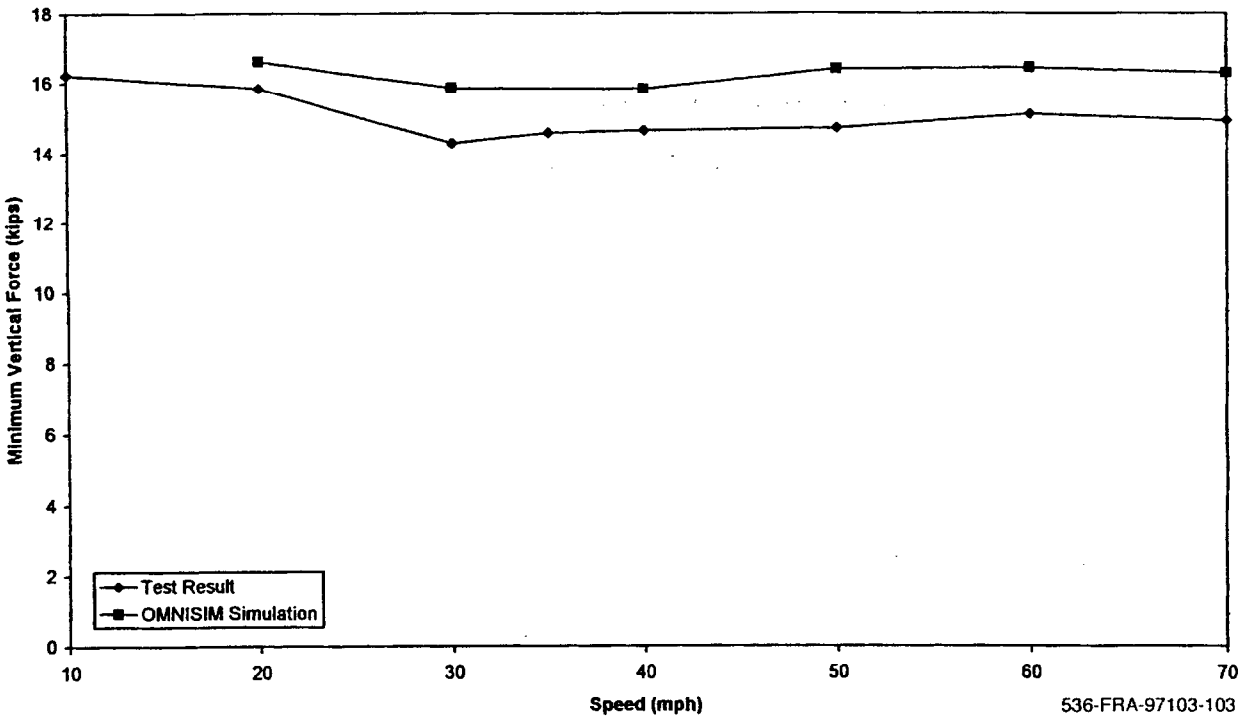

Figure A-35. Pitch and bounce - minimum vertical force (lead left wheel)

A.7 Hunting Test with Initial Alignment Defects

In both the test data and the simulations no evidence of sustained vehicle hunting is observed in the 80 to 130 mph speed range. Additional computer simulations conducted at higher speeds indicated that the vehicle hunting speed is in excess of 200 mph. Comparisons of lateral measured and simulated forces resulting from track perturbation are plotted in Figure A-36 for all four wheels of the trailing truck for the 130 mph case. Both the test and simulation data show no evidence of sustained hunting and in general have lateral force variations of less than ±2 kips.

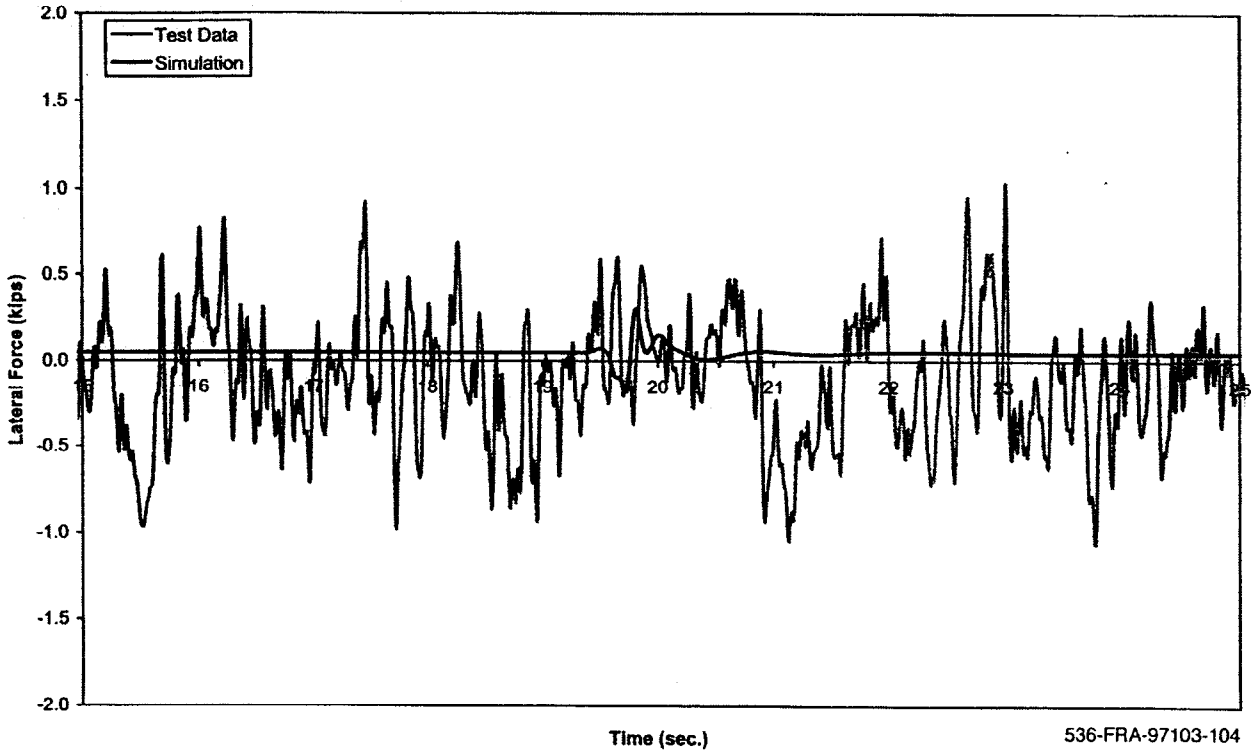

Figure A-36(a). Hunting test - lateral force time history, 130 mph (lead left wheel)

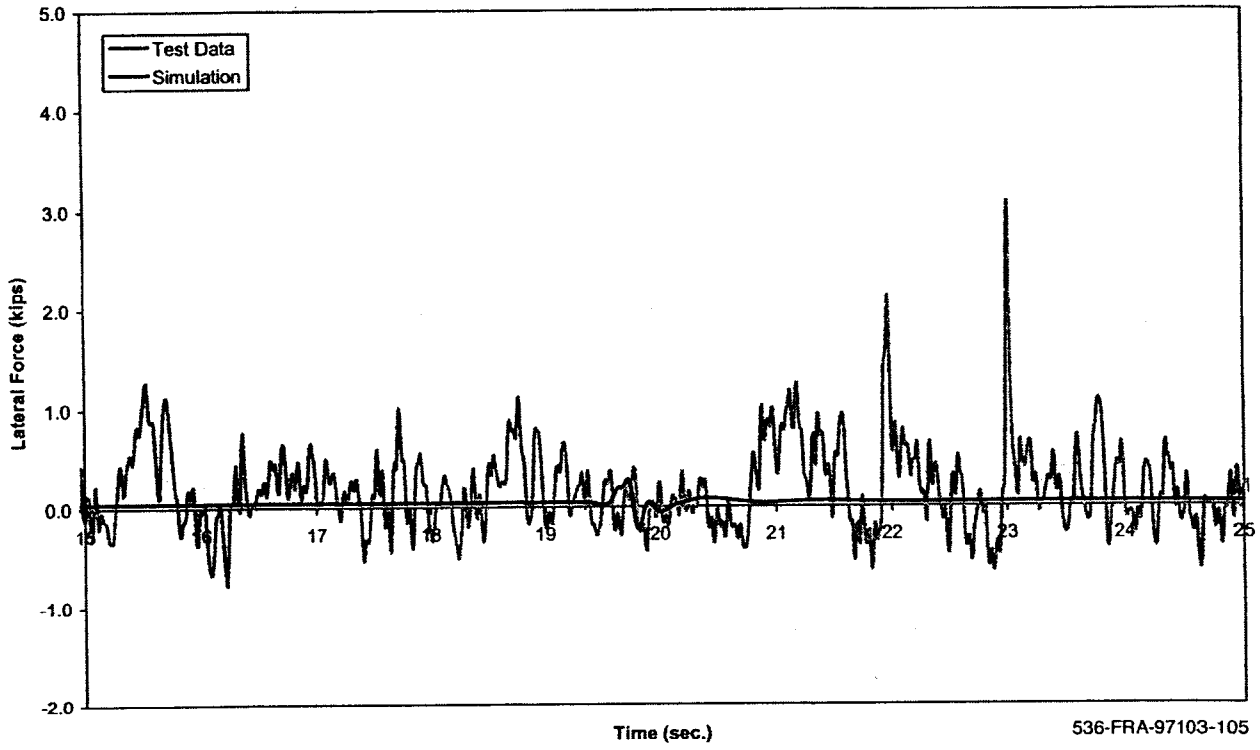

Figure A-36(b). Hunting test - lateral force time history, 130 mph (lead right wheel)

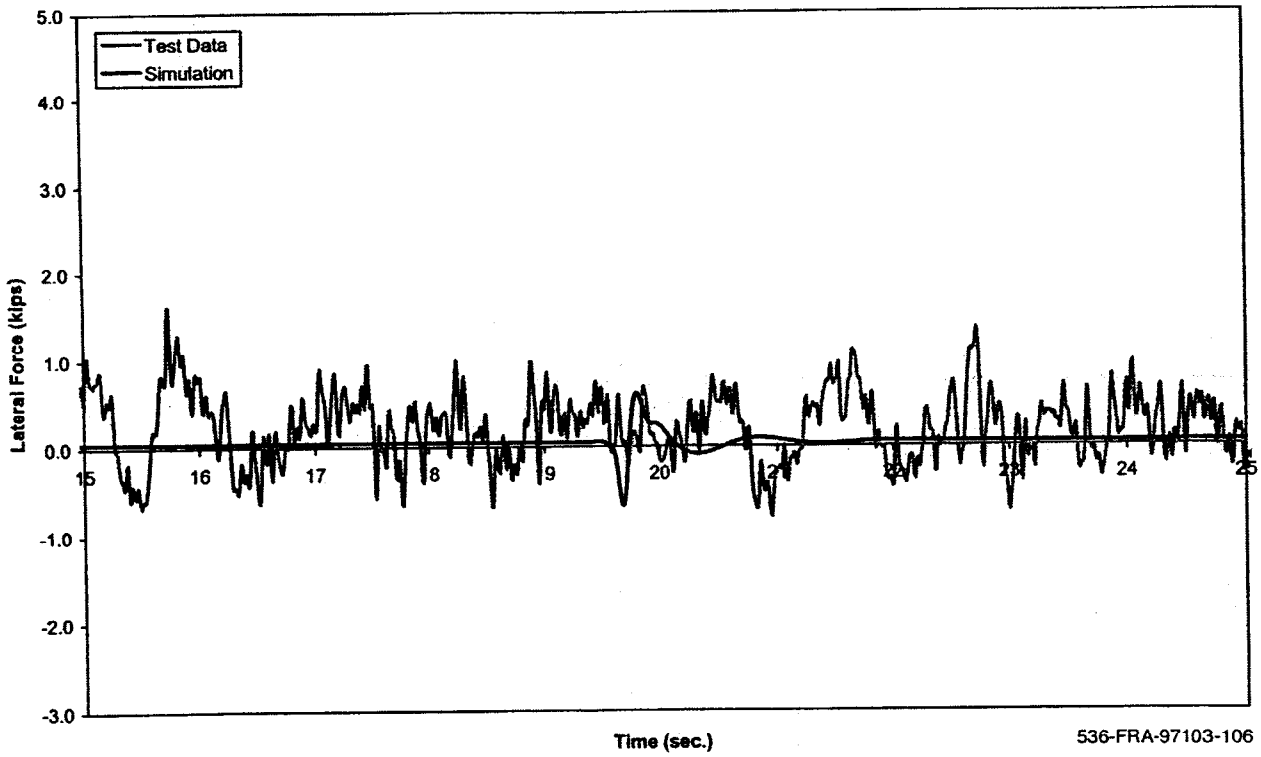

Figure A-36(c). Hunting test - lateral force time history, 130 mph (trailing left wheel)

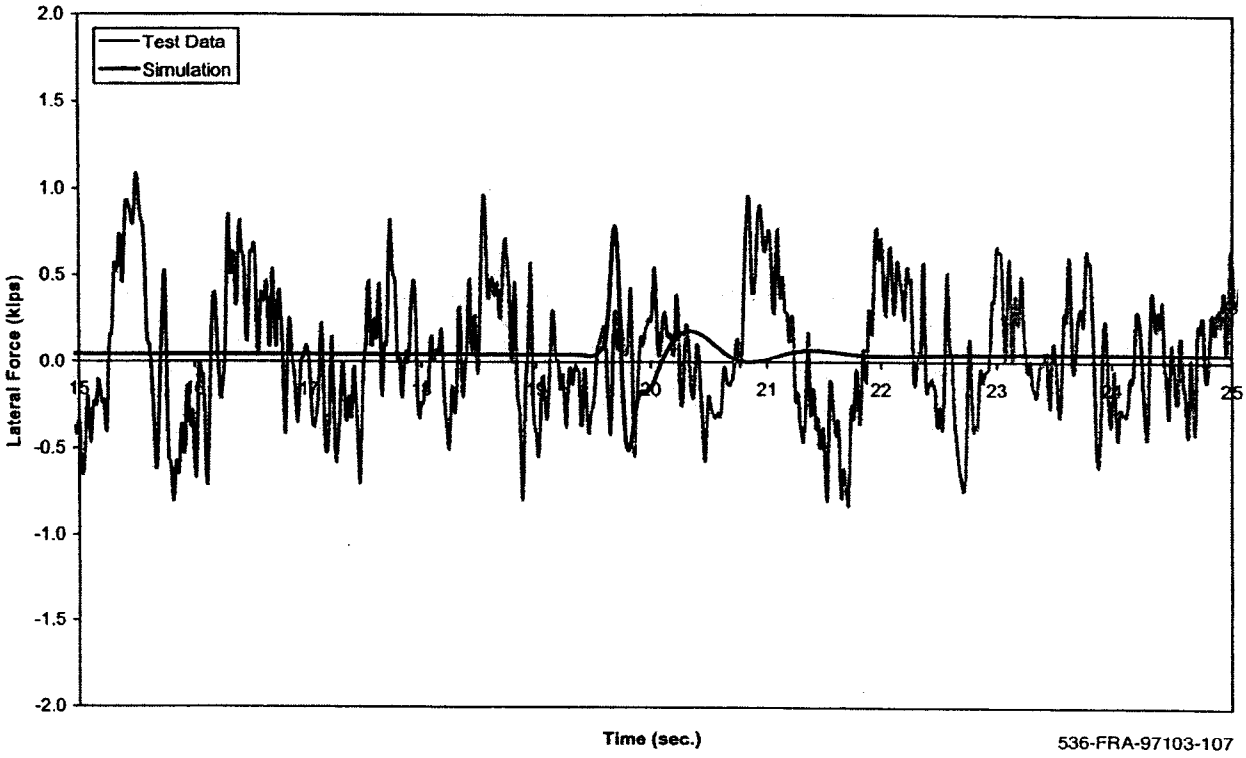

Figure A-36(d). Hunting test - lateral force time history, 130 mph (trailing left wheel)

APPENDIX B

COMPARISON OF TESTS TO SIMULATIONS (PASSENGER RAIL VEHICLE WITH EQUALIZED TRUCKS)

B.1 Vehicle Response to Variations in Vertical Alignment

Test data and simulation results for the wheel vertical and lateral forces resulting from the traverse of the vertical bump are displayed in Figures B-1 and B-2 for 24 mph operation and in Figures B-3 and B-4 for 15 mph. The simulation and the test data indicate wheel unloading condition occurring at all speeds in the test range. For both 15 and 24 mph cases, good agreement is found between the predicted and measured vertical forces at all four wheels of the instrumented truck.

At 24 mph, the inner wheel of the lead axle vertical force increases to a value of approximately 21 to 22 kips just prior to reducing to 9.5 kips (maximum wheel unloading). At 15 mph, the inner wheel of the lead axle vertical force similarly increases to a value of approximately 22 kips, decreases to a minimum of approximately 14 kips and then increases again to approximately 20 kips with good correspondence between the test data and simulation.

The measured and predicted lateral forces have similar shapes and levels of magnitude, however, the correlations are not as good as found for the vertical force. For the 24 mph case, the lateral force on the lead axle prior to entering the bump is approximately 9 kips (simulation) and 8 kips (test) for the outer wheel and 6 kips (simulation and test) for the inner wheel. The lateral forces for both the simulation and test data on the outer and inner wheel changes abruptly at the point of maximum wheel unloading. The trailing axle lateral forces test data are in the approximately ±1.0 kips range for the outer wheel and 2 kips range for the inner wheel. The simulation results have similar waveforms but at reduced levels with the outer wheel lateral forces varying from 0.5 kips and the inner wheel lateral force a maximum of 2 kips.

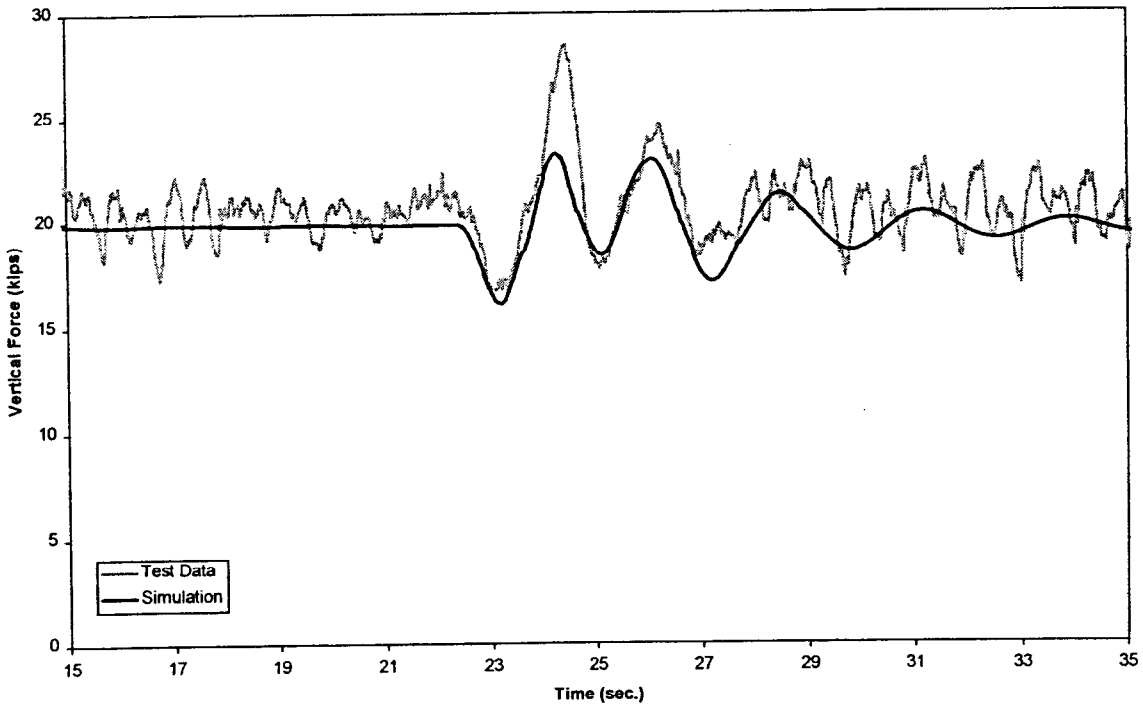

Figure B-1(a). Vertical bump test - vertical force time history, 24 mph (lead outer wheel)

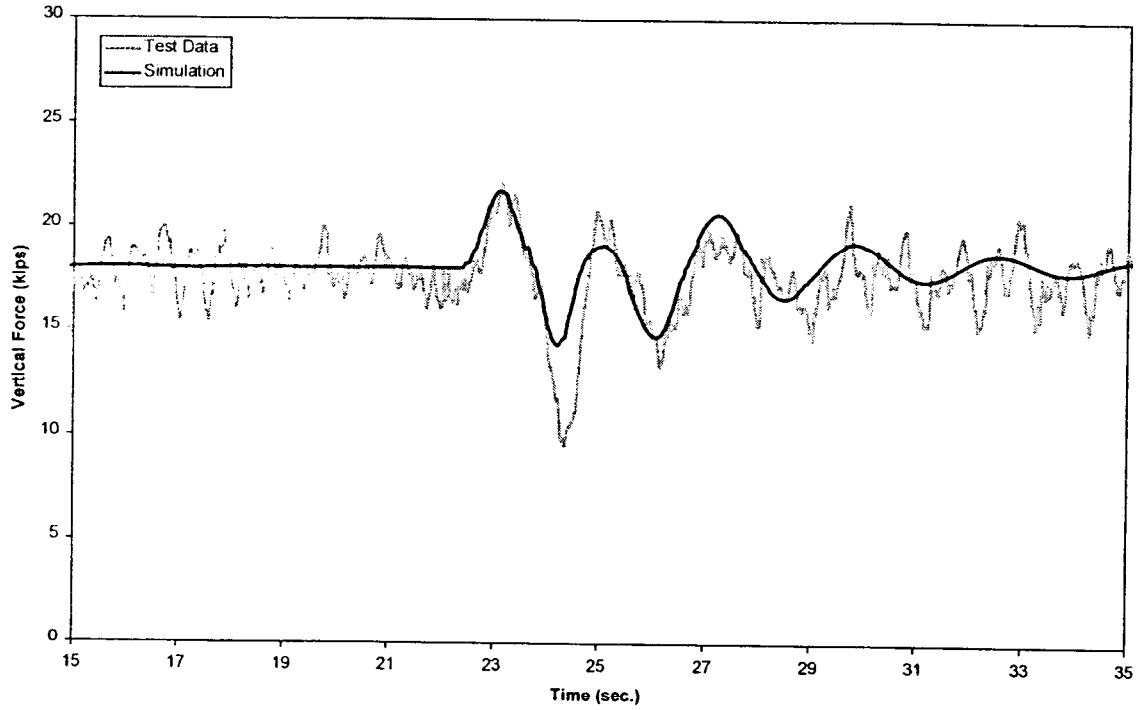

Figure B-1(b). Vertical bump test - vertical force time history, 24 mph (lead inner wheel)

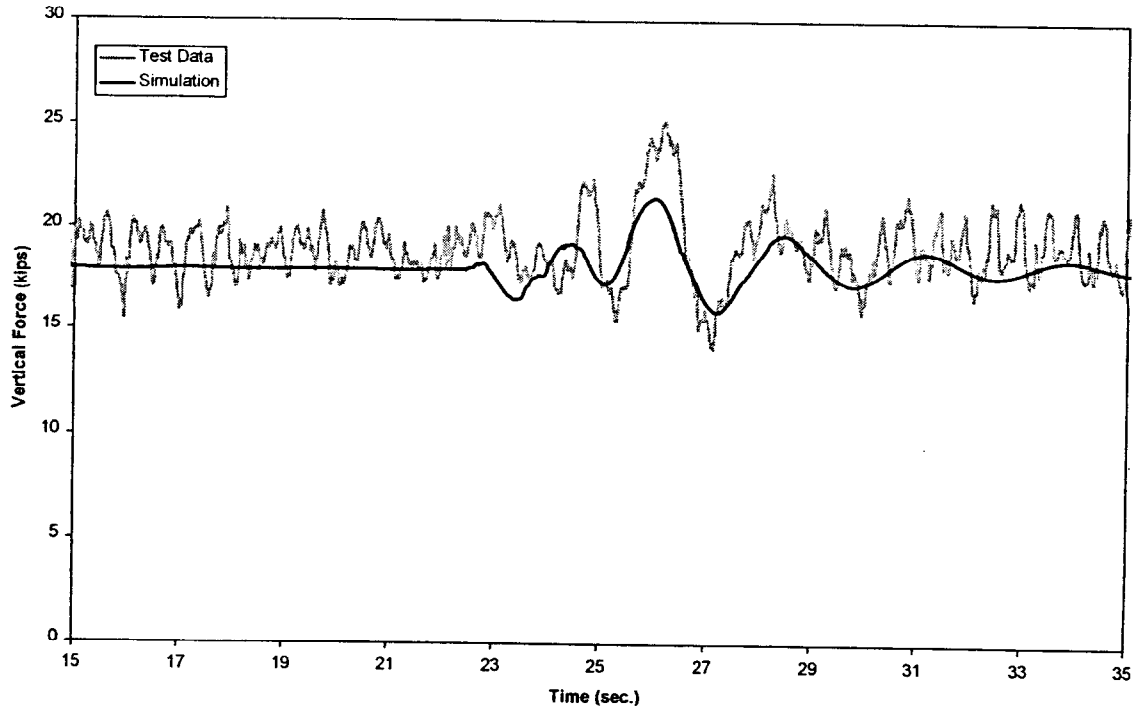

Figure B-1(c). Vertical bump test - vertical force time history, 24 mph (trailing outer wheel)

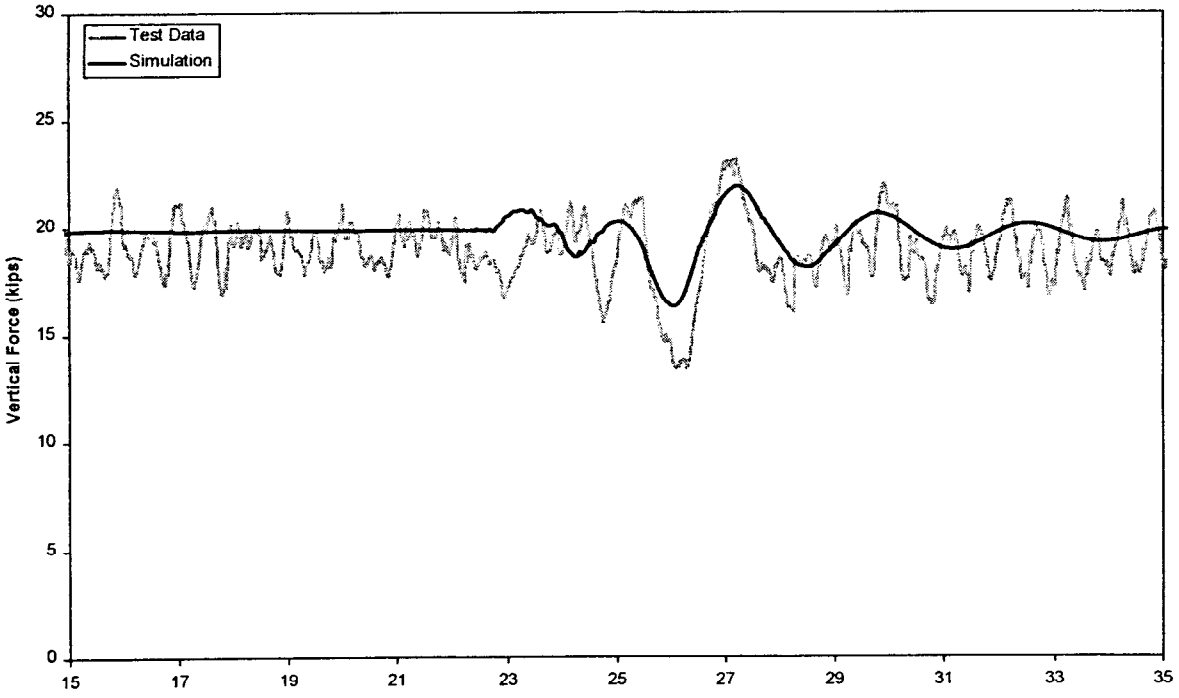

Figure B-1(d). Vertical bump test - vertical force time history, 24 mph (trailing inner wheel)

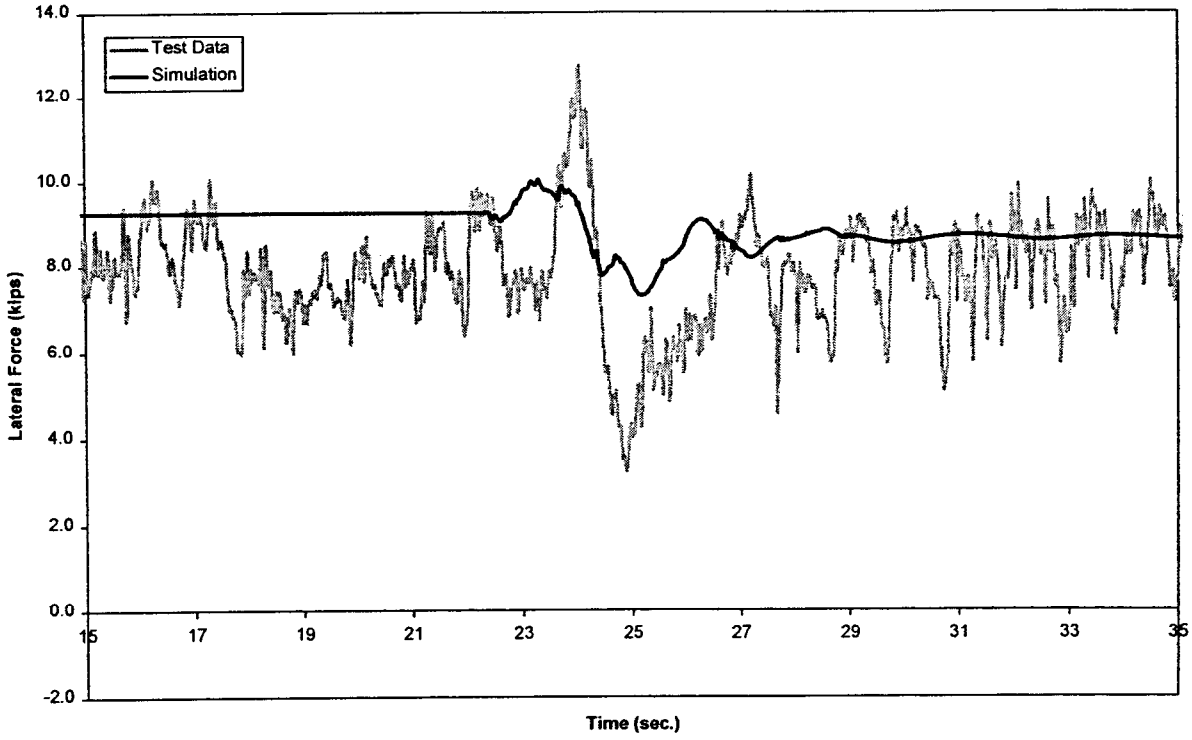

Figure B-2(a). Vertical bump test - lateral force time history, 24 mph (lead outer wheel)

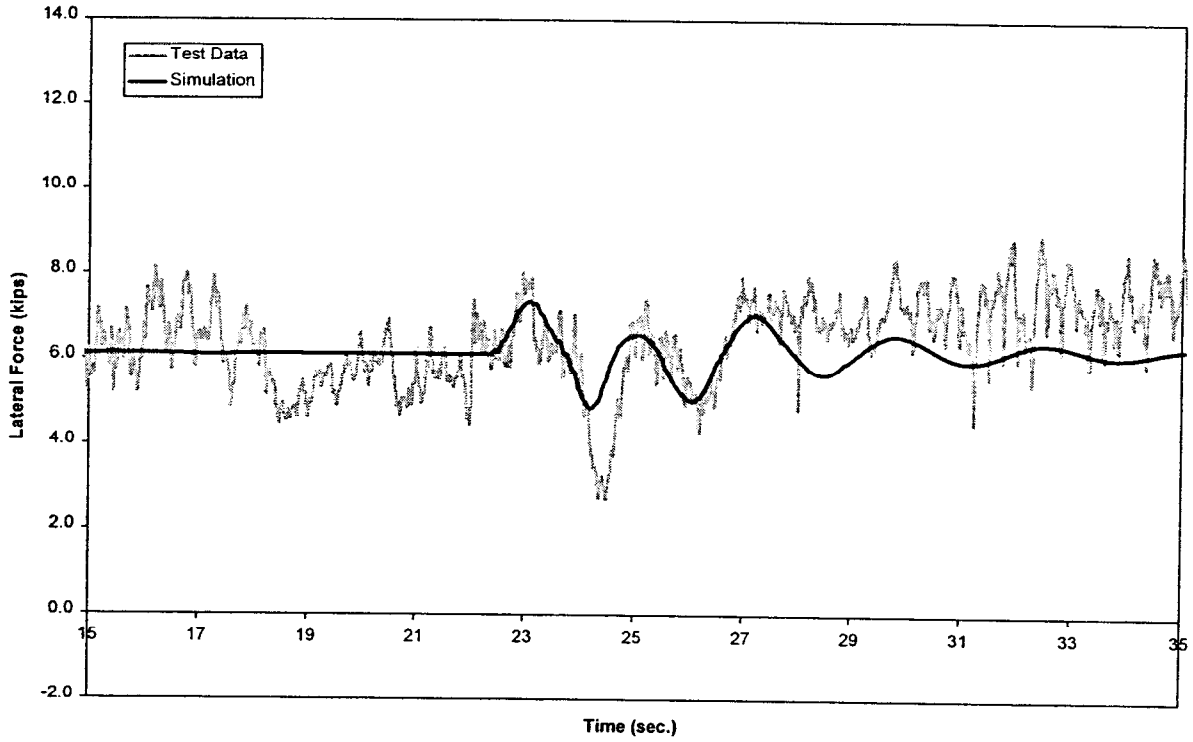

Figure B-2(b). Vertical bump test - lateral force time history, 24 mph (lead inner wheel)

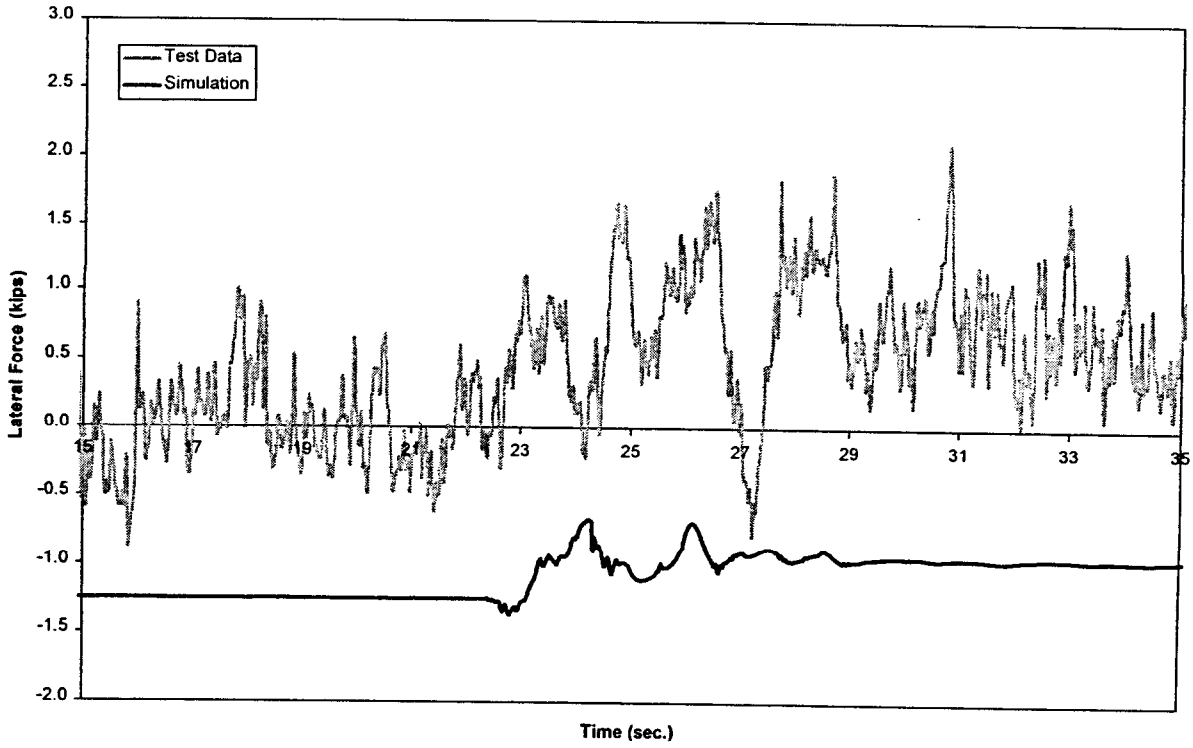

Figure B-2(c). Vertical bump test - lateral force time history, 24 mph (trailing outer wheel)

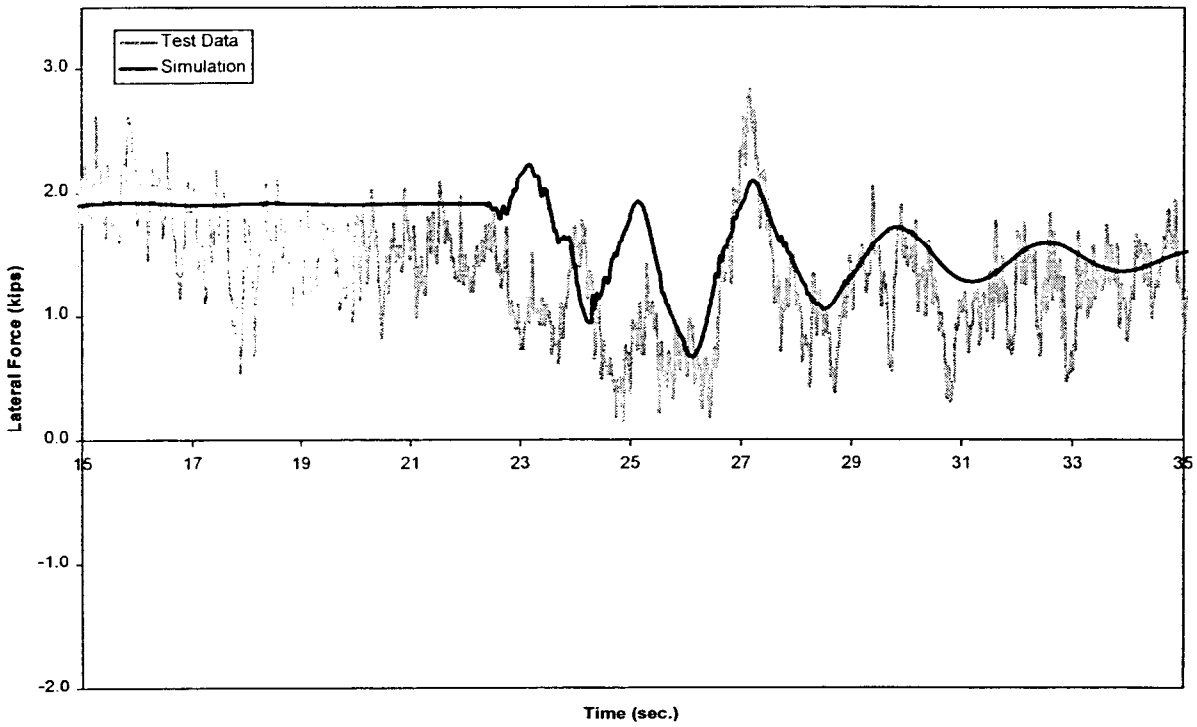

Figure B-2(d). Vertical bump test - lateral force time history, 24 mph (trailing inner wheel)

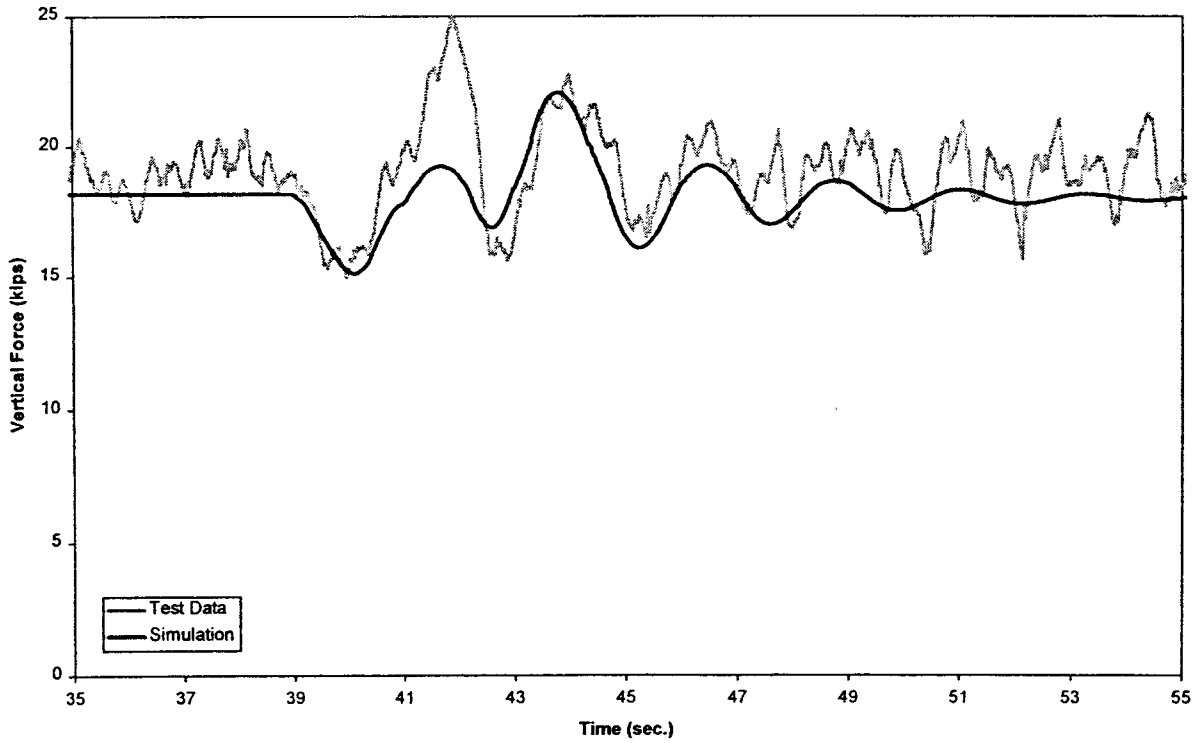

Figure B-3(a). Vertical bump test - vertical force time history, 15 mph (lead outer wheel)

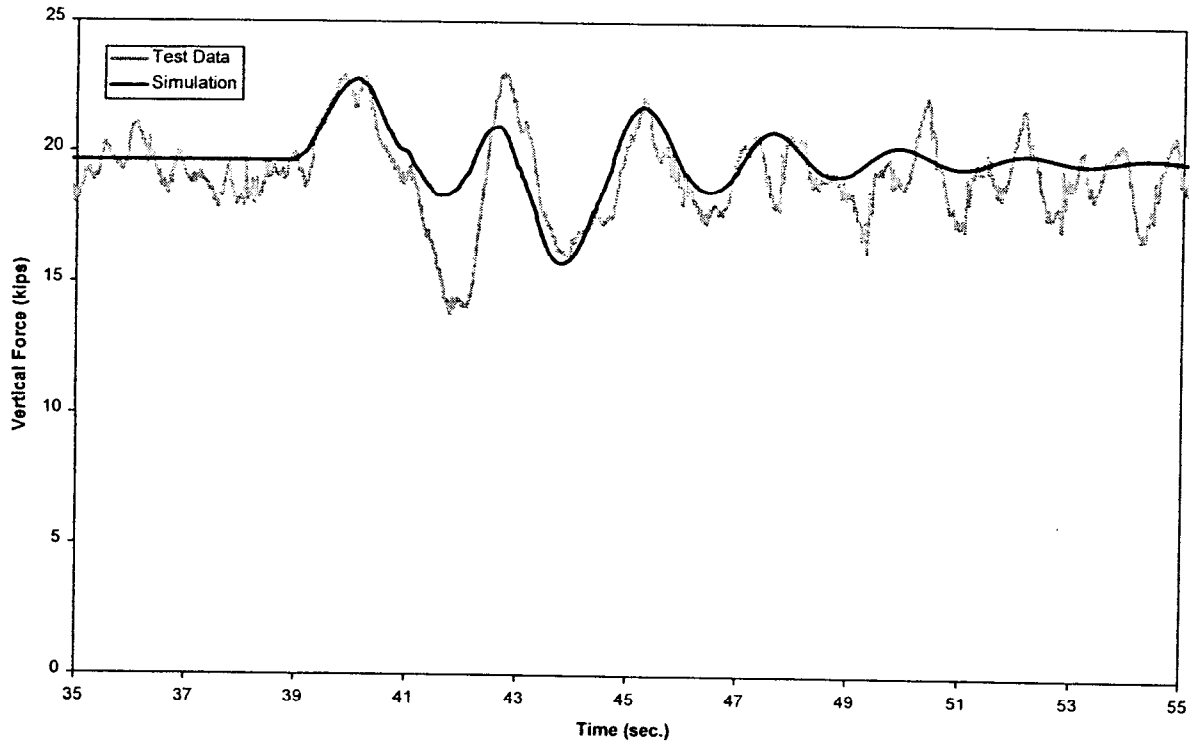

Figure B-3(b). Vertical bump test - vertical force time history, 15 mph (lead inner wheel)

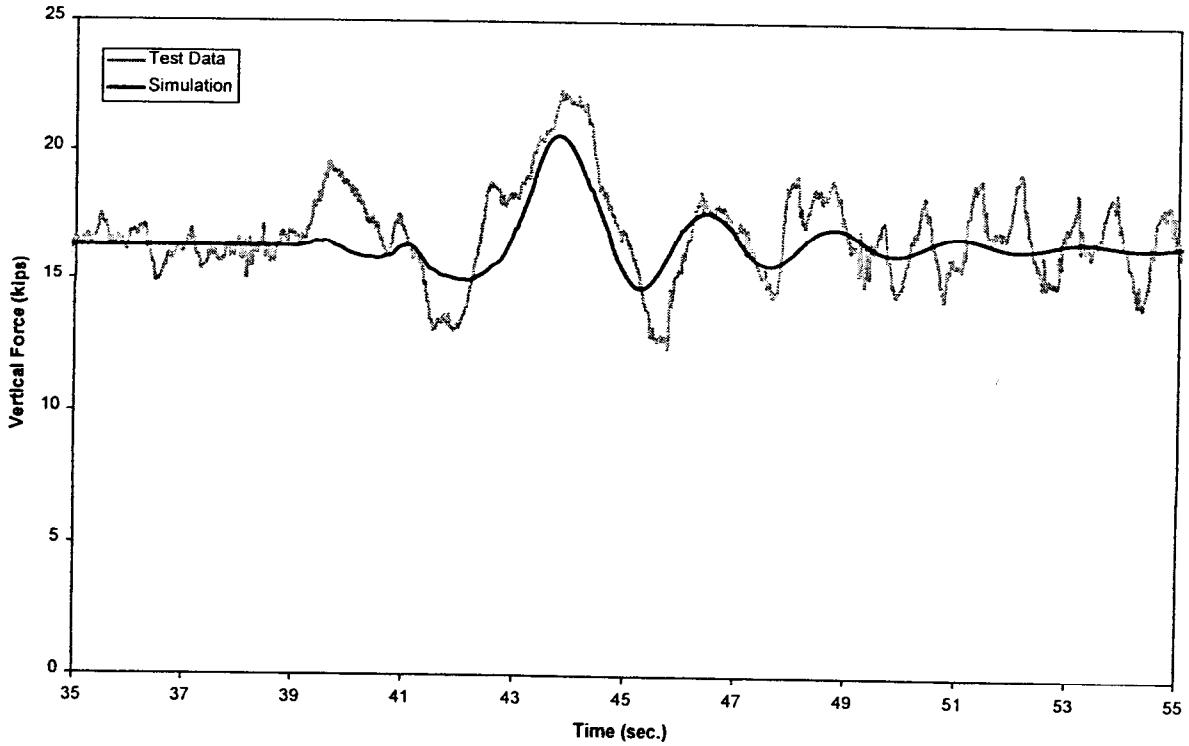

Figure B-3(c). Vertical bump test - vertical force time history, 15 mph (trailing outer wheel)

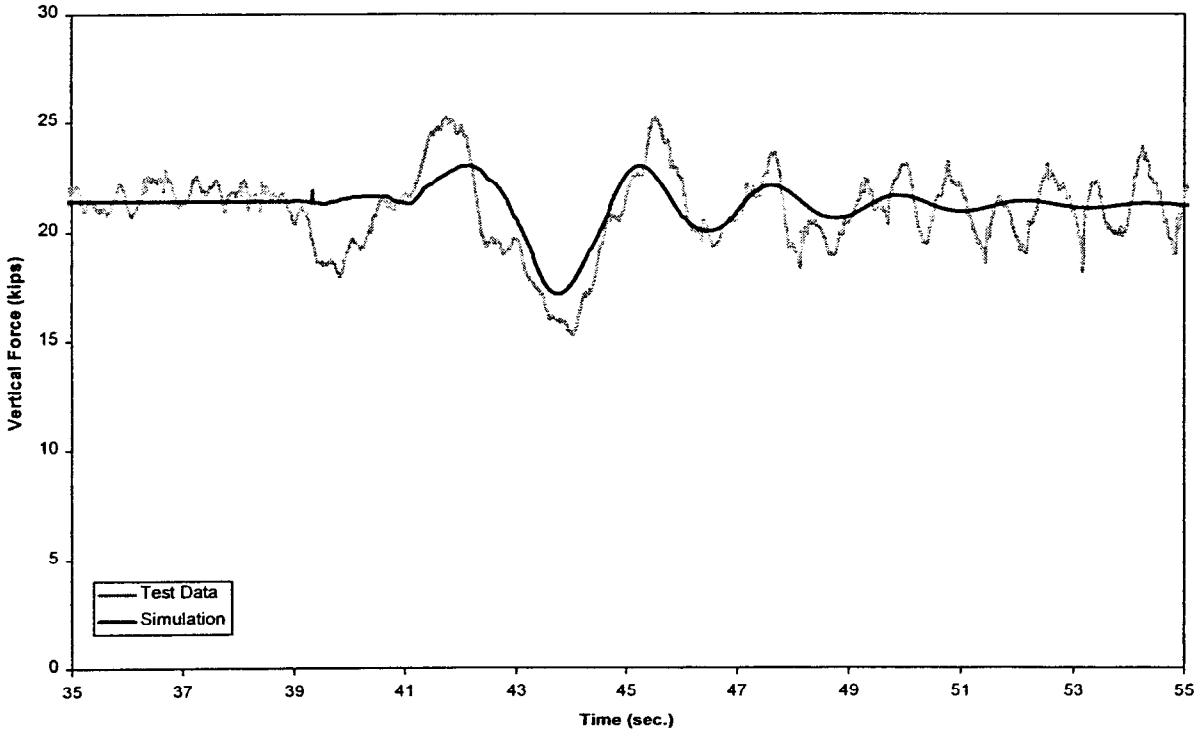

Figure B-3(d). Vertical bump test - vertical force time history, 15 mph (trailing inner wheel)

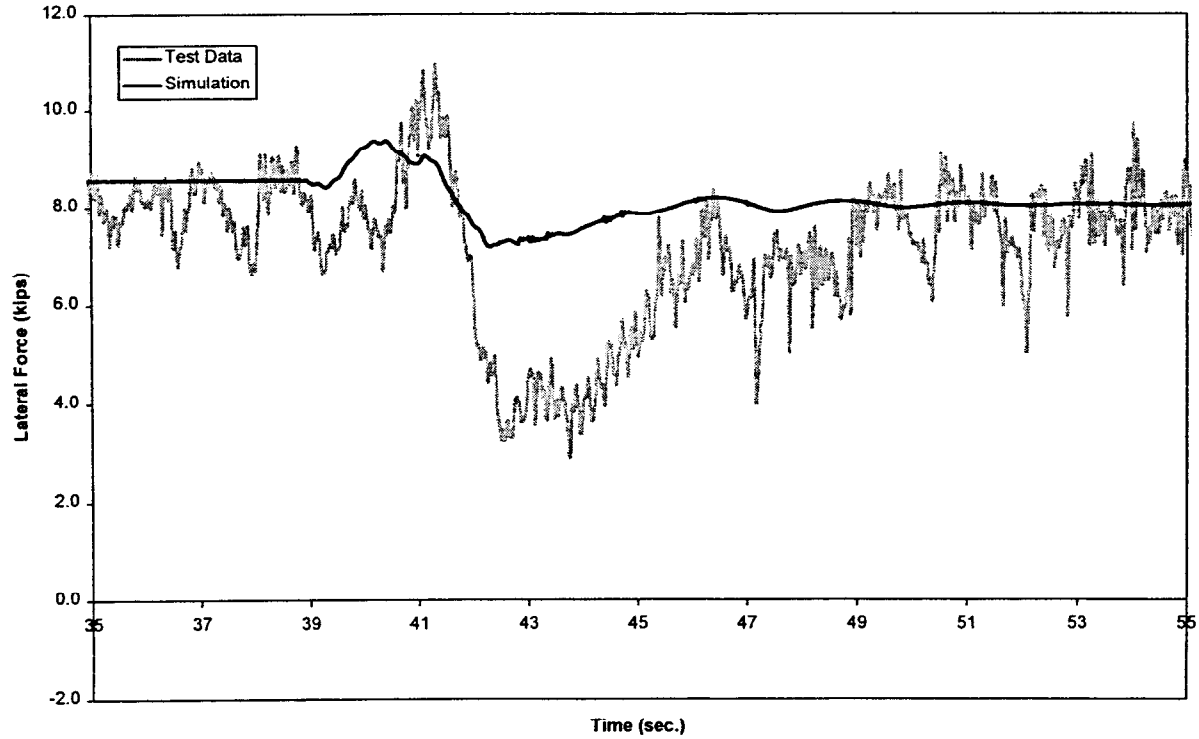

Figure B-4(a). Vertical bump test - lateral force time history, 15 mph (lead outer wheel)

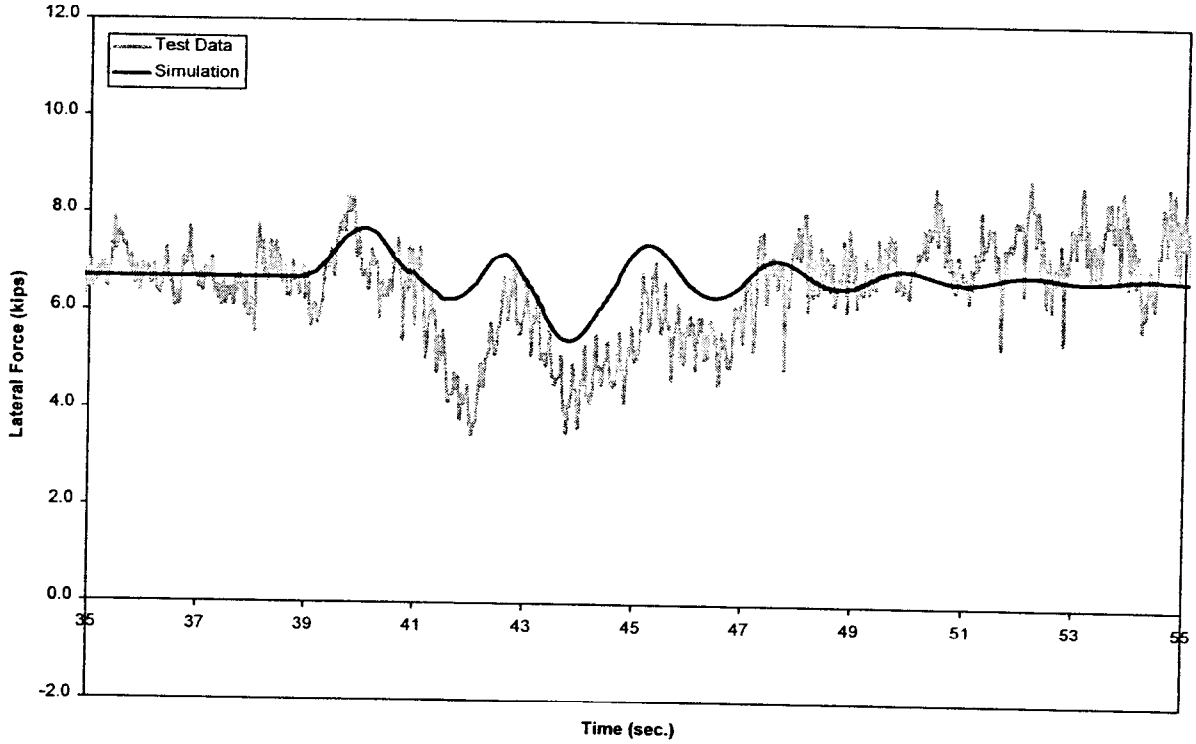

Figure B-4(b). Vertical bump test - lateral force time history, 15 mph (lead inner wheel)

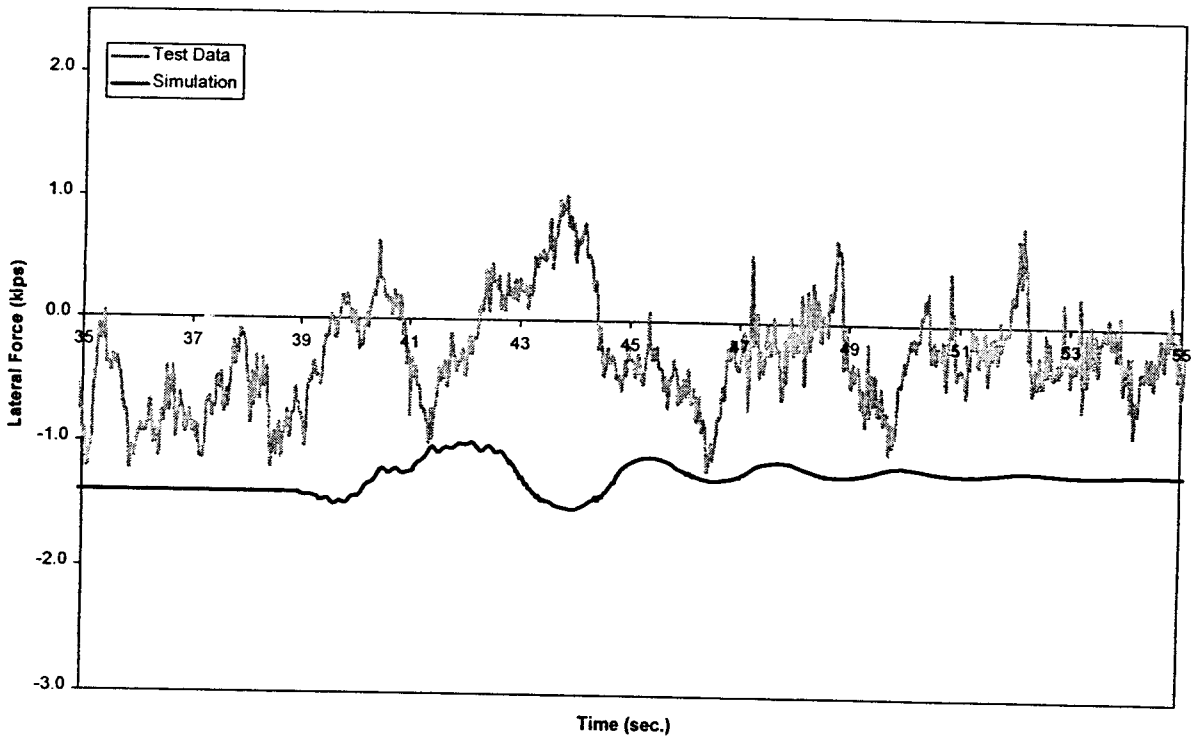

Figure B-4(c). Vertical bump test - lateral force time history, 15 mph (trailing outer wheel)

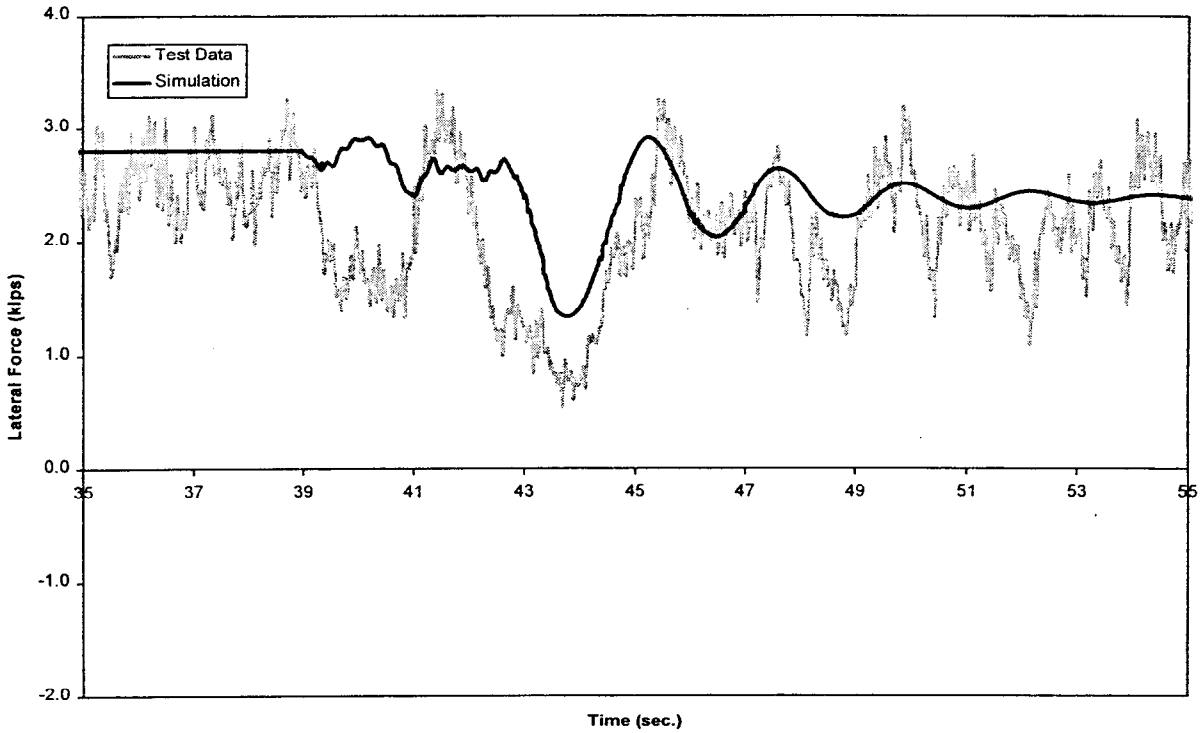

Figure B-4(d). Vertical bump test - lateral force time history, 15 mph (trailing inner wheel)

At 15 mph the lateral force test data have relatively good agreement with the simulation data for the initial lateral force values prior to entering the bump. The waveforms of the simulations are similar to the test data during passage through the bump, but have larger amplitudes than the test data by 3 to 4 kips for the lead axle outer wheel.

A plot of the minimum vertical force occurring during negotiation of the bump for a range of speeds is shown in Figure B-5 for the outer wheel on the lead axle of the trailing truck. Good correlation is shown over the speed range for the vertical force.

B.2 Constant Curving with Spirals

Test data and simulation results for passage through the 7.5 deg curve are presented in Figures B-6, B-7 and B-8 for operation at 24 mph (balance speed) and in Figures B-9, B-10 and B-11 for operation at 32 mph. Only the results for the 7.5 deg will be shown because the other correlations (10 and 12 deg) are similar. Vertical force data in Figure B-6 for operation at balance speed show that both the test data and simulation indicate that the vertical forces remain very close to their nominal values for all four wheels during the curve negotiation. The variations in the test data (Figure B-6) from the nominal value are believed due to local track perturbations. The lateral data (Figure B-7) for the individual wheels also have close agreement between the simulation and the test data. The lead axle test data is 1 to 3 kips less than the simulation value for the outer and inner wheels. The trailing axle test data is 0.5 to 1 kips less than the simulation data for the outer and inner wheels. Comparison of the simulation and test data for the net lateral force on the lead and trailing axles, summarized in Figure B-8, has closer

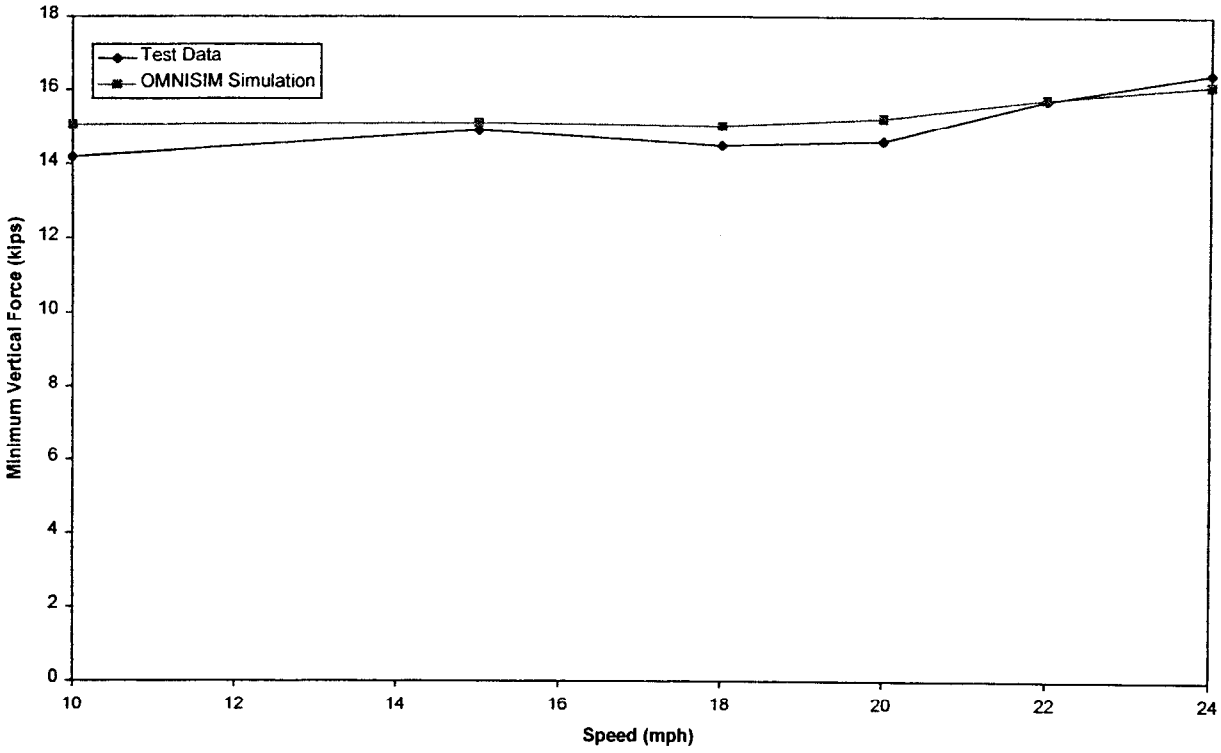

Figure B-5. Vertical bump test - minimum vertical force

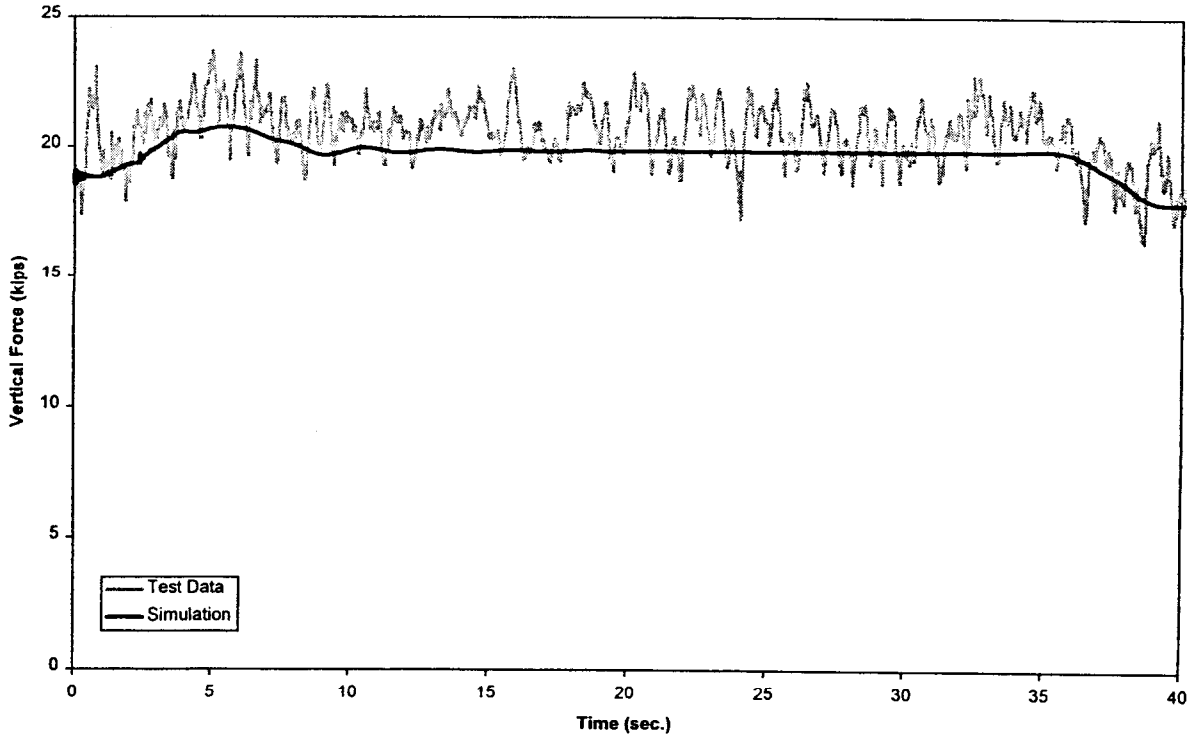

Figure B-6(a). Constant curving - vertical force time history, 24 mph (lead outer wheel)

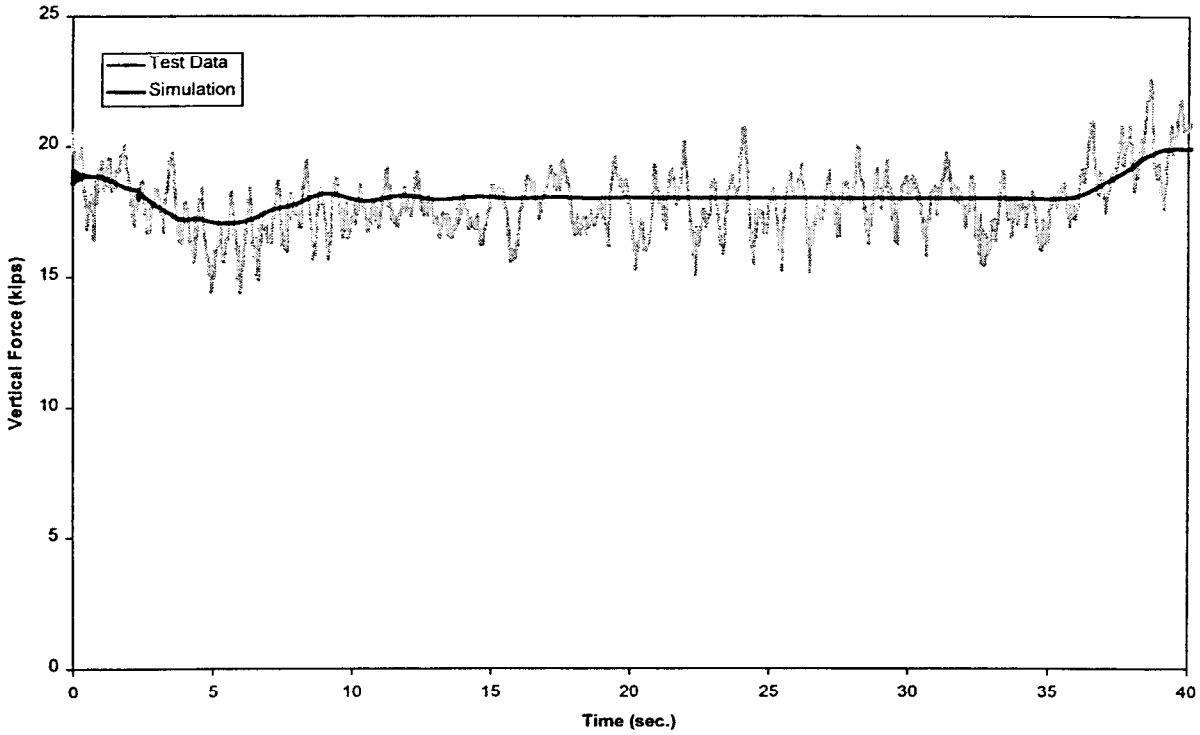

Figure B-6(b). Constant curving - vertical force time history, 24 mph (lead inner wheel)

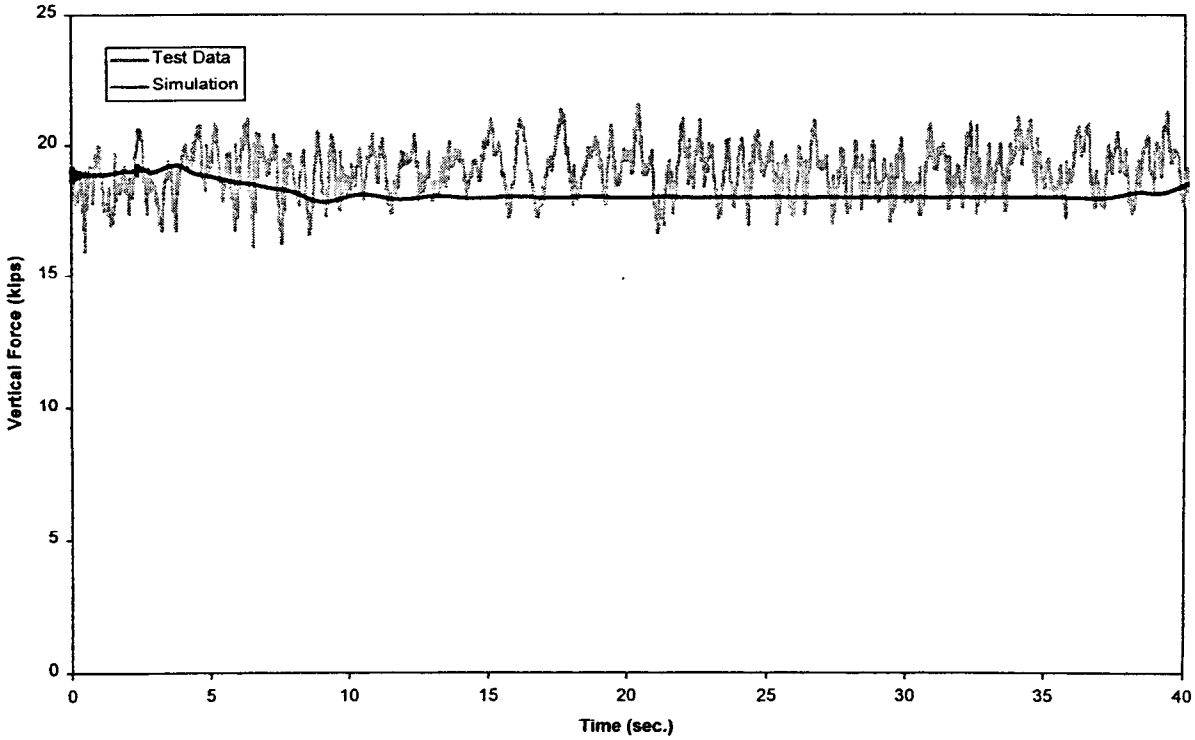

Figure B-6(c). Constant curving - vertical force time history, 24 mph (trailing outer wheel)

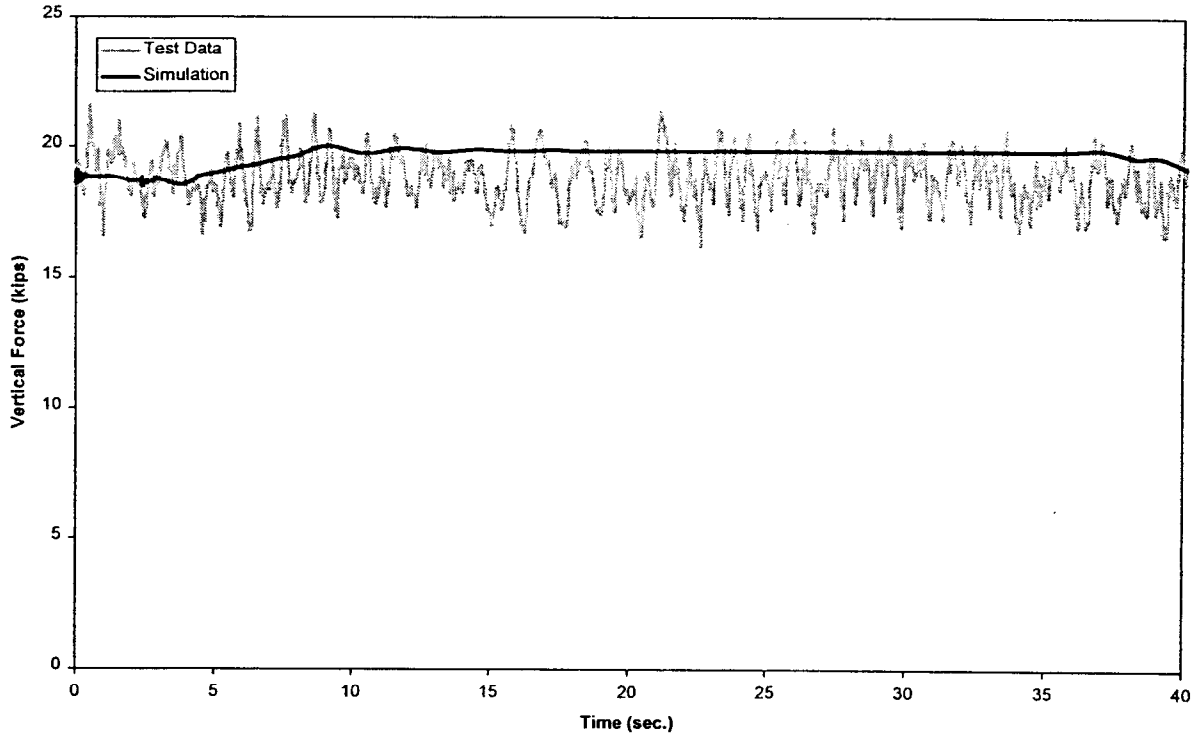

Figure B-6(d). Constant curving - vertical force time history, 24 mph (trailing outer wheel)

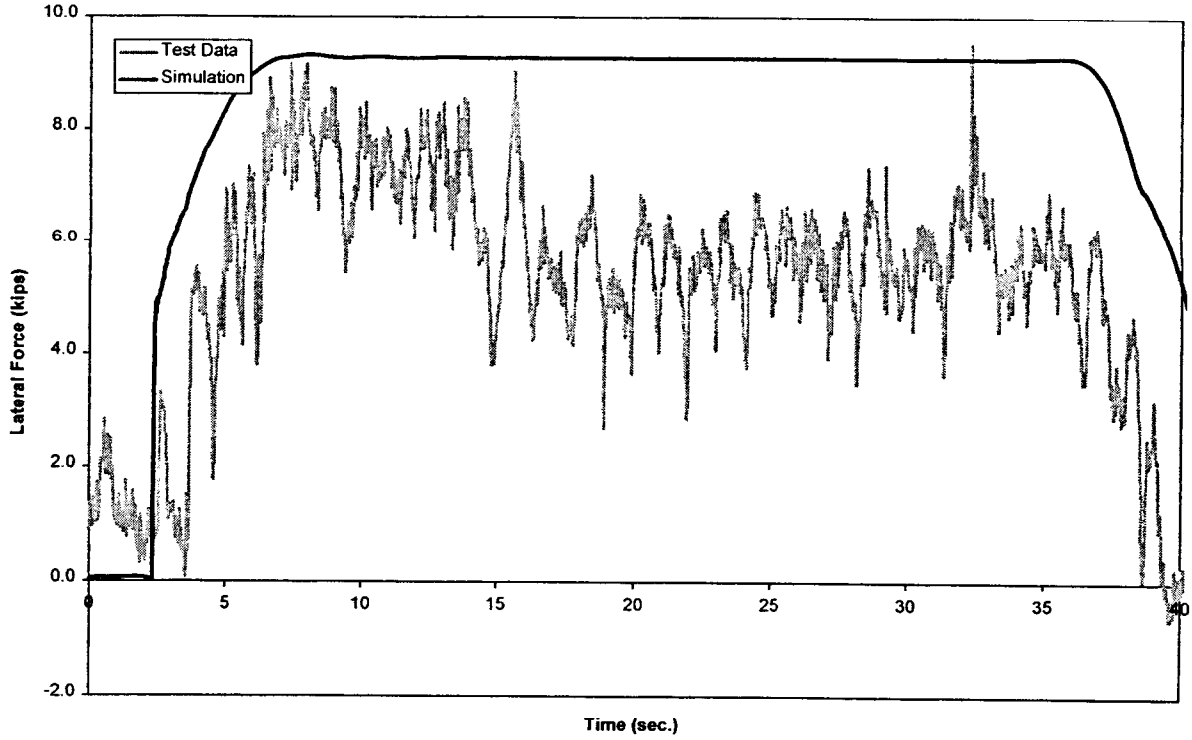

Figure B-7(a). Constant curving - lateral force time history, 24 mph (lead outer wheel)

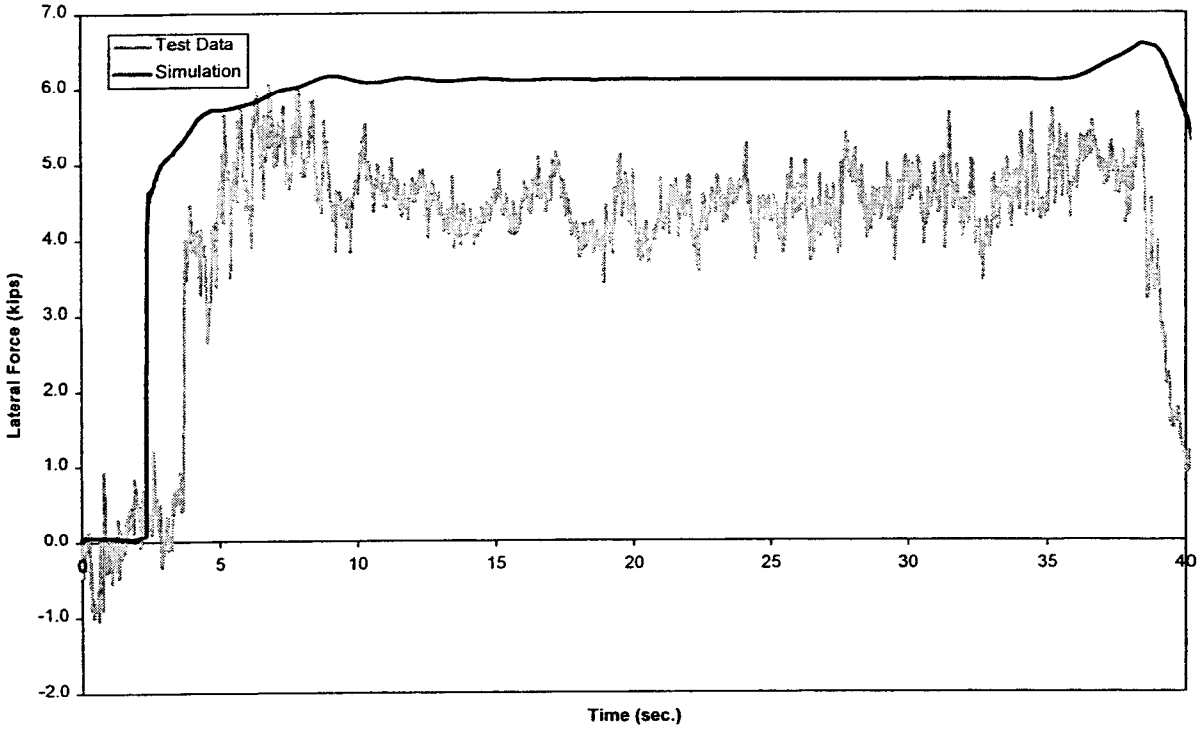

Figure B-7(b). Constant curving - lateral force time history, 24 mph (lead inner wheel)

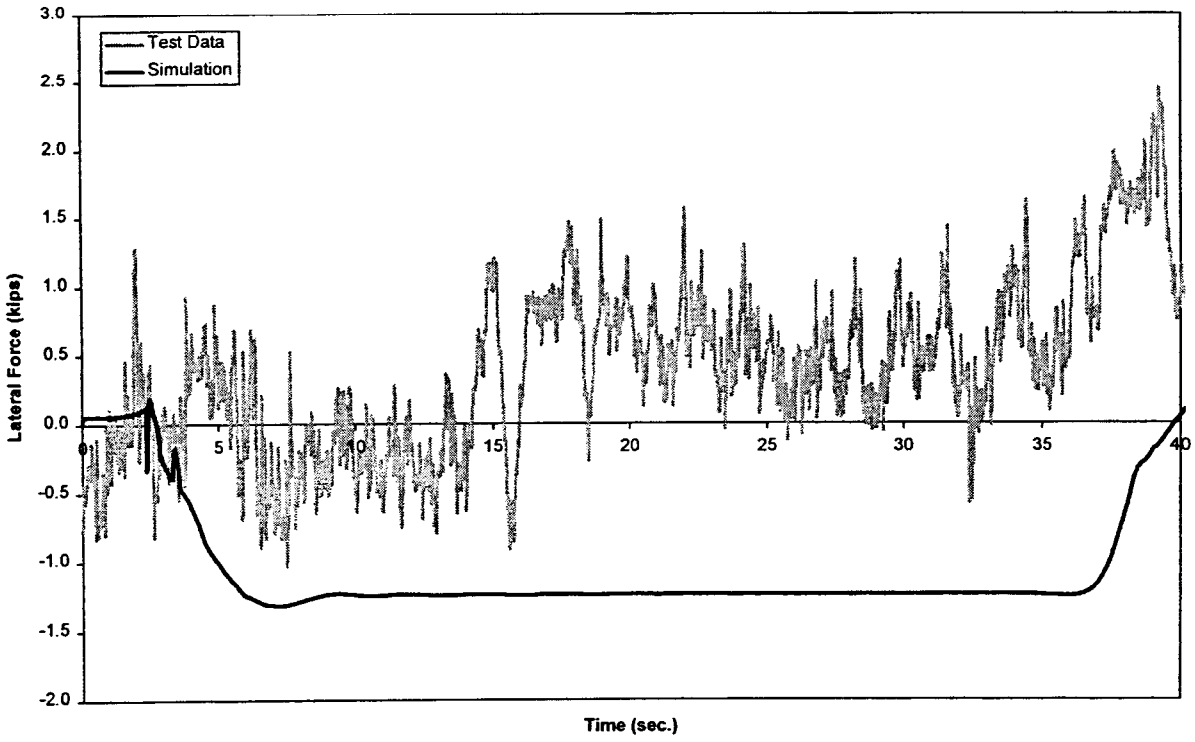

Figure B-7(c). Constant curving - lateral force time history, 24 mph (trailing outer wheel)

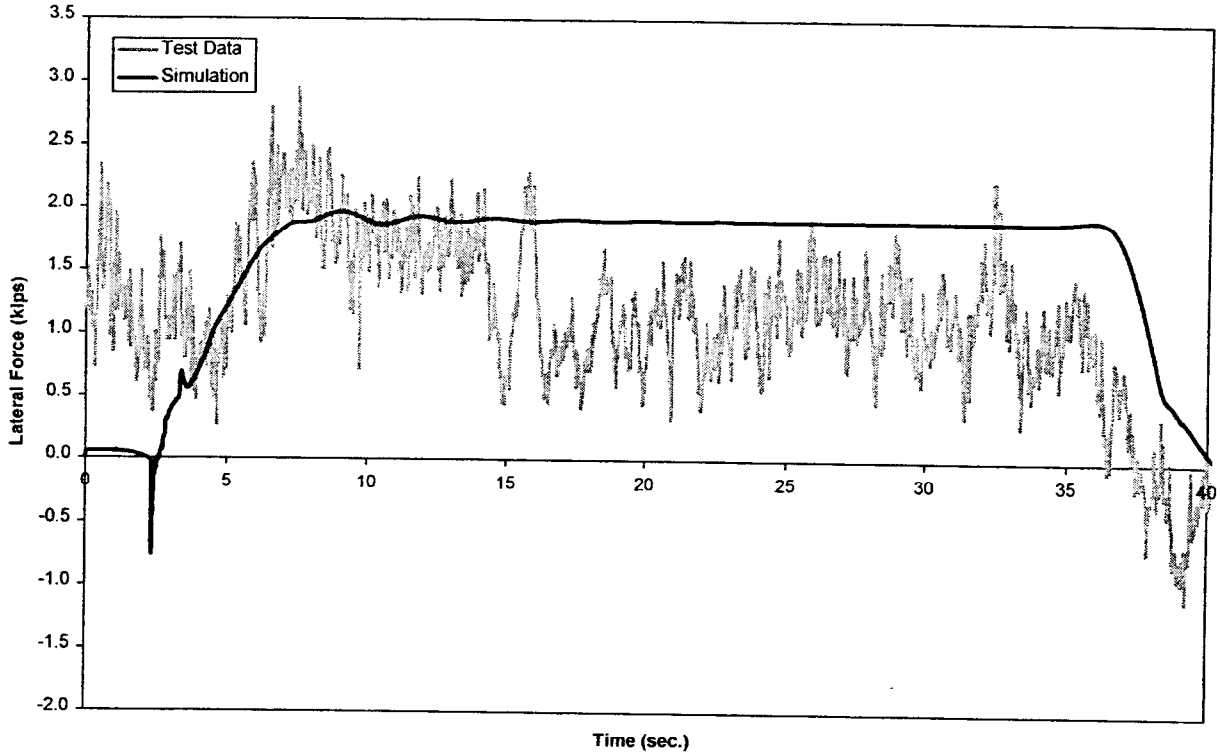

Figure B-7(d). Constant curving - lateral force time history, 24 mph (trailing inner wheel)

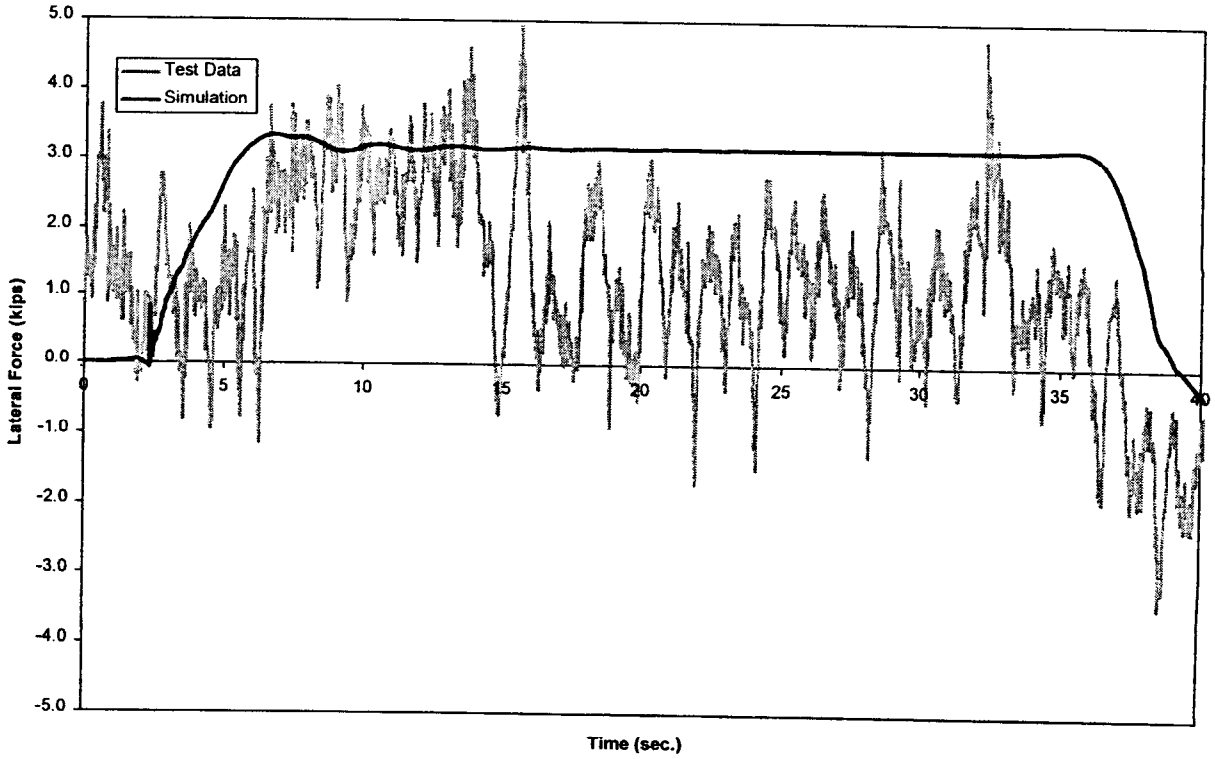

Figure B-8(a). Constant curving - net axle lateral force time history, 24 mph (lead axle)

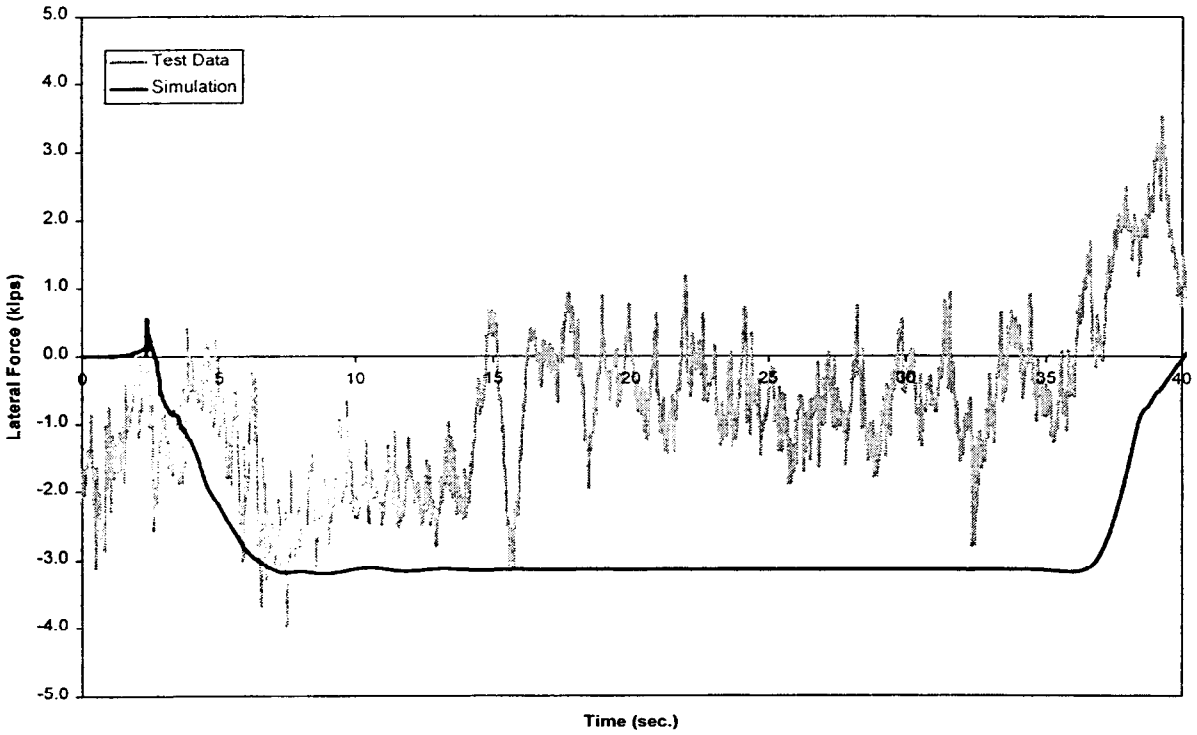

Figure B-8(b). Constant curving - net axle lateral force time history, 24 mph (trailing axle)

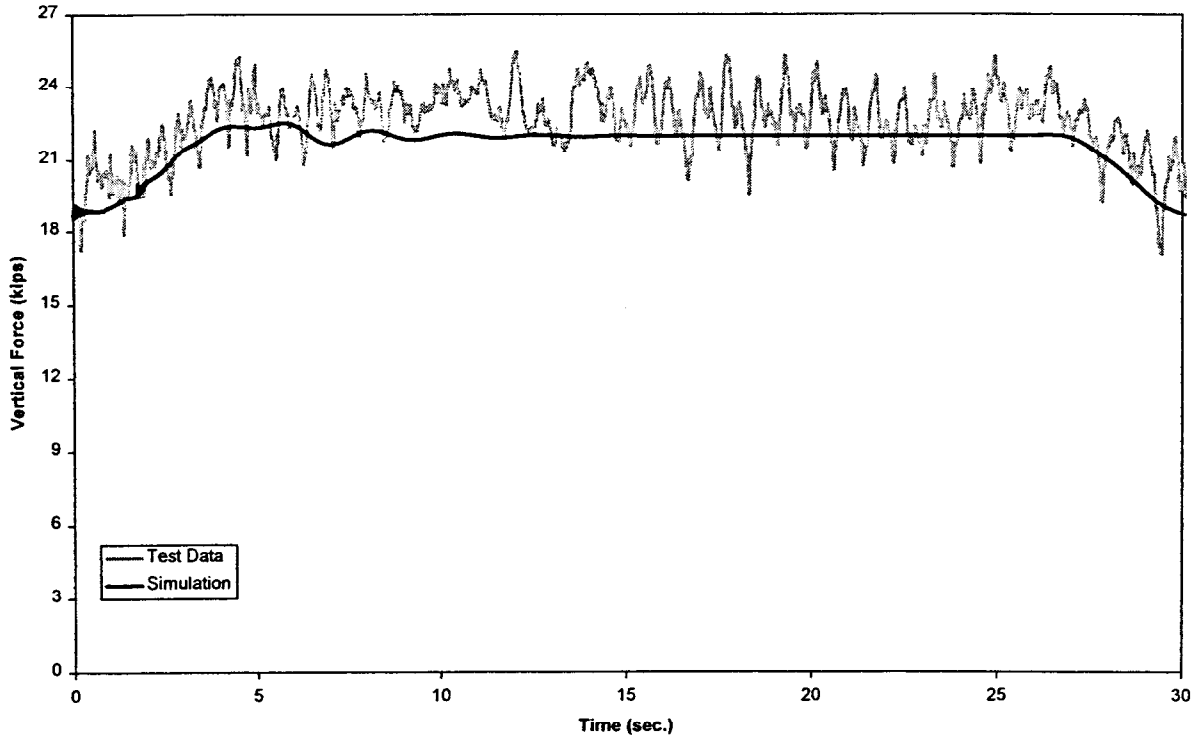

Figure B-9(a). Constant curving - vertical force time history, 32 mph (lead outer wheel)

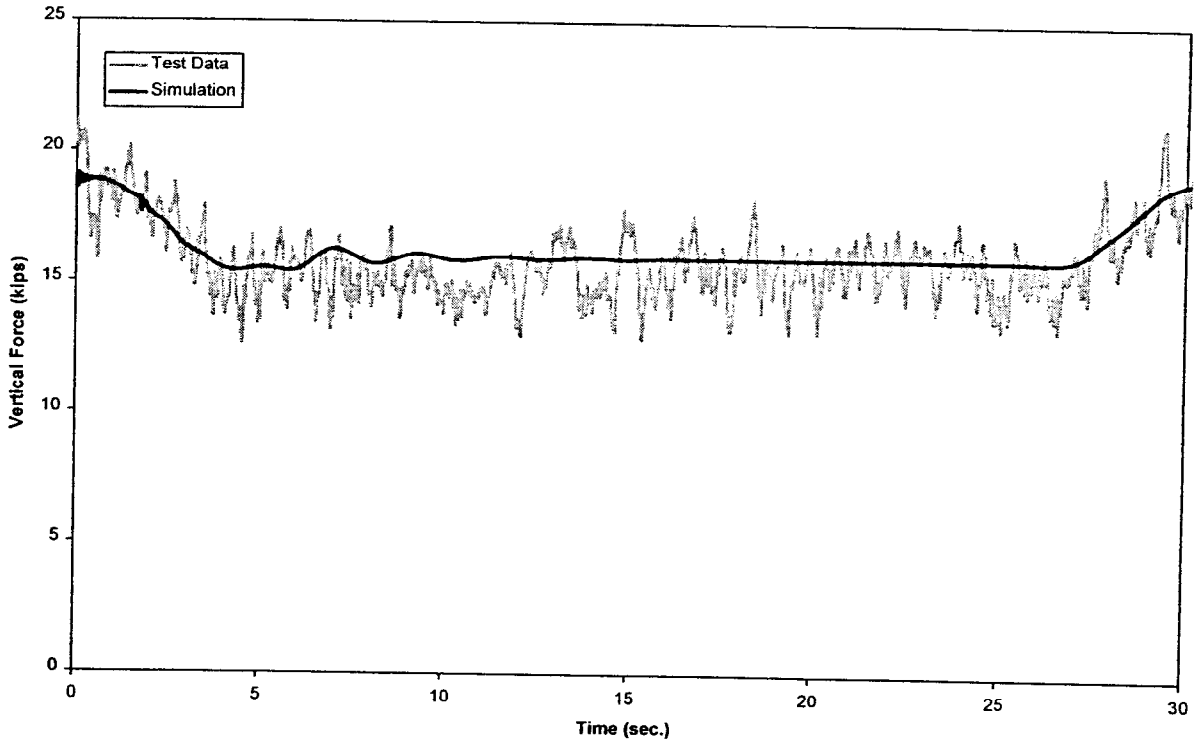

Figure B-9(b). Constant curving - vertical force time history, 32 mph (lead inner wheel)

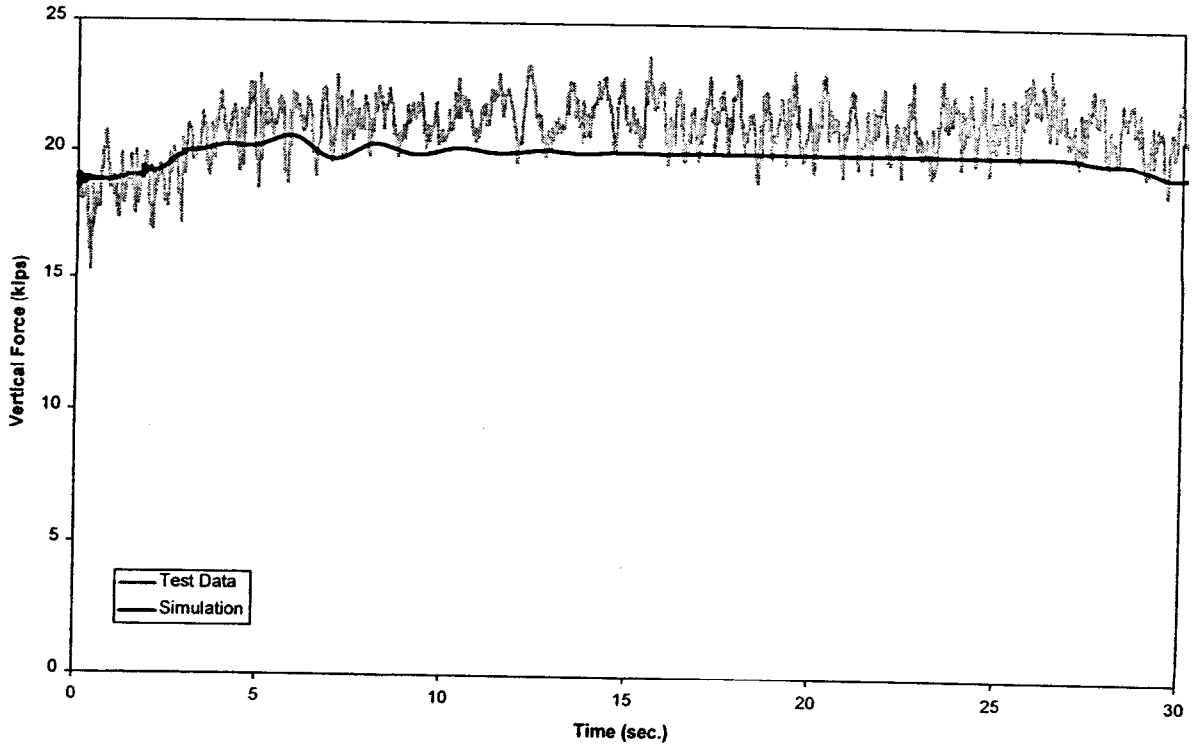

Figure B-9(c). Constant curving - vertical force time history, 32 mph (trailing outer wheel)

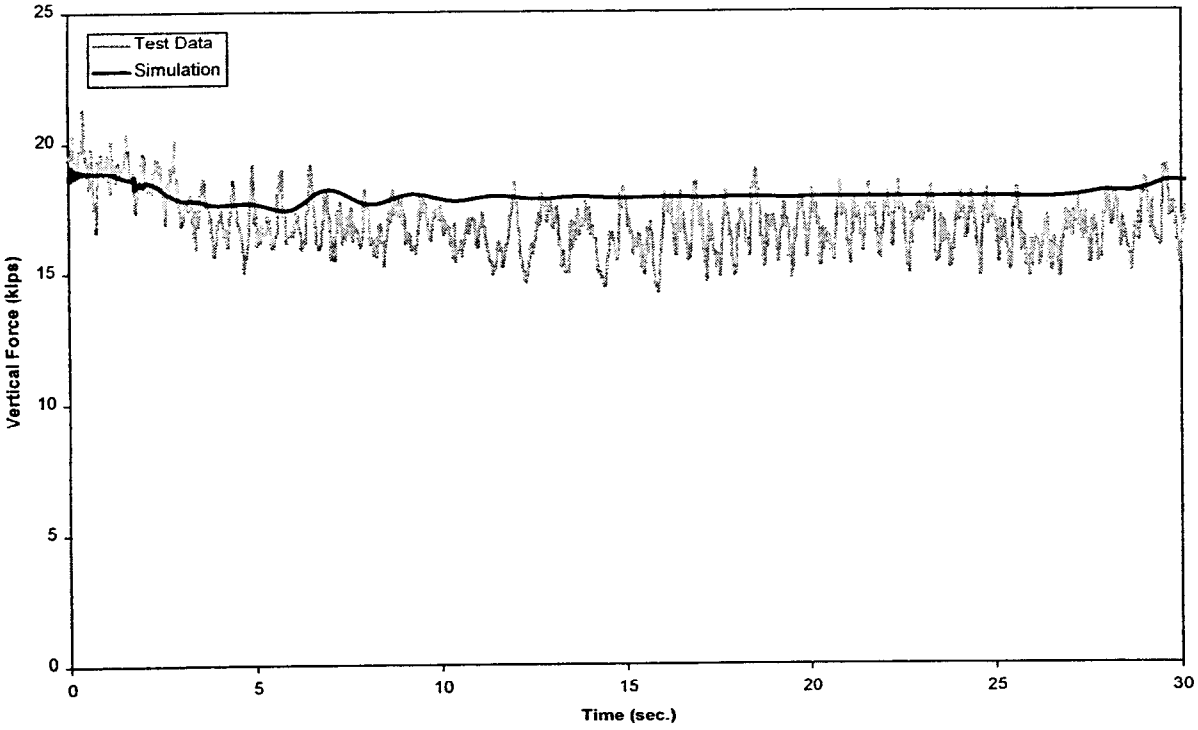

Figure B-9(d). Constant curving - vertical force time history, 32 mph (trailing inner wheel)

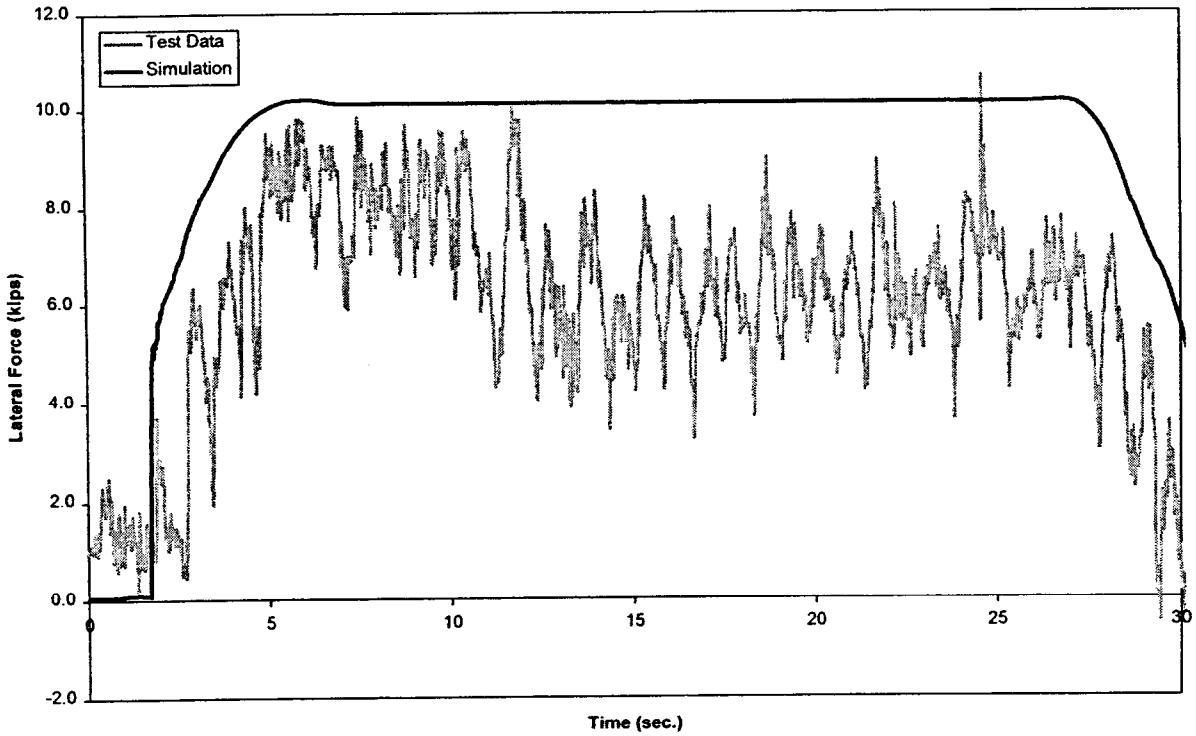

Figure B-10(a). Constant curving - lateral force time history, 32 mph (lead outer wheel)

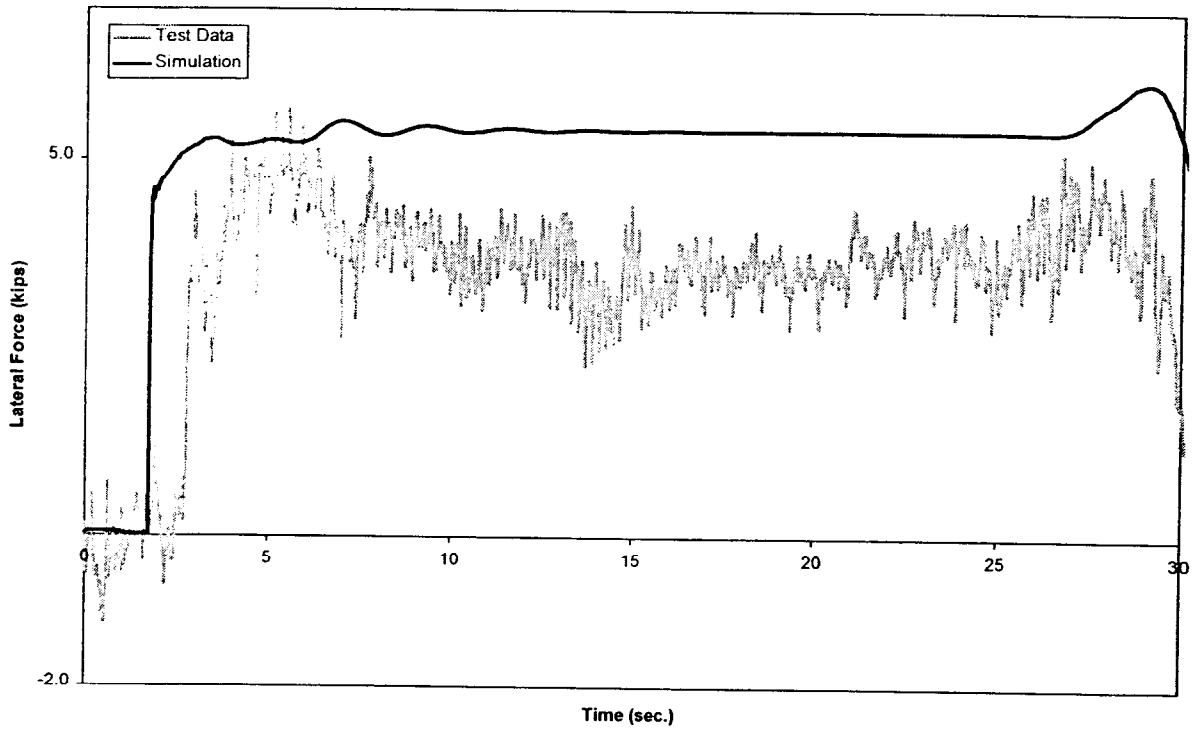

Figure B-10(b). Constant curving - lateral force time history, 32 mph (lead inner wheel)

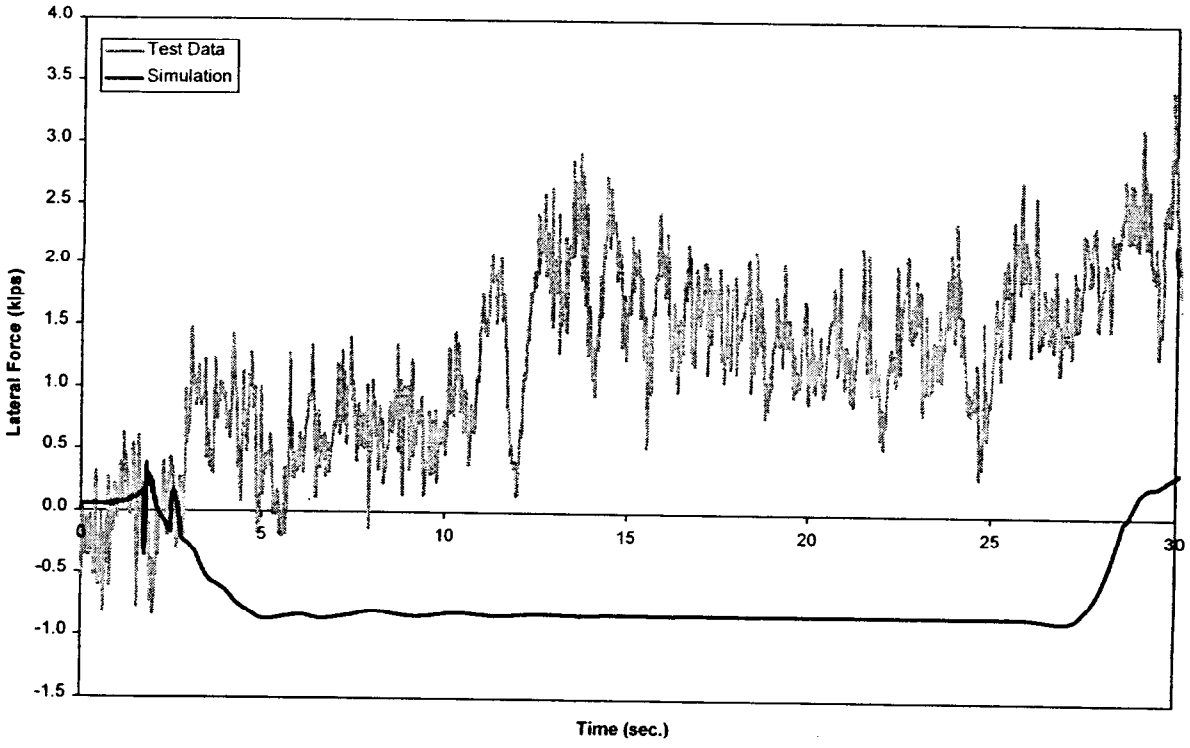

Figure B-10(c). Constant curving - lateral force time history, 32 mph (trailing outer wheel)

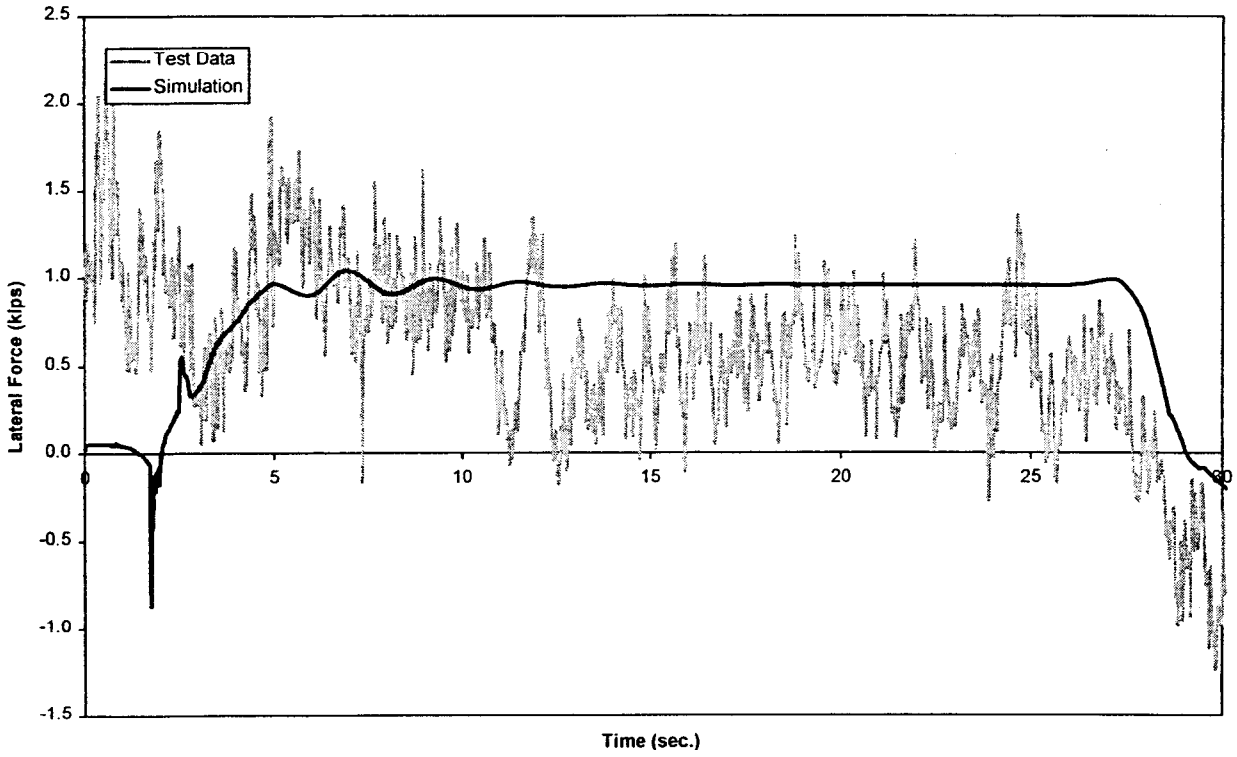

Figure B-10(d). Constant curving - lateral force time history, 32 mph trailing inner wheel)

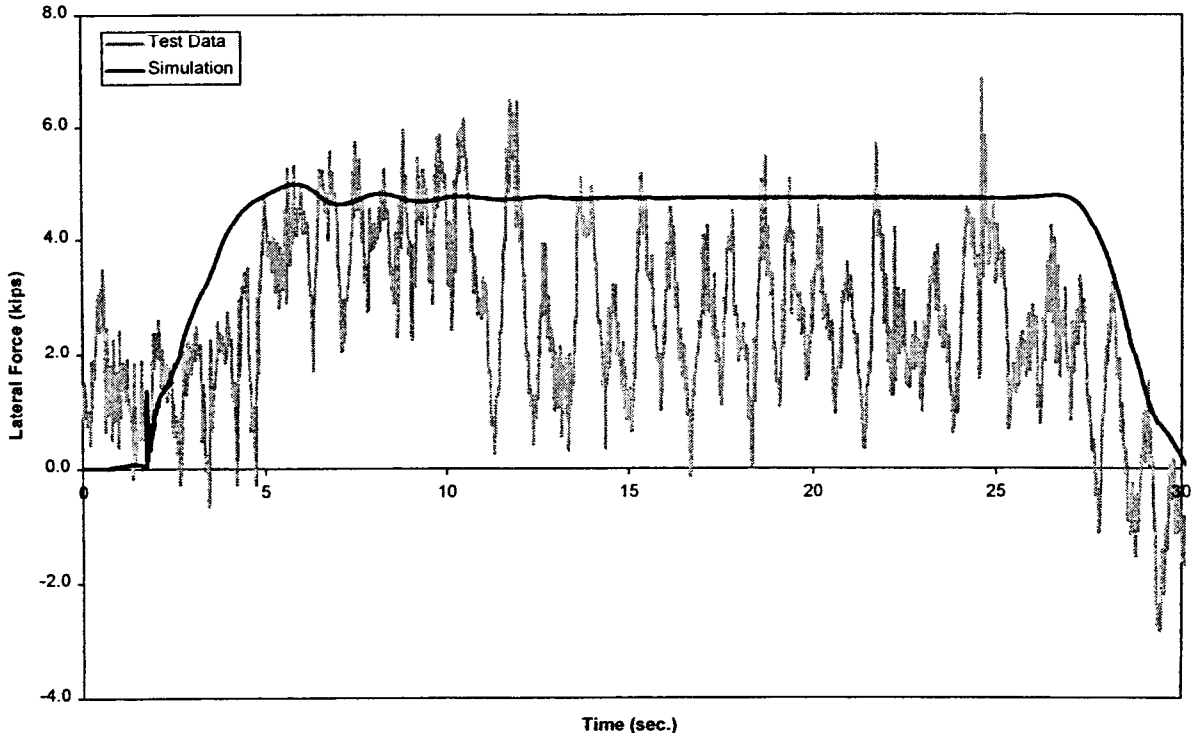

Figure B-11(a). Constant curving - net axle lateral force time history, 32 mph (lead axle)

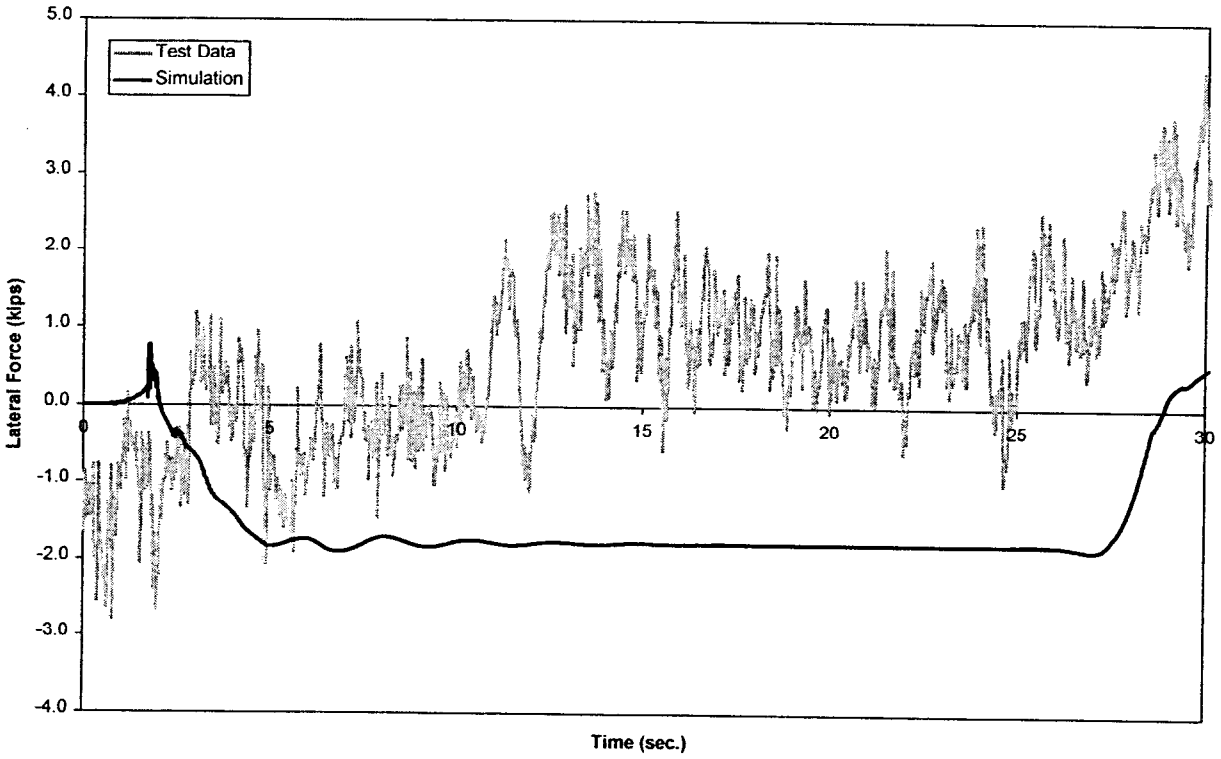

Figure B-11(b). Constant curving - net axle lateral force time history, 32 mph trailing axle)

correlations. For the lead axle, simulation gives 3.0 kips compared with test data of approximately 2.0 kips. For the trailing axle, simulation gives –3.0 kips compared with test data of approximately –2.0 kips. The sum of the two net axle loads is approximately zero for operation at balance speed in both the simulation and test data, as one would expect.

The vertical force data, presented in Figure B-9, shows that at 32 mph, the outer wheel vertical force increases to approximately 23 to 25 kips and the inner wheel value decreases to approximately 15 kips for both axles. The test and simulation data are close. Lead axle lateral force data (Figure B-10) shows that the outer wheel is approximately 10 kips for the simulation in comparison to 7 kips for the test data, whereas the inner wheel is 5.0 kips for the simulation and approximately 3.5 kips for the test data. The trailing axle lateral force for the outer wheel is –1 kip in the simulation and approximately 1.5 kips in the test data and for the inner wheel is 1 kip for the simulation in comparison to approximately 0.5 kips for the test data.

The net axle lateral force for both axles is presented in Figure B-11. The lead axle net lateral force is approximately 4 kips with close agreement between the simulation and test data while the trailing axle lateral force is 1 kip for the simulation and approximately –1 kip for the test data. The net axle lateral forces are in relatively good agreement between the simulation and test data and reflect a net truck lateral force of approximately 3 kips for the over balance speed of 32 mph. The theoretical value is 2.9 kips and is calculated as the difference between the centripetal force and the horizontal component of weight.

A plot of the minimum vertical force and the maximum lateral force occurring during negotiation of the 7.5 deg curve for a range of speeds is shown in Figure B-12 for the outer wheel on the lead axle of the trailing truck. Good correlation is shown over the speed range for the vertical and lateral force. Similar plots are shown in Figures B-13 and B-14 for the 10 and 12 deg curves, respectively.

B.3 Dynamic Curving

The vertical and lateral forces for the trailing truck wheels are shown in Figures B-15 and B-16, respectively for operation at 18.6 mph. The vertical force simulation and test data are in good agreement. The vertical forces vary from 16 to 24 kips as the perturbations are negotiated. The lateral force waveforms for the simulation and test data are similar for the trailing axle wheels, and the amplitudes are in good agreement. For the lead axle, simulation data shows higher (by approximately 5 kips) average values of force on both the outer and inner wheels. (This difference is similar to the difference seen in the steady-state curving tests.)

Data for operation at 28 mph, illustrated in Figure B-17, also indicate good correspondence between the vertical forces predicted and measured for all four wheels. The lateral force data of Figure B-18 for the trailing axle are also in reasonable agreement. The lead axle simulation has an average value of approximately 3 to 9 kips greater than the test data for the inner and outer wheels.

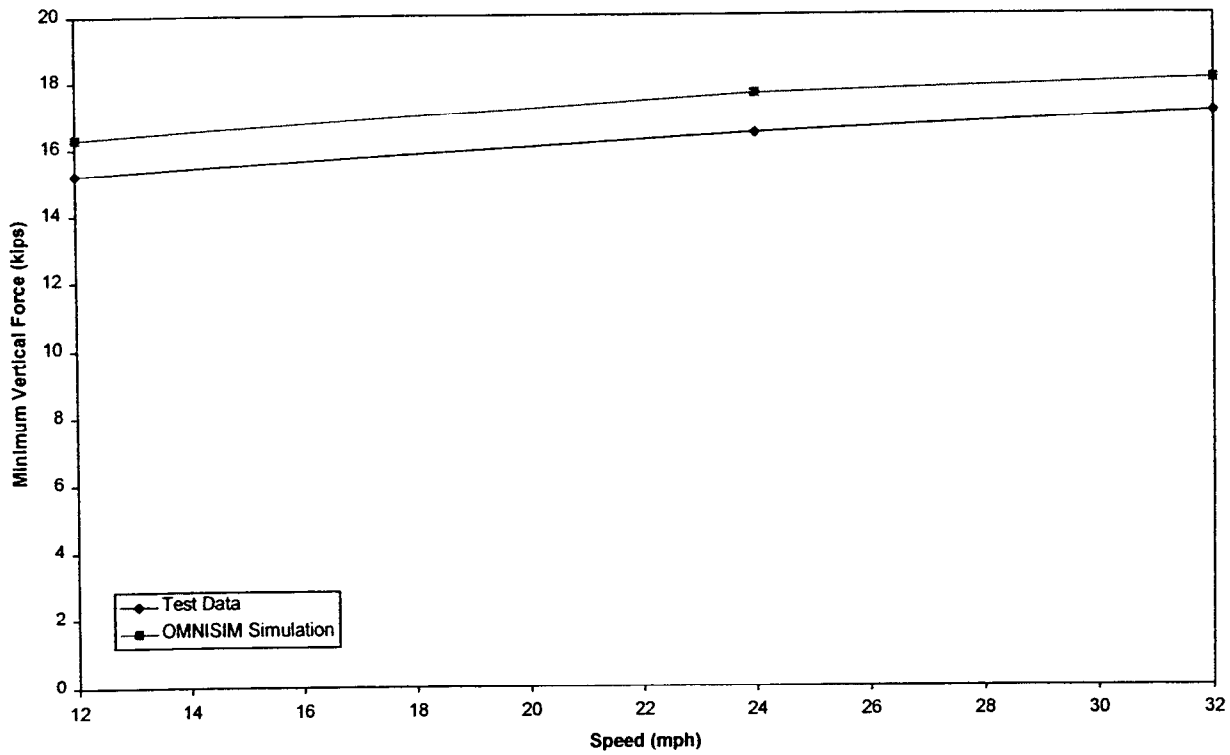

Figure B-12(a). Constant curving (7.5 deg curve) - minimum vertical force

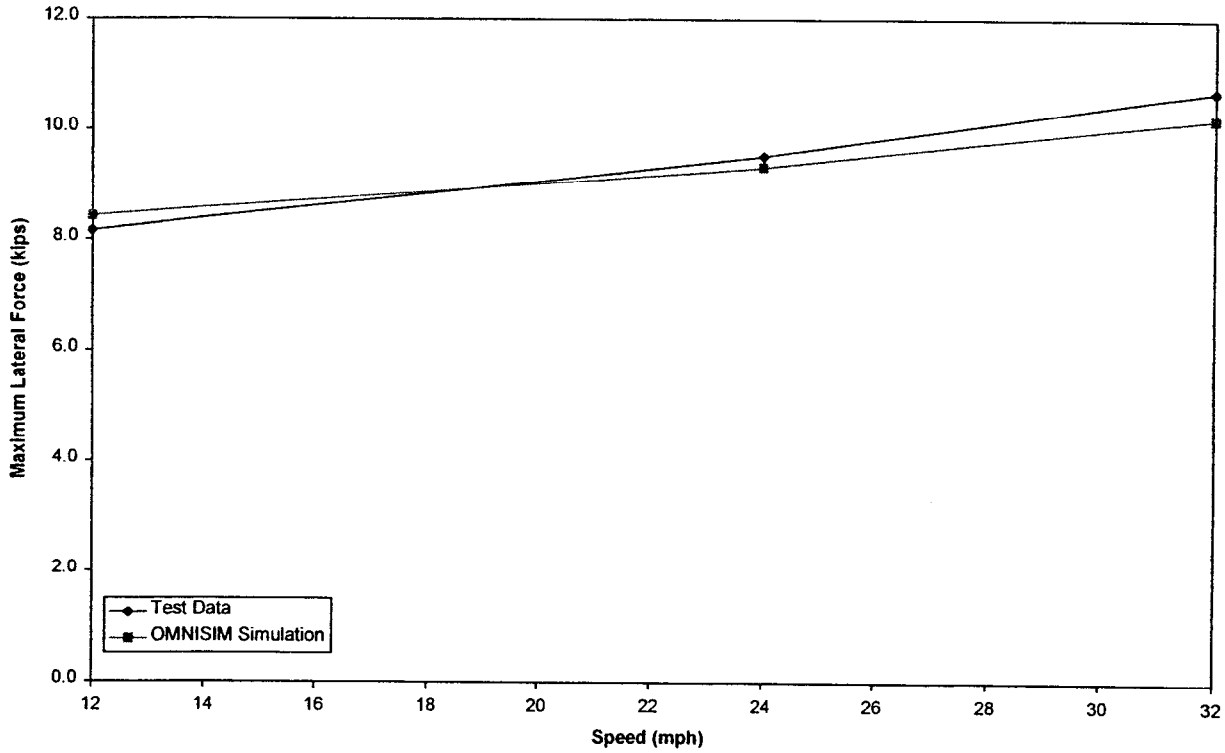

Figure B-12(b). Constant curving (7.5 deg curve) - maximum lateral force

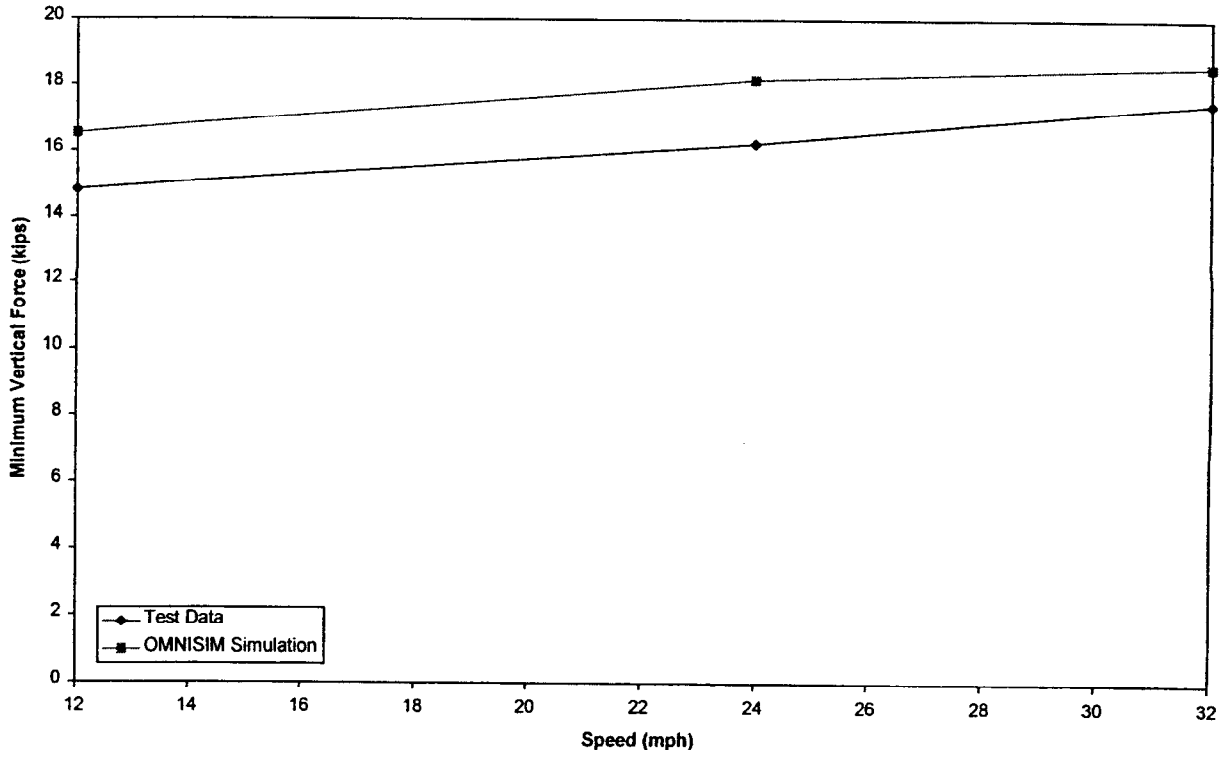

Figure B-13(a). Constant curving (10 deg curve) - minimum vertical force

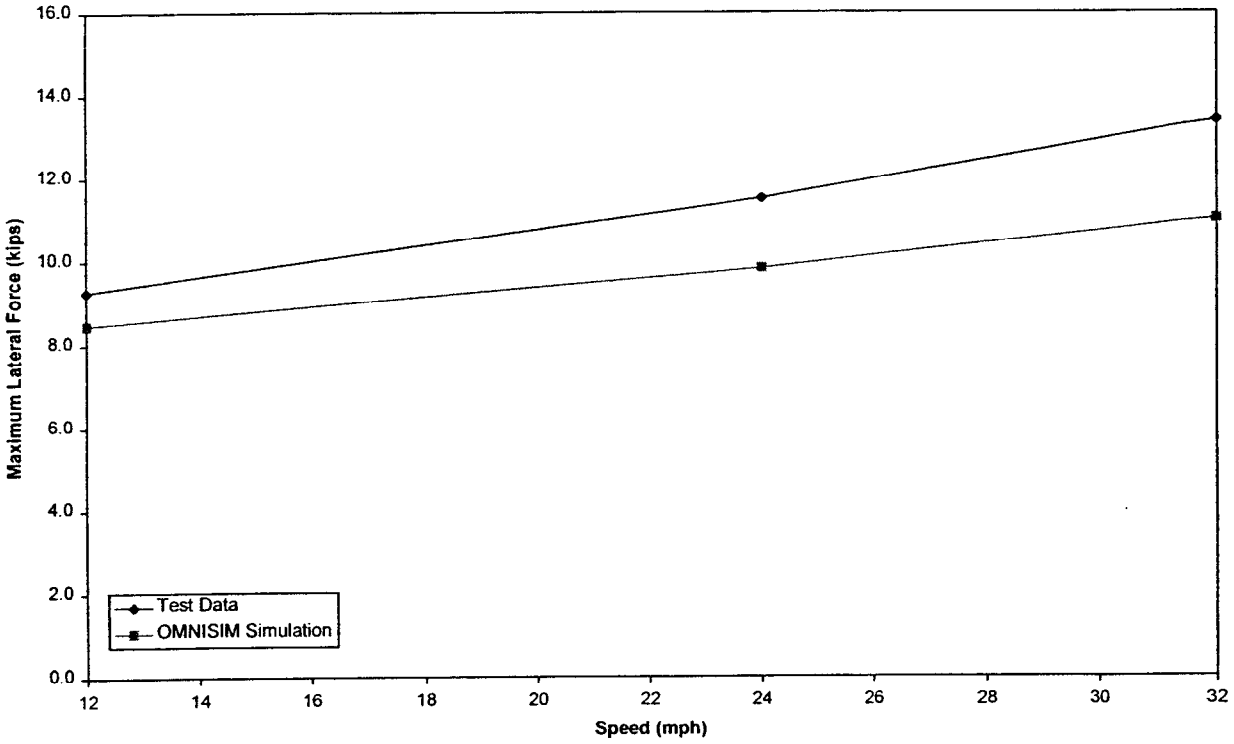

Figure B-13(b). Constant curving (10 deg curve) - maximum lateral force

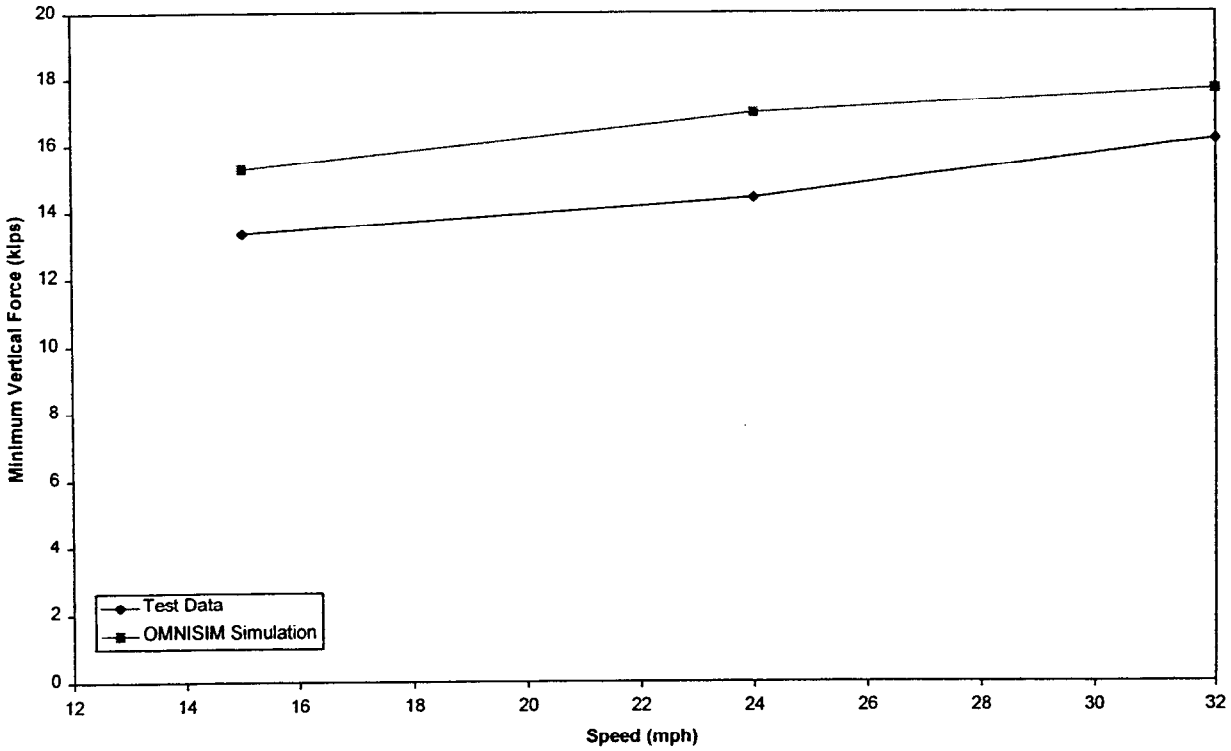

Figure B-14(a). Constant curving (12 deg curve) - minimum vertical force

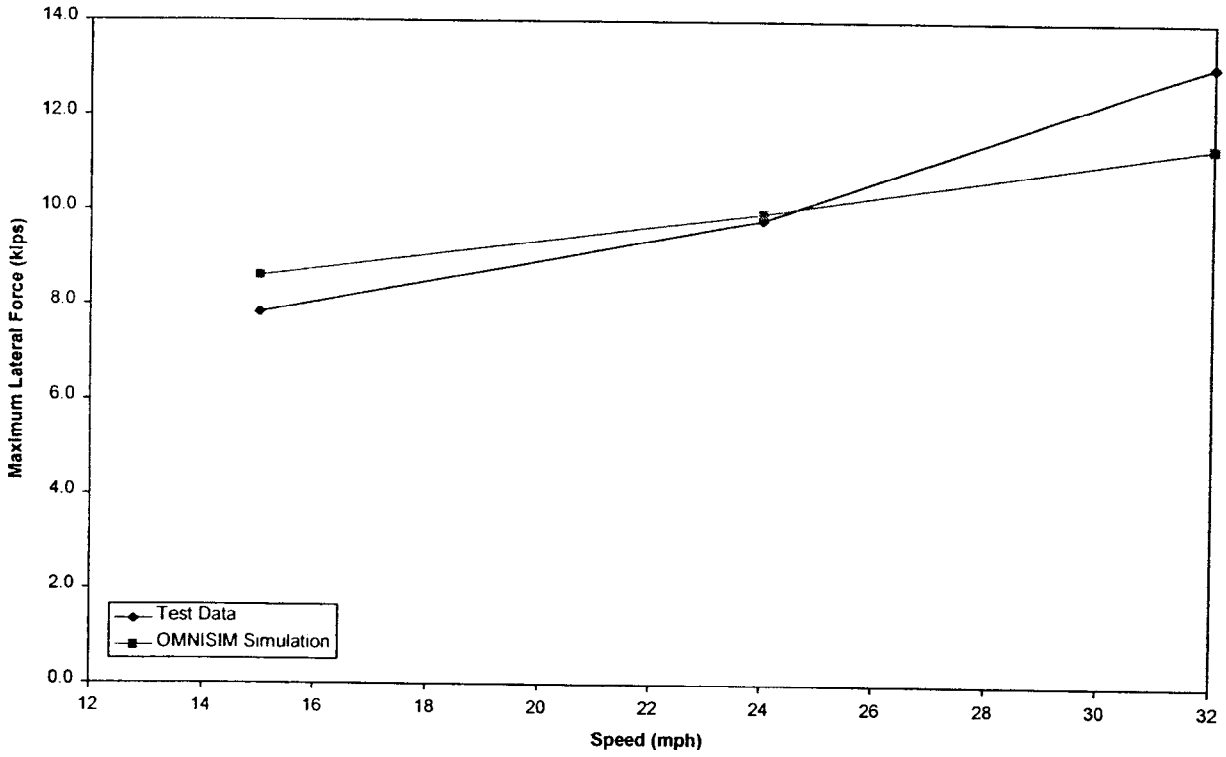

Figure B-14(b). Constant curving (12 deg curve) - maximum lateral force

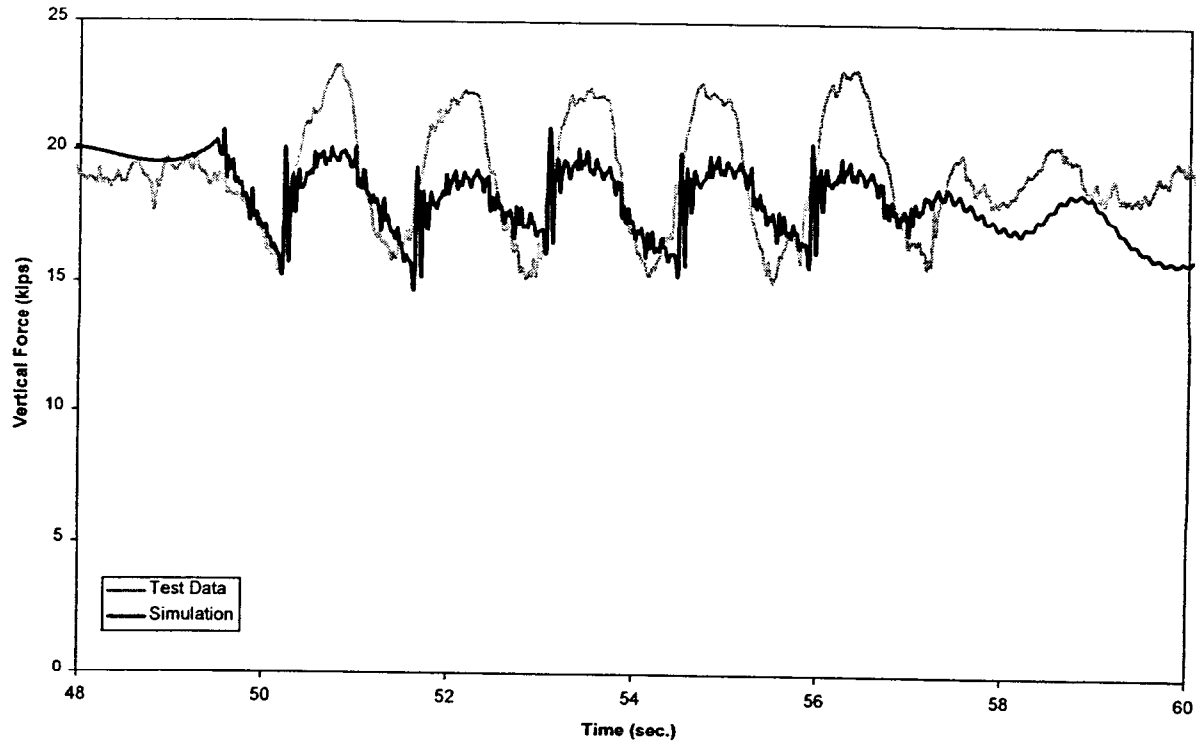

Figure B-15(a). Dynamic curving - vertical force time history, 18.6 mph (lead outer wheel)

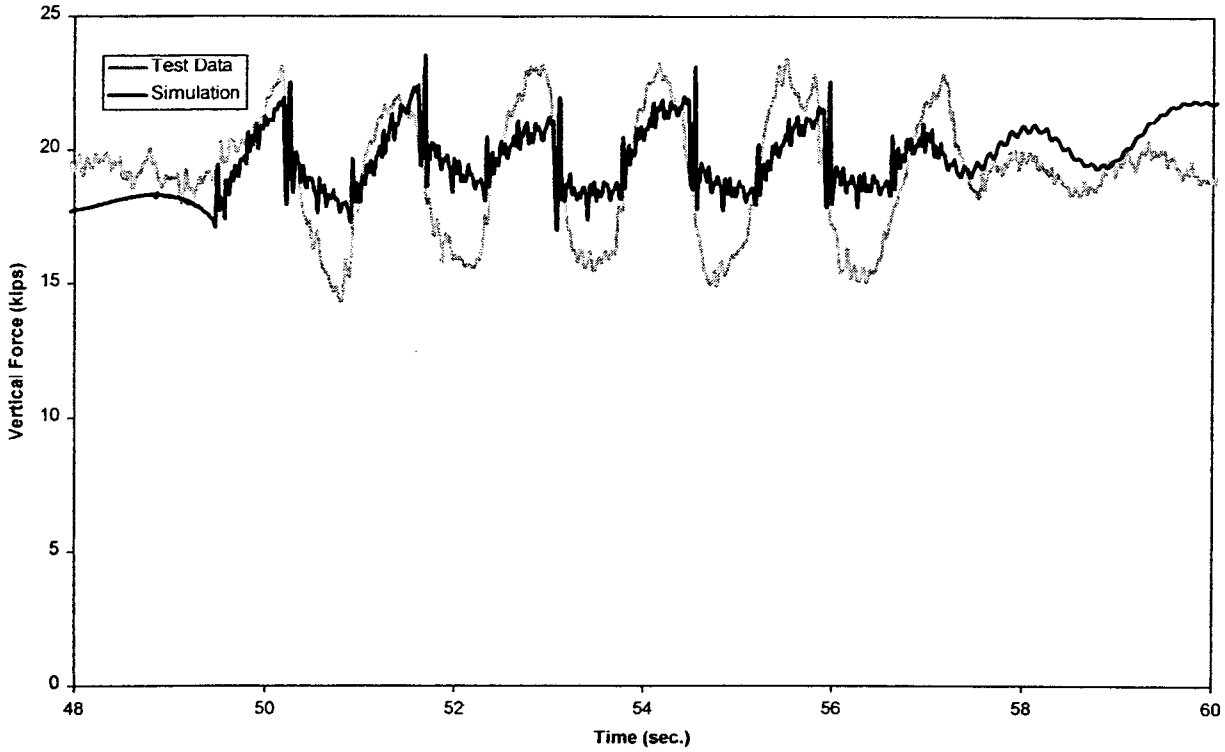

Figure B-15(b). Dynamic curving - vertical force time history, 18.6 mph (lead inner wheel)

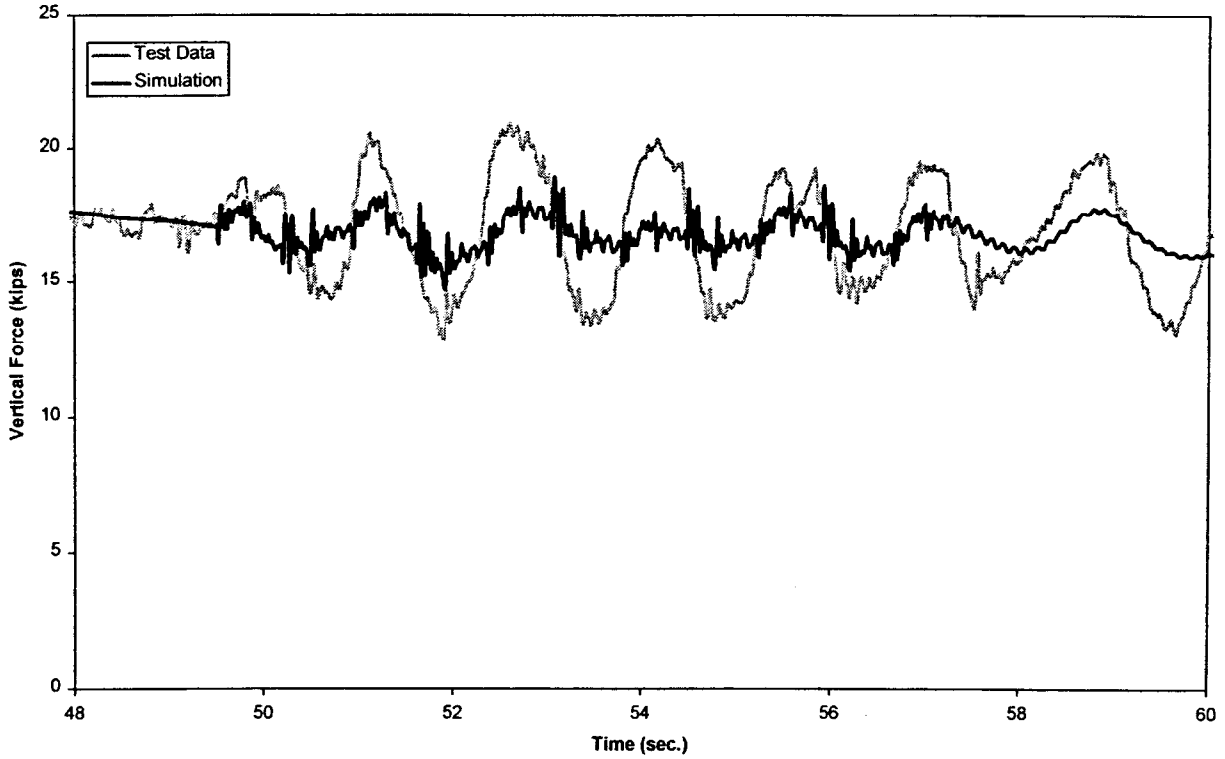

Figure B-15(c). Dynamic curving - vertical force time history, 18.6 mph (trailing outer wheel)

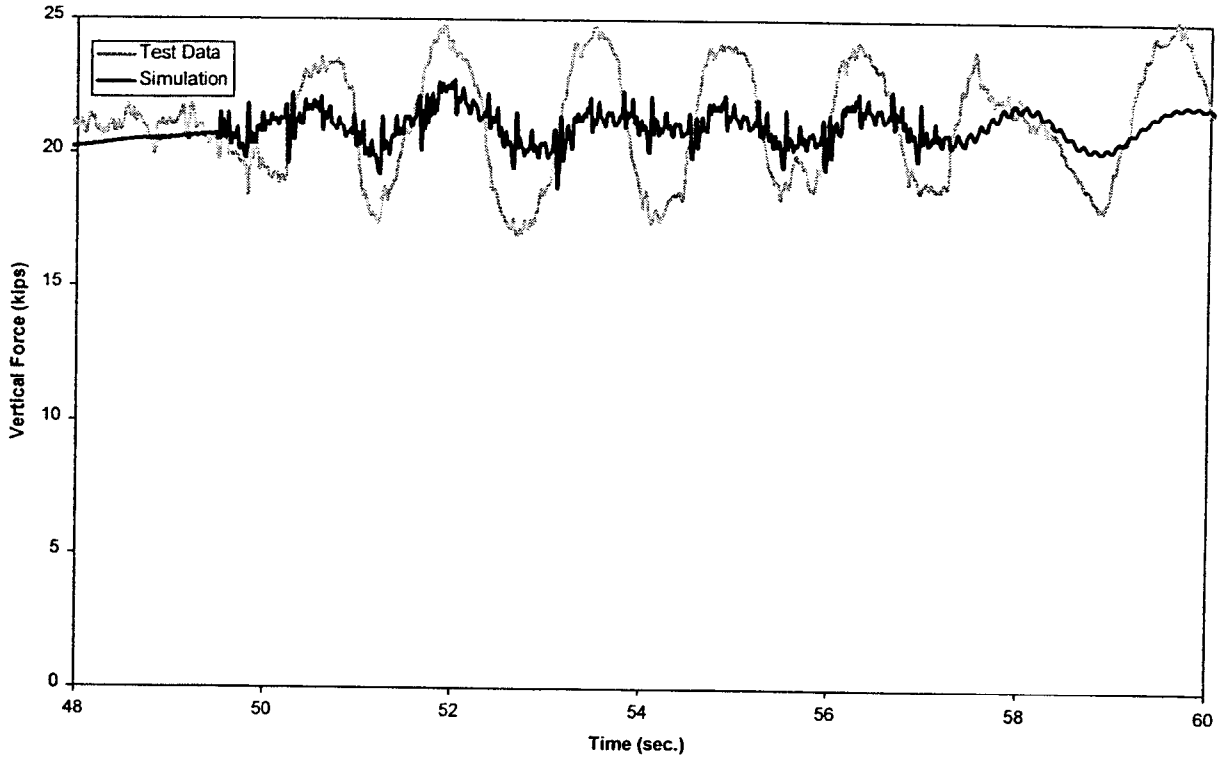

Figure B-15(d). Dynamic curving - vertical force time history, 18.6 mph (trailing inner wheel)

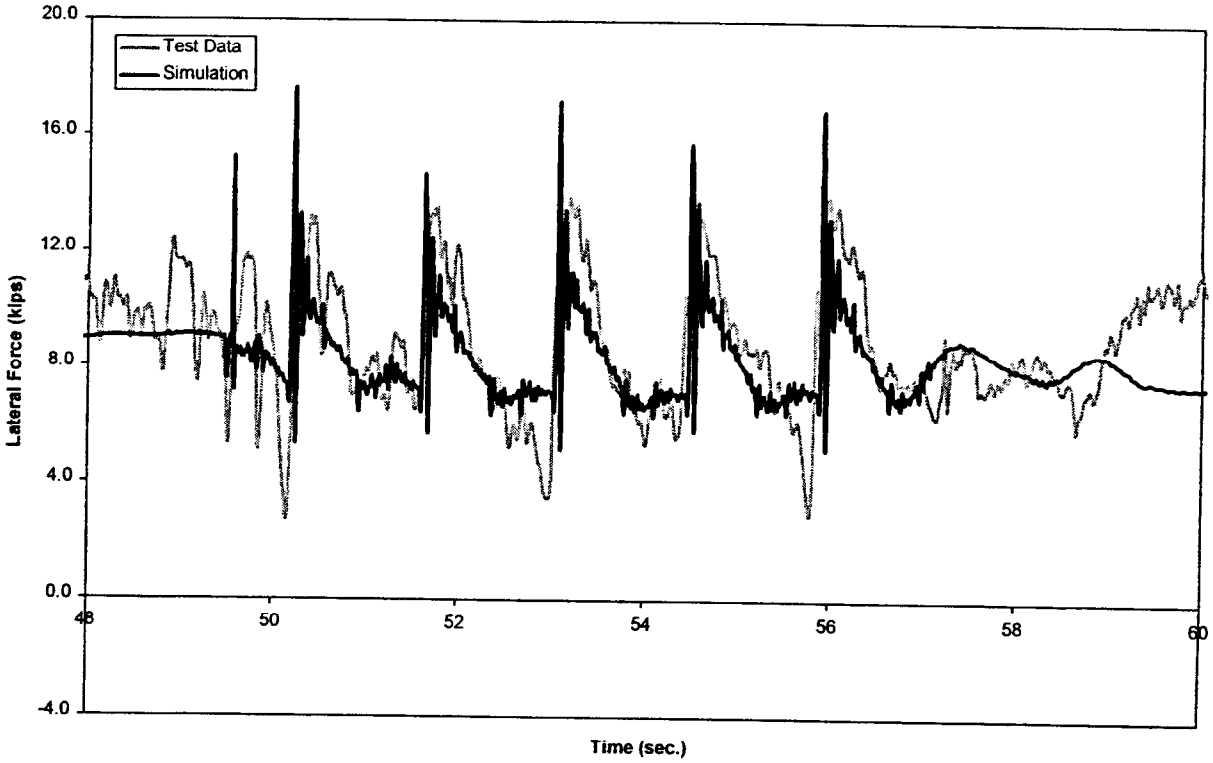

Figure B-16(a). Dynamic curving - lateral force time history, 18.6 mph (lead outer wheel)

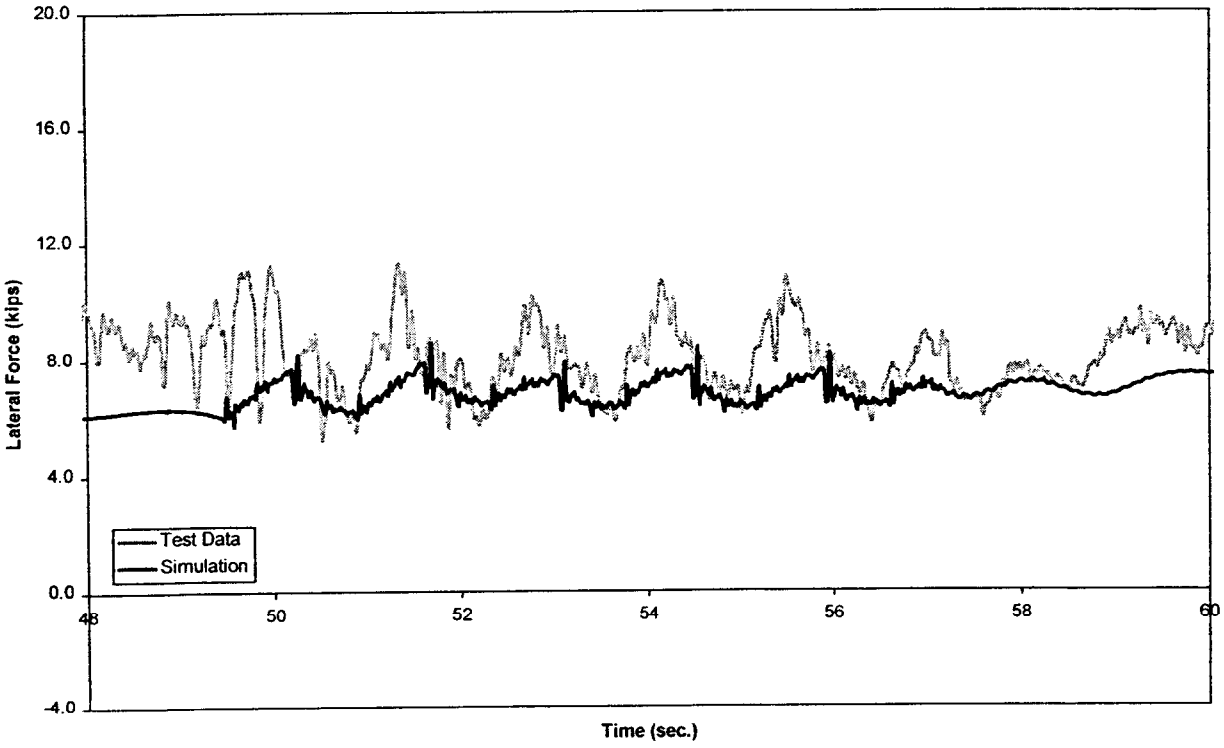

Figure B-16(b). Dynamic curving - lateral force time history, 18.6 mph (lead inner wheel)

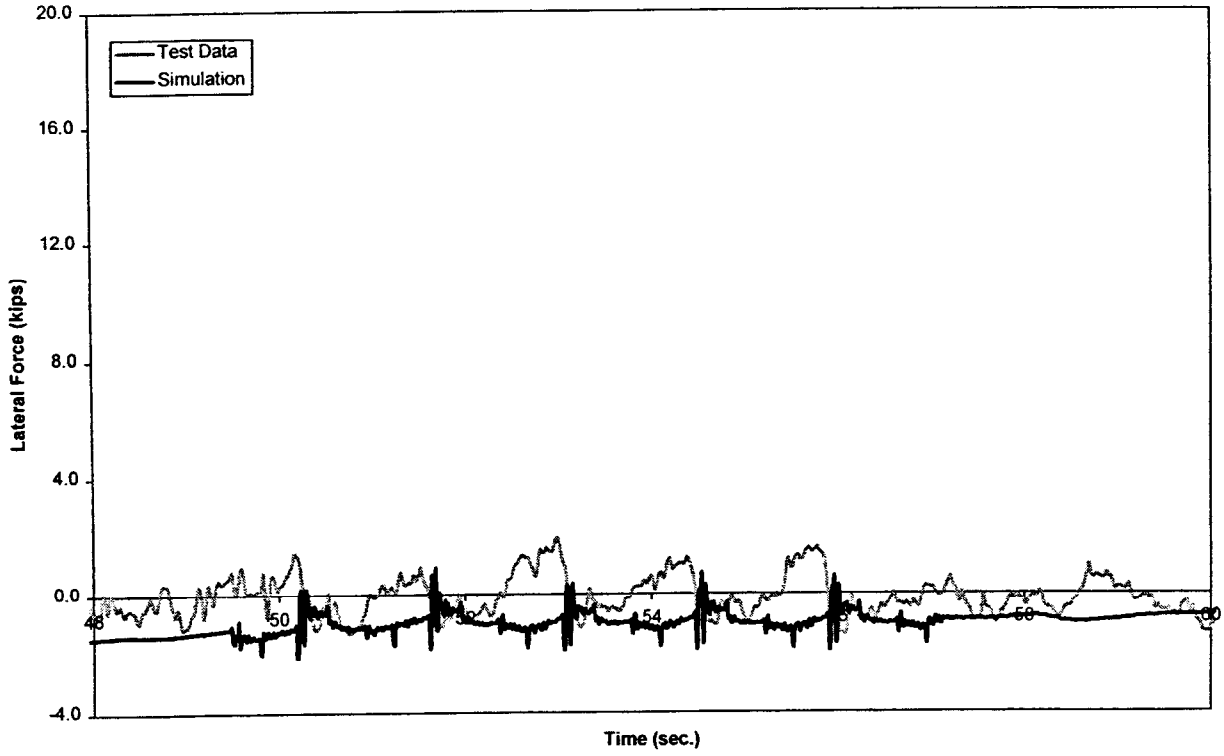

Figure B-16(c). Dynamic curving - lateral force time history, 18.6 mph (trailing outer wheel)

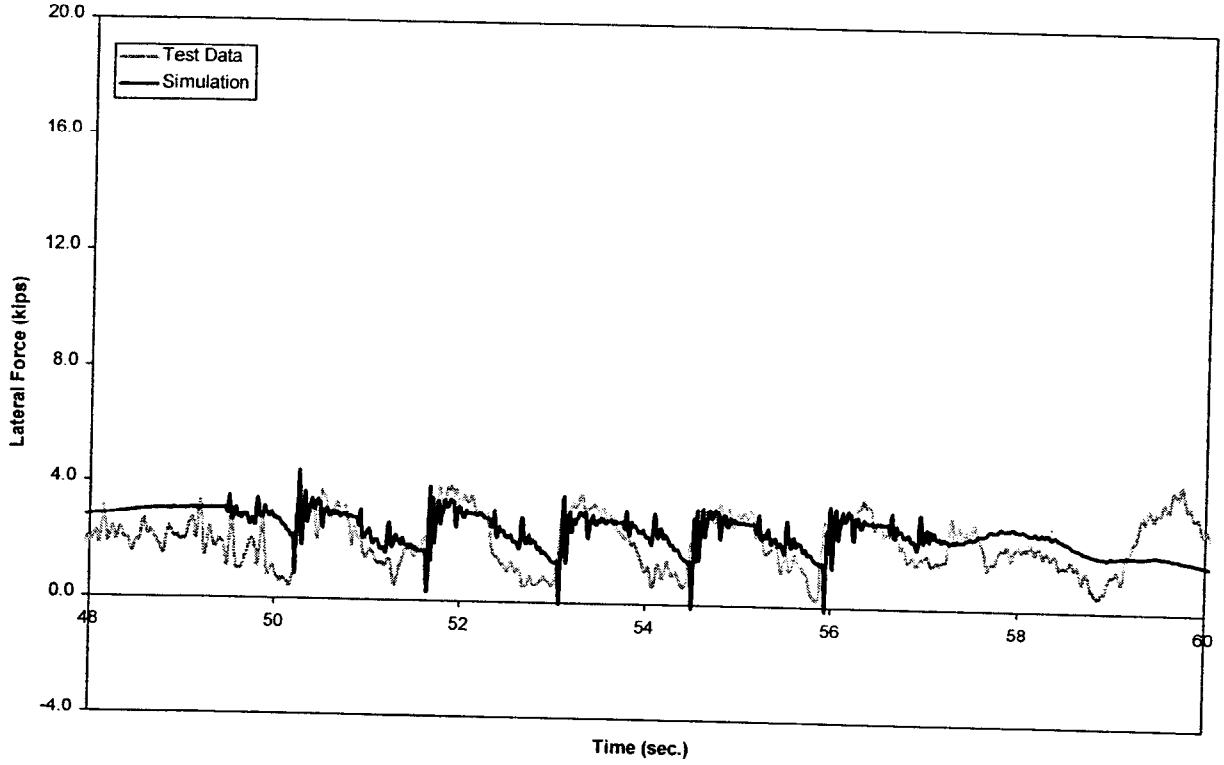

Figure B-16(d). Dynamic curving - lateral force time history, 18.6 mph (trailing inner wheel)

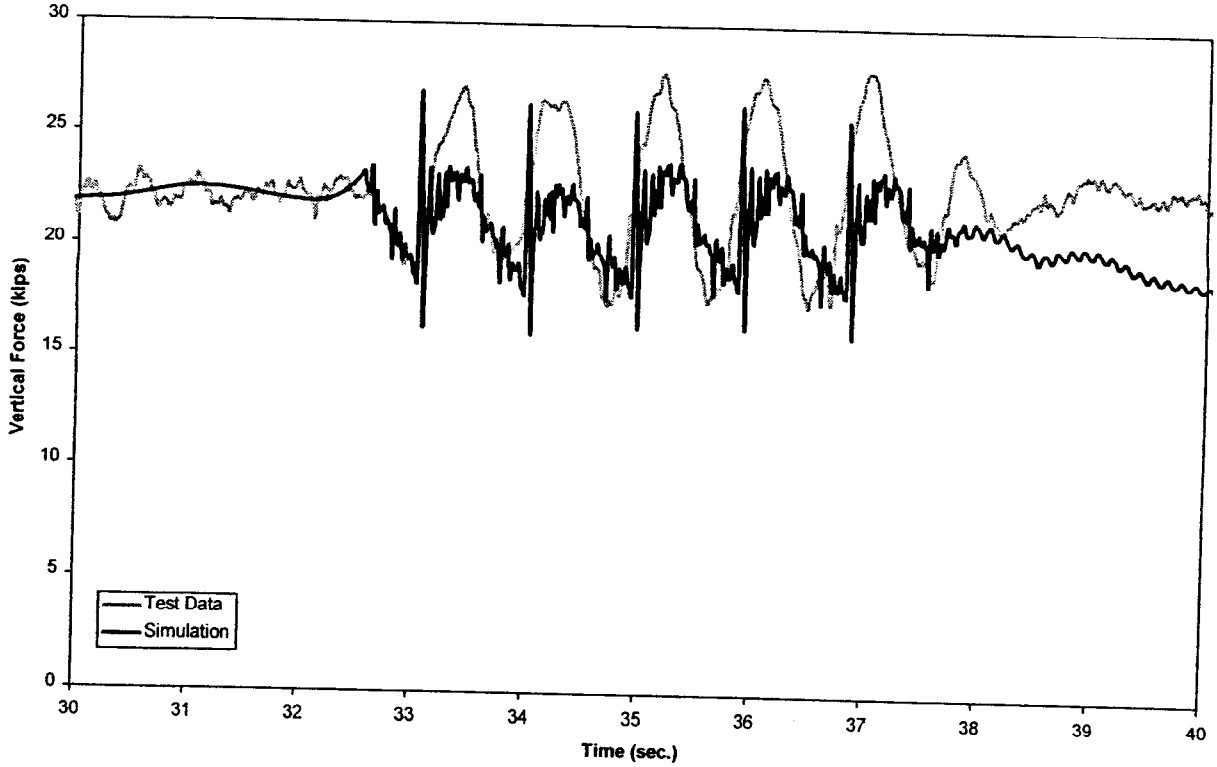

Figure B-17(a). Dynamic curving - vertical force time history, 28 mph (lead outer wheel)

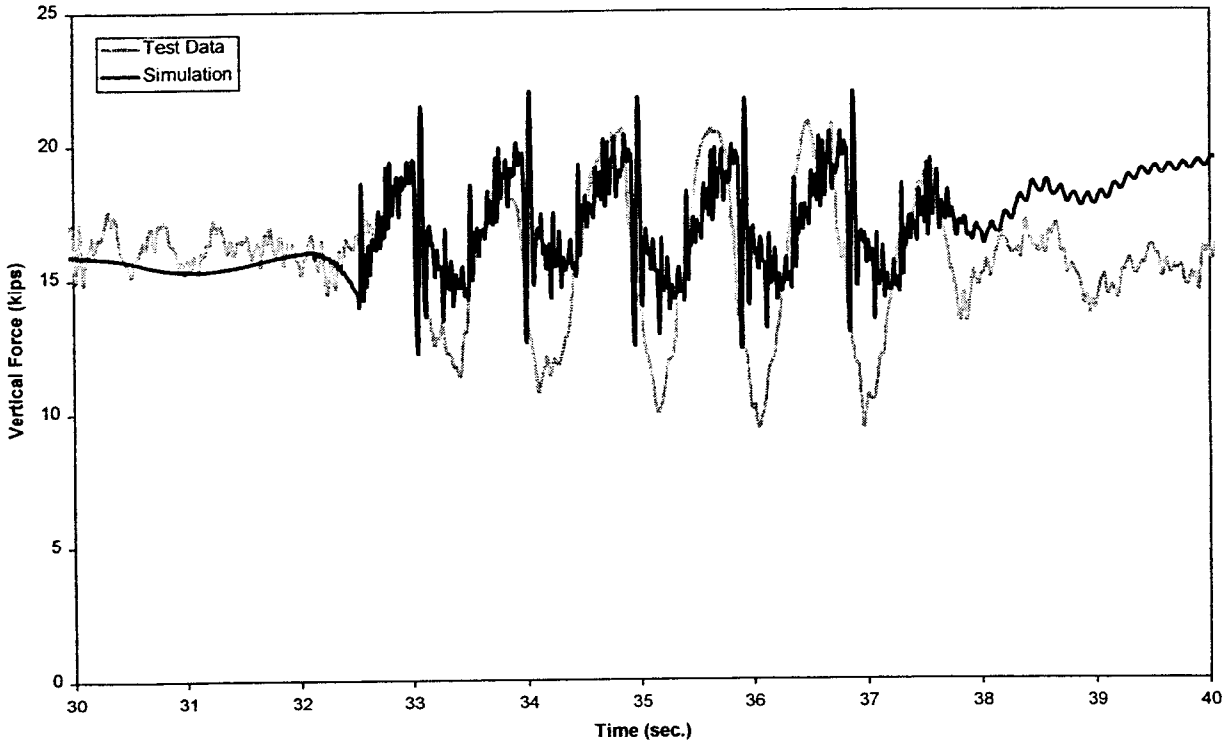

Figure B-17(b). Dynamic curving - vertical force time history, 28 mph (lead inner wheel)

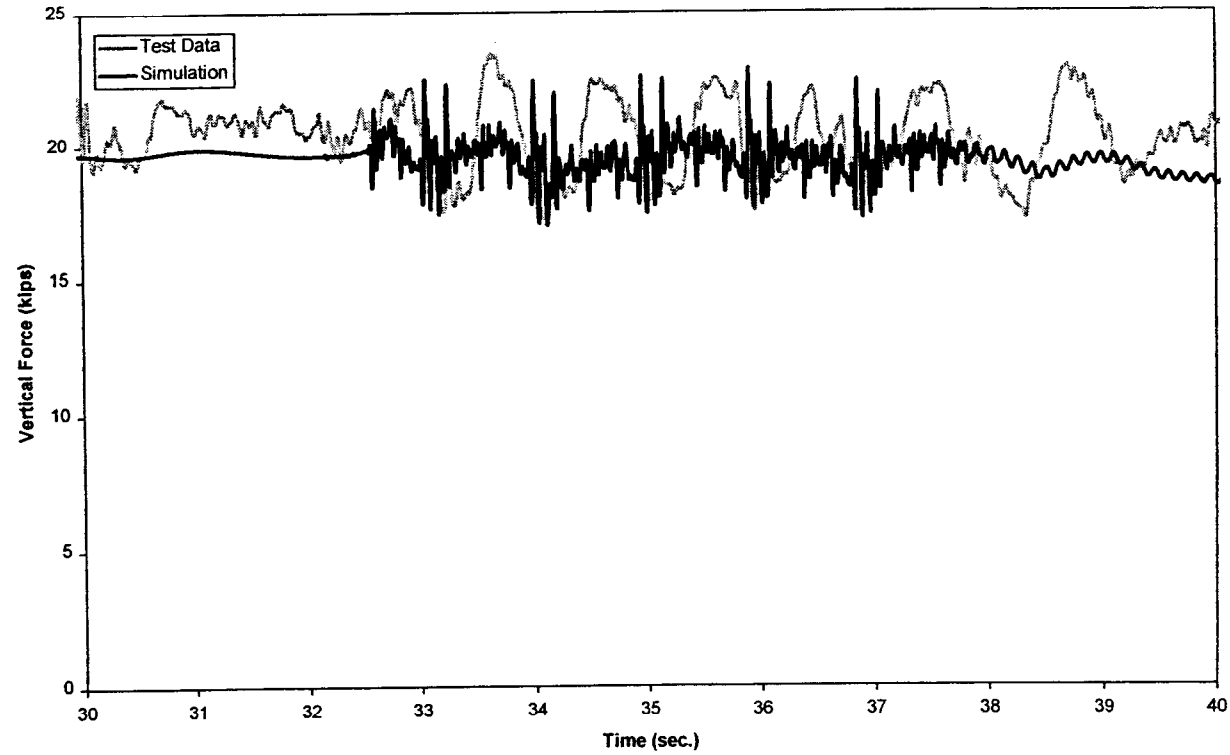

Figure B-17(c). Dynamic curving - vertical force time history, 28 mph (trailing outer wheel)

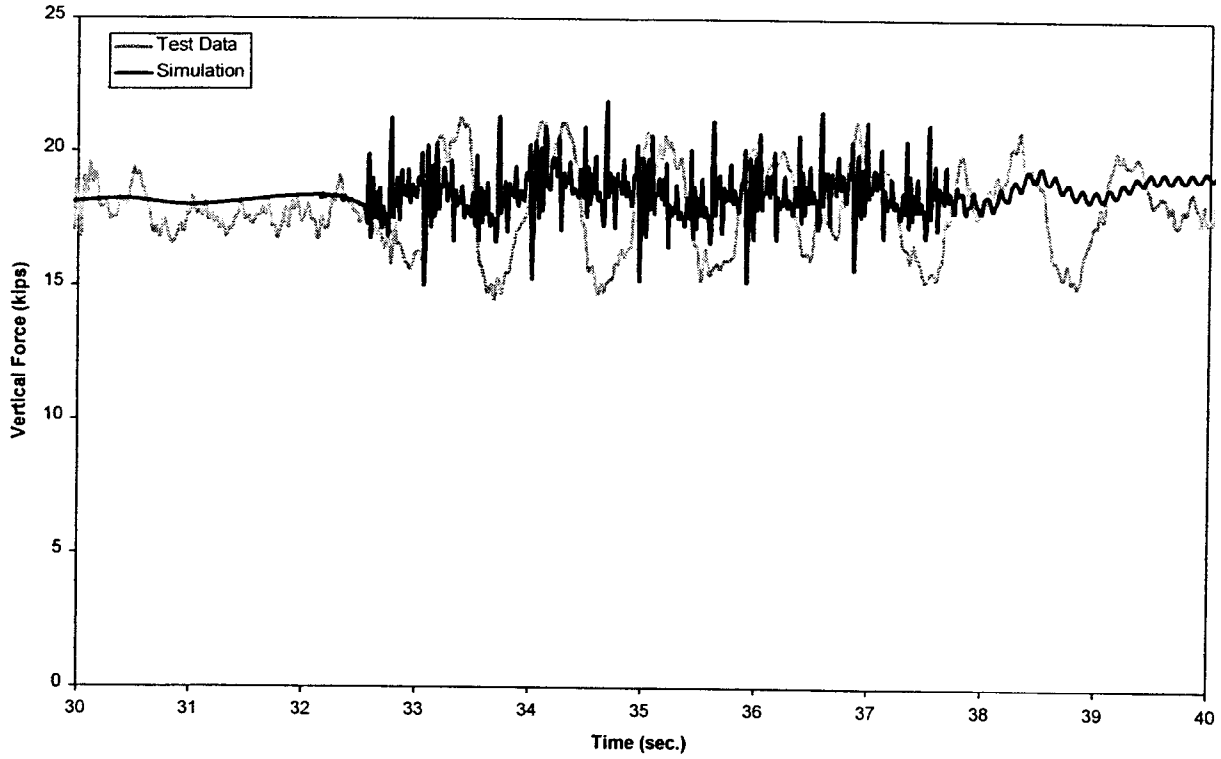

Figure B-17(d). Dynamic curving - vertical force time history, 28 mph (trailing inner wheel)

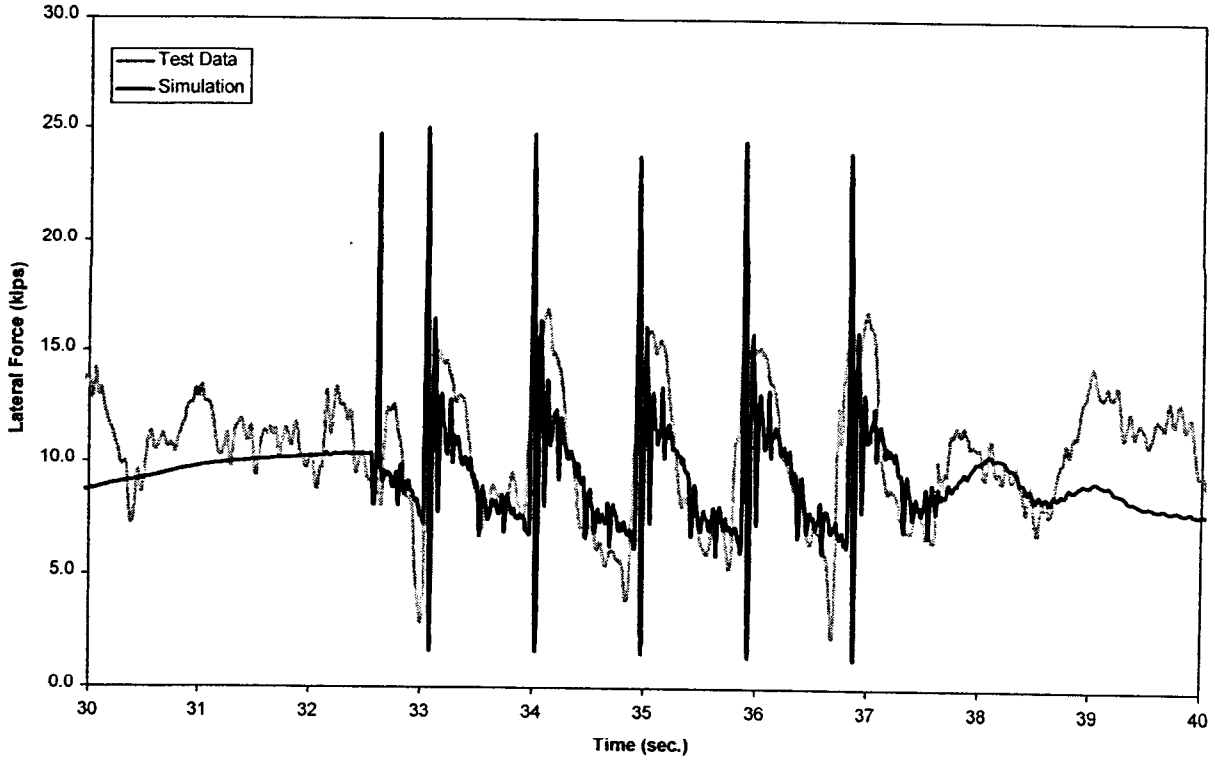

Figure B-18(a). Dynamic curving - lateral force time history, 28 mph (lead outer wheel)

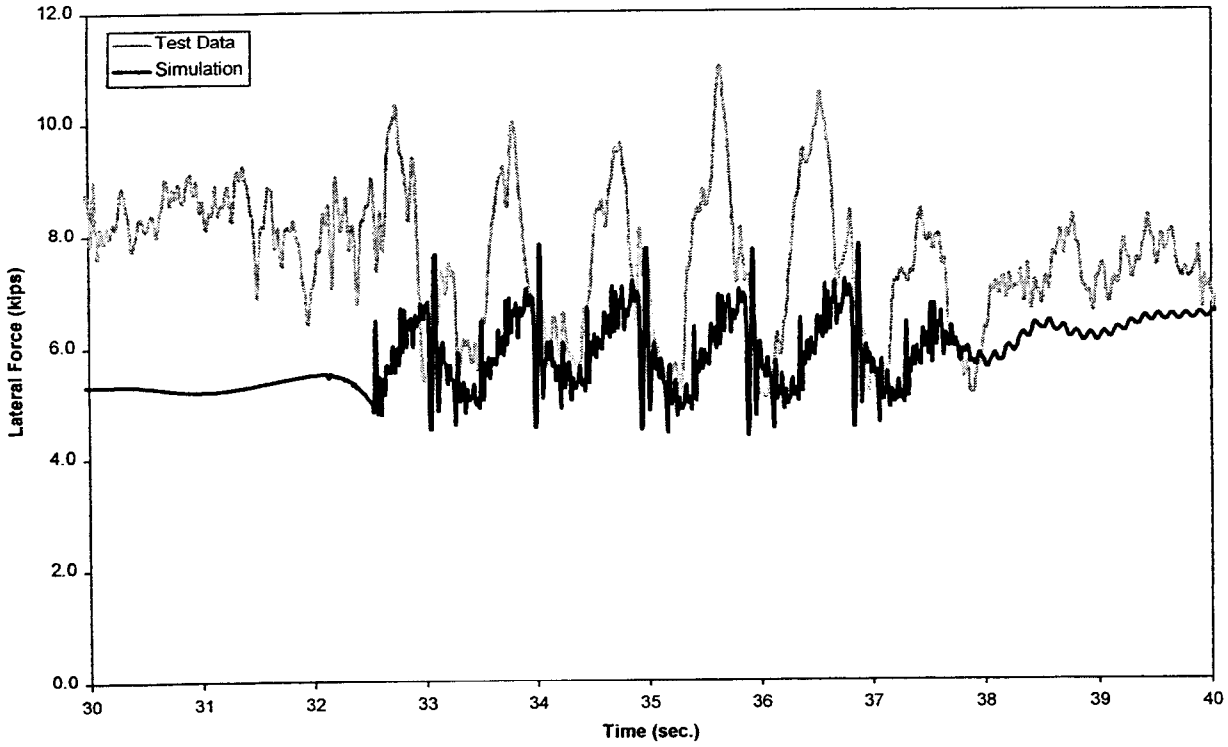

Figure B-18(b). Dynamic curving - lateral force time history, 28 mph (lead inner wheel)

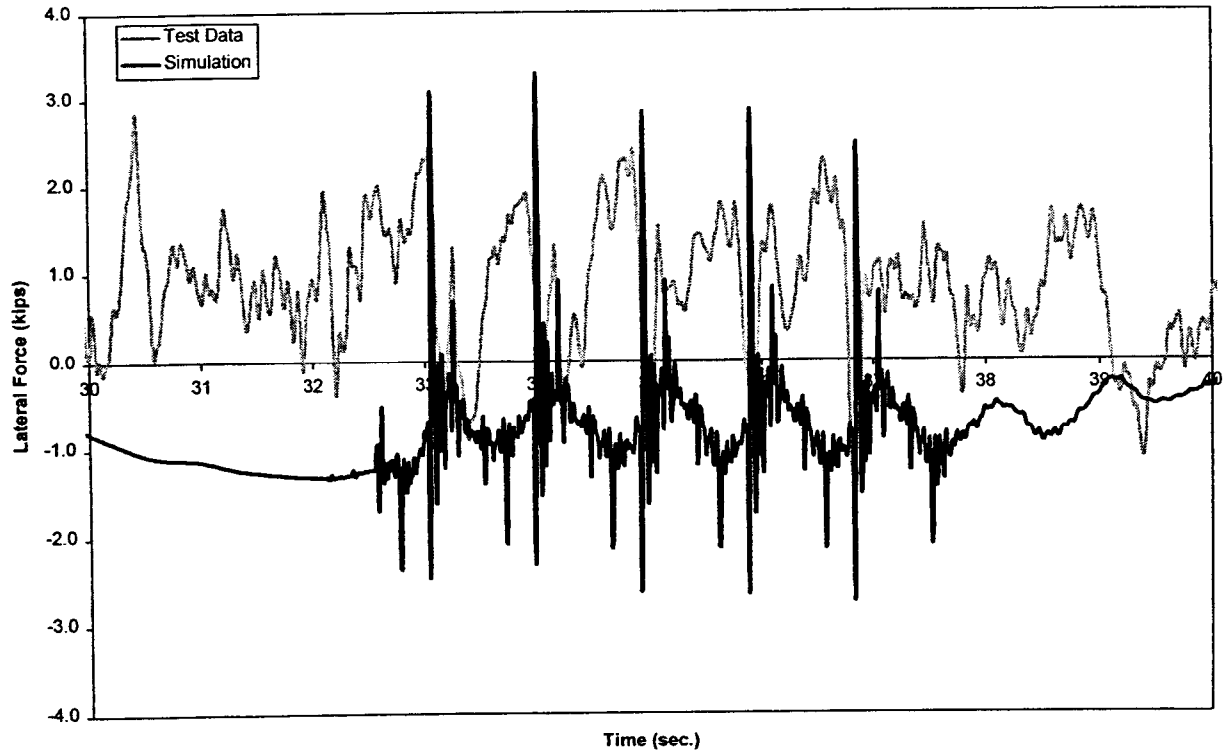

Figure B-18(c). Dynamic curving - lateral force time history, 28 mph (trailing outer wheel)

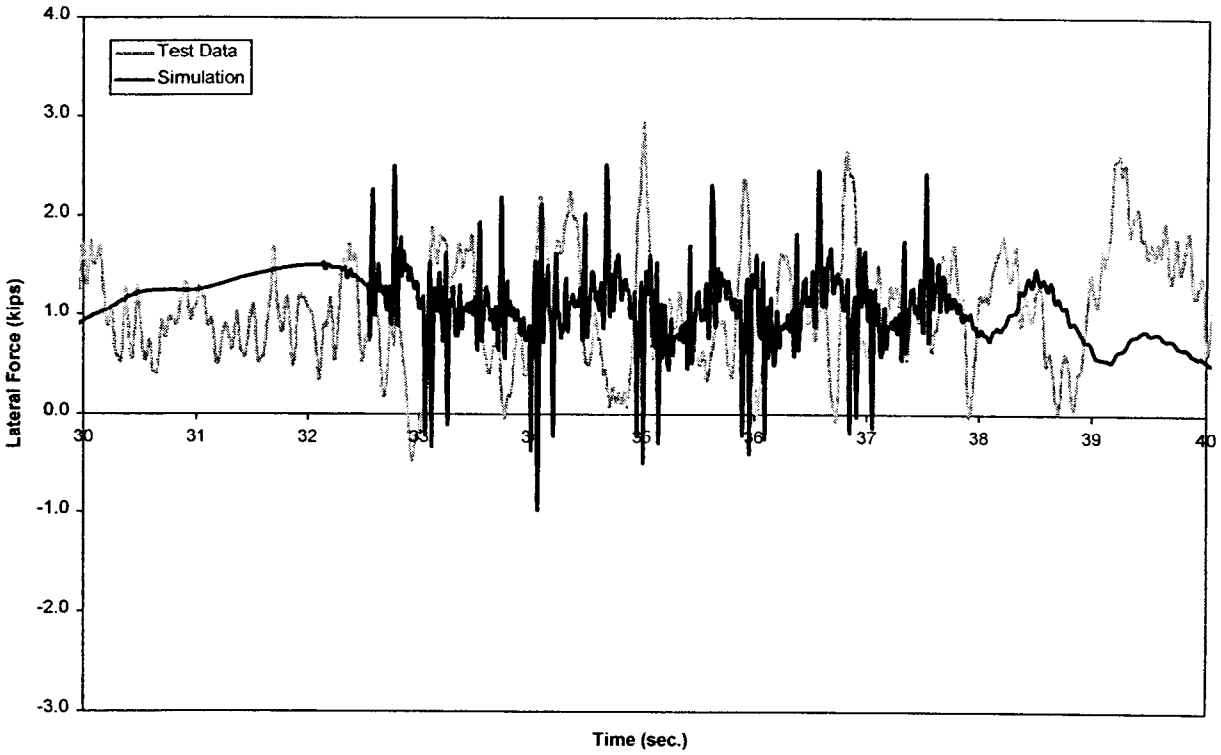

Figure B-18(d). Dynamic curving - lateral force time history, 28 mph (trailing inner wheel)

A plot of the minimum vertical force and maximum lateral force occurring during the tests is shown in Figures B-19 and B-20. Good correlation is shown through the speed range for the vertical force. The lateral force correlation is not as good. The maximum absolute lateral carbody acceleration at the "B" end is shown in Figure B-21. The test data generally have higher values of acceleration than the simulation over the speed range.

The simulation has good correlation for the vertical force at all speeds, however, the correlation for the lateral force is not as good. The simulation predicts well the shape and amplitude of the vertical forces. The predicted lateral forces have the same shape as test lateral forces but their amplitudes are larger. The overall safe behavior of the vehicle observed in the test is consistent with the simulation predictions.

B.4 Yaw and Sway

Comparisons of the test and simulation data are shown in Figures B-22 and B-23 for vertical and lateral forces, respectively for 20 mph and in Figures B-24 and B-25 for 60 mph. For the tests at both speeds, the vertical data have relative small variations on the order of ±1 kip from the nominal value of vertical load of 19.5 kips. While the lead axle test data indicates nominally equal loads on each wheel, the trailing axle test data shows a nominal load of 18 kips on the left wheel and 19.5 kips on the right wheel. The five cycle variation in vertical load illustrated in the simulation is also reflected in the test data. The lateral test data on all four wheels at both speeds have a series of sharp "spikes" of lateral force with amplitudes typically of 1 to 5 kips. These spikes occur at 39 ft intervals.

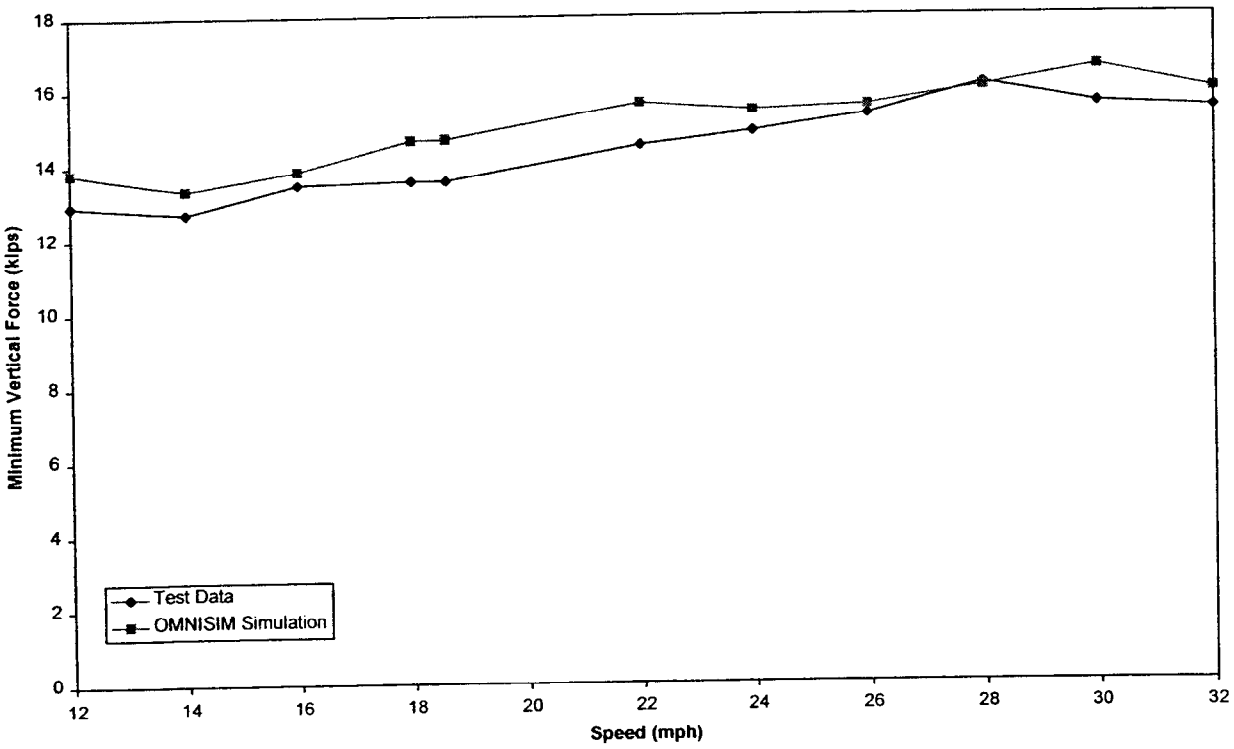

Figure B-19. Dynamic curving - minimum vertical force

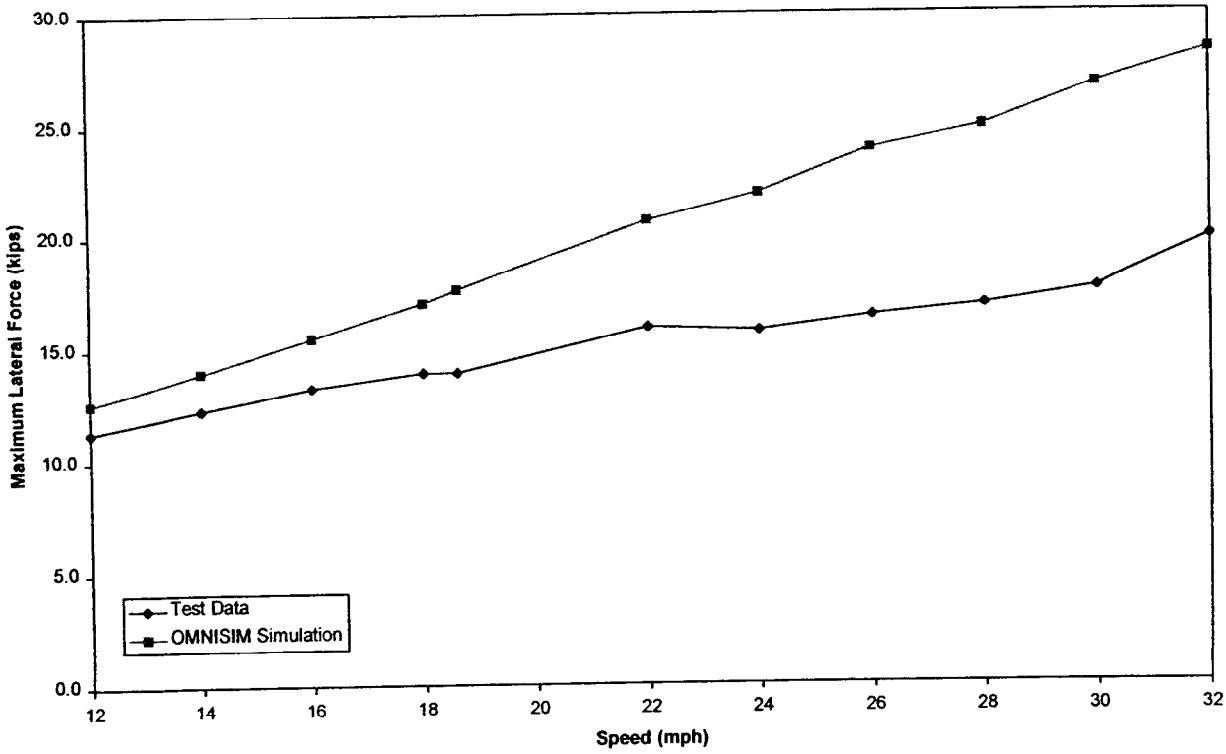

Figure B-20. Dynamic curving - maximum lateral force

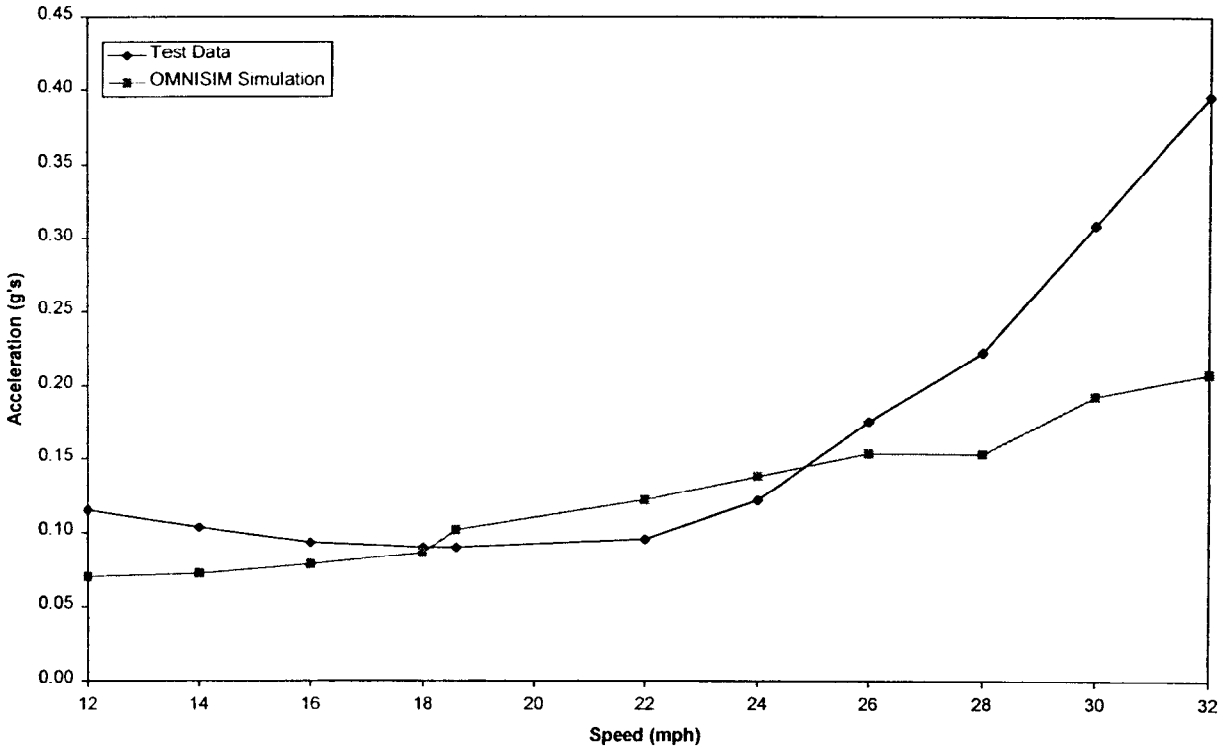

Figure B-21. Dynamic curving - maximum absolute lateral carbody acceleration

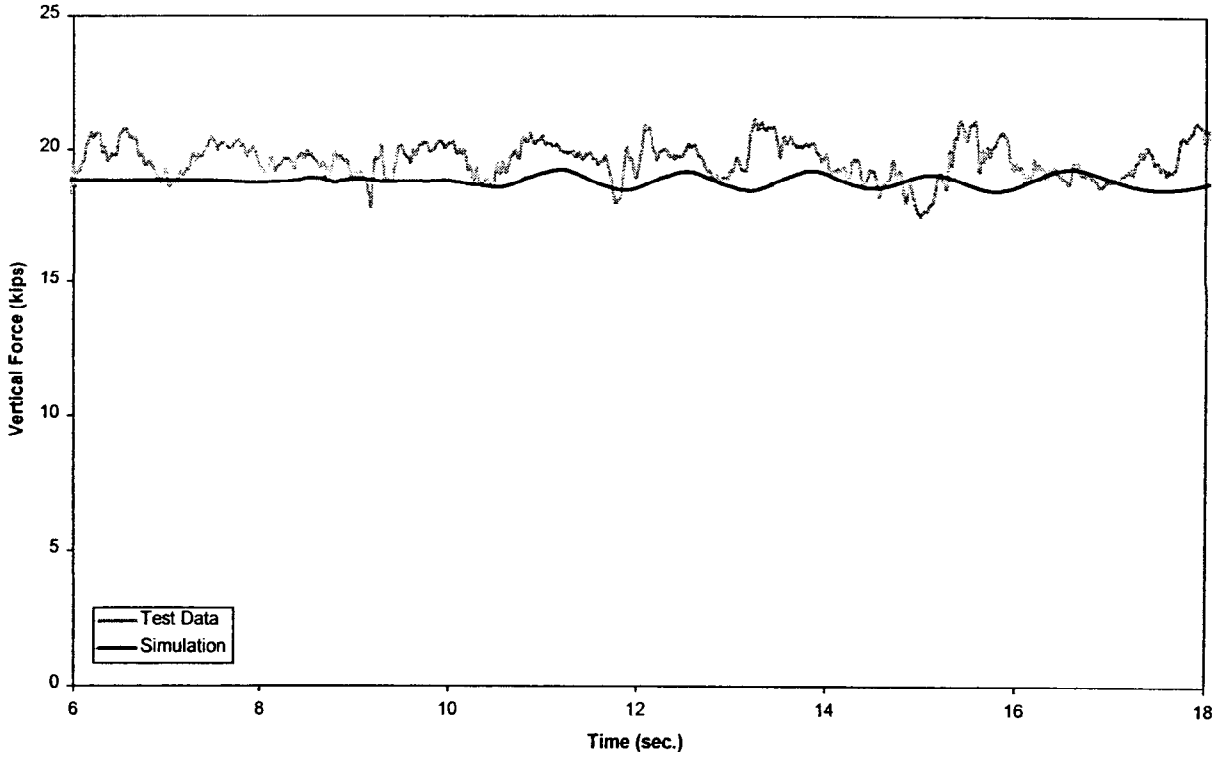

Figure B-22(a). Yaw and sway - vertical force time history, 20 mph (lead left wheel)

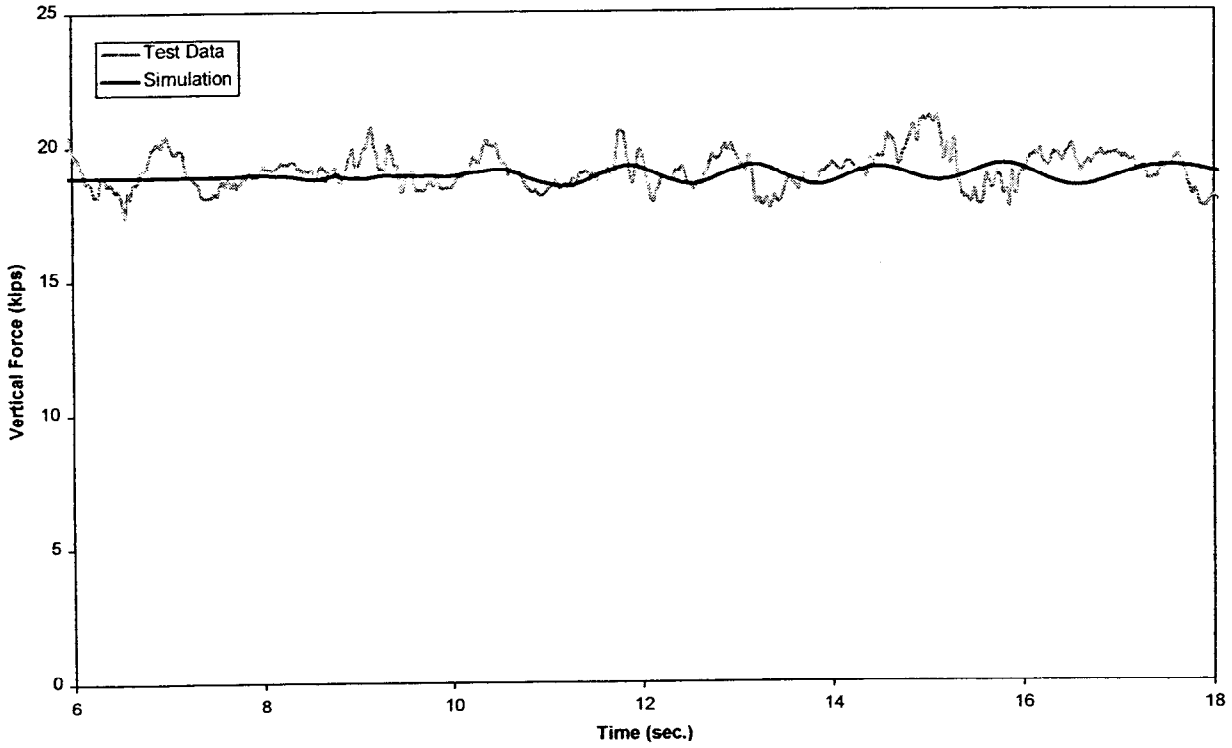

Figure B-22(b). Yaw and sway - vertical force time history, 20 mph (lead right wheel)

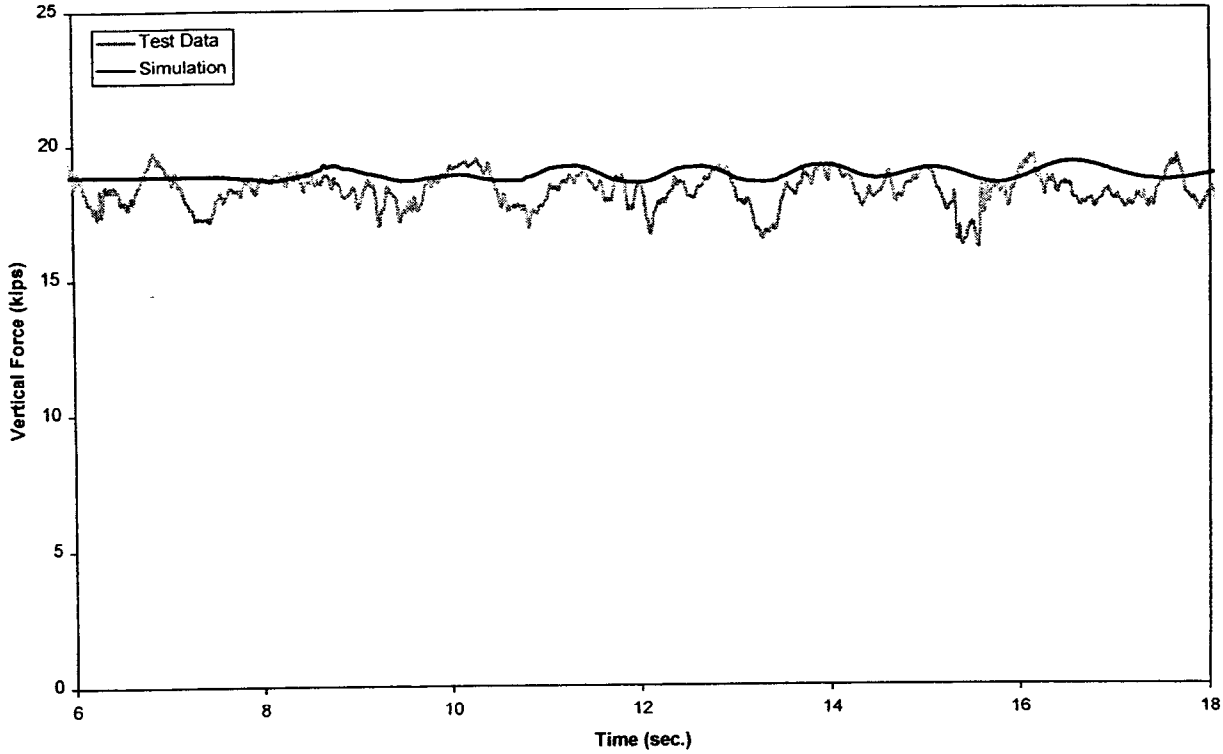

Figure B-22(c). Yaw and sway - vertical force time history, 20 mph (trailing left wheel)

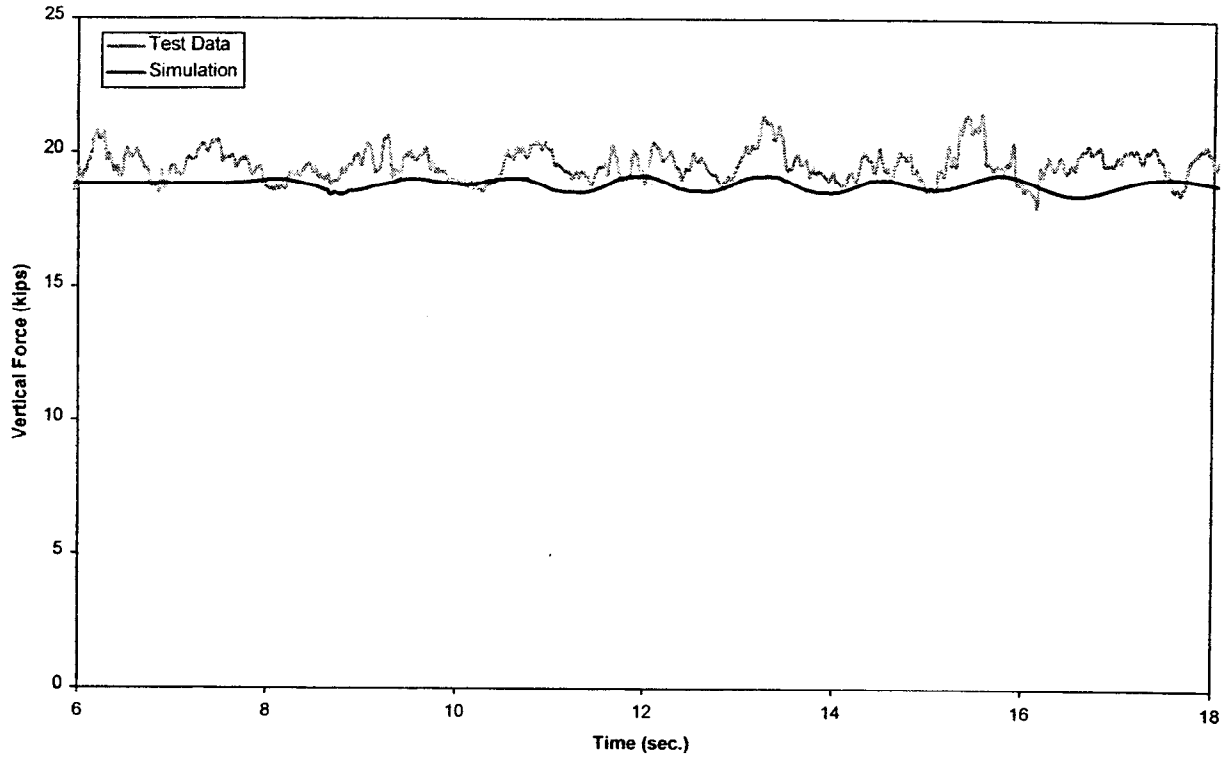

Figure B-22(d). Yaw and sway - vertical force time history, 20 mph (trailing right wheel)

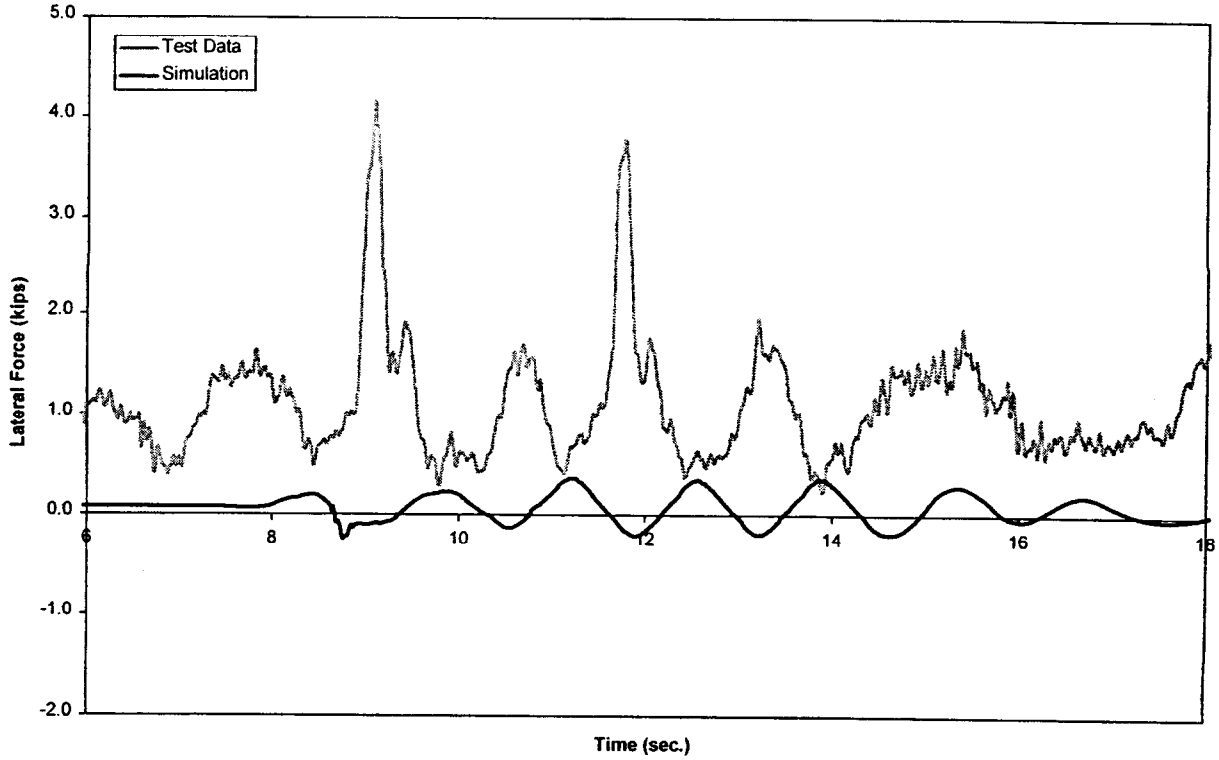

Figure B-23(a). Yaw and sway - lateral force time history, 20 mph (lead left wheel)

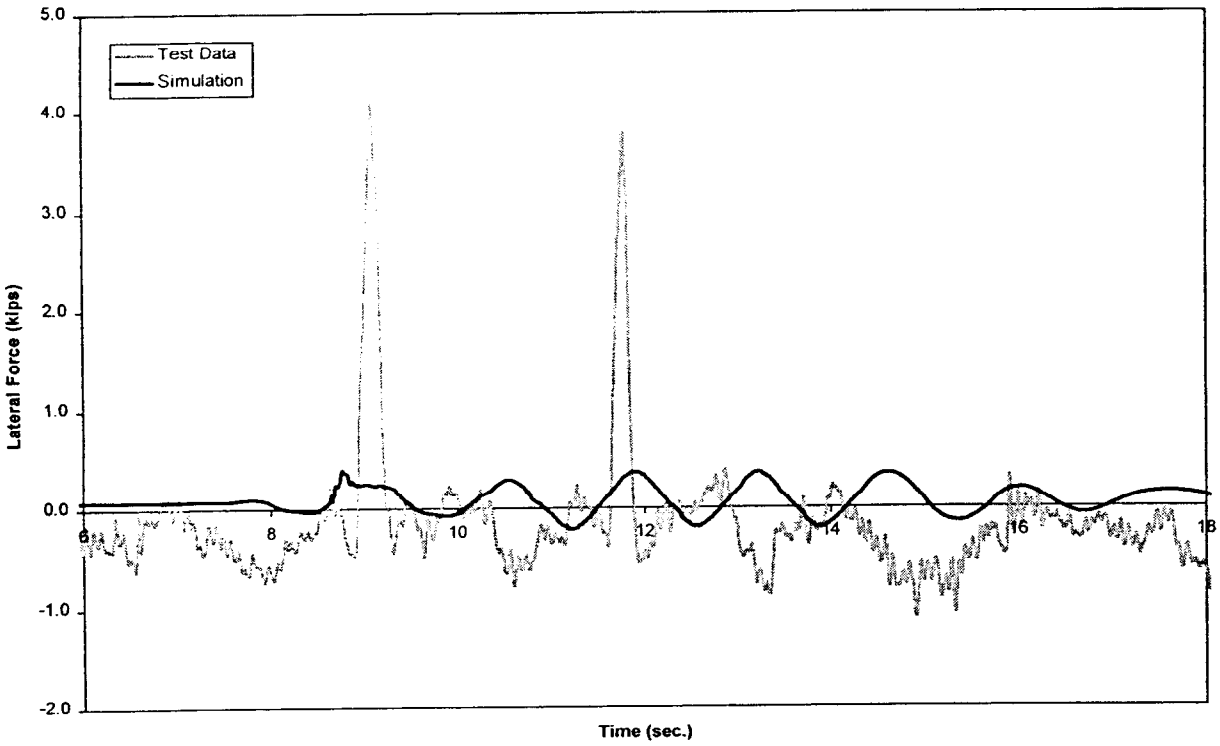

Figure B-23(b). Yaw and sway - lateral force time history, 20 mph (lead right wheel)

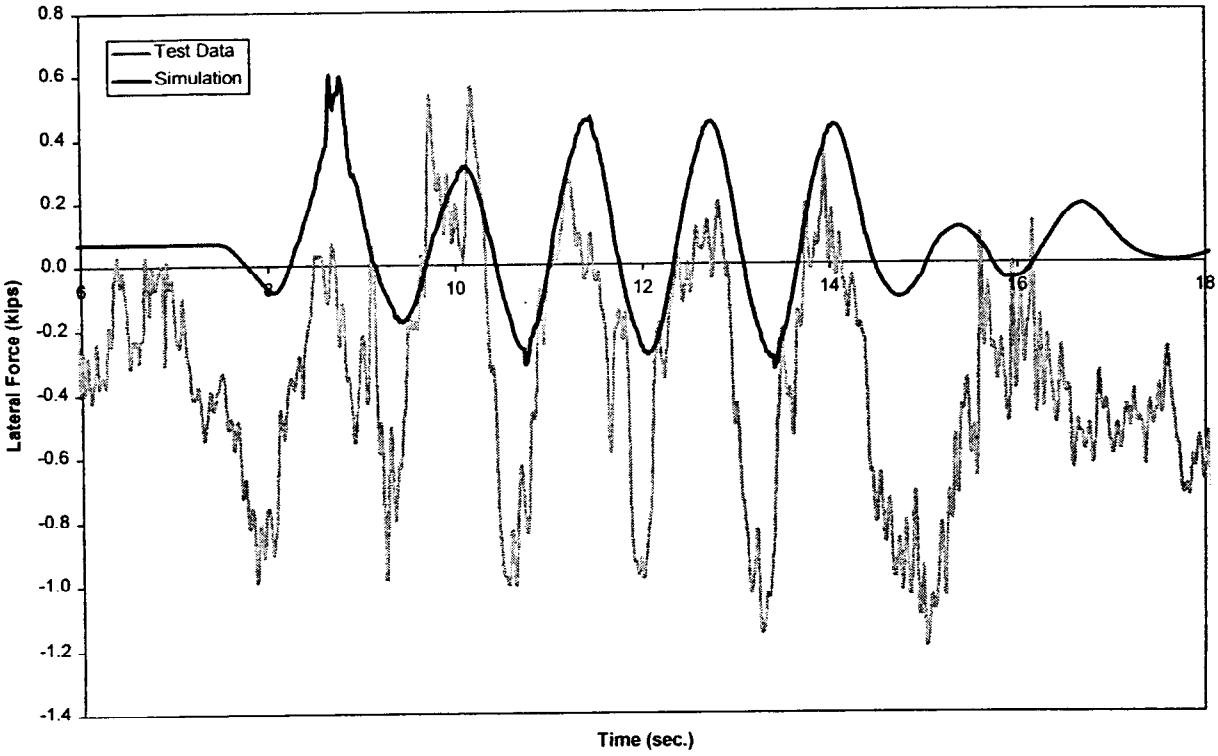

Figure B-23(c). Yaw and sway - lateral force time history, 20 mph (trailing left wheel)

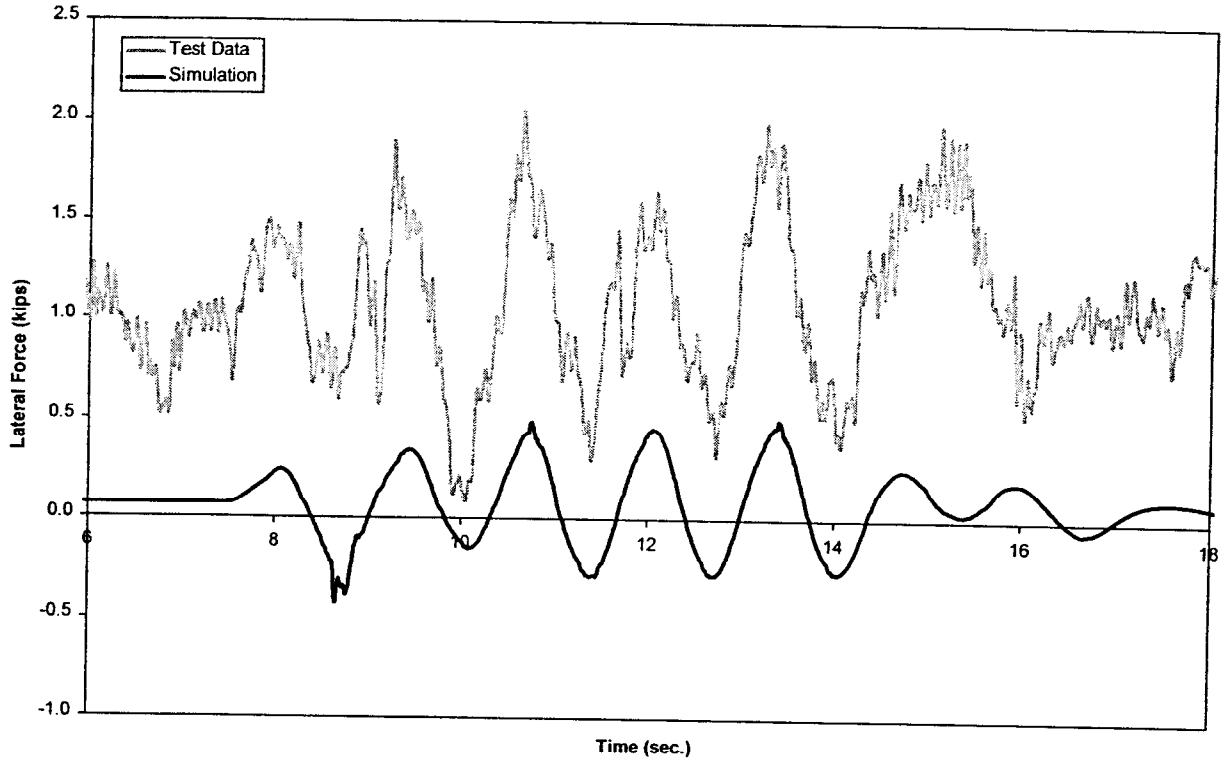

Figure B-23(d). Yaw and sway - lateral force time history, 20 mph (trailing right wheel)

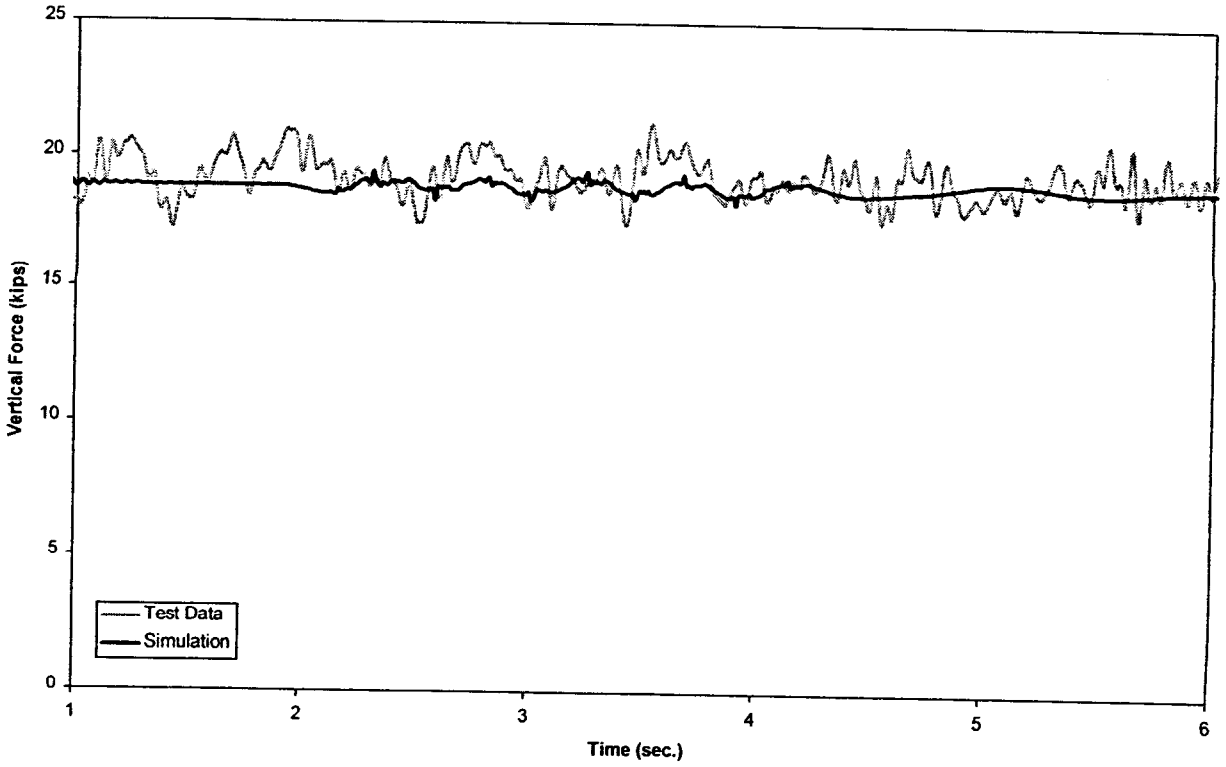

Figure B-24(a). Yaw and sway - vertical force time history, 60 mph (lead left wheel)

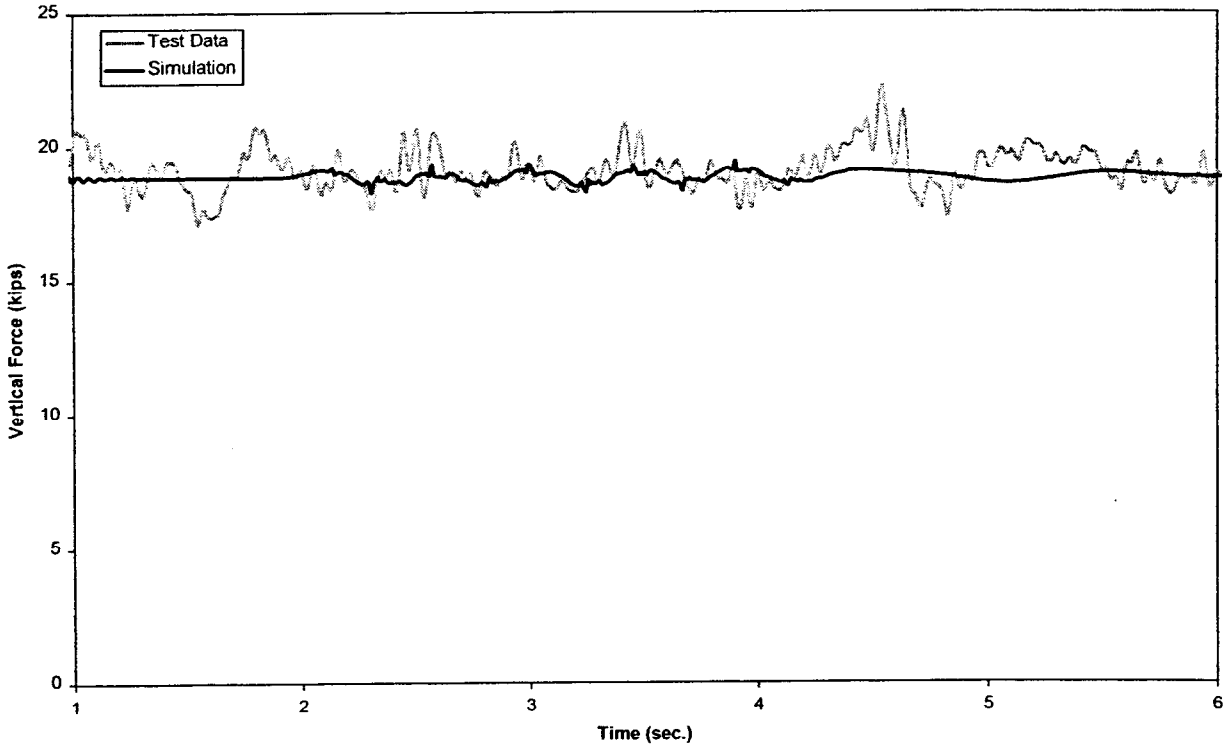

Figure B-24(b). Yaw and sway - vertical force time history, 60 mph (lead right wheel)

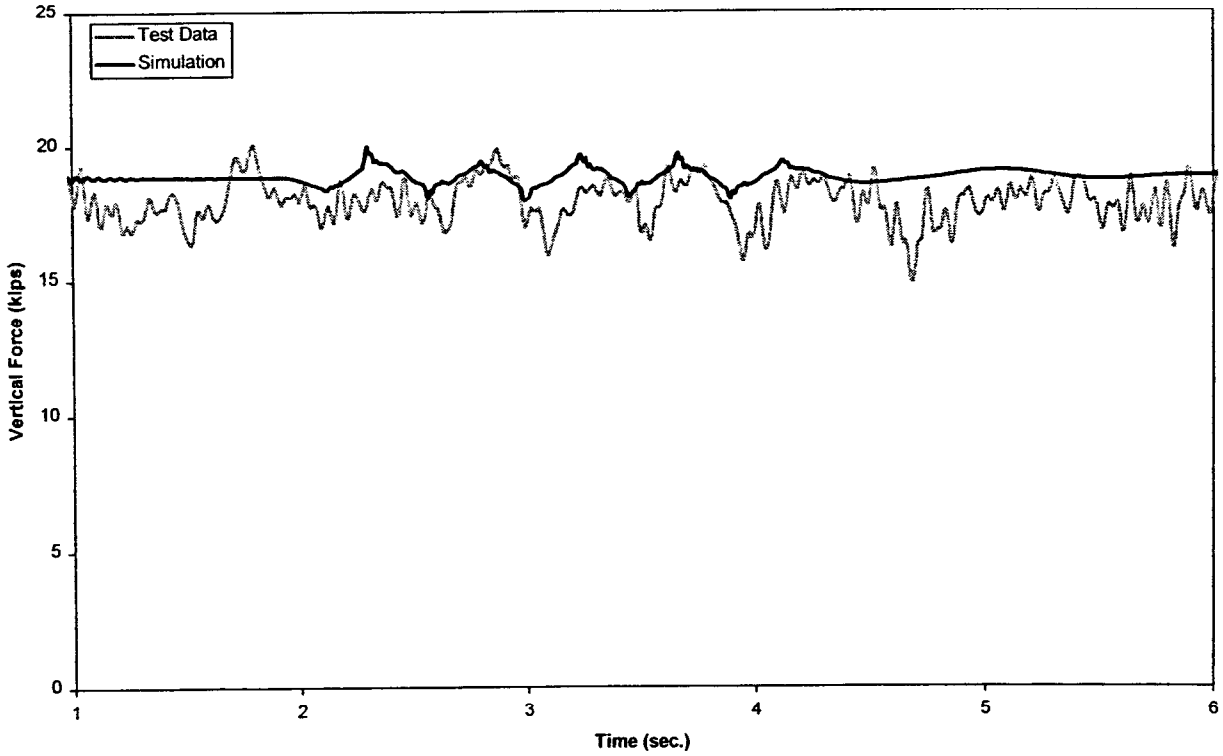

Figure B-24(c). Yaw and sway - vertical force time history, 60 mph (trailing left wheel)

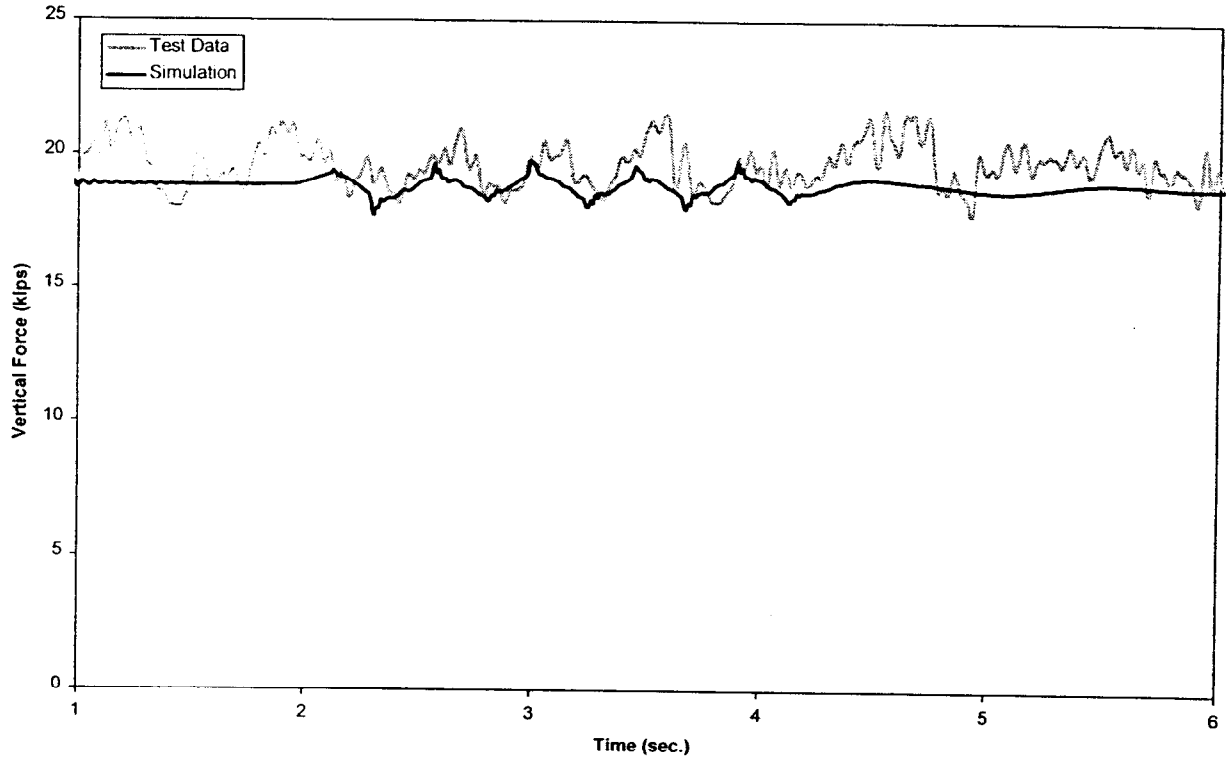

Figure B-24(d). Yaw and sway - vertical force time history, 60 mph (trailing right wheel)

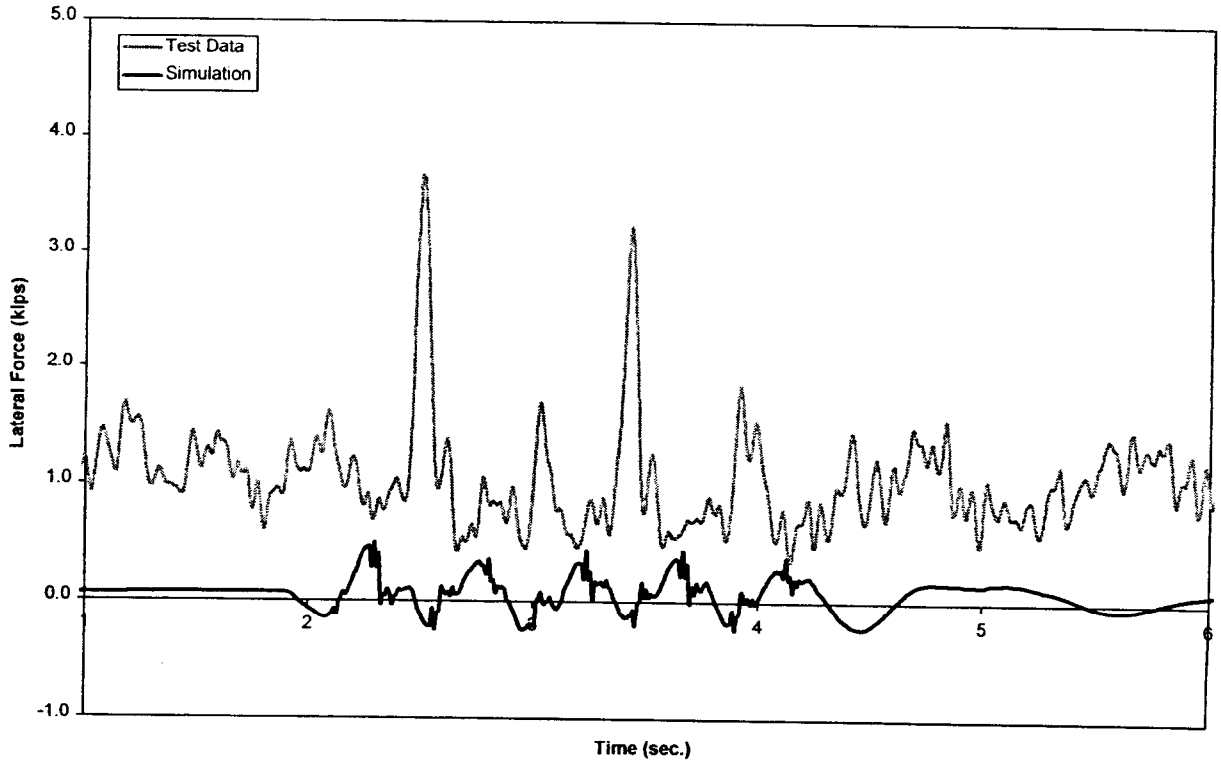

Figure B-25(a). Yaw and sway - lateral force time history, 60 mph (lead left wheel)

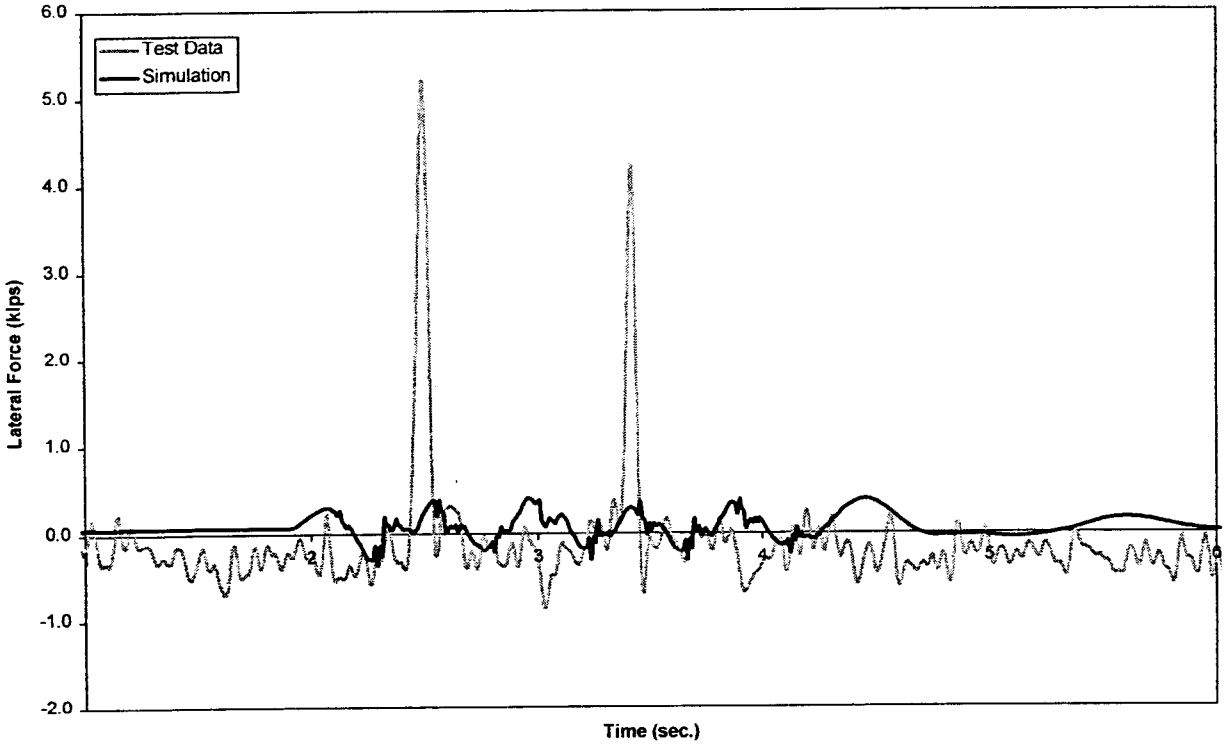

Figure B-25(b). Yaw and sway - lateral force time history, 60 mph (lead right wheel)

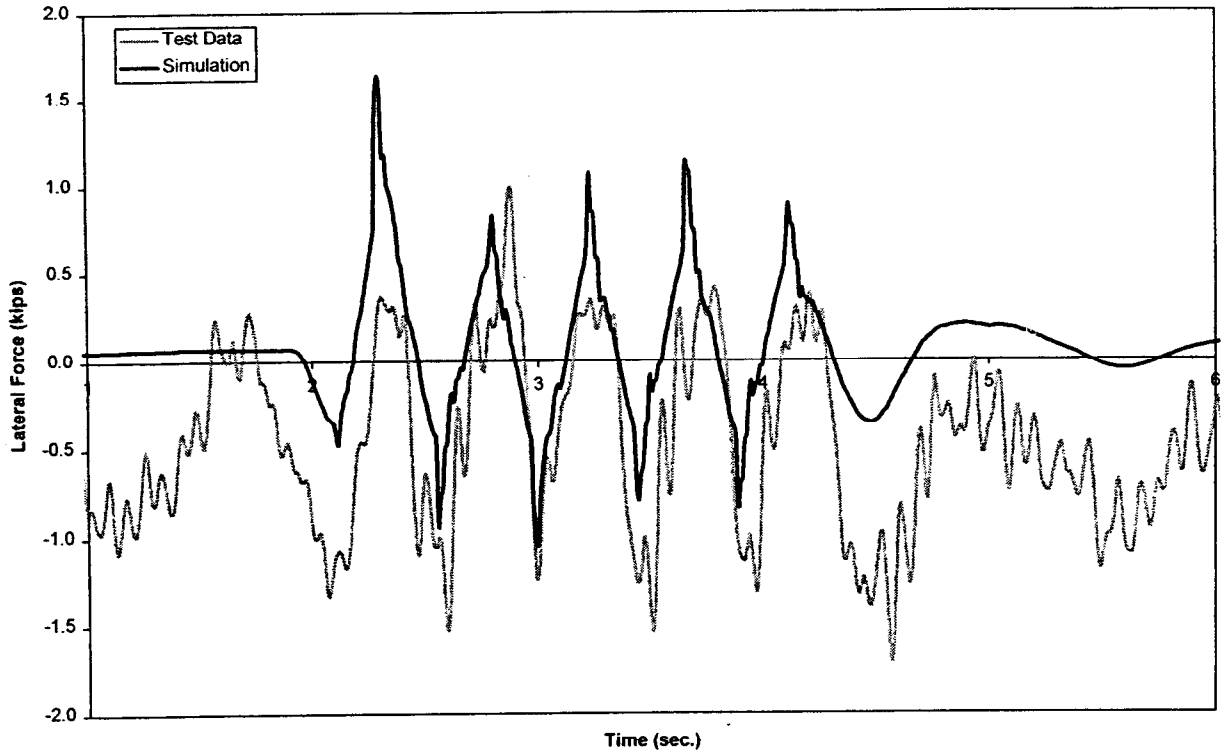

Figure B-25(c). Yaw and sway - lateral force time history, 60 mph (trailing left wheel)

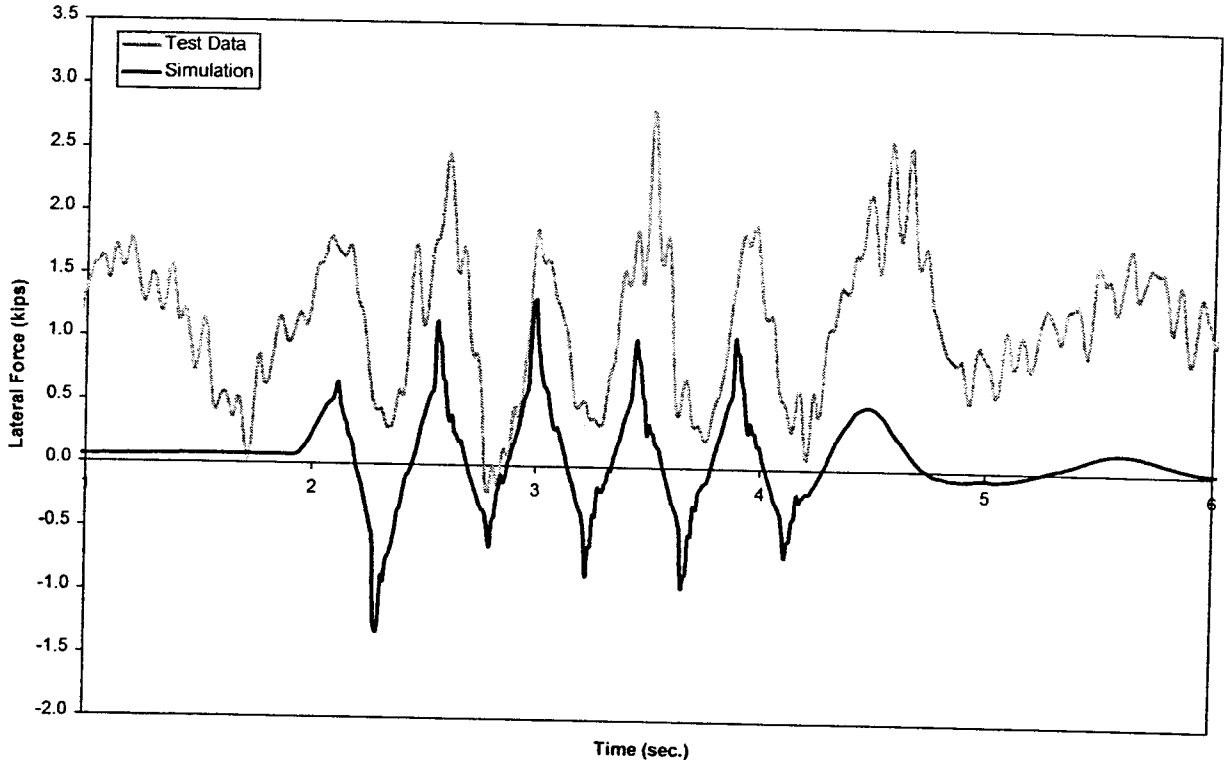

Figure B-25(d). Yaw and sway - lateral force time history, 60 mph (trailing right wheel)

The minimum vertical force over the speed range of 15 to 90 mph occurring during a test run is plotted in Figure B-26 for the left front axle wheel. The maximum lateral force and maximum lateral carbody acceleration at the B end are plotted respectively in Figures B-27 and B-28. The lateral maximum wheel force and carbody acceleration data exceed the simulation data significantly if the "spikes" in the test data due to the joints are included. The resonant condition is not obvious from the test data possibly due to large damping in the system.

B.5 Twist and Roll

Comparisons of the test data for all four wheels of the trailing truck vertical and lateral forces are summarized in Figures B-29 and B-30 for 19.2 mph and Figures B-31 and B-32 for 60 mph tests. The comparisons illustrate good agreement in vertical force waveforms and amplitudes.

The vertical force amplitude at 19.2 mph of the four wheels varies between approximately 17 and 21 kips and shows good agreement between the test and simulation. The lateral force data for the lead axle vary between about –1.0 to +4 kips. The lateral force data for the trailing axle vary from –1 to +2 kips for the tests and ±0.5 kips in the simulation and are considered to be approaching values small enough to represent the test accuracy limits. The vertical force test and simulation data at 60 mph vary from approximately 15 to 22 kips and are in excellent agreement. The test and lateral force simulation data for the lead axle vary from approximately –0.5 to +5 kips. The lateral test and simulation force data for the trailing axle vary from –1.0 to +1.5 kips with the general levels in agreement.

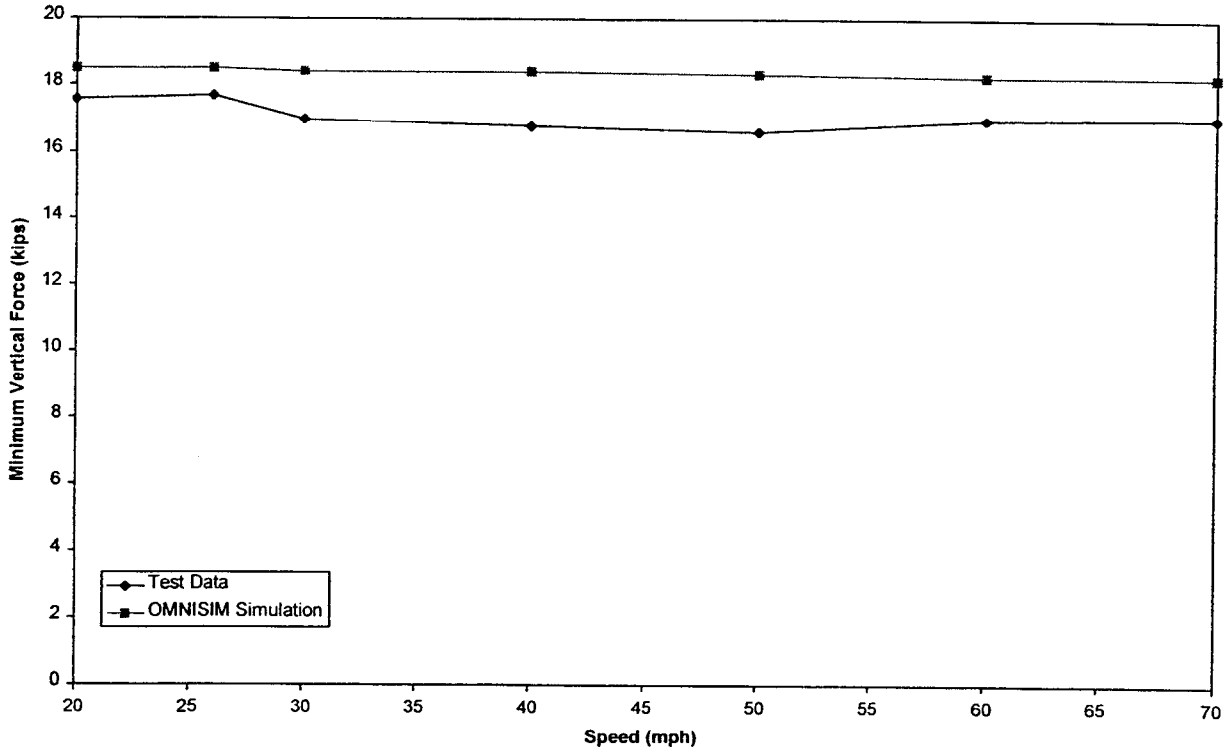

Figure B-26. Yaw and sway - minimum vertical force

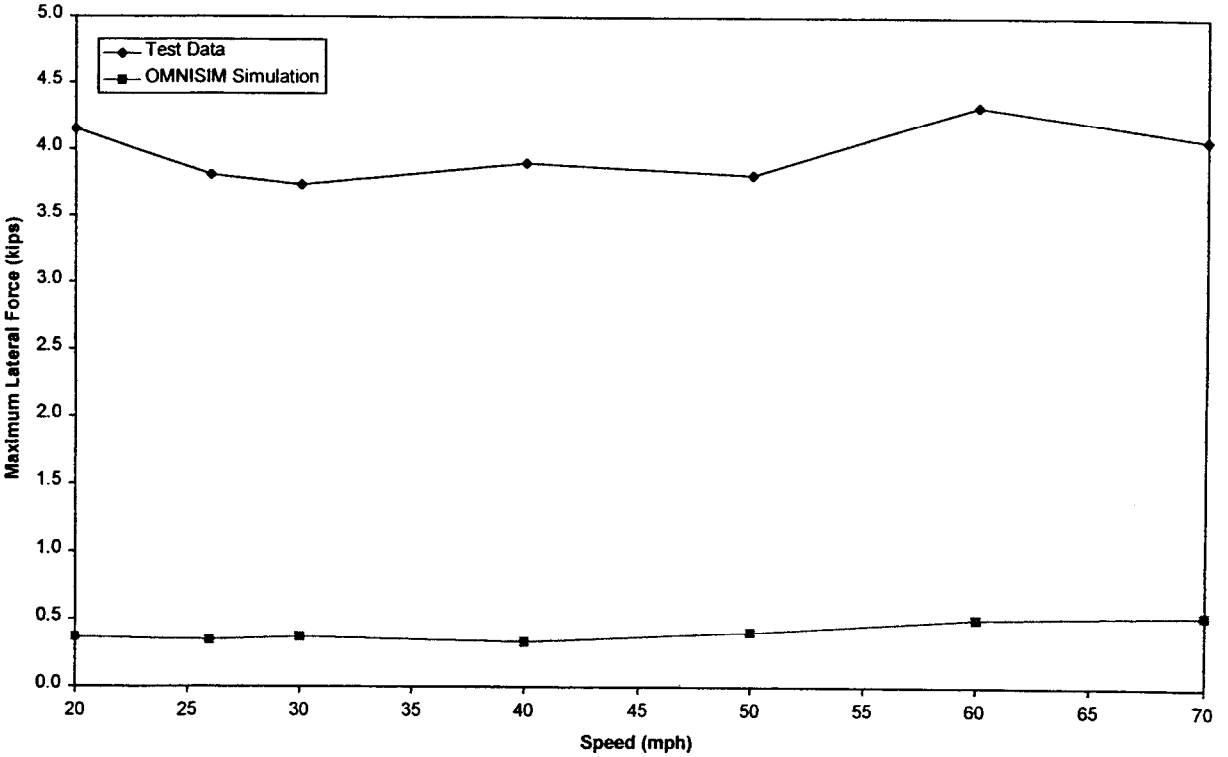

Figure B-27. Yaw and sway - maximum lateral force

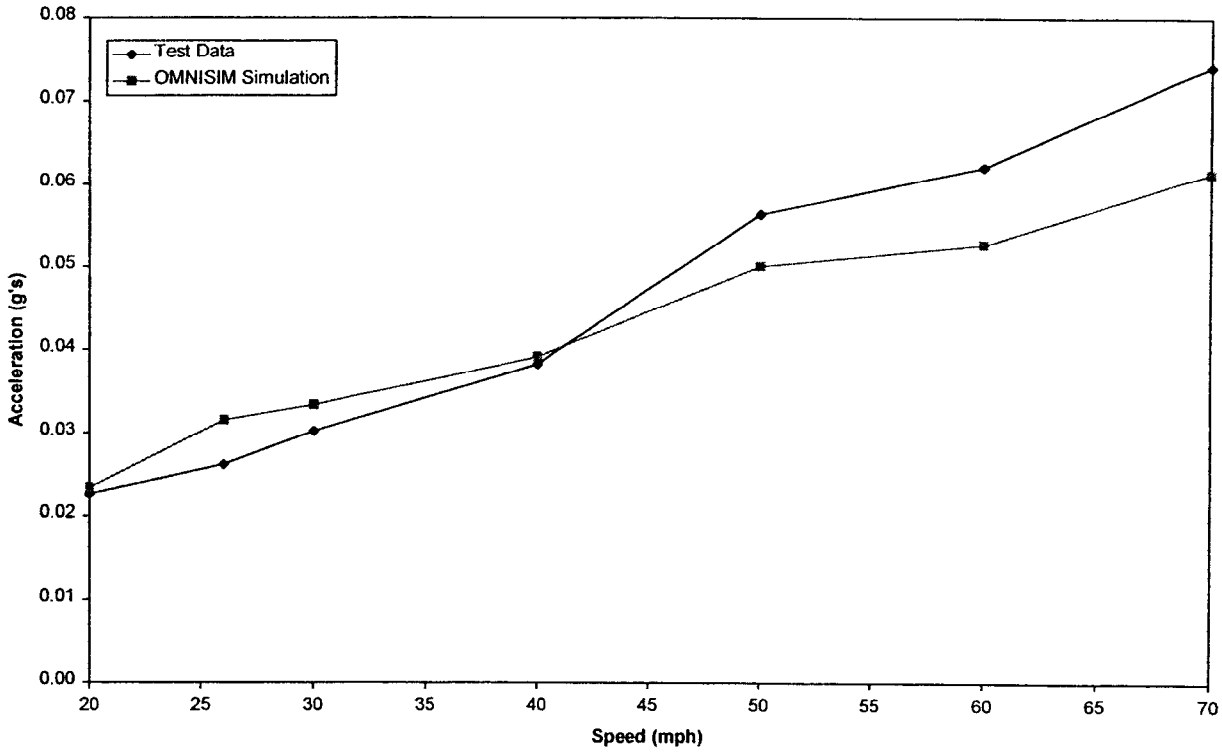

Figure B-28. Yaw and sway - maximum absolute lateral carbody acceleration

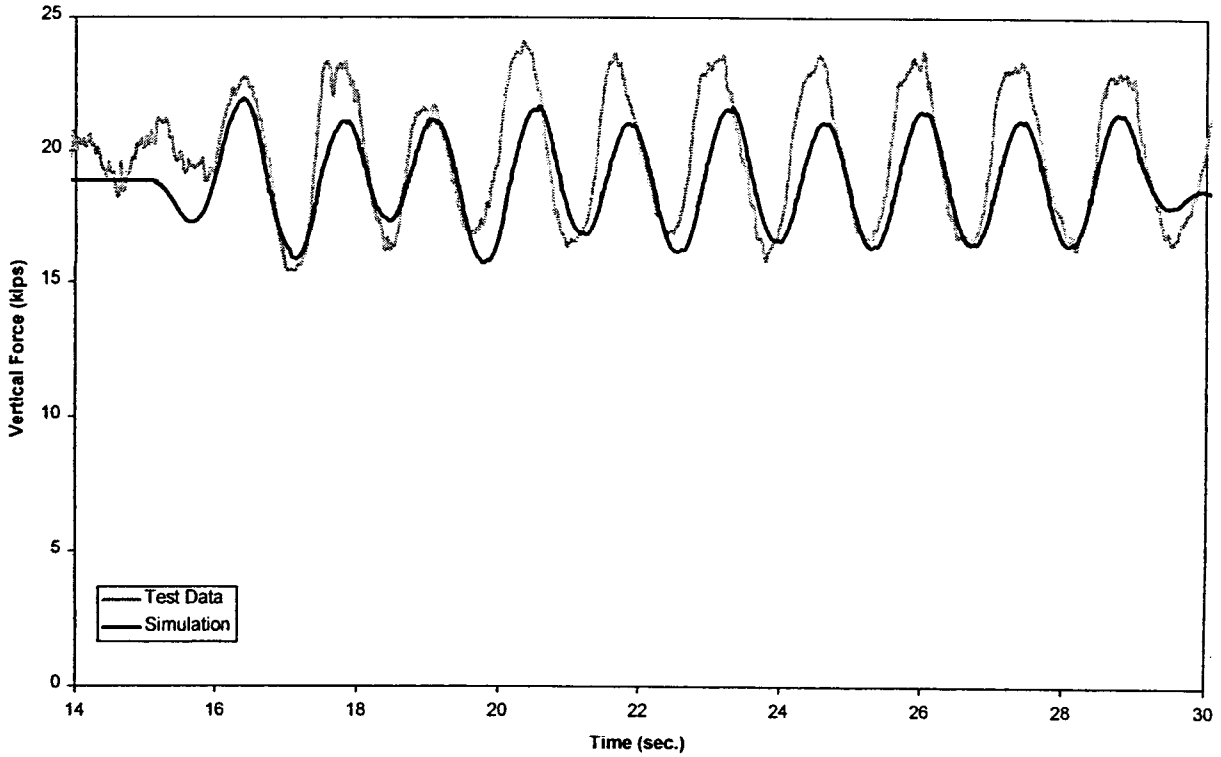

Figure B-29(a). Twist and roll - vertical force time history, 19.2 mph (lead left wheel)

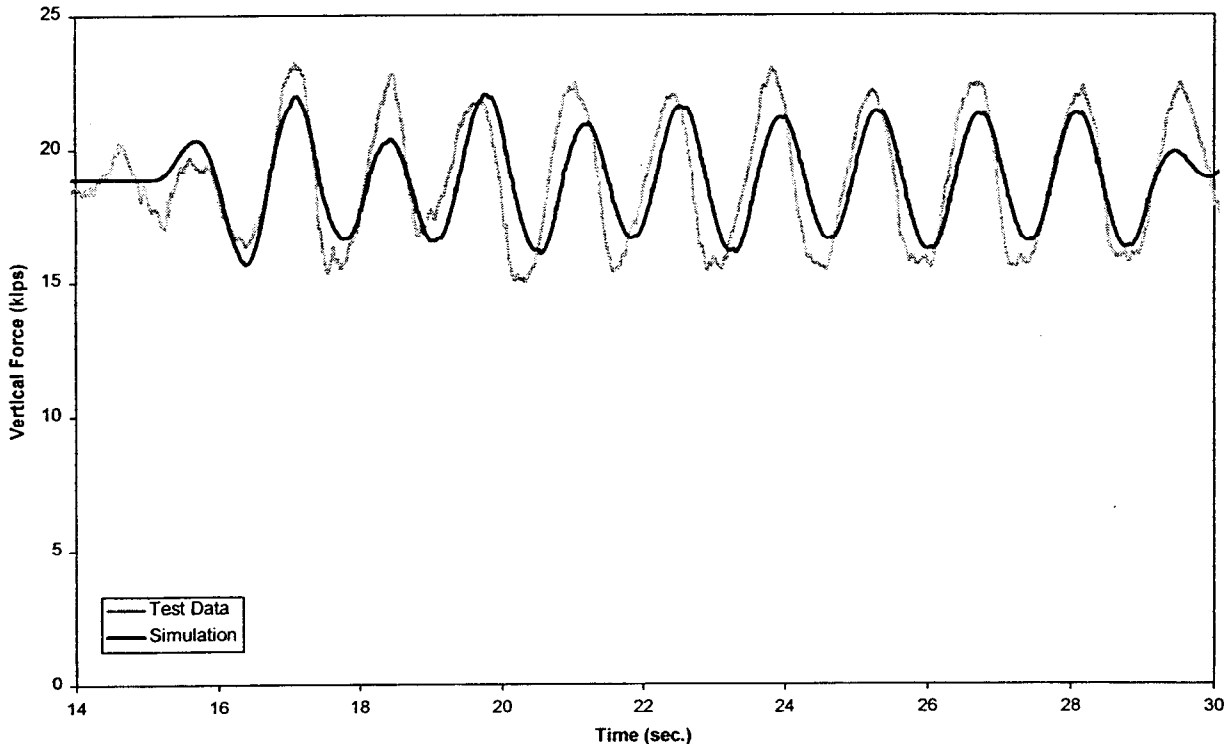

Figure B-29(b). Twist and roll - vertical force time history, 19.2 mph (lead right wheel)

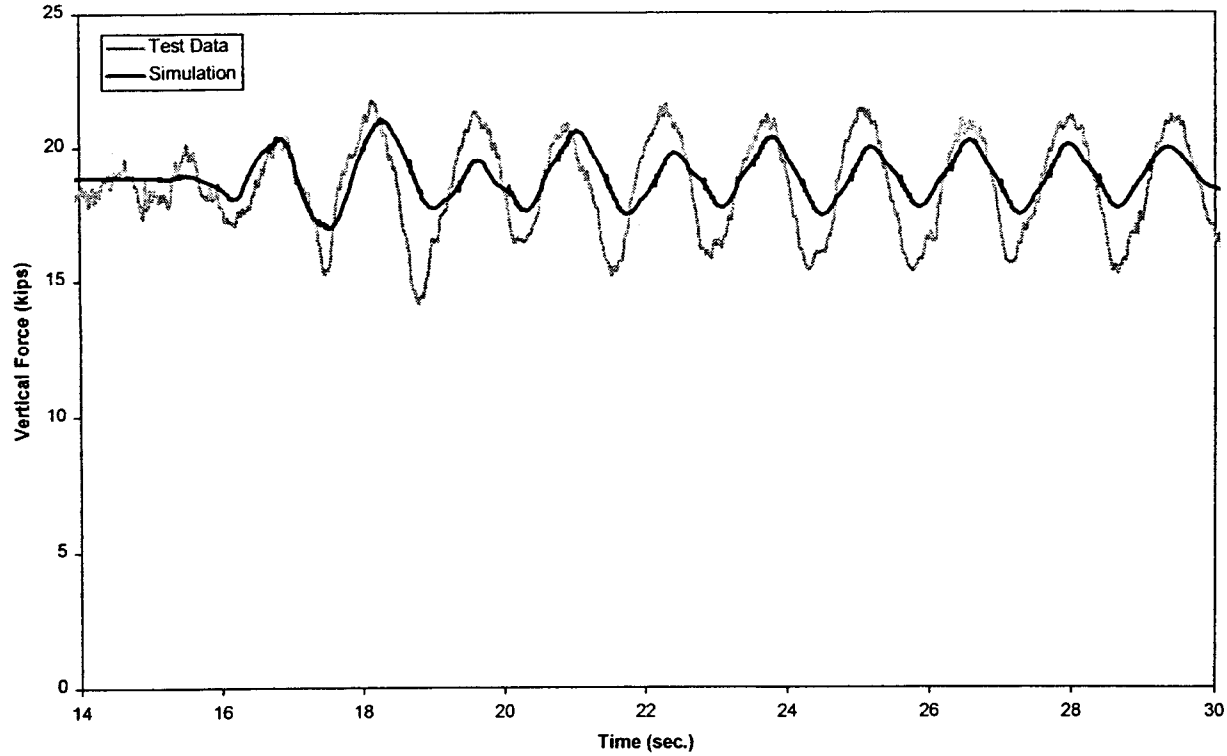

Figure B-29(c). Twist and roll - vertical force time history, 19.2 mph (trailing left wheel)

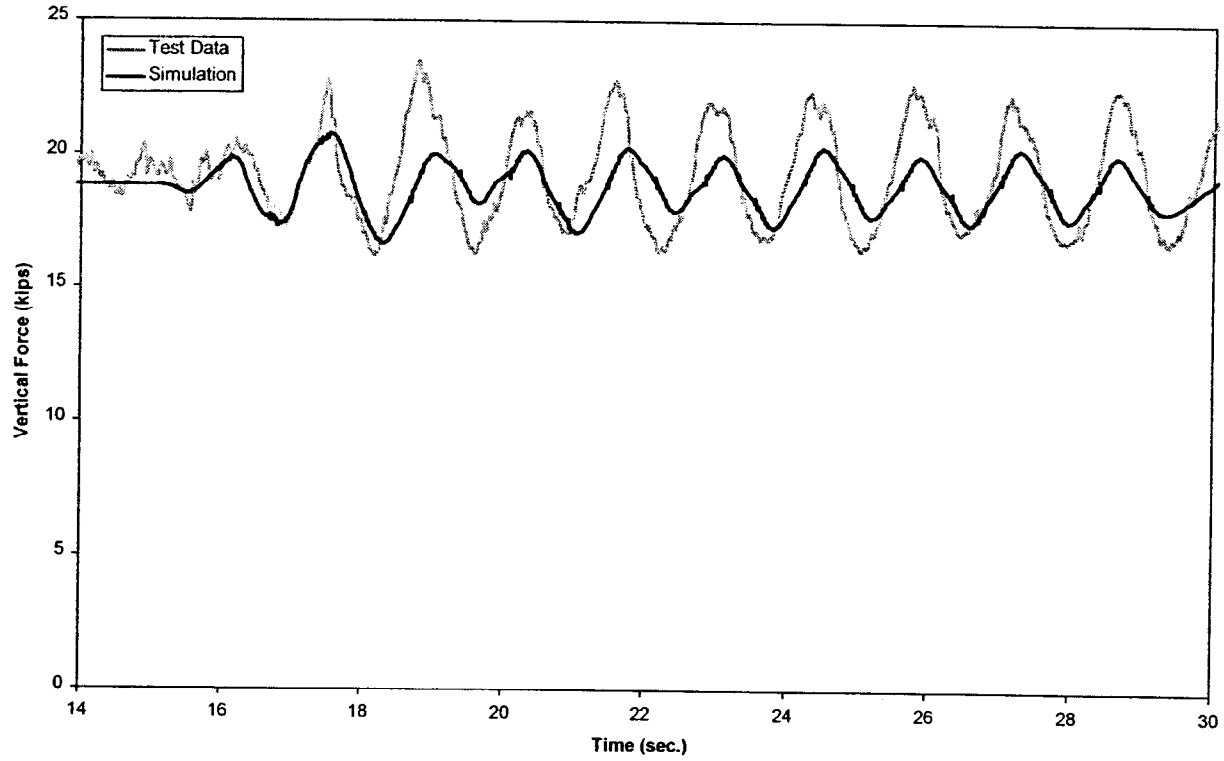

Figure B-29(d). Twist and roll - vertical force time history, 19.2 mph (trailing right wheel)

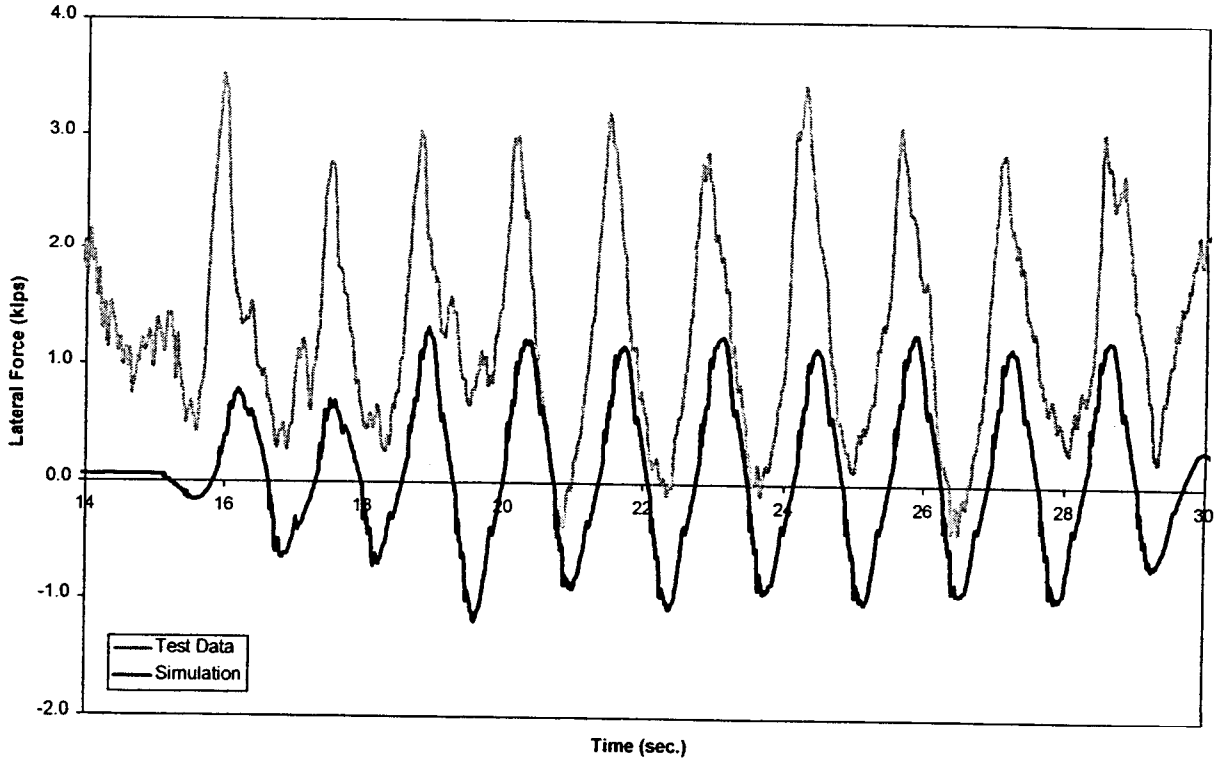

Figure B-30(a). Twist and roll - lateral force time history, 19.2 mph (lead left wheel)

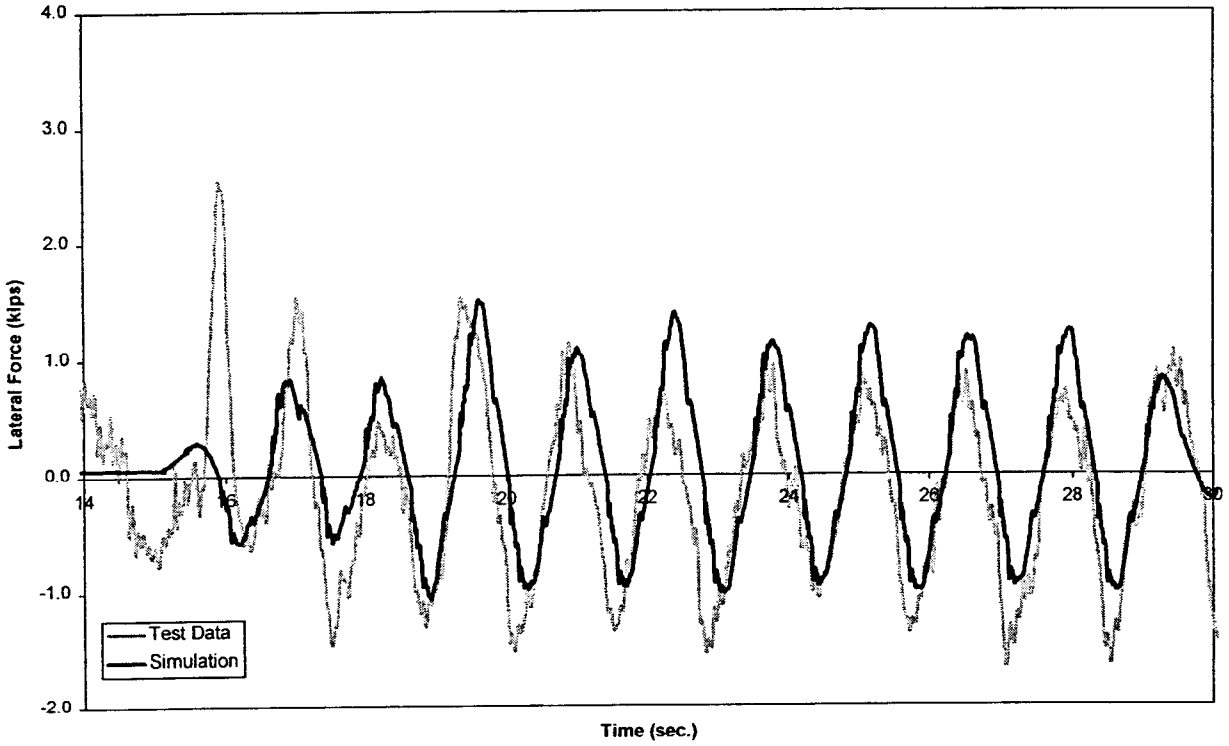

Figure B-30(b). Twist and roll - lateral force time history, 19.2 mph (lead right wheel)

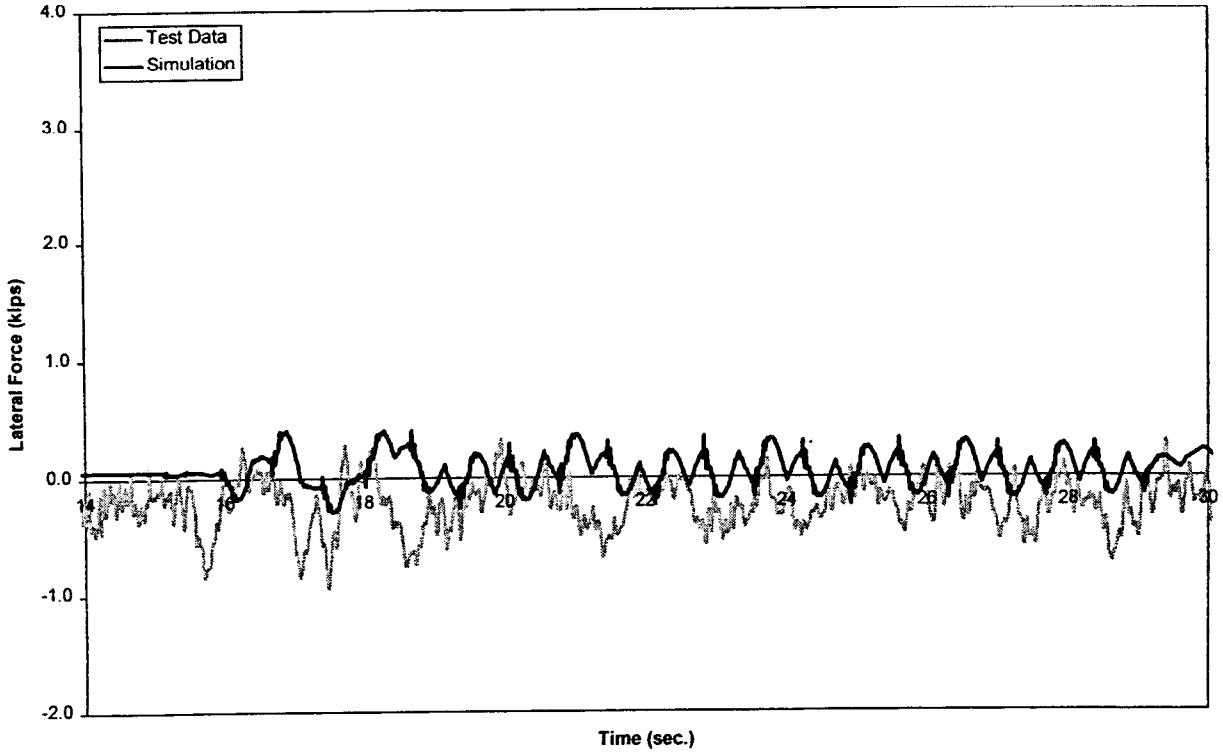

Figure B-30(c). Twist and roll - lateral force time history, 19.2 mph (trailing left wheel)

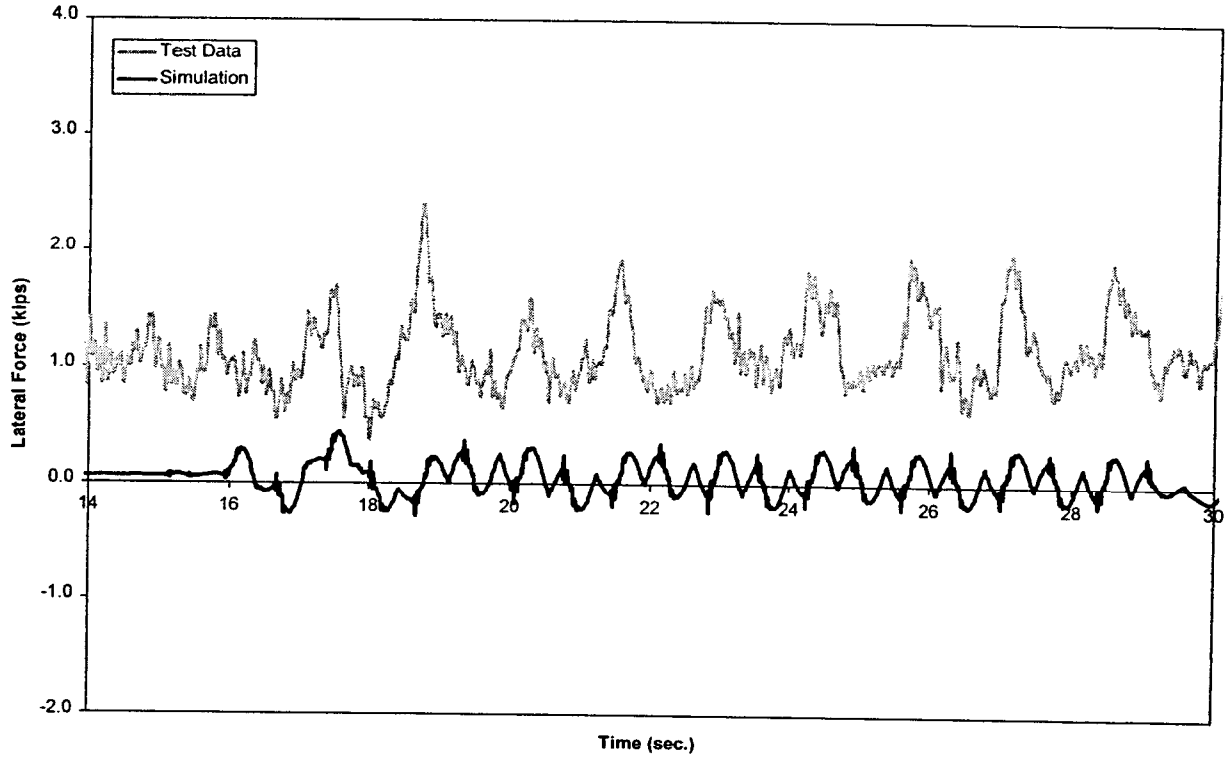

Figure B-30(d). Twist and roll - lateral force time history, 19.2 mph (trailing right wheel)

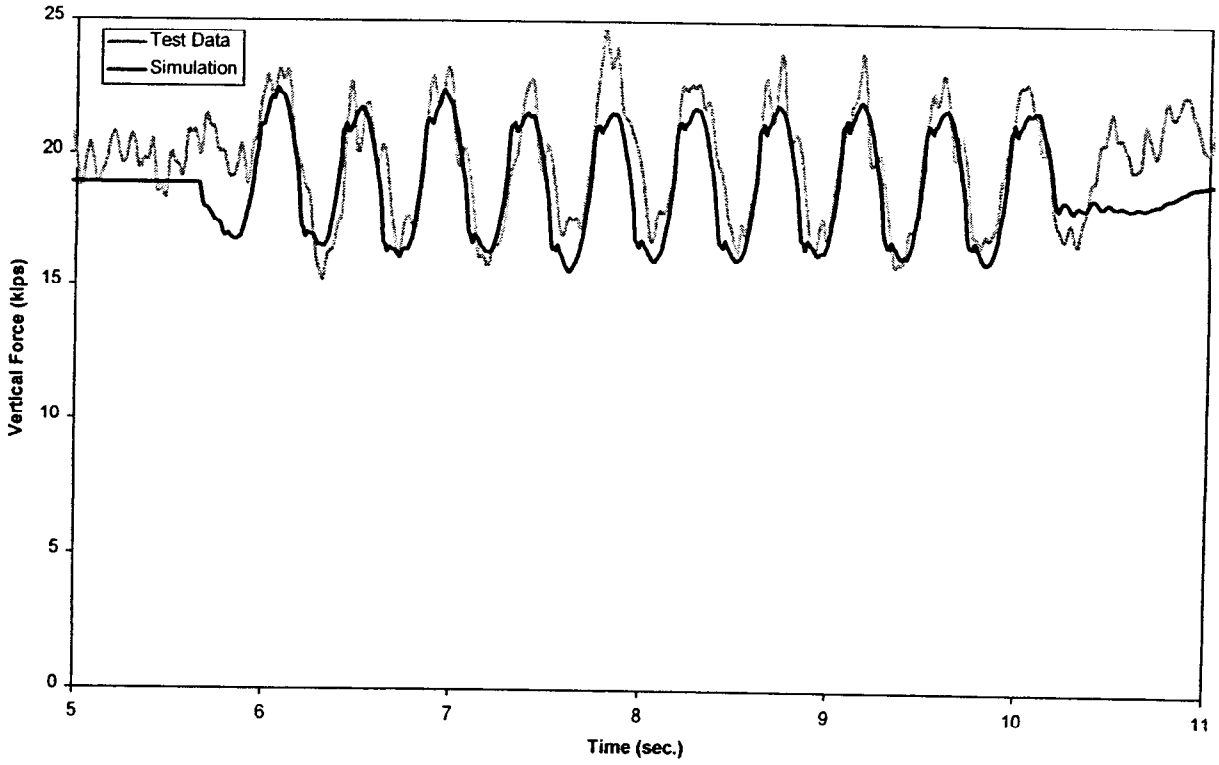

Figure B-31(a). Twist and roll - vertical force time history, 60 mph (lead left wheel)

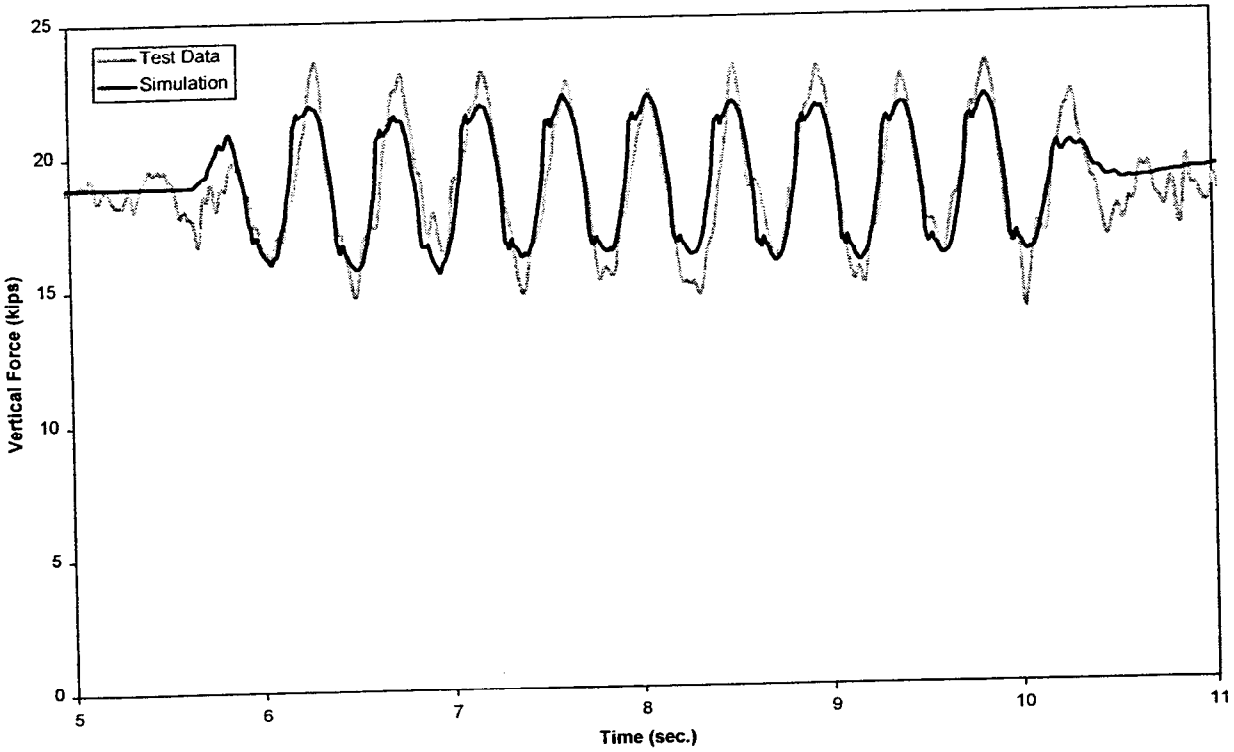

Figure B-31(b). Twist and roll - vertical force time history, 60 mph (lead right wheel)

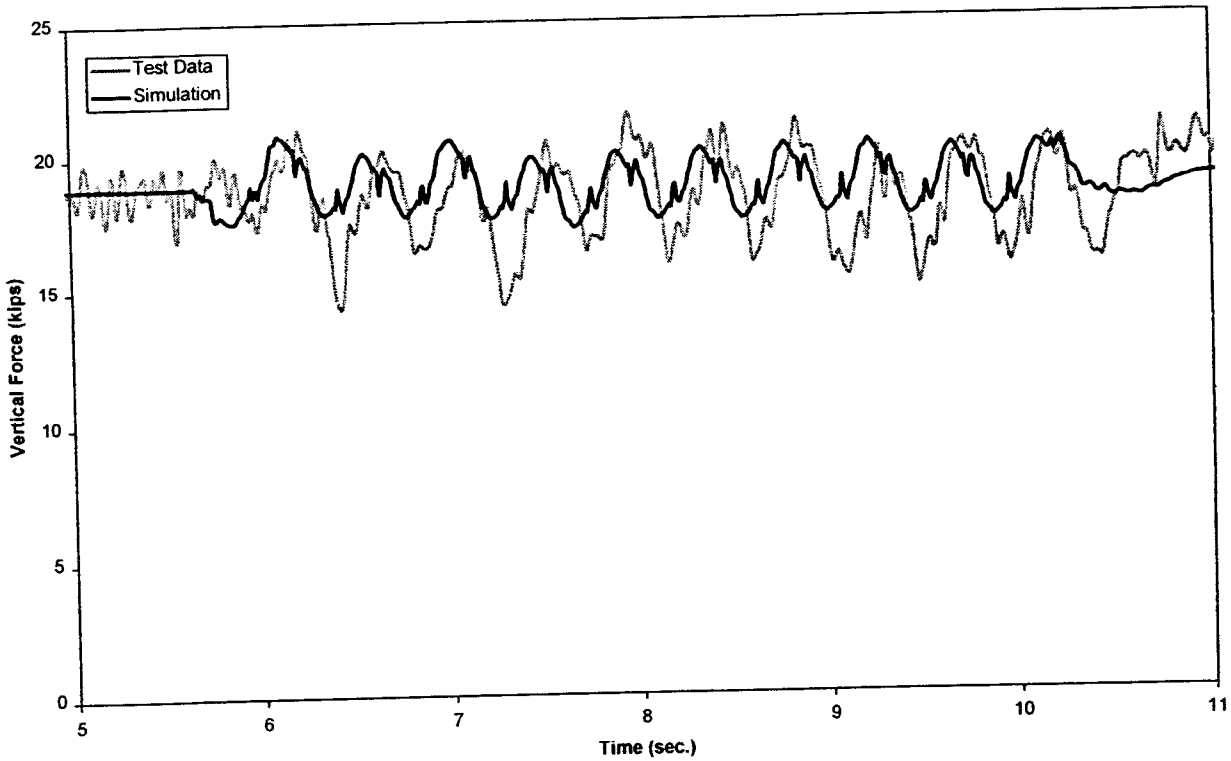

Figure B-31(c). Twist and roll - vertical force time history, 60 mph (trailing left wheel)

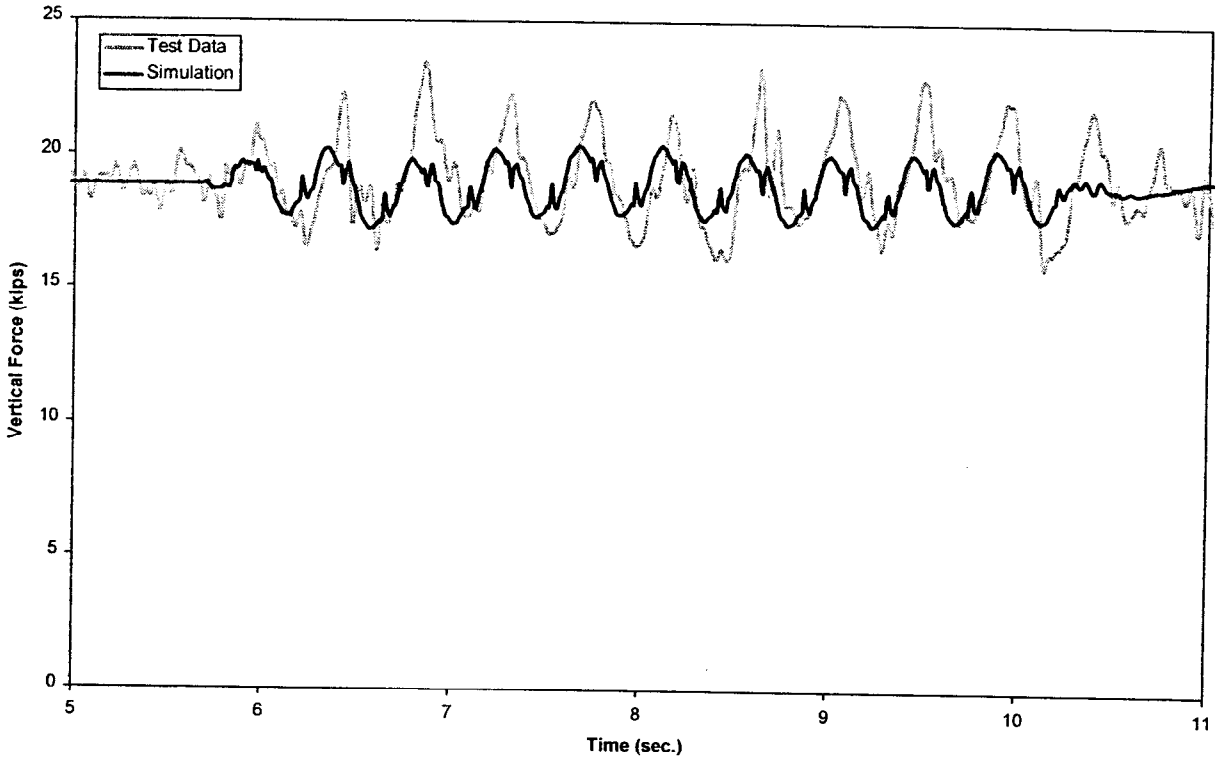

Figure B-31(d). Twist and roll - vertical force time history, 60 mph (trailing right wheel)

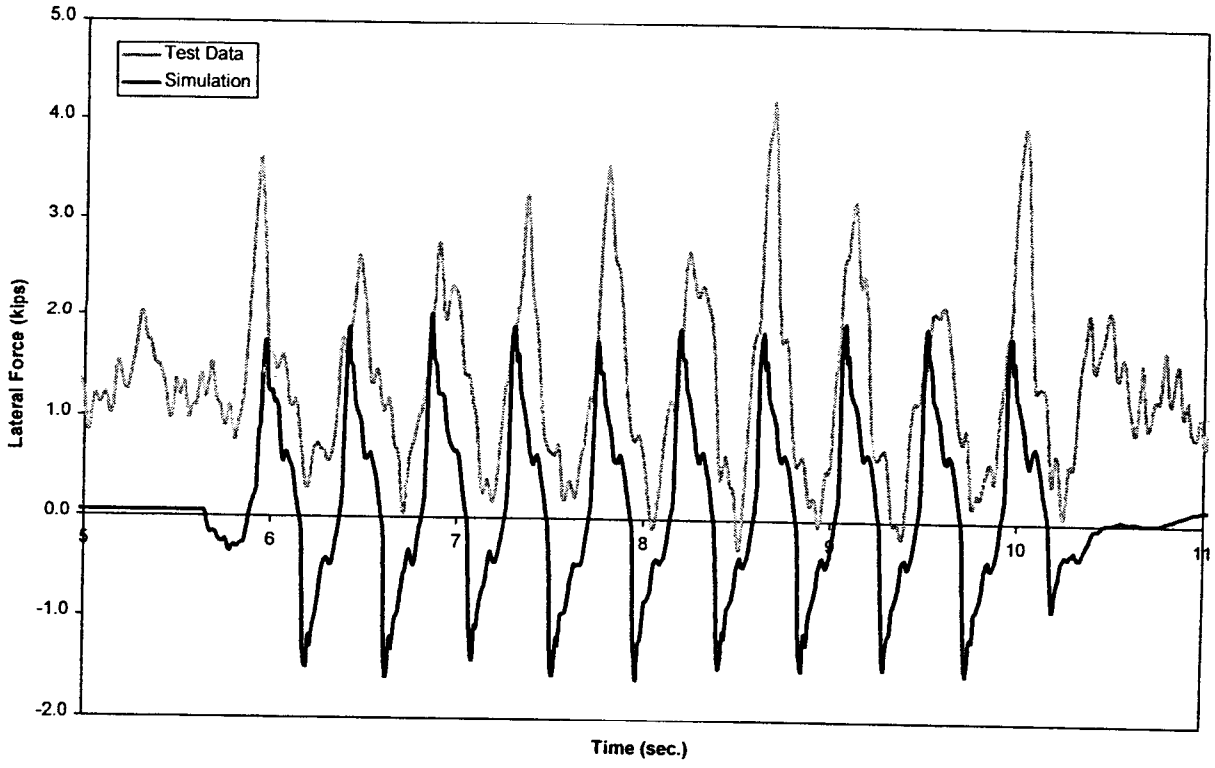

Figure B-32(a). Twist and roll - lateral force time history, 60 mph (lead left wheel)

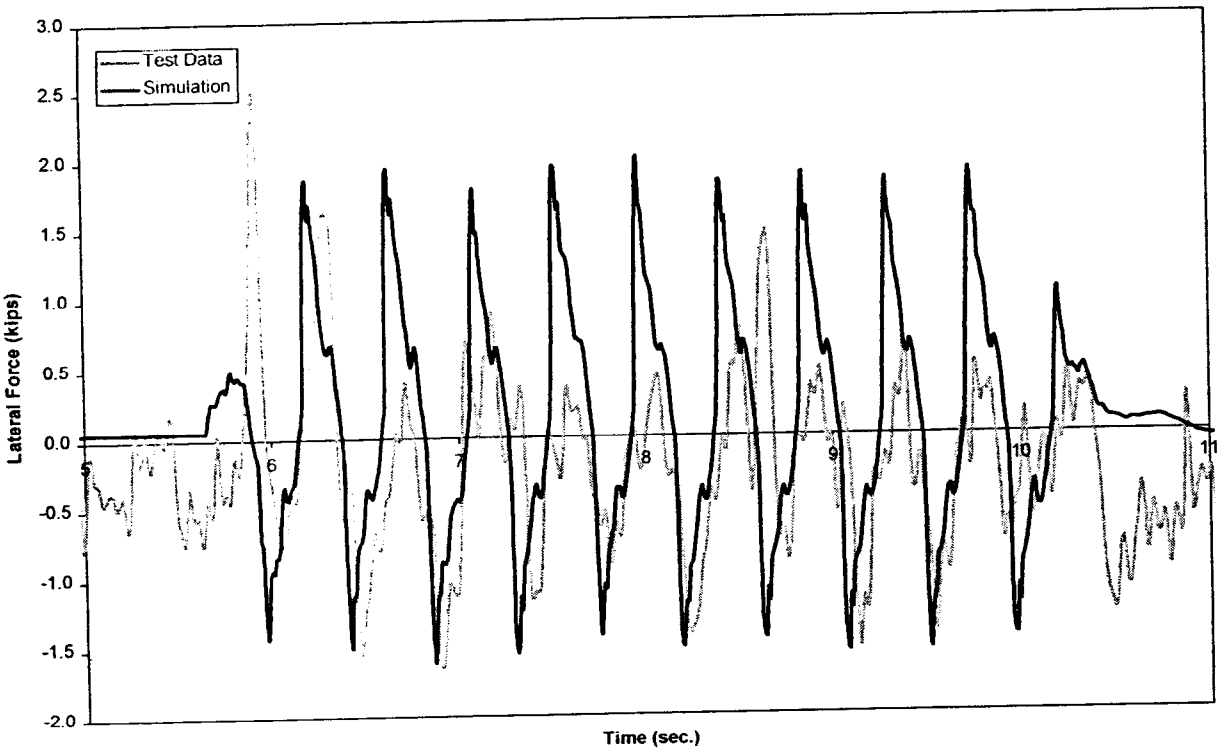

Figure B-32(b). Twist and roll - lateral force time history, 60 mph (lead right wheel)

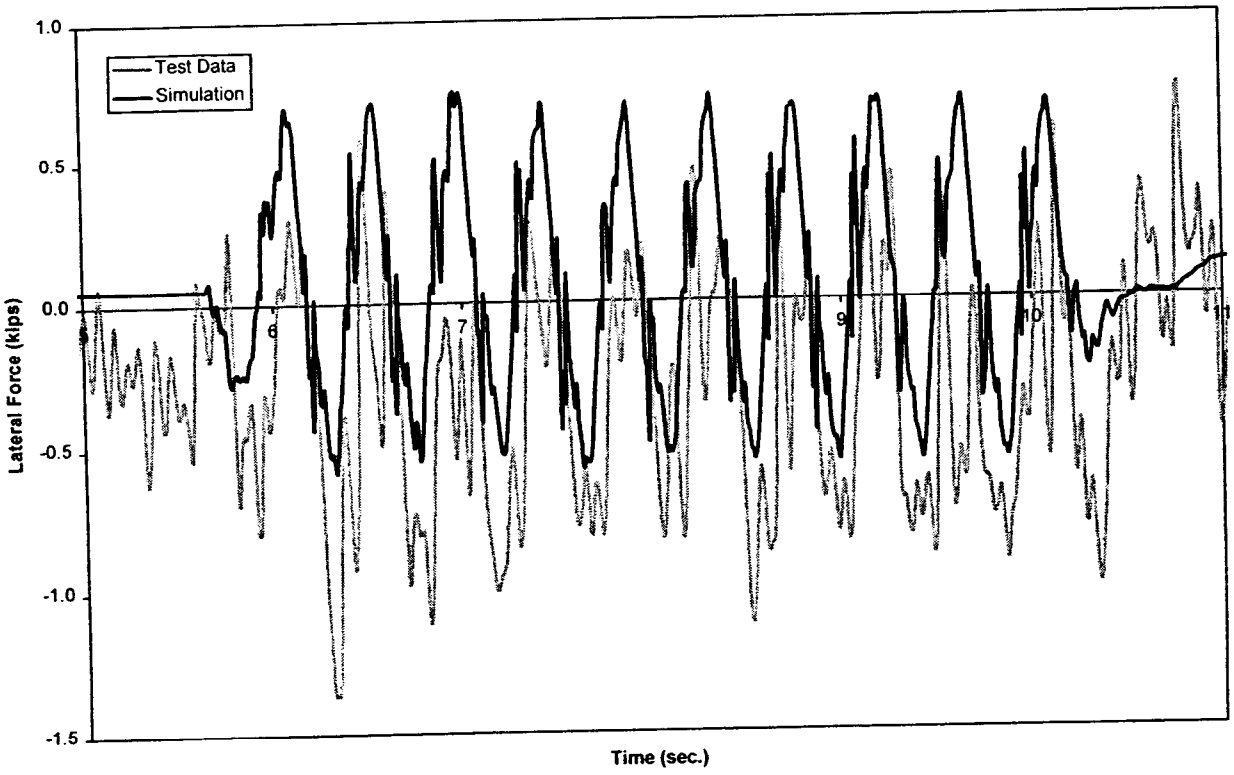

Figure B-32(c). Twist and roll - lateral force time history, 60 mph (trailing left wheel)

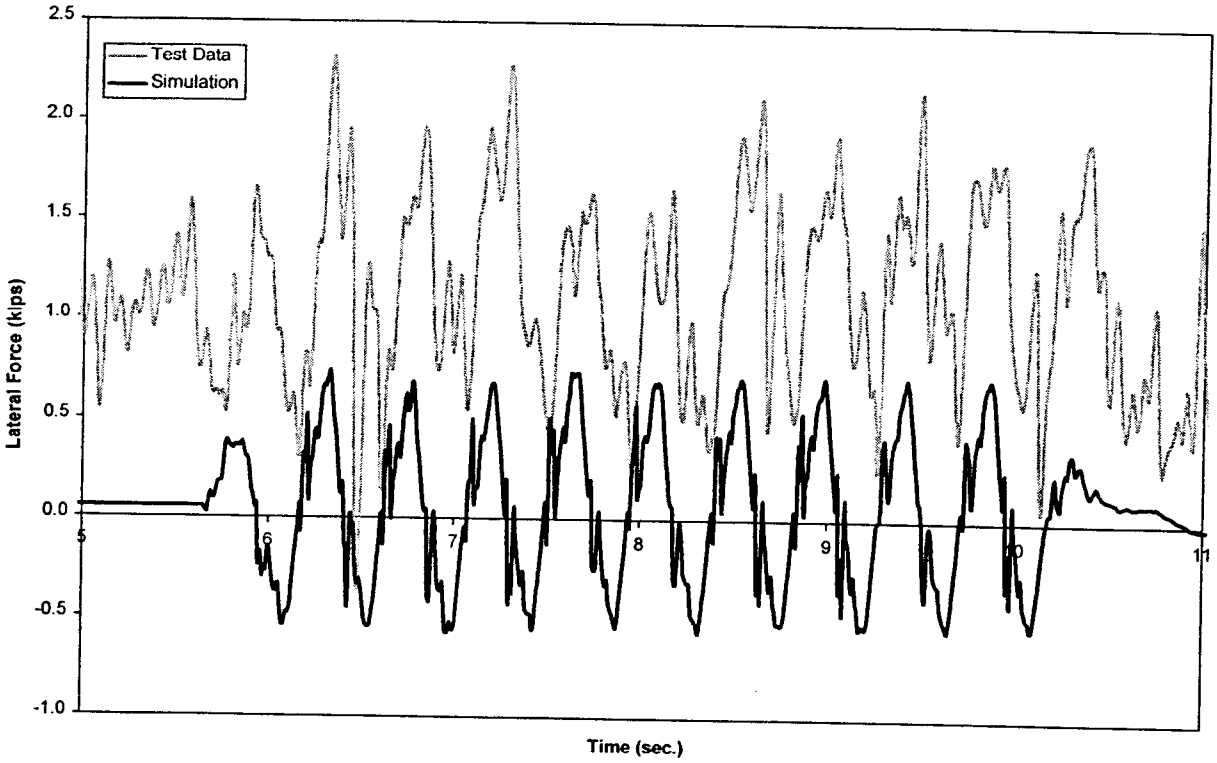

Figure B-32(d). Twist and roll - lateral force time history, 60 mph (trailing right wheel)

Plots of the test and simulation of minimum vertical force and maximum lateral force are shown in Figures B-33 and B-34 for the lead axle left wheel of the trailing truck. Good correlation is seen for the vertical force in the speed range while the lateral force test data is approximately 3 times greater than the simulation. The maximum absolute lateral carbody acceleration at the "B" end is shown in Figure B-35. The simulation underestimates the values by 0.04g, though the general trend of the car body acceleration with speed is well predicted by the simulation.

B.6 Pitch and Bounce

Figure B-36 illustrates the case of a pitch and bounce correlation of the vertical force for the four wheels of the trailing truck at a speed of 30 mph. Good correlation is seen between the test data and simulation results. The small fluctuations in the test data are attributed to the inherent variations in the rail vertical profile data, not modeled in the simulation. The lateral force levels are too small to be of any practical significance and are not shown. Similar results were obtained for other speeds.

Figure B-37 shows the vertical forces for the four wheels for a pitch and bounce test conducted at 60 mph. The correlation for the vertical force levels is good for all wheels.

A plot of the correlation of test and simulation data of minimum vertical force is shown in Figure B-38 for the left wheel on the lead axle of the trailing truck. Good correlation is shown through the speed range for the vertical force. The minimum vertical force is about 31 mph in both the test data and simulation. This occurs at the resonance speeds. The resonant condition is not noticeably strong.

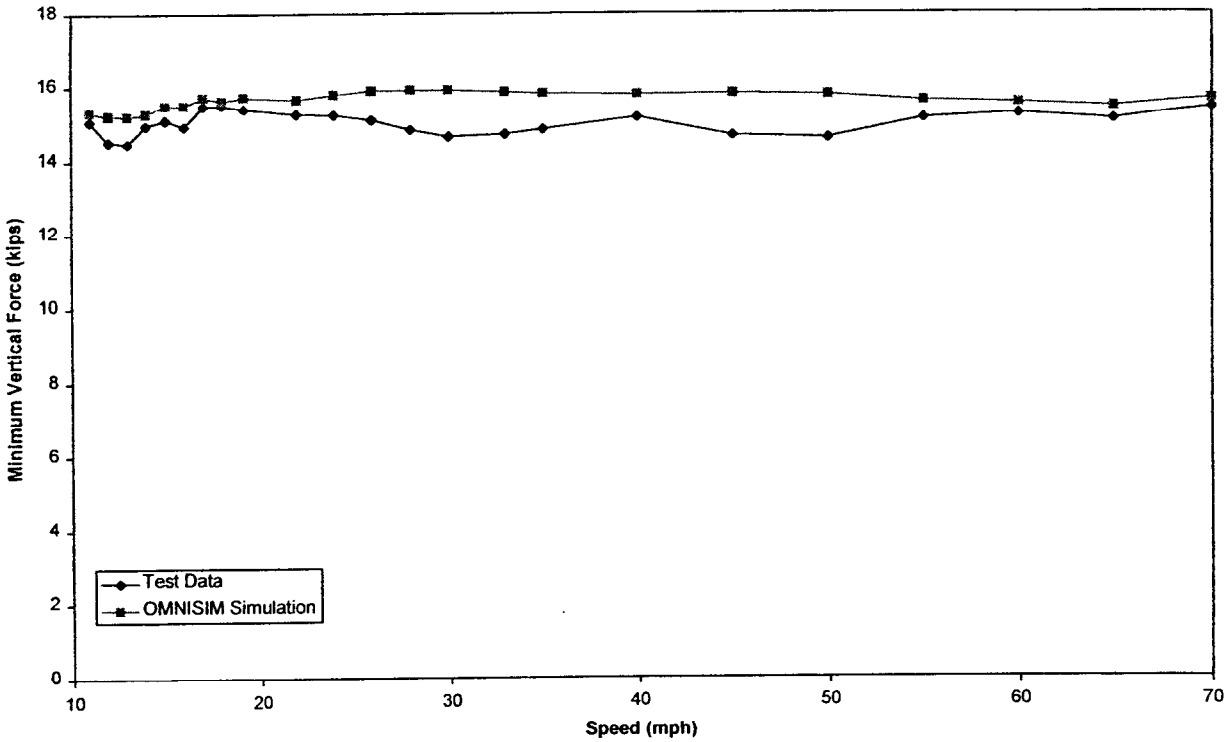

Figure B-33. Twist and roll - minimum vertical force

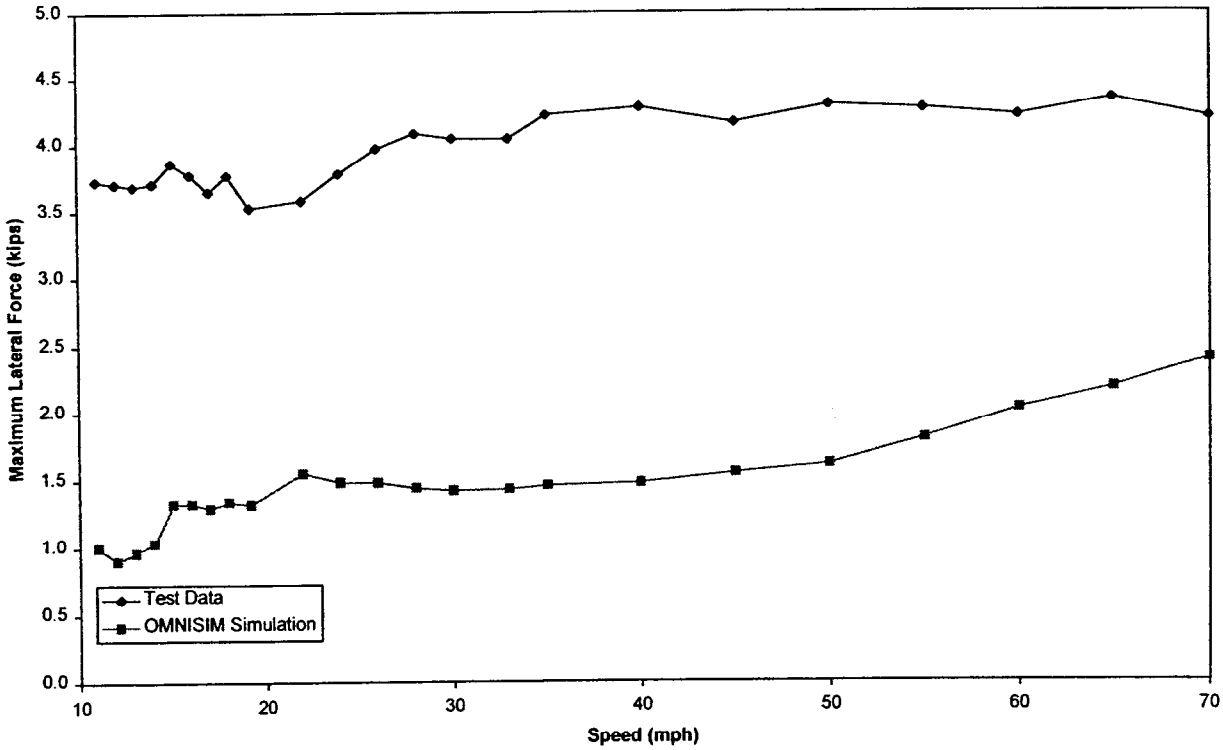

Figure B-34. Twist and roll - maximum lateral force

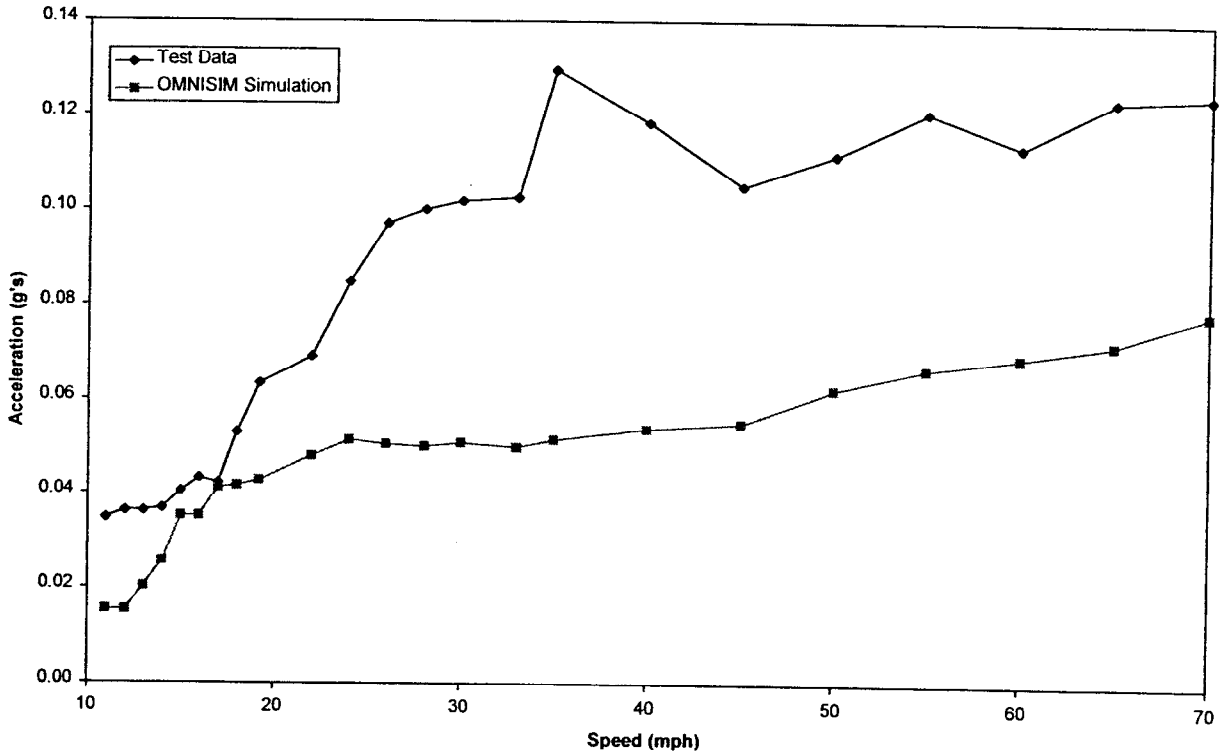

Figure B-35. Twist and roll - maximum absolute lateral carbody acceleration

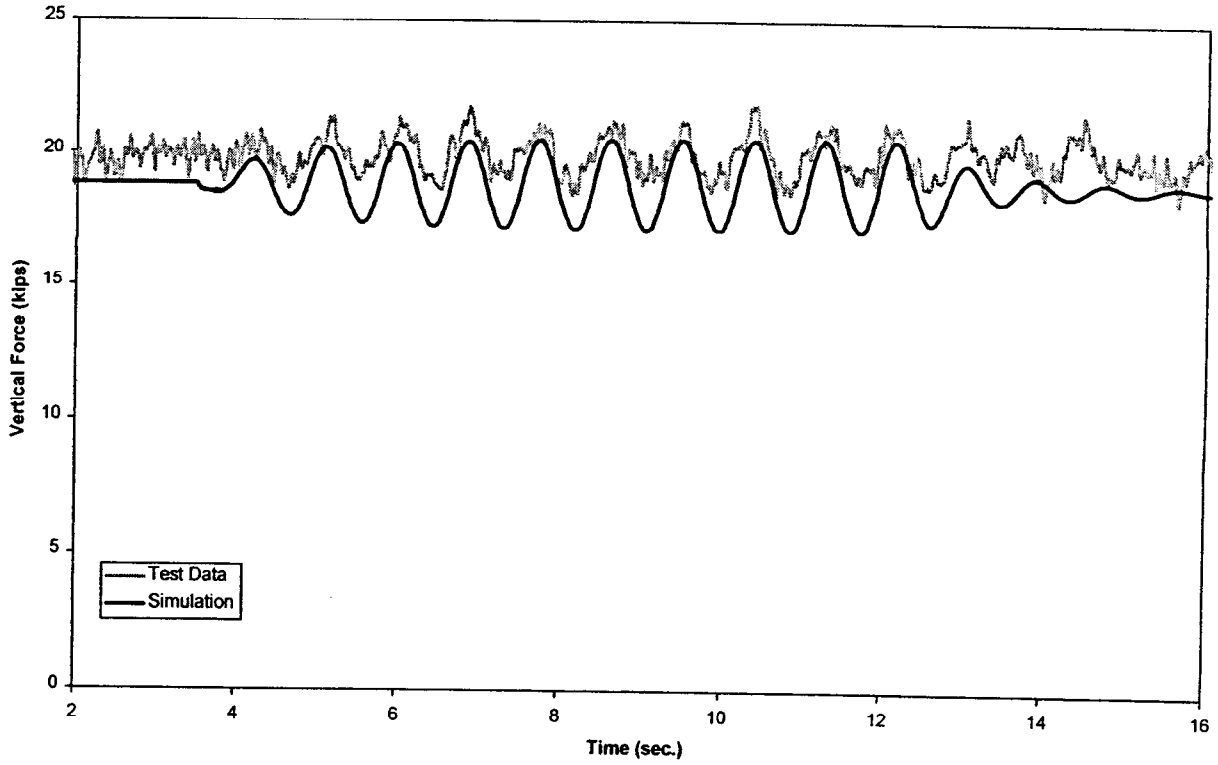

Figure B-36(a).Pitch and bounce - vertical force time history, 30 mph (lead left wheel)

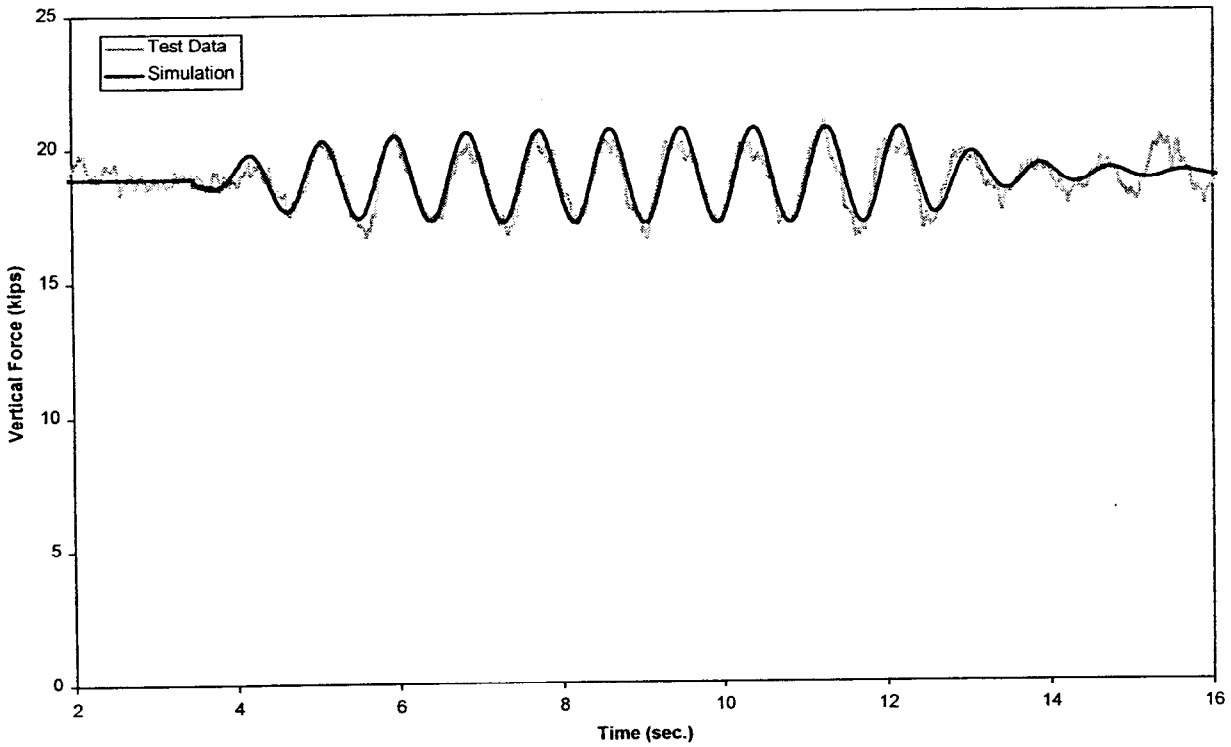

Figure B-36(b). Pitch and bounce - vertical force time history, 30 mph (lead right wheel)

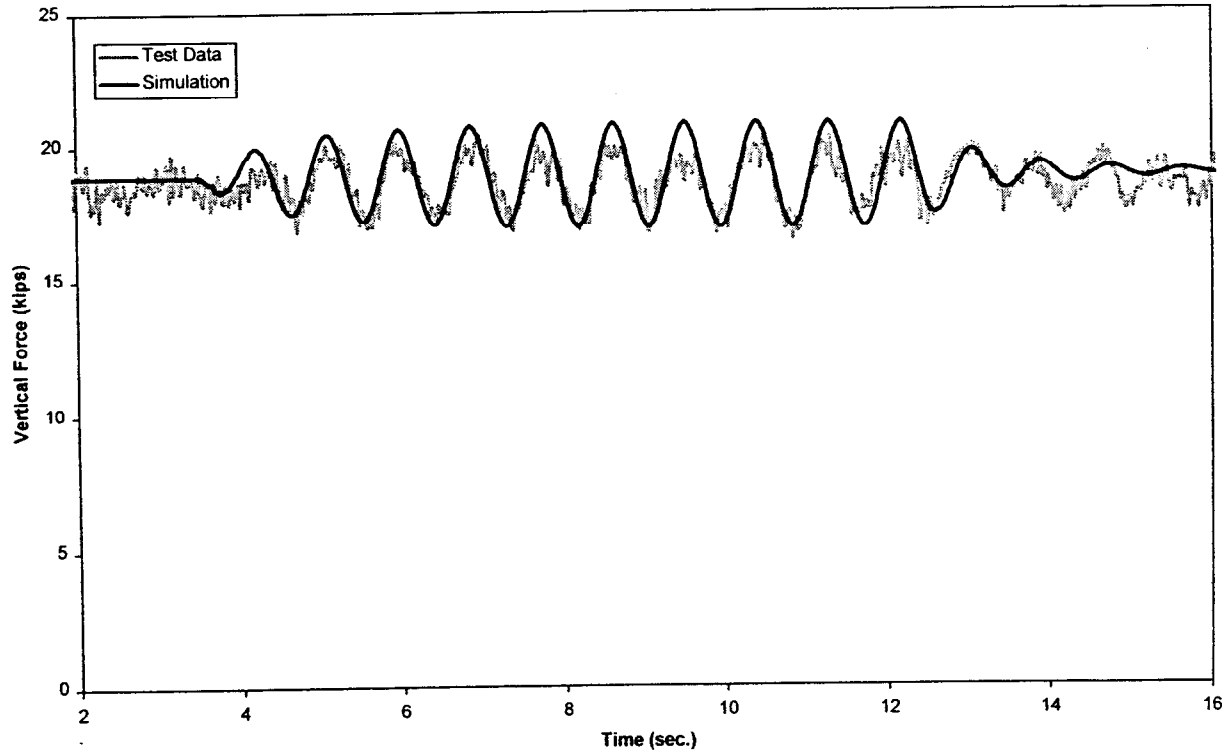

Figure B-36(c). Pitch and bounce - vertical force time history, 30 mph (trailing left wheel)

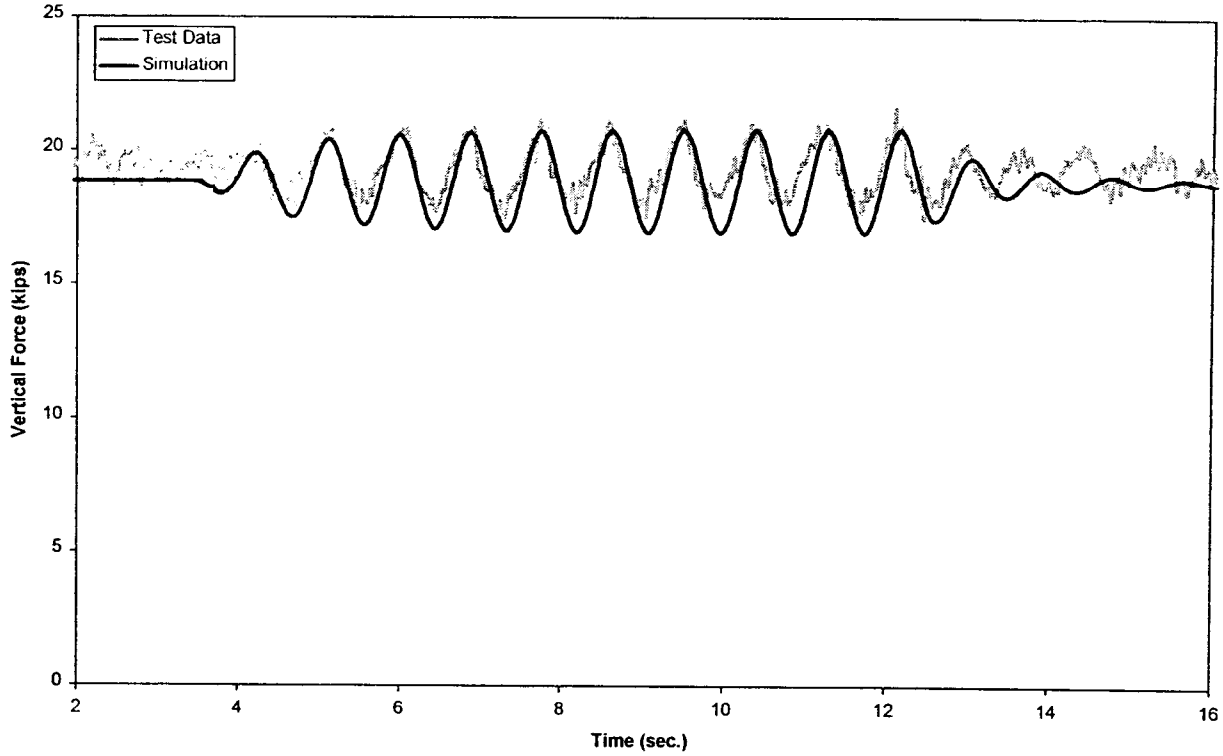

Figure B-36(d). Pitch and bounce - vertical force time history, 30 mph (trailing right wheel)

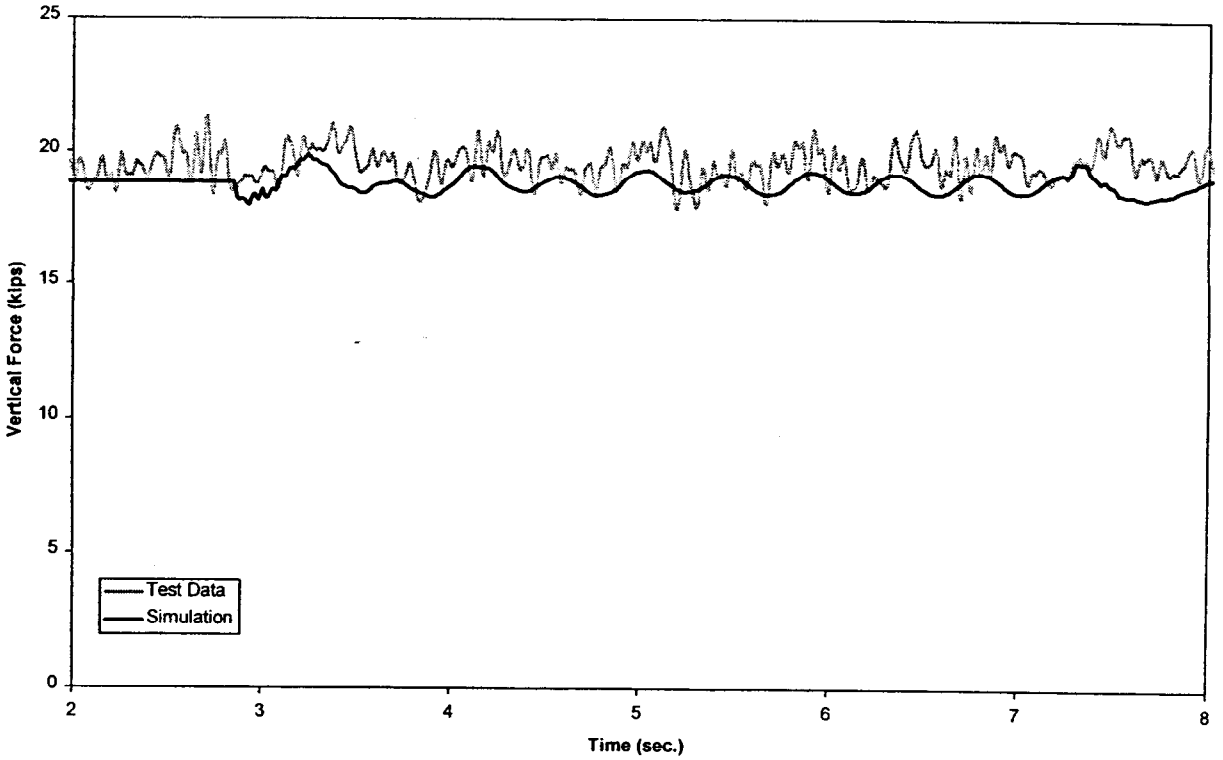

Figure B-37(a). Pitch and bounce - vertical force time history, 60 mph (lead left wheel)

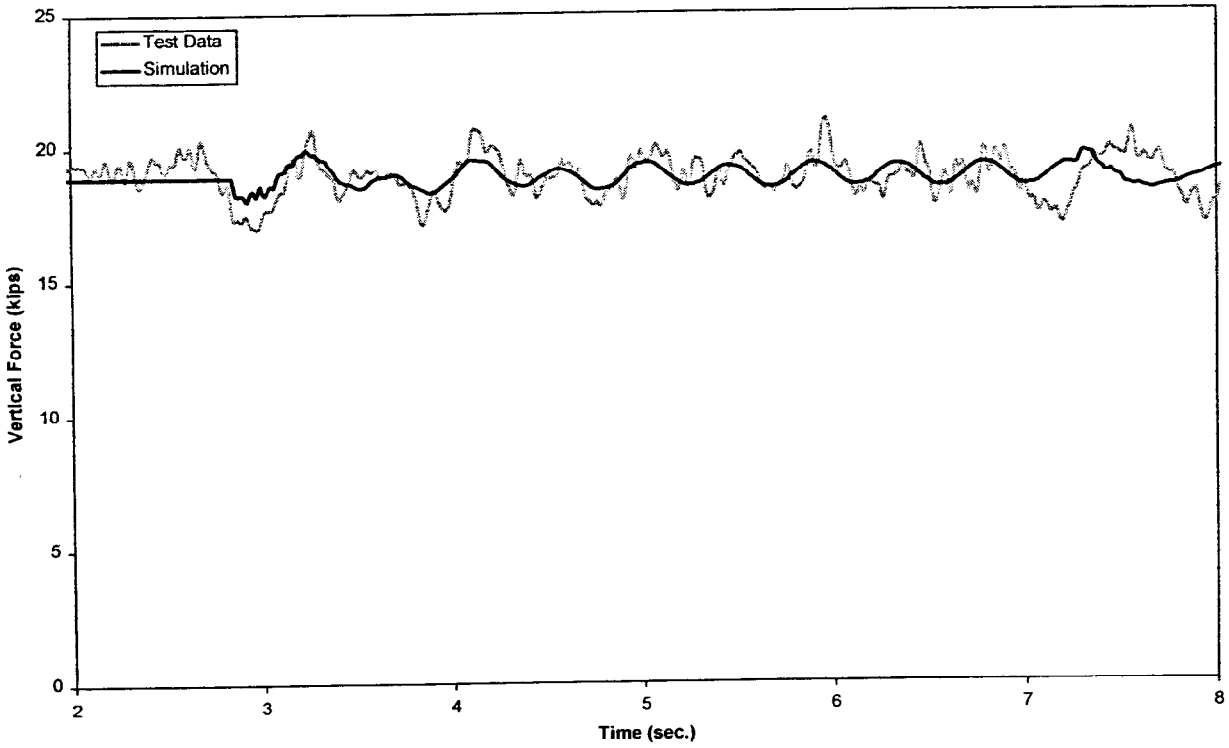

Figure B-37(b). Pitch and bounce - vertical force time history, 60 mph (lead right wheel)

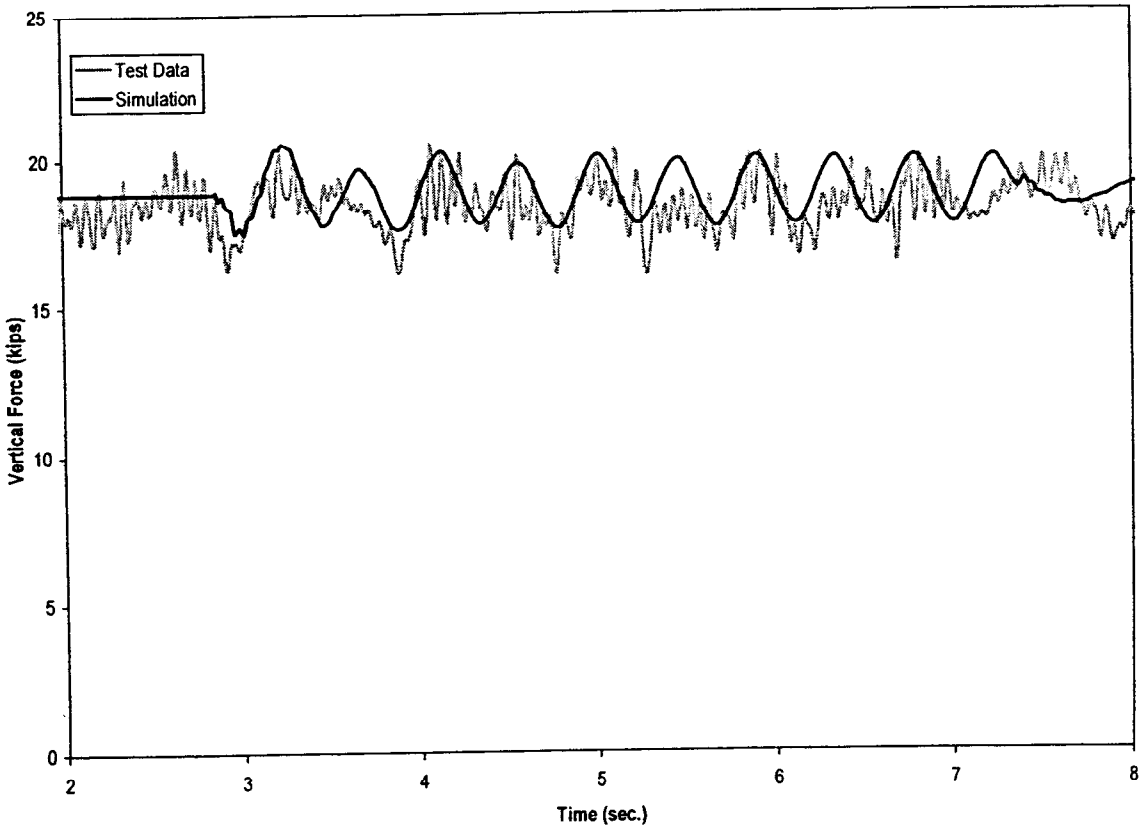

Figure B-37(c). Pitch and bounce - vertical force time history, 60 mph (trailing left wheel)

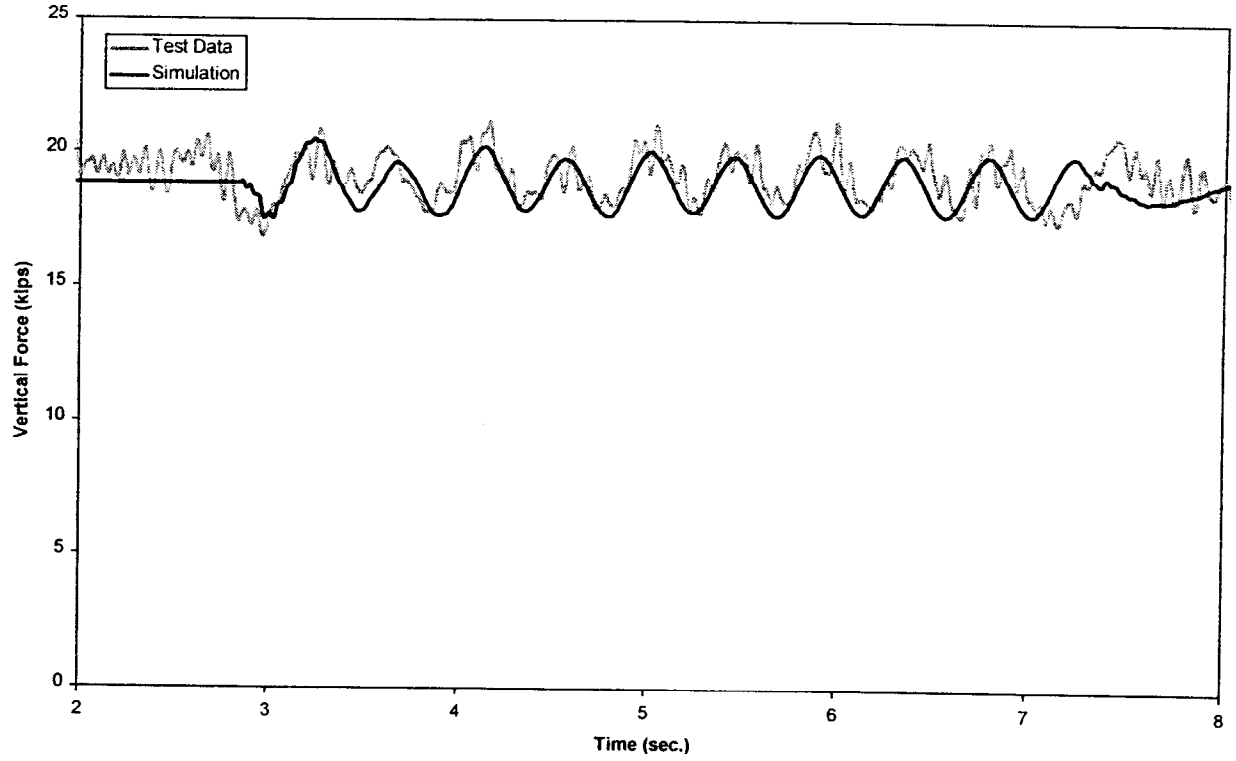

Figure B-37(d). Pitch and bounce - vertical force time history, 60 mph (trailing right wheel)

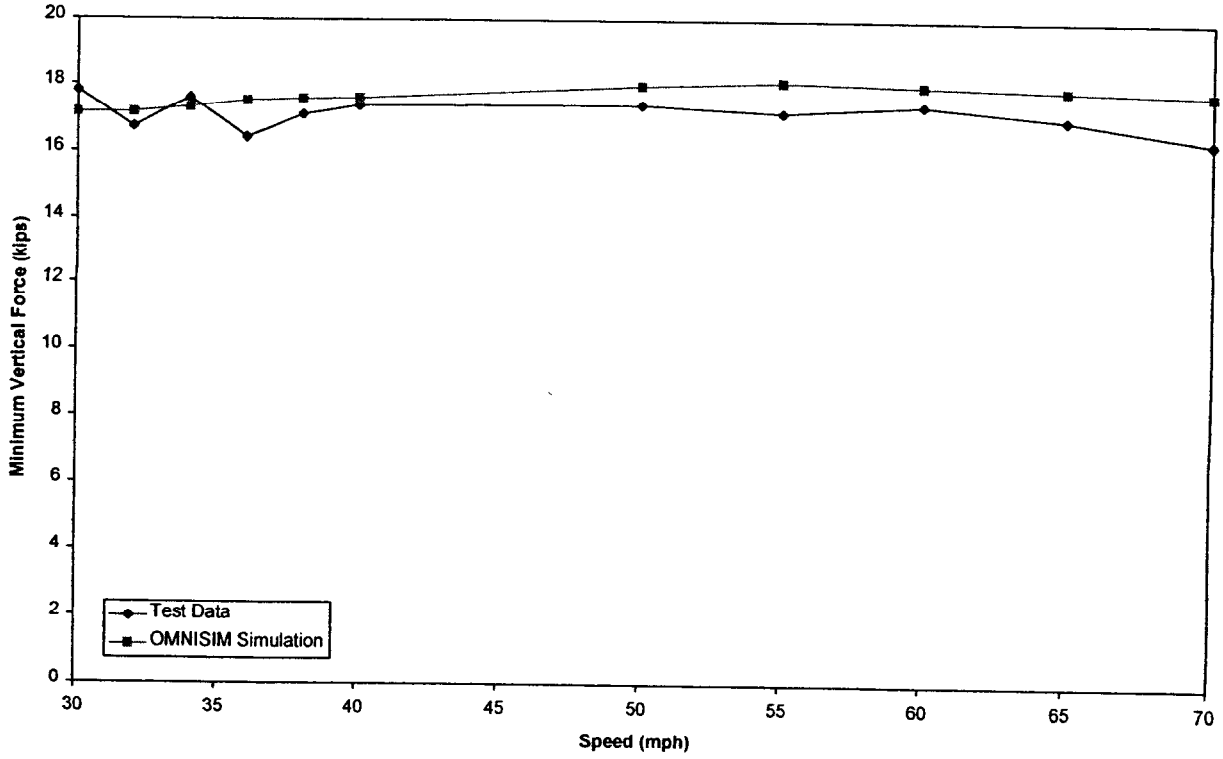

Figure B-38. Pitch and bounce - minimum vertical force